



University
of Glasgow

McColl, Barry (2004) *Pathophysiology of cerebral ischaemia: effects of APOE genotype on outcome and endocytosis.*

PhD thesis

<http://theses.gla.ac.uk/4324/>

Copyright and moral rights for this thesis are retained by the author

A copy can be downloaded for personal non-commercial research or study, without prior permission or charge

This thesis cannot be reproduced or quoted extensively from without first obtaining permission in writing from the Author

The content must not be changed in any way or sold commercially in any format or medium without the formal permission of the Author

When referring to this work, full bibliographic details including the author, title, awarding institution and date of the thesis must be given



UNIVERSITY
of
GLASGOW

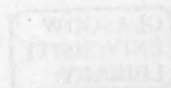
**PATHOPHYSIOLOGY OF CEREBRAL ISCHAEMIA:
EFFECTS OF *APOE* GENOTYPE ON OUTCOME AND
ENDOCYTOSIS**

Barry McColl BSc (Hons)

A thesis submitted for the degree of Doctor of Philosophy to the
Faculty of Medicine, University of Glasgow

Wellcome Surgical Institute and Hugh Fraser Neuroscience Laboratories
Division of Clinical Neuroscience
University of Glasgow
Garscube Estate
Bearsden Road
Glasgow G61 1QH

© Barry McColl, May 2004



DECLARATION

I declare that this thesis comprises my own original work and has not been submitted previously for any degree. The work comprising this thesis was carried out by myself, except where acknowledged in the text. All sources of data and information have been specifically referenced.

A handwritten signature in black ink, appearing to read 'Barry McColl'. The signature is written in a cursive style with a large initial 'B' and 'M'.

Barry McColl

ACKNOWLEDGEMENTS

During my PhD I have been fortunate to work and form friendships with a number of individuals who, collectively, have offered assistance (both in the lab and in the pub), advice, guidance, criticism (of varying forms), and probably the two most important aids to completing this thesis – some much needed laughter and the occasional boot up the ****. I would like to take this opportunity to sincerely thank these people.

My greatest thanks go to my principal supervisor, Dr Karen Horsburgh, for her scientific guidance and advice, practical expertise and assistance, and unwavering support throughout. I hope I haven't been too much trouble! I am also deeply grateful to Prof David Graham for his willingness to provide his expert opinion, advice and guidance when needed. Likewise, I am extremely grateful to Prof Jim McCulloch for his guidance, advice and input to several experiments, and for being the principal source of the boot up the ****. I would also like to thank Dr Fiona White, Dr Eileen McCracken, Dr Debbie Dewar and Prof Mhairi Macrae for their help and advice in various matters. Special thanks to Dr Hilary Carswell for her input to the blood flow experiments and help in unravelling the mysteries of blood flow analysis on the MCID, and to Dr Ailsa McGregor, Dr Sandra Magnoni and Andrew Wong for their contributions to the adenovirus study.

I am indebted to the technical staff for their expert training and assistance. Thanks to Linda Carberry, Lindsay Gallagher, Eileen Harrop, Janice Stewart, Joan Stewart and Margaret Stewart. Similarly, I would like to thank the animal technicians and vets in both Glasgow and Edinburgh for their advice and assistance.

I would also like to acknowledge my fellow PhD students (Dan, David, Debbie, Debs, Jetta and Kirsty) at the Wellcome Surgical Institute, in particular for creating a colourful and unique environment (both visual and auditory) in which to work and for providing the “fun” element in my PhD. Likewise, I am grateful to the students and post-docs in Edinburgh for their help, and for easing the cultural and language difficulties for a born-and-bred Glaswegian working in Edinburgh!

Finally, I would like to thank Laura (who for some reason thought the beginning of a PhD would be a good time to go out with me) for her support and understanding (“You’re not taking more ***** photos, are you?”), and mum and dad for their immense support, encouragement and inspiration.

CONTENTS

	Page
Declaration	II
Acknowledgements	III
Contents	IV
List of figures	XII
List of tables	XV
List of abbreviations	XVI
List of publications	XIX
Summary	XXI
Chapter 1: Introduction	1
1.1 Cerebral ischaemia	2
1.1.1 Focal cerebral ischaemia	3
1.1.2 Global cerebral ischaemia	7
1.1.3 Involvement of cerebral ischaemia in traumatic brain injury	9
1.1.4 Animal models of cerebral ischaemia	9
1.1.5 Pathophysiology of ischaemic cell death	12
1.2 Apolipoprotein E (ApoE)	19
1.2.1 Plasma apolipoproteins	19
1.2.2 ApoE in plasma	20
1.2.3 ApoE in the nervous system	20
1.2.4 Molecular biology of apoE	22
1.2.5 ApoE receptors	24
1.2.6 ApoE response to peripheral nerve injury – first indication of a role for apoE in nervous system pathology	27
1.3 APOE polymorphism and human brain injury and disease	27
1.3.1 APOE polymorphism and Alzheimer's disease	28
1.3.2 APOE polymorphism and traumatic brain injury	29
1.3.3 APOE polymorphism and cerebral ischaemia	30

1.3.4	Stroke and TBI as risk factors for dementia - association with <i>APOE</i> polymorphism	32
1.4	Role of apoE in brain injury – insight from animal models and <i>APOE</i> deficient and transgenic mice	33
1.4.1	Cellular localisation of apoE after acute brain injury	33
1.4.2	Studies in <i>APOE</i> deficient mice	34
1.4.3	<i>APOE</i> transgenic mice	34
1.5	Mechanisms underlying <i>APOE</i> genotype effects	37
1.5.1	ApoE and excitotoxicity	37
1.5.2	ApoE and oxidative stress	38
1.5.3	ApoE and cytoskeletal interactions	39
1.5.4	Toxic effects of apoE	39
1.5.5	Plasma and brain apoE levels	40
1.6	Endocytosis	41
1.6.1	Endocytic pathway	41
1.6.2	Rab proteins	42
1.6.3	Trafficking of apoE through the endocytic pathway	44
1.6.4	ApoE receptors, endocytosis and signal transduction	44
1.6.5	Endocytic alterations in Alzheimer's disease	45
1.7	Modulation of apoE levels by <i>APOE</i> gene transfer	46
1.7.1	<i>APOE</i> as a candidate for gene transfer to the brain	46
1.7.2	Viruses as vectors for gene transfer	47
1.7.3	Adenoviral vectors	48
1.7.4	Adenoviral transduction and transgene expression in the brain	49
1.7.5	Adenoviral vector-mediated gene transfer and cerebral ischaemia	50
1.8	Hypotheses and aims of thesis	51
Chapter 2:	Materials and Methods	52
2.1	Human post-mortem brain tissue	53
2.1.1	Tissue processing and selection	53

2.1.2	<i>APOE</i> genotyping	54
2.2	Mice	55
2.2.1	C57Bl/6J mice	55
2.2.2	<i>APOE</i> transgenic mice	56
2.3	Surgical procedures	58
2.3.1	Stereotaxic injection	58
2.3.2	Intraluminal filament occlusion	60
2.3.3	Monitoring of mean arterial blood pressure	64
2.3.4	Examination of cerebrovascular anatomy	64
2.4	Assessment of neurological deficit	65
2.5	Perfusion fixation	65
2.6	Paraffin processing, embedding and cutting	66
2.6.1	Paraffin processing	66
2.6.2	Cutting	67
2.7	Histological staining	67
2.7.1	Haematoxylin and eosin	67
2.7.2	Thionin	68
2.8	Volumetric measurement of ischaemic damage	69
2.8.1	Selection of sections at eight coronal levels	69
2.8.2	Identification of areas of ischaemic damage	72
2.8.3	Calculation of volume of ischaemic damage	73
2.9	Immunohistochemistry	74
2.9.1	Antibodies	74
2.9.2	Avidin-biotin (ABC) method of immunohistochemistry	74
2.9.3	Peroxidase single-labelling immunohistochemistry	77
2.9.4	Fluorescent double-labelling immunohistochemistry	77
2.9.5	GFP fluorescence	78
2.9.6	Quantification of immunostaining	78
2.10	Measurement of apoE levels	79
2.10.1	Tissue harvesting	79
2.10.2	Sample homogenisation and protein extraction	81

2.10.3	Protein assay	81
2.10.4	ELISA	82
2.11	Measurement of local cerebral blood flow	83
2.11.1	Utility of ¹⁴ C-iodoantipyrine as a radioactive tracer	83
2.11.2	Administration of ¹⁴ C-IAP	83
2.11.3	Measurement of terminal heart blood sample ¹⁴ C-IAP concentration	84
2.11.4	Measurement of local brain tissue ¹⁴ C-IAP concentration	85
2.11.5	Calculation of local cerebral blood flow	86
2.12	Adenoviral vectors	88
2.13	Statistical analysis	88
Chapter 3:	Endocytic pathway alterations in human temporal lobe after global cerebral ischaemia and association with <i>APOE</i> genotype	89
3.1	Introduction and aims	90
3.2	Materials and methods	90
3.2.1	Post-mortem human brain tissue	90
3.2.2	Immunohistochemistry	90
3.2.3	Ischaemic neuronal damage	91
3.2.4	Statistical analysis	91
3.3	Results	92
3.3.1	Ischaemic neuronal damage	92
3.3.2	Rabaptin-5 immunostaining	94
3.3.3	Rab4 immunostaining	100
3.3.4	Association between <i>APOE</i> genotype and alterations in neuronal rabaptin-5 and rab4 immunostaining after global ischaemia	107
3.3.5	β -amyloid deposition and neurofibrillary tangles	110
3.4	Discussion	111
3.4.1	Global ischaemia and ischaemic neuronal damage	111
3.4.2	Endocytic pathway alterations	112

3.4.3	<i>APOE</i> genotype and endocytic pathway alterations	114
3.4.4	Conclusions	116
Chapter 4:	Characterisation and validation of the intraluminal filament model of focal cerebral ischaemia in C57Bl/6J mice	117
4.1	Introduction and aims	118
4.2	Materials and methods	118
4.2.1	Mice	118
4.2.2	Development of model	118
4.2.3	Characterisation of model	119
4.2.4	Examination of cerebrovascular anatomy	120
4.2.5	Operational definition of MCA territory	120
4.2.6	Immunohistochemistry	121
4.2.7	Statistical analysis	121
4.3	Results	122
4.3.1	Development of model	122
4.3.2	Characterisation of model	125
4.3.3	Cerebrovascular anatomy	136
4.3.4	Immunohistochemistry	136
4.4	Discussion	139
4.4.1	Technical and methodological considerations	139
4.4.2	Ischaemic damage after intraluminal occlusion	143
4.4.3	Cerebral blood flow during intraluminal occlusion	145
4.4.4	Implications for utility of model in further studies	148
4.4.5	Conclusions	148
Chapter 5:	Association between <i>APOE</i> genotype and differences in outcome and endocytic pathway alterations after focal cerebral ischaemia in mice	149
5.1	Introduction and aims	150
5.2	Materials and methods	150

5.2.1	Mice	150
5.2.2	Focal ischaemia and evaluation of neurological deficit	150
5.2.3	Measurement of ischaemic damage	150
5.2.4	Immunohistochemistry	151
5.2.5	Statistical analysis	151
5.3	Results	152
5.3.1	Mortality rate, haemorrhage rate and absence of ischaemic damage	152
5.3.2	Effect of <i>APOE</i> genotype on ischaemic damage	153
5.3.3	Effect of <i>APOE</i> genotype on neurological deficit	155
5.3.4	ApoE immunostaining	156
5.3.5	Rabaptin-5 immunostaining	162
5.3.6	Rab4 immunostaining	165
5.3.7	Correlations of apoE, rabaptin-5 and apoE immunoreactivity	169
5.4	Discussion	171
5.4.1	<i>APOE</i> genotype and outcome after focal ischaemia	171
5.4.2	ApoE alterations after focal ischaemia	174
5.4.3	ApoE and mechanisms of neuroprotection in acute brain injury	177
5.4.4	Endocytic pathway alterations after focal ischaemia	179
5.4.5	<i>APOE</i> genotype-dependent differences in endocytic pathway alterations after focal ischaemia	180
5.4.6	Implications of elevated endocytic pathway activity after cerebral ischaemia	182
5.4.7	Alterations in the endocytic pathway - possible mechanism underlying <i>APOE</i> genotype differences in outcome to acute brain injury	183
5.4.8	Conclusions	186

Chapter 6: Adenoviral-mediated gene transfer of <i>APOE</i> ϵ3 markedly reduces ischaemic brain damage after transient focal cerebral ischaemia in mice	188
6.1 Introduction and aims	189
6.2 Materials and methods	189
6.2.1 Mice	189
6.2.2 Adenoviral (Ad) vectors	189
6.2.3 Preliminary characterisation of adenoviral transduction and transgene expression	189
6.2.4 Effects of Ad- <i>APOE</i> administration on outcome and apoE immunostaining after focal ischaemia	190
6.2.5 Effect of Ad- <i>APOE</i> administration on apoE levels	191
6.2.6 Statistical analysis	192
6.3 Results	193
6.3.1 Preliminary characterisation of adenoviral transduction and transgene expression	193
6.3.2 Effect of Ad- <i>APOE</i> administration on apoE levels	201
6.3.3 Effect of Ad- <i>APOE</i> administration on ischaemic damage after focal ischaemia	202
6.3.4 Effect of Ad- <i>APOE</i> administration on neurological deficit after focal ischaemia	205
6.3.5 Effect of Ad- <i>APOE</i> administration on apoE immunostaining after focal ischaemia	206
6.4 Discussion	212
6.4.1 Adenoviral vector transduction and transgene expression	212
6.4.2 Adenoviral vector cytotoxicity	214
6.4.3 Neuroprotection by administration of Ad- <i>APOE</i>	214
6.4.4 Inflammatory and immune responses to adenoviral vectors	217
6.4.5 Potential for adenoviral vector administration post-ischaemia	218
6.4.6 Conclusions	219

Chapter 7: General discussion	220
7. Human stroke therapy and the therapeutic potential of apoE	221
Appendices	225
Appendix A Stock solutions	226
Appendix B Summary of mouse numbers for all experiments	227
Appendix C Control and global ischaemic cohort: clinical details	228
Appendix D Semi-quantification of immunoreactivity in human temporal lobe: validation and reproducibility	230
Appendix E Volumetric measurement of ischaemic damage: reproducibility	232
Appendix F Measurement of local cerebral blood flow: reproducibility	233
Appendix G Volumetric measurement of apoE immunostaining in <i>APOE</i> transgenic mice: reproducibility	234
Appendix H Semi-quantification of immunoreactivity in <i>APOE</i> transgenic mice: reproducibility	235
Appendix I Volumetric measurement of apoE immunostaining after viral vector or vehicle administration: reproducibility	236
Appendix J Association between ischaemic damage and apoE immunoreactivity after <i>Ad-APOE</i> administration	237
References	238

LIST OF FIGURES

	Page
Chapter 1	
1. Focal ischaemic brain damage	6
2. Influence of duration and severity of focal ischaemia on extent of damage	6
3. Selective and delayed neuronal damage after global ischaemia	8
4. Simplified schema of pathophysiological mechanisms after ischaemic brain injury	14
5. Structure of a lipoprotein particle	19
6. ApoE polymorphism	23
7. Schematic overview of the endocytic pathway	42
8. Role of rab proteins in endocytosis	43
Chapter 2	
9. Genotyping of <i>APOE</i> transgenic mice	58
10. Location of stereotaxic injections	59
11. Intraluminal filament occlusion technique – surgical approach	62
12. Coronal levels for quantification of ischaemic damage	70
13. Identification of areas of ischaemic damage	72
14. “ABC” immunohistochemistry method	76
15. Sandwich ELISA method	80
16. Representative time course of arterial ¹⁴ C radioactivity after intraperitoneal injection of ¹⁴ C-IAP	84
17. Representative standard curve of relative optical density readings from ¹⁴ C standards	86
18. Operational equation for calculation of cerebral blood flow	87
19. Schematic representation of adenoviral vector containing <i>APOE</i> gene	88
Chapter 3	
20. Ischaemic neuronal damage after global ischaemia	93
21. Rabaptin-5 immunostaining	96
22. Semi-quantitative assessment of rabaptin-5 immunoreactivity	97
23. Association between ischaemic neuronal damage and neuronal rabaptin-5 immunoreactivity	98

24. Association between survival time after global ischaemia and neuronal rabaptin-5 immunoreactivity	99
25. Rab4 immunostaining	102
26. Semi-quantitative assessment of rab4 immunoreactivity	103
27. Association between ischaemic neuronal damage and neuronal rab4 immunoreactivity	104
28. Association between survival time after global ischaemia and neuronal rab4 immunoreactivity	105
29. Association between neuronal rabaptin-5 and rab4 immunoreactivity	106
30. Effect of <i>APOE</i> genotype on alterations in neuronal rabaptin-5 immunoreactivity after global ischaemia	108
31. Effect of <i>APOE</i> genotype on alterations in neuronal rab4 immunoreactivity after global ischaemia	109
32. Effect of <i>APOE</i> genotype on ischaemic neuronal damage	116
 Chapter 4	
33. Effect of filament size on hypoperfusion in MCA territory	123
34. Validation of adapted method for measurement of ischaemic damage	124
35. Effect of occlusion duration on ischaemic damage	127
36. Representative ¹⁴ C-IAP autoradiograms after 15min and 60min sham occlusion	130
37. Representative ¹⁴ C-IAP autoradiograms after 15min and 60min intraluminal occlusion	132
38. Effect of occlusion duration on local cerebral blood flow in the dorsolateral caudate nucleus and hippocampus (CA1)	134
39. Effect of occlusion duration on local cerebral blood flow in the ventromedial thalamus and cerebellum	135
40. Mean arterial blood pressure during 60min occlusion	137
41. Integrity of the circle of Willis in C57Bl/6J mice	138
 Chapter 5	
42. Effect of <i>APOE</i> genotype on volume of ischaemic damage	154
43. Effect of <i>APOE</i> genotype on neurological deficit	155
44. Control apoE immunostaining in the non-ischaemic hemisphere	158
45. Alterations in apoE immunostaining in the ischaemic hemisphere	159
46. Effect of <i>APOE</i> genotype on volume of apoE immunoreactivity	160
47. Semi-quantification of apoE immunoreactivity	161

48. Rabaptin-5 immunostaining	163
49. Semi-quantification of rabaptin-5 immunoreactivity	164
50. Rab4 immunostaining	167
51. Semi-quantification of rab4 immunoreactivity	168
52. Association between rabaptin-5 and rab4 immunoreactivity	169
53. Association between apoE and rabaptin-5 or rab4 immunoreactivity	170
54. ApoE levels in APOE ϵ3-437 and APOE ϵ4-81 lines of mice	175
55. APOE genotype-dependent differences in the response of the endocytic pathway to cerebral ischaemia	181
Chapter 6	
56. Effect of adenoviral vector dose on distribution of GFP expression	194
57. GFP expression in the caudate nucleus and subcortical white matter	195
58. Tissue damage after vehicle or adenoviral vector injection	197
59. ApoE immunostaining after vehicle or vector administration without subsequent ischaemia	199
60. ApoE immunostaining after Ad-APOE injection	200
61. Quantification of apoE levels by ELISA	201
62. Measurement of ischaemic damage	203
63. Neurological deficit after focal ischaemia	205
64. ApoE staining in the contralateral hemisphere after focal ischaemia	207
65. ApoE immunostaining in the ipsilateral hemisphere after focal ischaemia	208
66. Volumetric measurement of apoE immunoreactivity	211

LIST OF TABLES

	Page
Chapter 2	
1. Paraffin processing protocol for whole brains	66
2. Coronal levels and their neuroanatomical landmarks	71
3. Primary antibodies, optimised concentrations and their corresponding secondary antibodies and blocking serum	75
Chapter 4	
4. Hypoperfusion associated with intraluminal occlusion with a 5-0 and thinner 6-0 filament	122
5. Mice excluded prior to measurement of ischaemic damage	125
6. Frequency of ischaemic damage in specific brain regions	128
7. Effect of sham occlusion duration on local brain tissue ¹⁴ C concentration	131
8. Effect of intraluminal filament occlusion duration on local cerebral blood flow	133
Chapter 5	
9. Mice excluded prior to measurement of ischaemic damage	152
10. Frequency of ischaemic damage in specific brain regions	153
Chapter 6	
11. Frequency of ischaemic damage in specific brain regions	204

LIST OF ABBREVIATIONS

β -gal	β -galactosidase
^{14}C -IAP	^{14}C -iodoantipyrine
4-HNE	4-hydroxynonenal
A β	β -amyloid
AAV	adeno-associated virus
ACA	anterior cerebral artery
Ad	adenovirus
AD	Alzheimer's disease
AMPA	α -amino-3-hydroxy-5-methyl-4-isoxazole propionic acid
ANOVA	analysis of variance
apoA-I	apolipoprotein A-I
apoA-IV	apolipoprotein A-IV
apoD	apolipoprotein D
apoE	apolipoprotein E (protein)
<i>APOE</i>	apolipoprotein E (gene)
apoER2	apolipoprotein E receptor 2
apoH	apolipoprotein H
apoJ	apolipoprotein J
APP	β -amyloid precursor protein
BA	basilar artery
BCA	bicinchoninic acid
BCCAo	bilateral common carotid artery occlusion
BDNF	brain-derived neurotrophic factor
BSA	bovine serum albumin
CA	cornu ammoni
CAA	cerebral amyloid angiopathy
CAR	coxsackie-adenovirus receptor
CBF	cerebral blood flow
CCA	common carotid artery
CCV	clathrin-coated vesicles
CMV	cytomegalovirus
CNS	central nervous system

CNTF	ciliary neurotrophic factor
CSF	cerebrospinal fluid
CT	computed tomography
CuZn-SOD	copper, zinc superoxide dismutase
DAB	diaminobenzidine
Dab-1	disabled-1
DMSO	dimethyl sulphoxide
ECA	external carotid artery
ECL	entorhinal cortex lesion
ELISA	enzyme-linked immunosorbent assay
GDNF	glial cell line-derived neurotrophic factor
GFAP	glial fibrillary acidic protein
GFP	green fluorescent protein
H & E	haematoxylin and eosin
HDL	high-density lipoprotein
HRP	horse-radish peroxidase
HSP	heat shock protein
ICA	internal carotid artery
ICH	intracerebral haemorrhage
IL-1 β	interleukin-1 β
IL-1ra	interleukin-1 receptor antagonist
K-PI	Kunitz-type protease inhibitor
LCBF	local cerebral blood flow
LDL	low-density lipoprotein
LRP	low density lipoprotein receptor-related protein
MABP	mean arterial blood pressure
MAP	microtubule associated protein
MCA	middle cerebral artery
NF	neurotrophic factor
NGF	nerve growth factor
NGS	normal goat serum
NHS	normal horse serum
NMDA	<i>N</i> -methyl- <i>D</i> -aspartate

NSE	neuron-specific enolase
OPD	o-phenylenediaminedihydrochloride
PAM	paraformaldehyde
PB	phosphate buffer
PBS	phosphate buffered saline
PBST	phosphate buffered saline-Tween 20
PCA	posterior cerebral artery
PcomA	posterior communicating artery
PCR	polymerase chain reaction
PD	Parkinson's disease
PET	positron emission tomography
PMSF	phenylmethylsulfonyl fluoride
PS1	presenilin 1
PSD-95	postsynaptic density-95
PTB	phosphotyrosine-binding
RAP	receptor-associated protein
ROD	relative optical density
SAH	subarachnoid haemorrhage
SCA	superior cerebellar artery
SEM	standard error of the mean
SOD	superoxide dismutase
TBI	traumatic brain injury
TNF- α	tumour necrosis factor- α
TUNEL	terminal deoxynucleosidyl transferase (TdT)-mediated biotinylated deoxyuridine triphosphate (dUTP) nick end labelling
VA	vertebral artery
VLDL	very low-density lipoprotein

LIST OF PUBLICATIONS

Papers

McColl BW, McGregor A, Wong A, Harris JD, Dickson G, Amalfitano A, Magnoni S, Baker A, Horsburgh K. Adenovirus-mediated gene transfer of *APOE* ϵ 3 attenuates ischaemic brain damage after transient focal cerebral ischaemia in mice. *In preparation*

McColl BW, Roses AD, Horsburgh K: Association between *APOE* genotype and differences in outcome and endocytic pathway alterations after transient focal cerebral ischaemia in mice. *In preparation*

McColl BW, Carswell HV, McCulloch J, Horsburgh K: Extension of cerebral hypoperfusion and ischaemic pathology beyond middle cerebral artery territory after intraluminal filament occlusion in C57Bl/6J mice. **Brain Res 2004, 997:15-23**

Horsburgh K, **McColl BW**, White F, McCulloch J: Apolipoprotein E influences neuronal death and repair. **International Congress Series 2003, 1737:1-8**

McColl BW, Graham DI, Weir CJ, White F, Horsburgh K: Endocytic pathway alterations in human hippocampus after global ischaemia and the influence of *APOE* genotype. **Am J Pathol 2003, 162:273-281**

Abstracts

McColl BW, McGregor A, Wong A, Harris JD, Dickson G, Amalfitano A, Magnoni S, Baker A, Horsburgh K. Adenovirus-mediated gene transfer of *APOE* ϵ 3 is neuroprotective in a mouse model of brain injury: implications for Alzheimer's disease therapy. **The 9th International Conference on Alzheimer's Disease and Related Disorders 2004.**

McColl BW, McCulloch J, Horsburgh K: The extent and distribution of neuronal damage is influenced by the duration and severity of cerebral hypoperfusion after transient middle cerebral artery occlusion in C57Bl/6J mice. **J Cereb Blood Flow Metab (Suppl 1) 2003, 19:191**

McColl BW, Roses AD, Horsburgh K: Increased susceptibility of *APOE* ϵ 4 transgenic mice to transient middle cerebral artery occlusion. **J Cereb Blood Flow Metab (Suppl 1) 2003, 19:588**

McColl BW, McCulloch J, Horsburgh K: The duration and severity of cerebral hypoperfusion influences the extent and distribution of neuronal damage after transient MCAo in C57Bl/6J mice. **British Neuroscience Association, 17th National Meeting 2003:60.07**

McColl BW, Roses AD, Horsburgh K: *APOE* epsilon 4 mice show poorer outcome after transient middle cerebral artery occlusion compared to epsilon 3 mice. **British Neuroscience Association, 17th National Meeting 2003:60.08**

McColl BW, McCulloch J, Horsburgh K: Characterisation of transient middle cerebral artery occlusion by intraluminal filament in mice. Society for Neuroscience, 32nd Annual Meeting 2002:488.1

McColl BW, Graham DI, White F, Horsburgh K: Endocytic pathway alterations in human hippocampus after global ischaemia and the influence of *APOE* genotype. Society for Neuroscience, 32nd Annual Meeting 2002:883.1

McColl BW, Graham DI, White F, Horsburgh K: Endocytic pathway alterations after brain injury and the influence of *APOE* genotype: implications for Alzheimer's disease. The 3rd Neurobiology of Aging Conference 2002:P25

SUMMARY

Apolipoprotein E (apoE denotes protein; *APOE* denotes gene) is a lipid-transport protein abundantly expressed in the brain and strongly upregulated after acute brain injury. The *APOE* ϵ 4 allele is the major genetic risk factor for Alzheimer's disease (AD) and has been associated with poorer outcome after various types of acute brain injury, including traumatic brain injury and subarachnoid haemorrhage. However, the role of *APOE* genotype in focal ischaemic stroke is less clear. The mechanism(s) by which *APOE* genotype may modulate outcome after acute brain injury are also unclear at present. Accordingly, the studies described in this thesis were undertaken to further address these issues.

Endocytic pathway alterations in human temporal lobe after global cerebral ischaemia and association with *APOE* genotype

The endocytic pathway is integral to the internalisation and intracellular trafficking of apoE. Marked upregulation and neuronal accumulation of apoE occur after cerebral ischaemia. Alterations in this pathway are therefore a potential mechanism that could contribute to *APOE* genotype effects in the injured brain. In the present study, endocytic pathway activity was assessed in post-mortem temporal lobe sections from patients who experienced an episode of global ischaemia (and controls) using antibodies to markers of endocytic pathway activity – rabaptin-5 (internalisation) and rab4 (recycling). Significant increases in the degree of neuronal rabaptin-5 and rab4 immunoreactivity were observed after global ischaemia, indicative of enhanced endocytic pathway activity in response to ischaemia. In addition, endocytic pathway alterations after global ischaemia were *APOE* genotype-dependent. There was a significant interaction between the effects of *APOE* genotype and an episode of global ischaemia on the degree of neuronal rab4 immunoreactivity. This indicated an attenuated endocytic recycling response after global ischaemia in *APOE* ϵ 4 carriers compared to individuals without an *APOE* ϵ 4 allele.

Characterisation and validation of the intraluminal filament model of focal cerebral ischaemia in C57Bl/6J mice

The intraluminal occlusion model of transient focal ischaemia was established and characterised in C57Bl/6J mice in order to systematically investigate the role of *APOE* genotype and endocytosis in cerebral ischaemia. The consequences of increasing

duration (15, 30 and 60min) of intraluminal occlusion on ischaemic damage (24h post-occlusion), cerebral blood flow and blood pressure were determined. The volume of ischaemic damage increased significantly with increasing occlusion duration, in part due to recruitment of tissue outside middle cerebral artery territory. The severity of cerebral hypoperfusion was significantly greater in 9 of 12 brain regions examined after 60min compared to 15min occlusion. Blood pressure during 60min occlusion remained stable for 25min after occlusion onset and declined thereafter. Cerebrovascular anatomy was examined and showed that a complete circle of Willis was present in only 10% of mice. A temporal decline in mean arterial blood pressure and increase in the severity of cerebral hypoperfusion with increasing occlusion duration likely underlie the high sensitivity of ischaemic damage to increasing occlusion duration.

Association between *APOE* genotype and differences in outcome and endocytic pathway alterations after focal cerebral ischaemia in mice

Characterisation of the intraluminal occlusion model enabled the effects of *APOE* genotype on outcome and endocytic pathway alterations to be investigated in *APOE* transgenic mice. Ischaemic damage, neurological deficit, and apoE and endocytic pathway alterations were assessed 24h after 15min focal ischaemia in mice expressing human *APOE* $\epsilon 3$ or *APOE* $\epsilon 4$. The volume of ischaemic damage and neurological deficit score were significantly greater in *APOE* $\epsilon 4$ mice, indicating a poorer outcome associated with *APOE* $\epsilon 4$. The volume of ischaemic damage correlated with neurological deficit. Focal ischaemia induced increased apoE immunoreactivity in areas of ischaemic damage in both *APOE* $\epsilon 3$ and *APOE* $\epsilon 4$ mice. The volume of apoE immunoreactivity correlated with the volume of ischaemic damage and was significantly greater in *APOE* $\epsilon 4$ mice. Increased immunoreactivity of the endocytic markers, rabaptin-5 and rab4 were also observed in areas of ischaemic damage indicating elevated endocytic pathway activity in response to focal ischaemia. These alterations were *APOE*-genotype dependent. The degree of rab4 immunoreactivity was significantly greater in *APOE* $\epsilon 3$ compared to *APOE* $\epsilon 4$ mice suggesting an attenuated endocytic recycling response associated with the *APOE* $\epsilon 4$ allele. *APOE* genotype-dependent differences in endocytic pathway alterations could modulate the response to cerebral ischaemia by influencing the intracellular trafficking of apoE and its interactions with cellular elements.

Adenovirus-mediated gene transfer of *APOE* ϵ 3 markedly reduces ischaemic brain damage after focal cerebral ischaemia in mice

A better outcome after focal ischaemia in *APOE* ϵ 3 mice (as determined in this thesis) is consistent with a number of previous studies showing favourable effects associated with the *APOE* ϵ 3 allele. Since exogenous administration of apoE has previously conferred neuroprotection after acute brain injury, increasing apoE3 levels to promote the beneficial effects of this isoform is a relevant strategy to improve outcome after focal ischaemia. In this study, a 2nd generation adenoviral vector containing the “beneficial” *APOE* ϵ 3 gene (Ad-*APOE*) was injected into the brain 3d prior to 60min focal ischaemia and outcome was determined 24h post-ischaemia. The volume of ischaemic damage was significantly reduced by 50% in Ad-*APOE* treated mice compared to mice treated with a control vector (Ad-GFP) or vehicle. There was a trend toward a lower neurological deficit score in Ad-*APOE* treated mice, although this did not reach statistical significance. ApoE immunohistochemistry and ELISA showed that levels of apoE were significantly increased in mice treated with Ad-*APOE* compared to a control vector (Ad-GFP) or vehicle. Thus, the neuroprotective effects achieved by adenoviral vector-mediated *APOE* ϵ 3 gene transfer may be mediated by elevated apoE3 levels and suggest that manipulation of apoE-sensitive mechanisms could be a realistic therapeutic strategy in human stroke.

The data presented in this thesis indicate an important role for *APOE* genotype in modulating outcome after ischaemic brain injury, further highlighting the favourable effects associated with the *APOE* ϵ 3 allele. *APOE* genotype-dependent alterations in the endocytic pathway are mechanisms which could contribute to differences in outcome. These data also highlight the neuroprotective effects achieved by manipulating apoE levels to promote the beneficial effects of apoE3. An apoE-based therapeutic strategy may be a potential approach for treatment of ischaemic brain injury in humans.

Chapter 1

Introduction

1.1 Cerebral ischaemia

The structural and functional integrity of the brain requires a continuous and adequate supply of oxygen and metabolic substrate (glucose) to meet the high metabolic demands of brain tissue. Cerebral ischaemia refers to a condition where there is inadequate cerebral blood flow to meet these demands with the consequence that normal brain function is perturbed. Cerebrovascular disease resulting from cerebral ischaemia is the third leading cause of death in developed countries behind ischaemic heart disease and cancer (Dirnagl *et al.*, 1999). Cerebrovascular disease is also the most common cause of long-term neurological disability in the adult population (Wolfe, 2000). As a consequence, treatment of cerebrovascular disease consumes a large proportion of the economic resources of health-care systems (Terent *et al.*, 1994; Rothwell, 2001). Furthermore, cerebral ischaemia is a major feature and cause of mortality and morbidity after traumatic brain injury resulting from head trauma (Graham *et al.*, 1978; Graham *et al.*, 1989), the leading cause of death under the age of 45 (Baethmann *et al.*, 1998). Significantly, there is no current effective treatment for ischaemic brain damage that is in widespread use. Thus, in view of the prevalence of ischaemic brain damage in brain injury and disease and the severity and impact of its sequelae on society, further understanding of the aetiology and pathophysiology of cerebral ischaemia and development of novel treatments are imperative.

There is increasing awareness of the important roles that genetic factors may play in modulating the risk of and outcome to cerebral ischaemia and their effects on the pathophysiology of ischaemic brain damage (Carr *et al.*, 2002; Alberts, 2003). Strong clinical evidence indicates a role for polymorphism in the apolipoprotein E (*APOE* denotes gene; apoE denotes protein) gene in outcome from various types of acute brain injury, although results have been inconclusive with regard to ischaemic stroke. A major aim of this thesis was to further investigate the effects of *APOE* polymorphism in a model of focal ischaemia. A potential mechanism – endocytic pathway alterations – by which *APOE* genotype may modulate the susceptibility of the brain to injury, was also investigated. In addition, the potential of exogenously administered apoE (via viral vector) to modulate ischaemic brain damage was determined.

1.1.1 Focal cerebral ischaemia

Two major types of cerebral ischaemia, focal and global (*see section 1.1.2*), are recognised based on the anatomical distribution of the ischaemic insult. Focal cerebral ischaemia occurs when there is diminished cerebral blood flow to a discrete brain region. In humans, when the ischaemic insult is severe enough, focal (or global) neurological deficits present clinically, a condition referred to as “stroke” if such deficits persist for longer than 24h or lead to death and have no apparent cause other than a vascular one (as defined by WHO). The most rigorous studies have indicated stroke incidence rates of approximately 300 – 500 per 100,000 in white populations (Sudlow and Warlow, 1997). The incidence of stroke increases dramatically with age, with three-quarters of all first strokes occurring after the age of 65, at least in white populations (Sudlow and Warlow, 1997). Overall, approximately 30% of hospitalised patients die within one year of a stroke (Warlow *et al.*, 2003).

1.1.1.1 Aetiology

The underlying cause of focal cerebral ischaemia in stroke may be occlusive (thrombotic or embolic blockage of an artery) or haemorrhagic (bleeding from a ruptured artery) in origin. The majority (approximately 80% in white populations) of strokes result from thrombotic or embolic occlusion of an artery (*for review see Kalimo et al.*, 2002). The middle cerebral artery (MCA) is the most commonly occluded intracranial vessel (Derouesne *et al.*, 1993), which may be due to its relatively large size and proportion of blood flow and proximity to the internal carotid artery from which circulating emboli may pass into the MCA (McAuley, 1995). The territory supplied by the MCA includes motor and somatosensory cortex, the striatum and the internal capsule. Consequently, ischaemic damage is observed in these areas in a high proportion of strokes. The clinical importance of the MCA in human stroke is reflected by the development of numerous animal models of focal cerebral ischaemia that involve MCA occlusion (*see section 1.1.4*).

Spontaneous intracranial haemorrhage is the underlying cause in approximately 20% of first-time strokes (Warlow *et al.*, 2001). The two major types of intracranial haemorrhage are intracerebral and subarachnoid, which account for approximately 15% and 5% of strokes (in white populations) (Warlow *et al.*, 2001). Intracerebral haemorrhage (ICH) is associated with formation of an intraparenchymal haematoma that may result in raised intracranial pressure, displacement of deep brain structures and

loss of consciousness (Massaro *et al.*, 1991). Hypertension is the most important cause of ICH and is primarily associated with haemorrhages located deep within the brain (caudate nucleus, putamen, cerebellum, brainstem). Cerebral amyloid angiopathy (CAA), a condition involving deposition of the β -amyloid protein in the walls of cerebral blood vessels, is also a major cause of ICH, particularly lobar haemorrhages located more superficially in the cerebral hemispheres (Massaro *et al.*, 1991). Subarachnoid haemorrhage (SAH) most frequently results from the rupture of a saccular aneurysm in a vessel on the brain surface leading to bleeding in to the subarachnoid space. Both SAH and ICH are associated with poorer clinical prognosis compared to occlusive stroke with mortality rates as high as 50% (Camarata, 1994).

1.1.1.2 CBF thresholds in focal ischaemia

Irrespective of the proximate cause of focal ischaemia, a characteristic topographical pattern develops consisting of a dense core region of hypoperfusion separated from normally perfused tissue by a zone of intermediate ischaemia, termed the ischaemic “penumbra” (Astrup *et al.*, 1981). This gradient of cerebral blood flow is associated with the development of irreversible damage in the ischaemic core and potentially reversible dysfunction in the surrounding tissue. Underlying this pattern is a series of critical thresholds of cerebral blood flow (CBF) at which various electrophysiological and biochemical alterations occur ultimately leading to irreversible injury. Experimental MCA occlusion in baboons and cats has shown that neuronal electrical function is affected when CBF falls below 40% (20ml/100g/min) of the normal value and is completely lost when CBF is 30% of the normal level. (Branston *et al.*, 1974; Heiss *et al.*, 1976). At this level of perfusion, ionic homeostasis and structural integrity is maintained. Ionic pump failure and accompanying membrane depolarisation and potassium efflux do not occur until CBF is further reduced to approximately 15% (10 – 12ml/100g/min) of normal levels (Astrup *et al.*, 1977; Branston *et al.*, 1977). Ionic pump and membrane failure results in energy metabolism failure and irreversible neuronal injury unless adequate perfusion is restored. The concept of the ischaemic penumbra arose from the above studies and describes the zone of tissue surrounding the central core that is perfused at a level between the upper threshold of electrical failure and the lower threshold of energy failure and ionic pump failure (Astrup *et al.*, 1981). Cells in this zone are therefore considered to be functionally impaired but structurally

intact. The existence of a spectrum of cerebral hypoperfusion and the ischaemic penumbra has also been demonstrated in rodent models of MCA occlusion using autoradiographic techniques (Memezawa *et al.*, 1992; Belayev *et al.*, 1997; Hata *et al.*, 1998; Ginsberg, 2003) and in human stroke patients by the use of PET and CT scanning (Hakim *et al.*, 1989; Kaufmann *et al.*, 1999; Heiss *et al.*, 2001).

1.1.1.3 Neuropathology

Pathologically, focal ischaemia is characterised by damage to a discrete brain region, for example, the territory of the MCA in the event this artery is occluded (**Figure 1**). The extent of ischaemic pathology following a focal ischaemic insult is strongly dependent on both the severity and duration of hypoperfusion (**Figure 2**). Studies assessing both CBF deficits and the topography and severity of histopathology after MCA occlusion in primates, cats and rats have demonstrated correlations between the level of hypoperfusion and the degree of ischaemic pathology suggesting that ischaemic thresholds for infarction (necrosis of all tissue elements) also exist (Morawetz *et al.*, 1979; Tamura *et al.*, 1980; Jones *et al.*, 1981; Heiss, 1983; Tyson *et al.*, 1984; Nagasawa *et al.*, 1989). Systematic experiments using MCA occlusion in rats have shown that the infarcted core corresponds to tissue with CBF less than 20% of normal levels, whereas, in the surrounding penumbra as CBF rises the risk of infarction declines (Memezawa *et al.*, 1992; Belayev *et al.*, 1997; Zhao *et al.*, 1997) A similar relationship between CBF deficits and the risk of infarction has also been shown in human stroke patients (Kaufmann *et al.*, 1999; Heiss *et al.*, 2001). The nature and development of ischaemic damage is also strongly dependent on the duration of the ischaemic insult (Jones *et al.*, 1981; Kaplan *et al.*, 1991) such that short periods of severe ischaemia or longer durations of milder hypoperfusion are both capable of inducing irreversible damage or infarction (**Figure 2**). Pathologically, permanent occlusion or extensive durations of transient occlusion (6 – 8h) of the MCA are associated with necrosis of all tissue elements (neurons, glia, vascular cells), or infarction, in the ischaemic core. The core is frequently surrounded by a thin zone of tissue displaying scattered neuronal damage reflecting the penumbral zone of intermediate ischaemia (Nedergaard, 1988). In contrast, focal ischaemia of short duration and/or moderate severity may produce only areas of selective neuronal necrosis (incomplete infarction) or a combination of infarcted areas and areas of selective neuronal injury (DeGirolami *et al.*, 1984; Nedergaard, 1987).

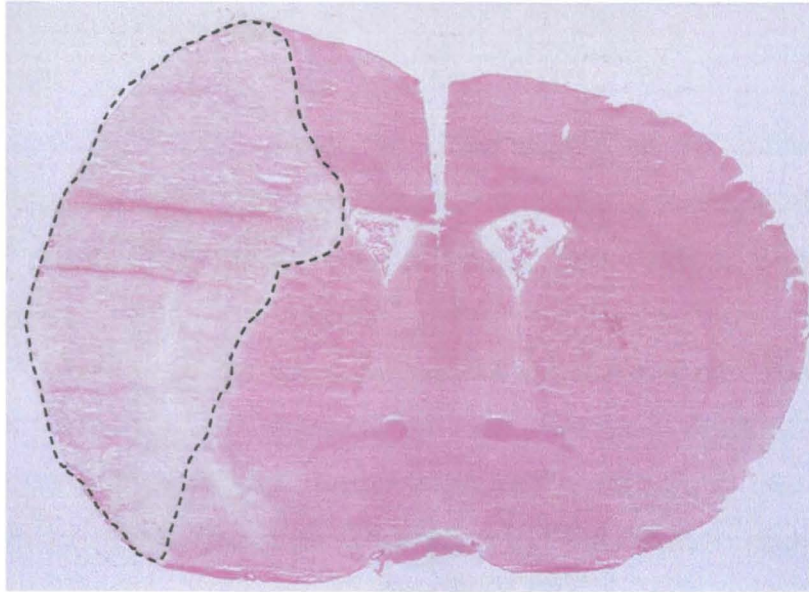


Figure 1. Focal ischaemic brain damage

Focal cerebral ischaemia typically produces damage in a discrete brain region. In this photomicrograph, the area of pallor (circumscribed area) represents the area of ischaemic damage which is confined to MCA territory. Photomicrograph shows a fresh-frozen haematoxylin and eosin stained section from a rat brain 24h after electrocoagulation of the MCA. Figure courtesy of Prof James McCulloch.

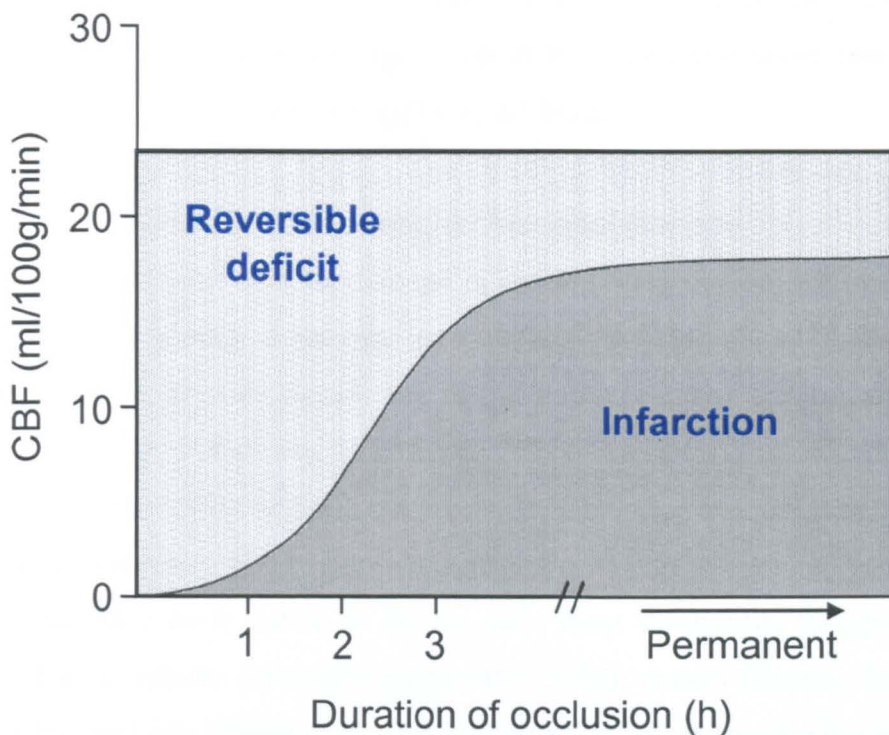


Figure 2. Influence of duration and severity of focal ischaemia on extent of damage

Development of irreversible brain damage (infarction) is acutely related to the severity of reduction in cerebral blood flow and the duration of the hypoperfusion. Adapted from Jones *et al.* (1981), data are from MCA occlusion in non-human primates.

1.1.2 Global cerebral ischaemia

1.1.2.1 Aetiology

Global cerebral ischaemia occurs when the blood supply to the entire brain is interrupted or severely reduced. In humans, the clinical syndrome resulting from global ischaemia is termed hypoxic-ischaemic encephalopathy. This condition is most often the result of cardiac arrest and resultant failure of the systemic circulation. Approximately 10 – 20% of cardiac arrest patients show a recovery after resuscitation, however, coma or persistence in a vegetative state and subsequent death within a few weeks are the most likely outcomes (Roine *et al.*, 1993; Bassetti *et al.*, 1996). In survivors of cardiac arrest, the neurological sequelae of global cerebral ischaemia are a major cause of morbidity with neuropsychological deficits prominent (Roine *et al.*, 1993; Rempel-Clower *et al.*, 1996). Other causes of global ischaemia include raised intracranial pressure as occurs following head trauma, severe arterial hypotension, carbon monoxide poisoning and heat stroke (cerebral hyperthermia).

Global ischaemia, like focal, can be either transient or permanent. Transient global ischaemia has assumed greater clinical relevance since permanent global ischaemia is generally synonymous with death. Transient global ischaemia is associated with a characteristic pattern of ischemic damage in which selective and delayed neuronal death is observed in selectively vulnerable regions of the brain.

1.1.2.2 Selective vulnerability and delayed neuronal damage

Development of selective neuronal damage in specific neuroanatomical locations is a feature of transient global ischaemia in both humans and animal models. These selectively vulnerable regions include the hippocampus, cerebral cortex, striatum and thalamus (*for review see Auer and Sutherland, 2002*). Hierarchies of vulnerability also exist within these susceptible regions, the precise pattern being dependent on the species and severity of ischaemia. For example, in the hippocampus, the pyramidal neurons of the CA1 sector have been shown to be the cells most susceptible to a mild global ischaemic insult in humans (Auer and Sutherland, 2002), gerbils (Kirino, 1982; Kirino and Sano, 1984) and rats (Smith *et al.*, 1984) (**Figure 3**). When the duration/severity of ischaemia is increased neuronal damage is also evident in the CA3 and CA4 sectors and even in the normally resistant dentate gyrus (Smith *et al.*, 1984; Auer and Sutherland, 2002). In contrast, in the mouse, neurons of the hippocampal CA2 sector and the caudate nucleus are most vulnerable to global ischaemia (Horsburgh *et al.*, 1999b; Kelly

et al., 2001b). The mechanisms underlying selective vulnerability are incompletely understood. One possible explanation in the hippocampus is that the vulnerable CA1 pyramidal neurons have a relatively greater abundance of NMDA receptors than adjacent sectors suggesting that these neurons may be more susceptible to glutamate-mediated excitotoxicity (Greenamyre *et al.*, 1985; Monaghan and Cotman, 1985).

Delayed neuronal death was described following observations in the hippocampus of rodents subjected to brief periods of global ischaemia (Ito *et al.*, 1975; Kirino, 1982; Pulsinelli *et al.*, 1982; Kirino and Sano, 1984; Smith *et al.*, 1984). The principal observation was that hippocampal neurons displaying characteristic ischaemic morphology were largely absent a few hours after the ischaemic insult but substantially increased after 2 - 3 days (Kirino, 1982; Pulsinelli *et al.*, 1982) (**Figure 3**). Delayed neuronal death is therefore thought to reflect neuronal degeneration that slowly matures hours to days after transient global ischaemia. Evidence of delayed neuronal damage in the hippocampus after global ischaemia (due to cardiac arrest) has also been observed in humans (Petito *et al.*, 1987; Horn and Schlote, 1992).

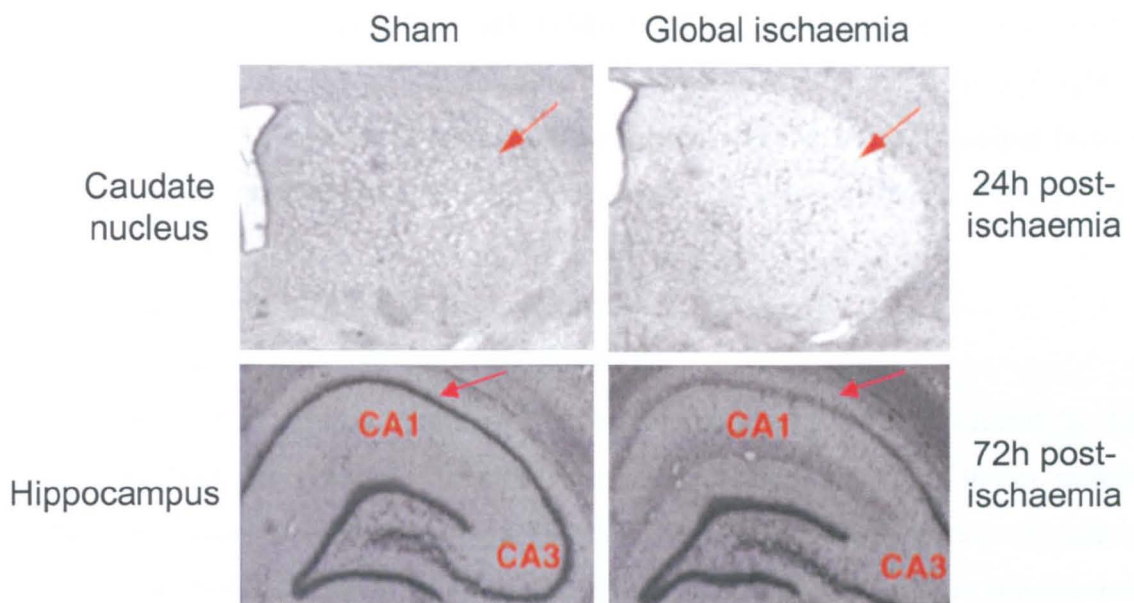


Figure 3. Selective and delayed neuronal damage after global ischaemia

The caudate nucleus and hippocampal CA1 sector (arrows) are particularly vulnerable to neuronal damage after global ischaemia. Delayed neuronal damage (e.g. 72h post-ischaemia) is a feature of global ischaemia, particularly in the hippocampus. Images, courtesy of Dr Karen Horsburgh, show tissue from rats after transient global ischaemia.

1.1.3 Involvement of cerebral ischaemia in traumatic brain injury

Cerebral ischaemia is also a major sequel of head trauma and resultant traumatic brain injury (TBI). TBI is the leading cause of mortality in those aged less than 45 years and also causes severe morbidity (Baethmann *et al.*, 1998). The prevalence of ischaemic brain damage after non-missile head injury was first recognised in the 1970s. In a comprehensive study involving 151 fatal head injuries, neuropathological evidence of ischaemic brain damage was observed in 138 (91%) individuals (Graham *et al.*, 1978). The basal ganglia and hippocampus were the most affected areas. In a follow-up study a decade later, a similar prevalence (88%) of ischaemic damage was reported despite improvements in management of head-injured patients (Graham *et al.*, 1989). Studies assessing CBF after head injury have demonstrated that cerebral hypoperfusion is a feature of the acute (hours) phase after injury (Bouma *et al.*, 1992; Sahuquillo *et al.*, 1993; Schroder *et al.*, 1995; Brown *et al.*, 1998). CBF deficits may be focal or global in nature and levels below the threshold for infarction have been reported in the 4 – 6 hours after injury (Bouma *et al.*, 1992; Saluquillo *et al.*, 1993; Schroder *et al.*, 1996). Furthermore, correlations between the degree of CBF deficit and Glasgow Coma Score during the first 24 hours have been shown (Marion *et al.*, 1991; Robertson *et al.*, 1992; Kelly *et al.*, 1997). The clinical importance of cerebral ischaemia in TBI is highlighted by the indication that hypoxic/ischaemic brain damage is one of the principal factors governing outcome and the degree of morbidity after head injury (Graham *et al.*, 2002).

1.1.4 Animal models of cerebral ischaemia

1.1.4.1 Importance and utility of animal models

The development of animal models of cerebral ischaemia has been central to the elucidation of key features of cerebral ischaemia such as the concepts of the ischaemic penumbra and delayed neuronal damage described above. The utility of animal models of cerebral ischaemia (and models of other nervous system pathologies) is underscored by a number of factors. The capacity to directly investigate pathophysiological features underlying diseases of and injuries to the nervous system in humans is limited, most notably due to important ethical considerations. In addition, human disease is often sporadic, random and variable, factors that do not facilitate dissection of molecular and biochemical mechanisms of disease. Consequently, a number of animal models of brain injury and disease have been developed that offer greater reproducibility and control of confounding variables and therefore enable more systematic investigation of

pathophysiology and therapeutic strategies. With regard to cerebral ischaemia there are a number of specific advantages of animal models. These include the absence of co-morbidity such as diabetes or hypotension and precise control over the location, duration and severity of the ischaemic insult, factors which may hamper interpretation of results in the clinical setting. Furthermore, in view of the development and increasing availability of genetically modified mice, the use of models of cerebral ischaemia in this species enables evaluation of the influence that single genes and their gene products may have in cerebral ischaemia. This powerful approach was exploited in this thesis to investigate the influence of polymorphism in the apolipoprotein E gene in cerebral ischaemia (*chapter 5*).

Initial models of cerebral ischaemia were developed in large animal species (primates, cats, rabbits), the major advantage of which is their homology with humans, particularly with regard to the primate brain. However, due to considerable ethical concerns over use of sub-human primates in experimental research and their high costs, their use has declined and the majority of studies are now performed in rodents. Rodents are particularly suitable for study for a number of reasons including: (1) similarities between the anatomy of the intracranial circulation of rodents and man, (2) availability of detailed information on gross rodent brain anatomy and organisation of neurotransmitter systems, (3) relatively low maintenance and procedural costs on account of their small size. With specific regard to the mouse, the development of genetically modified strains is the major factor underlying their increasing use in cerebral ischaemia research (and other fields). Rodent models of both focal and global cerebral ischaemia have been successfully developed to simulate the corresponding clinical conditions of stroke and cardiac arrest. Throughout this thesis, a mouse model of focal cerebral ischaemia was used and therefore this section will focus on the development of the model and its important features.

1.1.4.2 Rodent models of focal cerebral ischaemia

MCA occlusion in the rat was first described in 1975 (Robinson *et al.*, 1975) using a trans-cranial approach to ligate the distal portion of the MCA and which produced a cortical lesion. Subsequent modifications of this technique enabled a striatal component to be incorporated into the ischaemic lesion (Albanese *et al.*, 1980; Tamura *et al.*, 1981). The Tamura model has been central to the understanding and evaluation of various therapeutic agents such as glutamate receptor (NMDA) antagonists (Park *et al.*,

1988c; Bielenberg and Beck, 1991). With regard to human stroke, however, a major limitation of these models was the inability to induce recirculation through the occluded vessel, an event that occurs spontaneously in the majority of human strokes and, via thrombolytic agents, is a major clinical strategy for treating stroke patients (Ringelstein *et al.*, 1992). These factors instigated the development of models that permit a transient period of ischaemia followed by a period of reperfusion. The most extensively used model incorporating reperfusion is the intraluminal filament occlusion model.

1.1.4.3 Intraluminal filament occlusion model

The intraluminal filament occlusion model of focal cerebral ischaemia was used throughout this thesis. Intraluminal occlusion involves the introduction of a filament of pre-determined diameter into the external or common carotid artery that is then advanced along the internal carotid artery until the filament tip is located in the proximal portion of the anterior cerebral artery and therefore blocking the origin of the MCA (*section 2.3.2*). Restoration of blood flow through the MCA is achieved by withdrawal of the filament and closure of the arteriotomy. Additional advantages of this model in comparison to the Tamura model include the avoidance of craniectomy and thermal and mechanical brain damage caused by electrocoagulation. Intraluminal filament occlusion was initially developed in rats using a silicon-treated (Koizumi *et al.*, 1986) or heat-blunted (Longa *et al.*, 1989) filament tip to occlude the origin of the MCA. In common with other models of brain injury, adaptation of the intraluminal filament model for use in mice was prompted by the development and rapidly increasing availability of genetically modified mice.

1.1.4.4 Mouse strain differences in susceptibility to cerebral ischaemia

The increasing use of different mouse strains has highlighted the effect of inter-strain differences in the sensitivity to cerebral ischaemia and is particularly relevant to intraluminal occlusion. Understanding the inherent features of the background strain of genetically modified mice is therefore an important element in ischaemia research. The C57Bl/6J mouse is the most common background strain used to generate genetically modified mice. In this thesis, the transgenic mice expressing human *APOE* were developed on a C57Bl/6J background. Studies have demonstrated an increased vulnerability of the C57Bl/6J strain to focal and global ischaemia in comparison to other strains such as DBA/2, MF1 and 129/Sv (Barone *et al.*, 1993; Connolly *et al.*, 1996;

Fujii *et al.*, 1997; Yang *et al.*, 1997a; Kitagawa *et al.*, 1998c; Kelly *et al.*, 2001b; Majid *et al.*, 2001). The relative vulnerability of the C57Bl/6J mouse has been ascribed to the absence of one or both posterior communicating arteries (PcomAs) (Fujii *et al.*, 1997; Yang *et al.*, 1997a; Kitagawa *et al.*, 1998c; Kelly *et al.*, 2001b). These arteries connect the anterior and posterior portions of the circle of Willis with blood flow derived from the internal carotid and vertebral arteries respectively. The PcomA is important for perfusion of structures outside MCA territory (such as the hippocampus) during intraluminal filament occlusion.

The topography and distribution of ischaemic damage following intraluminal occlusion in the mouse differs from that observed in rats and may be related to PcomA hypoplasticity. In the mouse, the ischaemic lesion lies more posteriorly in the hemisphere such that ischaemic damage has been consistently observed in the thalamus and hippocampus, structures not commonly affected in the rat (Belayev *et al.*, 1999). Variability in the extent of ischaemic damage has been widely reported following transient intraluminal occlusion in both mice and rats (Connolly *et al.*, 1996; Clark *et al.*, 1997; Takano *et al.*, 1997) as has a relatively high mortality rate in comparison to permanent models of MCA occlusion (Koizumi *et al.*, 1986; Longa *et al.*, 1989; Connolly *et al.*, 1996; Kitagawa *et al.*, 1998c). In this thesis, comprehensive characterisation of the intraluminal filament model was performed in the mouse in order to assess the variables described above and enable optimisation of the technique.

1.1.5 Pathophysiology of ischaemic cell death

1.1.5.1 Necrosis and apoptosis

Cell death following ischaemic brain damage may involve both necrotic and apoptotic mechanisms with the predominating mode likely dependent on intrinsic (e.g. cell type) and extrinsic (e.g. nature and severity of insult) factors (Martin *et al.*, 1998; Snider *et al.*, 1999; Leker and Shohami, 2002).

Necrotic cell death occurs only after an exogenous insult and is thought to represent the most prevalent form of ischaemic cell death (Lipton, 1999). Briefly, necrosis is characterised by pronounced darkening and shrinkage of the nucleus and cytoplasm with the cell often assuming a triangular shape (Brown and Brierley, 1972). Cytoplasmic changes include markedly swollen mitochondria, disruption of the Golgi and endoplasmic reticulum organisation and disappearance of polyribosomes (Brown and Brierley, 1972). The cytoplasm is strongly acidophilic, a defining feature of this

form of cell death, which can be identified under the light microscope with use of acidic dyes such as eosin. Morphological evidence of necrotic cell death has been widely described after focal ischaemia where it is thought to be the predominant form of cell death (DeGirolami *et al.*, 1984; Lipton, 1999; Snider *et al.*, 1999) and has also been observed after global ischaemia in rodents (Kirino and Sano, 1984; Kirino *et al.*, 1984; Petit and Pulsinelli, 1984).

Apoptosis can occur under normal physiological conditions, in particular during development (Kerr *et al.*, 1972; Johnson and Deckwerth, 1993), or be activated by various types of insult, including cerebral ischaemia (Snider *et al.*, 1999). In contrast to necrosis, apoptosis is primarily a nuclear event. Characteristic morphological features include the formation of regularly-shaped masses of chromatin within the nucleus and the formation of apoptotic bodies in the cytoplasm (Arends and Wyllie, 1991). Unlike necrosis, cytoplasmic organelles appear relatively normal and the cytoplasm does not become acidophilic (Arends and Wyllie, 1991; Martin *et al.*, 1998). A strong indicator of apoptosis is the breakdown of DNA into nucleosomal fragments (DNA laddering) 180 – 200 base pairs in length (Arends *et al.*, 1990; Orrenius, 1995) that can be identified using the terminal deoxynucleosidyl transferase (TdT)-mediated biotinylated deoxyuridine triphosphate (dUTP) nick end labelling (TUNEL) technique (Gavrieli *et al.*, 1992). This pattern of DNA fragmentation is not an explicit marker of apoptosis, however, since it may occur during necrosis and therefore ultrastructural confirmation is required. There is strong morphological (formation of spherical chromatin masses and apoptotic bodies) and biochemical (DNA fragmentation, caspase activation, cytochrome *c* release from mitochondria) evidence that apoptosis can occur after focal ischaemia, particularly in regions where the insult is less severe (e.g. penumbra) (Li *et al.*, 1995a; Li *et al.*, 1995b; Linnik *et al.*, 1995; Charriaut-Marlangue *et al.*, 1996; Du *et al.*, 1996). It has been proposed that the delayed neuronal damage observed after global ischaemia may reflect apoptosis (Nitatori *et al.*, 1995). Although there is biochemical evidence to support this, morphological evidence of apoptosis after global ischaemia is weak (*for review see Lipton, 1999*).

The initiating event in cerebral ischaemia that ultimately leads to ischaemic cell death is energy failure, which in turn activates a number of pathogenetic mechanisms that culminate in cell death (necrotic and/or apoptotic) (**Figure 4**). These include excitotoxicity, oxidative stress, inflammation and induction of pro-apoptotic factors that mediate damage through their impact on important subcellular components.

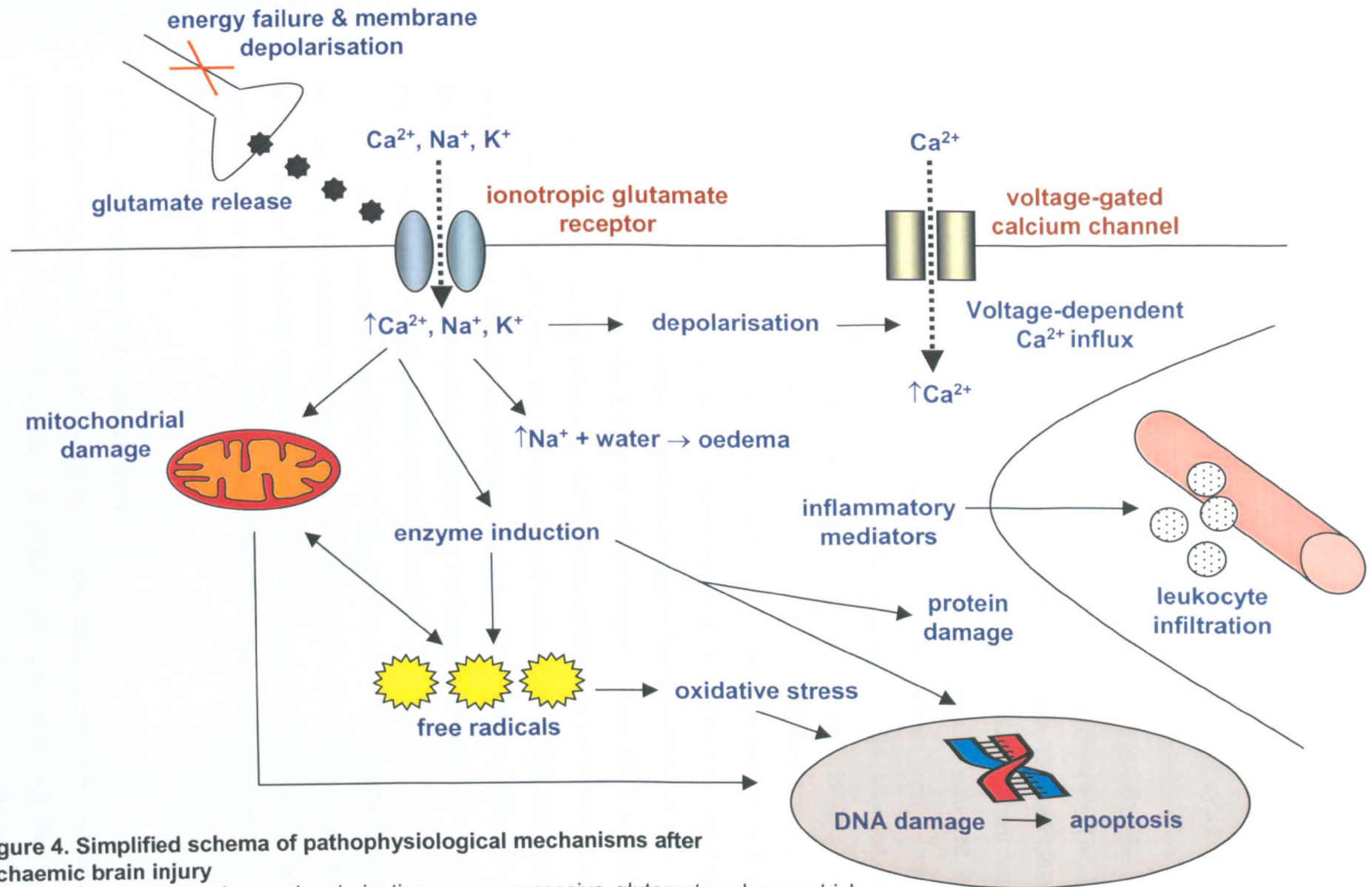


Figure 4. Simplified schema of pathophysiological mechanisms after ischaemic brain injury

Energy failure and membrane depolarisation cause excessive glutamate release which triggers a number of pathological processes including excitotoxicity, oedema, free radical formation and oxidative stress, mitochondrial damage, apoptosis and inflammation.

1.1.5.2 Glutamate and excitotoxicity

Glutamate is generally accepted as being the major excitatory neurotransmitter in the brain (Monaghan *et al.*, 1989) and is integral to normal neuronal function. However, the neurotoxic potential of glutamate is well established and is thought to play a key role in the pathophysiology of ischaemic cell death (Olney, 1978). Microdialysis has shown that normal levels of extracellular glutamate in the brain are 1 – 5 μ M (Butcher *et al.*, 1990; Wahl *et al.*, 1994) but are substantially increased after focal (Butcher *et al.*, 1990; Wahl *et al.*, 1994) and global (Benveniste *et al.*, 1984) ischaemia. Elevated glutamate arises from energy depletion, loss of ionic homeostasis and resultant cellular depolarisation. Presynaptic voltage-dependent calcium channels are activated that in turn trigger glutamate release into the extracellular space. Other energy-dependent processes, notably neurotransmitter reuptake mechanisms are also impeded, which further elevates extracellular glutamate levels (Dirnagl *et al.*, 1999). Elevated extracellular glutamate over-activates the ionotropic NMDA and AMPA receptors and leads to an excessive influx of Ca²⁺, Na⁺ and K⁺. A key event in excitotoxicity is the excessive influx of Ca²⁺ and ensuing calcium overload. Acting as a universal second messenger, an array of downstream processes is triggered by an increase in intracellular Ca²⁺ that can have detrimental effects on cellular integrity (Choi, 1988; Kristian and Siesjo, 1998; Arundine and Tymianski, 2003). These include direct activation of various enzymes such as proteases, phospholipases, and endonucleases that may result in structural damage to key cellular components (Leker and Shohami, 2002; Lo *et al.*, 2003). Other important processes triggered by an increase in intracellular Ca²⁺ are oxidative stress and apoptotic pathways (*see section 1.1.5.4*).

The most compelling evidence to support the role of glutamate-mediated excitotoxicity in ischaemic brain damage has arisen from numerous studies showing that ionotropic glutamate receptor antagonists are neuroprotective in experimental models of cerebral ischaemia (Simon *et al.*, 1984; Park *et al.*, 1988b; Park *et al.*, 1988c; McCulloch, 1992).

1.1.5.3 Free radicals and oxidative stress

Oxidative stress results when the generation of free radical species and their products exceeds intrinsic antioxidant capacity. Important free radicals include the reactive oxygen species (superoxide radical, hydroxyl radical, hydrogen peroxide), nitric oxide

and peroxynitrite. After brain injury, abnormally high production of free radicals overwhelms endogenous scavenging mechanisms (Lo *et al.*, 2003). A multiplicity of mechanisms is involved in the genesis of these reactive oxygen and nitrogen species (Lipton, 1999; Lewen *et al.*, 2000; Tyurin *et al.*, 2000; Chan, 2001). Of particular importance is the elevation of intracellular Ca^{2+} resulting from glutamate receptor activation. Irrespective of their source, however, the toxicity of free radicals results from their modification of macromolecules, namely lipids, carbohydrates, proteins and nucleic acids that critically alter cellular function. The importance of oxidative stress following cerebral ischaemia has been highlighted by studies in genetically modified mice either over-expressing or deficient in antioxidant enzymes (Chan *et al.*, 1995; Chan, 2001). Reduction of ischaemic damage after focal ischaemia has been demonstrated in mice over-expressing the copper, zinc superoxide dismutase (CuZn-SOD) gene (Kinouchi *et al.*, 1991; Noshita *et al.*, 2002; Saito *et al.*, 2003). An extensive number of studies have also shown that administration of agents with antioxidant properties (e.g. vitamin E, SOD enzymes, ebselen, tirilazad) confers neuroprotection in rodent models of cerebral ischaemia.

1.1.5.4 Induction of apoptotic pathways

Glutamate receptor over-activation and calcium overload are key events following brain injury that can induce a number of pro-apoptotic pathways (Zipfel *et al.*, 2000) including caspase activation and induction of pro-apoptotic members of the bcl family. Excessive production of free radicals is also an important mechanism leading to caspase activation via cytochrome c release from mitochondria (Skulachev, 1998; Sugawara *et al.*, 2002). Pharmacological and genetic manipulation of molecules involved in apoptotic pathways has provided evidence for the importance of apoptotic cell death after ischaemic injury. Administration of small peptide inhibitors of caspases reduces the amount of tissue damage, TUNEL-positive staining and attenuates neurological deficit after experimental focal ischaemia (Hara *et al.*, 1997; Mouw *et al.*, 2002). Furthermore, transgenic and viral vector mediated overexpression of survival promoting members of the bcl-2 family, such as bcl-2 and bcl-X_L, have neuroprotective effects in models of cerebral ischaemia (Martinou *et al.*, 1994; Kitagawa *et al.*, 1998b; Kilic *et al.*, 2002; Zhao *et al.*, 2003).

1.1.5.5 Inflammation

Experimentally and clinically, an acute and prolonged inflammatory response follows cerebral ischaemia (Zhang and Stanimirovic, 2002; Allan and Rothwell, 2003). Production and activation of inflammatory mediators such as complement, adhesion molecules and cytokines - notably interleukin-1 and tumour necrosis factor- α - are substantially increased in injured cells as early as 1 hour after an ischaemic insult (Rothwell and Hopkins, 1995; Feuerstein *et al.*, 1997; Feuerstein *et al.*, 1998). These mediators promote inflammatory responses by stimulating expression of adhesion molecules that facilitate the migration of inflammatory cells such as neutrophils, macrophages and monocytes into the injured brain (del Zoppo *et al.*, 2000). Resident brain microglia also contribute to the acute inflammatory response becoming activated within 4 – 6 hours after injury and producing a well developed microglial response by 24 hours (Dirnagl *et al.*, 1999). Administration and viral vector-mediated overexpression of the interleukin-1 receptor antagonist has been shown to reduce ischaemic brain damage (Betz *et al.*, 1995; Loddick and Rothwell, 1996; Yang *et al.*, 1997b; Yang *et al.*, 1999; Tsai *et al.*, 2003).

1.1.5.6 Endogenous protective mechanisms

In addition to the above mediators of ischaemic damage, cerebral ischaemia also induces synthesis and activation of a variety of molecules that are potentially protective. Among these, evidence of protective effects is strongest for heat shock proteins and neurotrophic factors (Lipton, 1999; Leker and Shohami, 2002).

Expression of the heat shock proteins HSP70 and HSP72 is induced after global ischaemia in rodents (Nowak, 1985; Dienel *et al.*, 1986; Nowak, 1991; Simon *et al.*, 1991; Kawagoe *et al.*, 1992; Liu *et al.*, 1993; Nishino and Nowak, 2004). Studies examining HSP immunoreactivity have shown that increased HSP70 immunoreactivity is most prominent in less vulnerable regions (dentate gyrus, CA3) but minimal in the vulnerable CA1 sector of the hippocampus (Vass *et al.*, 1988; Kawagoe *et al.*, 1992). After focal ischaemia, neurons in the core rarely display HSP70 immunoreactivity, whereas in the penumbra there is marked induction of HSP70 mRNA and neuronal HSP70 immunoreactivity suggesting that HSP70 may confer resistance to damage (Kinouchi *et al.*, 1993; Li *et al.*, 1993). Over-expression of HSP by viral vectors or genetic manipulation confers neuroprotection in models of focal and global ischaemia

(Rajdev *et al.*, 2000; Kelly *et al.*, 2001a; Tsuchiya *et al.*, 2003b) while HSP knockouts display greater ischaemic damage (Lee *et al.*, 2001).

Neurotrophic factors (NTFs) are vital for the survival and differentiation of normally developing neurons but are also thought to be integral to neuroprotective pathways under pathological conditions (Abe, 2000). Induction of several types of NTFs occurs in response to cerebral ischaemia, including nerve growth factor (NGF), brain derived neurotrophic factor (BDNF) and glial cell line derived neurotrophic factor (GDNF) (Abe, 2000; Leker and Shohami, 2002). Topical administration and viral vector-mediated overexpression of various NTFs have shown consistent effects in reducing the extent of damage after focal ischaemia (Abe *et al.*, 1997a; Hayashi *et al.*, 1998; Kitagawa *et al.*, 1998a; Kitagawa *et al.*, 1999; Zhang *et al.*, 1999; Wang *et al.*, 2000; Yagi *et al.*, 2000; Hermann *et al.*, 2001b; Zhang *et al.*, 2001; Zhang *et al.*, 2002).

Apolipoprotein E is another molecule upregulated after acute brain injury that may contribute to endogenous protective mechanisms in the brain (*for reviews see Laskowitz et al., 1998; Horsburgh et al., 2000a*). Furthermore, polymorphism in the apolipoprotein gene may be associated with disparities in the outcome/response to brain injury. Major components of this thesis were to further investigate this genetic influence and the neuroprotective potential of apolipoprotein E in cerebral ischaemia and as such the following sections focus on this molecule.

1.2 Apolipoprotein E (ApoE)

1.2.1 Plasma apolipoproteins

Apolipoprotein E (apoE denotes protein, *APOE* denotes gene) is one of numerous classes and sub-classes of apolipoproteins. Apolipoproteins comprise a group of molecules primarily synthesised in the liver that are intimately involved in directing plasma lipoprotein metabolism and maintaining cholesterol homeostasis. They are components of lipoprotein particles which transport and deliver lipids and cholesterol from one tissue or location to another (Borghini *et al.*, 1995). Lipoprotein particles consist of a triglyceride and cholesteryl-ester core surrounded by a phospholipid and free cholesterol shell (Figure 5). Plasma lipoproteins can be separated into four major classes on account of their size and density: chylomicrons, very low-density lipoprotein (VLDL), low-density lipoprotein (LDL) and high-density lipoprotein (HDL). Apolipoproteins reside on the surface of these molecules where they perform several important functions that include stabilising the particles, serving as co-factors in enzymatic reactions (Fielding *et al.*, 1972) and acting as ligands for lipoprotein receptors (Brown and Goldstein, 1986; Li *et al.*, 1988).

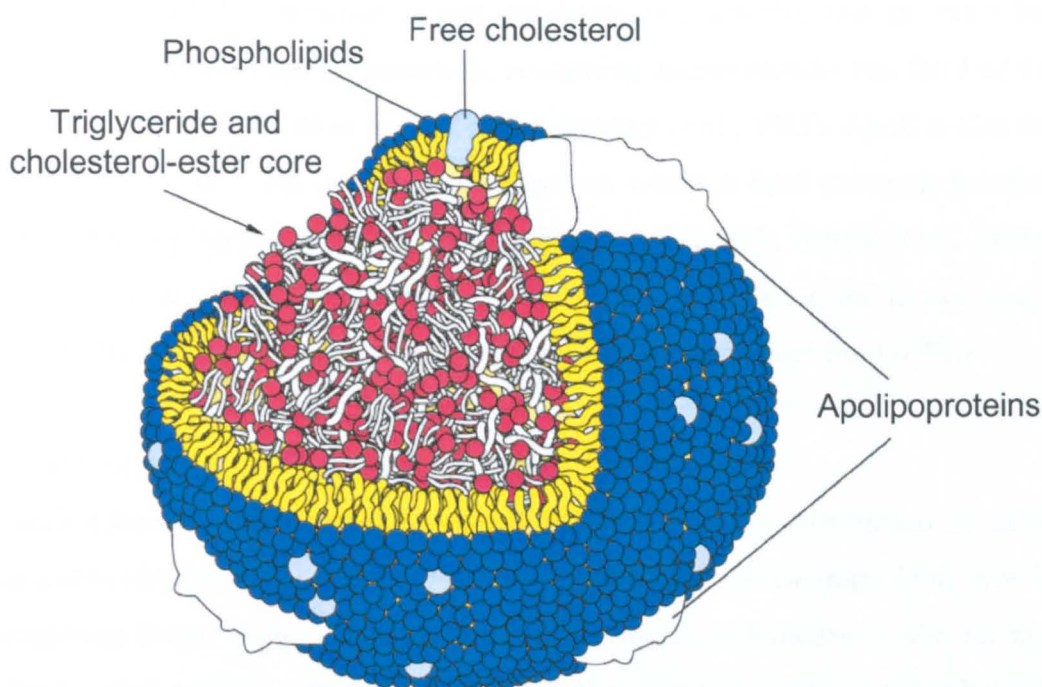


Figure 5. Structure of a lipoprotein particle

A cholesterol and phospholipid shell surrounds a triglyceride and cholesteryl-ester core. Apolipoproteins are located on the surface of the particle. Adapted from http://cwx.prehall.com/horton/medialib/media_portfolio/16.html.

1.2.2 ApoE in plasma

ApoE was discovered in 1973 as a protein constituent of triglyceride-rich plasma lipoproteins (Shore and Shore, 1973). In plasma, apoE is a component of several classes of lipoprotein particles including very low density lipoprotein (VLDL), chylomicron remnants and a subset of high density lipoprotein (HDL) (Mahley, 1988). ApoE associates with VLDL released from the liver and chylomicron remnants from the small intestine where it influences the hydrolysis of triglycerides and release of fatty acids from these particles for cellular uptake and energy metabolism (Mahley, 1988). As a constituent of VLDL apoE can direct triglycerides and cholesterol to extrahepatic sites whereas apoE associated with chylomicrons and their remnants delivers dietary triglycerides and cholesterol to the liver. In addition to promoting cellular uptake of cholesterol, apoE when associated with a subclass of HDL can support cholesterol efflux. This function of apoE is prominent in reverse cholesterol transport, a pathway that transports excess cellular cholesterol via apoE-containing HDL to the liver for excretion (Mahley and Innerarity, 1983; Huang *et al.*, 1994).

1.2.3 ApoE in the nervous system

Analysis of apoE mRNA expression in rats and marmosets revealed that the brain has the second highest level of apoE expression, containing approximately one third of the levels of apoE mRNA produced in the liver (Elshourbagy *et al.*, 1985). ApoE is also the most abundant apolipoprotein in the nervous system where a lipid transport function analogous to that in plasma has been proposed (Pitas *et al.*, 1987b; Poirier *et al.*, 1993a; Poirier, 1994; Poirier, 2000). Within the nervous system, apoE is located in two major environments, the brain parenchyma and the circulating cerebrospinal fluid (CSF).

1.2.3.1 Localisation of apoE in “normal” brain parenchyma

Several techniques have been used to investigate the regional distribution of apoE synthesis and to identify the specific cell types responsible for production of this protein in the uninjured brain. Using RNA dot blot hybridisation techniques in the rat and human brain, apoE mRNA was detected in several regions including the cerebellum, brain stem, medulla, pons and cerebral cortex (Elshourbagy *et al.*, 1985). A similarly extensive distribution of apoE transcripts was demonstrated in a comprehensive study utilising *in situ* hybridisation in the mouse brain; regions displaying apoE mRNA

included the choroid plexus and ependyma, cerebral cortex, thalamic nuclei, hypothalamus and hippocampus, particularly the molecular layer (Lorent *et al.*, 1995).

In general, it is thought that apoE is synthesised and secreted mostly by glial cells, particularly astrocytes (Boyles *et al.*, 1985; Pitas *et al.*, 1987a), although there is evidence of substantial inter-species variability in the cellular localisation of apoE. In the normal rodent brain, apoE is essentially restricted to glial cells. Intense apoE immunoreactivity has been shown in protoplasmic astrocytes of grey matter and fibrous astrocytes of white matter (Boyles *et al.*, 1985). Other non-neuronal cells, such as microglia, oligodendrocytes and ependymal cells also stain positively for apoE. In the normal primate and human brains, however, there is evidence of apoE localisation to both glial cells and neurons (Han *et al.*, 1994a; Han *et al.*, 1994b; Metzger *et al.*, 1996; Xu *et al.*, 1999). In the human brain, neuronal apoE immunoreactivity has been detected in pyramidal neurons of the cerebral cortex and hippocampus (Han *et al.*, 1994b; Bao *et al.*, 1996). Furthermore, regionally specific neuronal *APOE* mRNA transcription has been revealed using *in situ* hybridisation (Xu *et al.*, 1999). *APOE* mRNA-containing neurons were observed in the frontal cortex, CA1 to CA4 regions of the hippocampus and the granule cell layer of the dentate gyrus but not in the cerebellar cortical neurons (Xu *et al.*, 1999). In the same study, apoE immunohistochemical localisation paralleled the regional and cellular pattern of *APOE* mRNA transcription thus supporting a role for intraneuronal synthesis of apoE in the human brain.

1.2.3.2 ApoE-containing lipoprotein particles in cerebrospinal fluid

ApoE is also found in CSF associated with lipoprotein particles analogous to those circulating in plasma. CSF lipoprotein particles contain higher proportions of apolipoproteins than their counterparts in plasma and accordingly are of higher density and most closely resemble plasma HDL (Roheim *et al.*, 1979; Pitas *et al.*, 1987b). At least three major subpopulations of CSF lipoprotein particles have been identified (Pitas *et al.*, 1987b; Borghini *et al.*, 1995; Yamauchi *et al.*, 1999a; Koch *et al.*, 2001). One is enriched in apoA-I and also contains significant quantities of apoE, apoD and apoJ, another is enriched in apoE and the third is less well defined and more heterogeneous in its composition (containing apoA-IV, apoD, apoH, apoJ). The apoE-enriched particles are among the largest in CSF, with a diameter of approximately 15nm (Pitas *et al.*, 1987b). These particles are similar to plasma HDL particles with regard to their density

and rich cholesteryl-ester content (Guyton *et al.*, 1998). Significantly, the smaller particles containing apoA-I and apoA-IV are not thought to be synthesised within the CNS, but rather originate in plasma and are filtered across the blood-brain barrier (Elshourbagy *et al.*, 1985; Karathanasis *et al.*, 1986). In contrast, several lines of evidence suggest that apoE-containing lipoprotein particles are synthesised locally in the CNS and are most probably of astrocytic origin. Most convincing evidence that apoE is synthesised locally within the brain was revealed in patients undergoing liver transplantation where the plasma apoE phenotype changed to that of the donor whereas the apoE phenotype in CSF was unchanged (Linton *et al.*, 1991). In addition, the sialylation pattern and molecular weight of CSF-apoE is distinct from the corresponding plasma species. Furthermore, comparison of lipoprotein particles isolated from human CSF and from primary astrocyte cultures revealed that CSF lipoproteins contained several apolipoproteins, including apoE, apoA-I, apoA-II and apoJ, whereas astrocyte-secreted lipoproteins contained only apoE and apoJ (LaDu *et al.*, 1998).

1.2.4 Molecular biology of apoE

1.2.4.1 Genetic polymorphism

Human apoE is a 34kDa glycoprotein composed of 299 amino acids in its mature form. Three isoforms of apoE are recognised in humans – apoE2, E3 and E4. This polymorphism is the result of three alleles at a single gene locus on chromosome 19. The corresponding alleles, *APOE* ϵ 2, ϵ 3 and ϵ 4, give rise to the three protein isoforms (Zannis *et al.*, 1982). Although geographical and ethnic differences in relative allele frequencies have been identified (Gerdes *et al.*, 1996; Schiele *et al.*, 2000), in all populations studied to date, the *APOE* ϵ 3 allele occurs with greatest frequency (~78%); also, in most cases the ϵ 4 allele (~14%) is more common than the ϵ 2 allele (~7%) (Davignon *et al.*, 1988). Thus, *APOE* genetic polymorphism results in six possible genotypes, three homozygous (ϵ 2/2, ϵ 3/3 and ϵ 4/4) and three heterozygous (ϵ 2/3, ϵ 2/4 and ϵ 3/4). As a consequence of the variation in allelic frequency, the occurrence of the six *APOE* genotypes is approximately: ϵ 3/3 (55%), ϵ 3/4 (25%) and ϵ 2/3 (15%), with the remaining three genotypes (ϵ 2/2, ϵ 2/4, ϵ 4/4) occurring with a frequency of 1 – 2% each (Mahley and Rall, 2000). Significantly, up to one third of the population may therefore inherit at least one copy of the *APOE* ϵ 4 allele.

1.2.4.2 Structure of human apoE

The apoE2, E3 and E4 isoforms differ sequentially by one unit of charge, a feature that has been demonstrated following isoelectric focussing (Utermann *et al.*, 1977). ApoE4 is the most cationic isoform, differing from apoE3 by one charge unit and from apoE2 by two charge units. These charge differences are the result of single amino acid substitutions at two sites in the apoE polypeptide (**Figure 6**). ApoE2 has cysteine at residues 112 and 158, apoE3 has cysteine at residue 112 and arginine at residue 158 and apoE4 has arginine at both residues 112 and 158. These isoform-specific differences in primary structure have important effects on the tertiary structure and hence functional properties of each isoform.

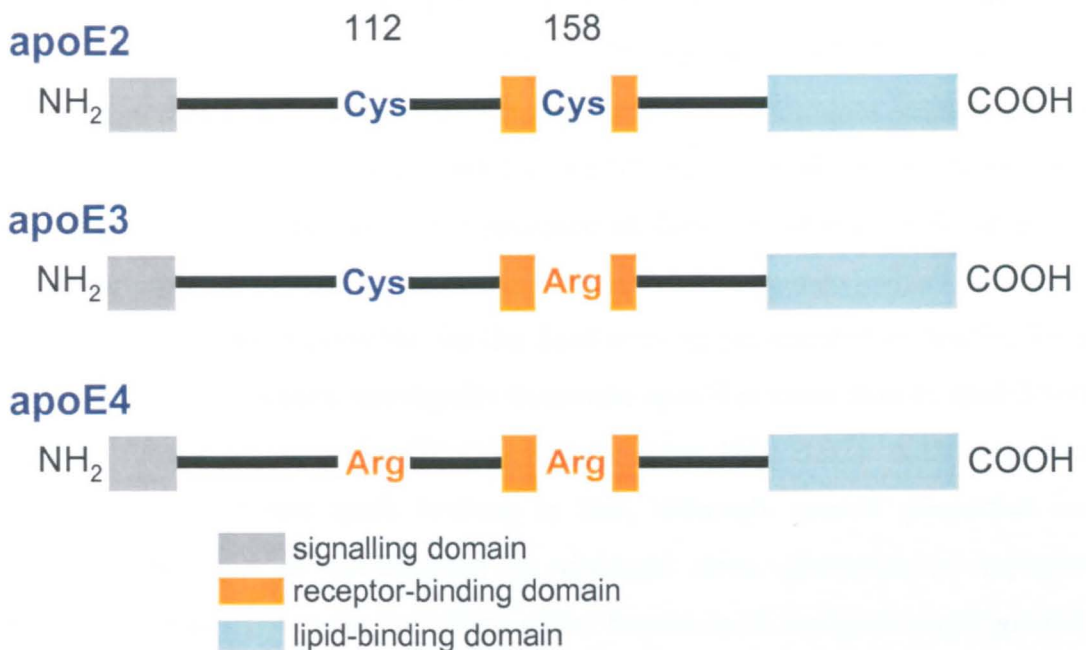


Figure 6. ApoE polymorphism

Polymorphism in apoE arises from amino acid substitutions at positions 112 and 158 of the protein.

ApoE contains two independently folded domains each with distinct physical and functional properties which are linked by a region of random structure (Aggerbeck *et al.*, 1988; Wetterau *et al.*, 1988; Weisgraber, 1994). The amino-terminal domain (residues 1-191) comprises five α -helices and contains the receptor-binding (residues 134-150) and heparin (proteoglycan)-binding regions (Weisgraber, 1994). ApoE isoform polymorphisms at residues 112 and 158 produce subtle but important variations in the tertiary structure of the amino-terminal domain which in turn generate isoform-

specific receptor binding activities (Zaiou *et al.*, 2000; Lund-Katz *et al.*, 2001). The lipid binding region of apoE (residues 244-272) is located within the carboxyl-terminal domain (residues 225-299) (Horie *et al.*, 1992). Polymorphisms at positions 112 and 158, although within the amino-terminal domain, also produce isoform-specific differences in lipid-binding properties which are thought to be mediated by alterations in inter-domain interactions among the three apoE isoforms (Raffai *et al.*, 2001).

1.2.4.3 Structure of mouse apoE

Mouse apoE, unlike in humans, does not display multiple isoforms. This feature is shared with other animals including all of the great apes, the closest living ancestors of humans (Hanlon and Rubinsztein, 1995). The mouse *APOE* gene encodes for arginine at the position corresponding to residue 112 in human apoE and therefore, mouse apoE is similar in primary structure to human apoE4 (Weisgraber, 1994). However, mouse apoE, in common with all other non-human apoE studied thus far, does not demonstrate the characteristic binding of human apoE4 to VLDL; mouse apoE preferentially binds to HDL. Underlying this feature is the presence of threonine at residue 61 in mouse apoE (in contrast to arginine at the corresponding position in humans) which diminishes the domain interactions responsible for the lipid-binding preferences of apoE4. Thus, mouse apoE, although related structurally to human apoE4 is more akin to apoE3 with regard to its functional properties (Strittmatter and Bova Hill, 2002). A key aspect of mice expressing only one apoE isoform is that, although general properties and functions of apoE can be investigated in wild-type mice, dissection of important differences that may exist in the behaviour of the human apoE isoforms is not possible. Accordingly, the development of transgenic mice expressing human *APOE* has been of huge importance to the investigation of isoform-specific differences in apoE that are pertinent to humans (*section 1.4.3*).

1.2.5 ApoE receptors

One of the most prominent functions of apoE is to serve as a ligand for receptors that mediate the cellular uptake of apoE and associated lipids. ApoE is a ligand for several structurally- and functionally-related cell surface receptors which are all members of the low-density lipoprotein (LDL) receptor family. In mammals, seven core members of this group have been identified each of which binds and internalises apoE-containing lipoproteins (Herz and Beffert, 2000). In the brain, the presence of three of these

receptors – LDL receptor, LDL receptor-related protein and the ApoER2 – has been most widely demonstrated.

1.2.5.1 Low density lipoprotein receptor

The LDL receptor was the first member of this group to be identified and elucidation of its role in lipid uptake was instrumental to understanding the mechanism of receptor-mediated endocytosis (Brown and Goldstein, 1986). During this process, cell surface receptors recognise specific ligands in the circulation or extracellular space, bind them, and mediate their internalisation via specialised regions of the plasma membrane called clathrin-coated pits (*see also section 1.6.1*). Humans and rabbits that are homozygous for spontaneous mutations that inactivate the LDL receptor display a grossly elevated plasma cholesterol level that leads to atherosclerosis and coronary artery disease early in life. These observations were explained by the inability to remove LDL from the circulation via receptor-mediated endocytosis in hepatocytes. Thus, the physiological role of the LDL receptor in the endocytosis of lipoproteins and lipid/cholesterol homeostasis provided a template that has been applied to other members of the LDL family of receptors subsequently discovered.

The LDL receptor is expressed in tissues throughout the body, including the brain. In the brain, most evidence suggests that the LDL receptor is primarily found in glial cells. Astrocytic localisation has been demonstrated in rats, marmosets and humans using immunohistochemistry (Pitas *et al.*, 1987b; Rebeck *et al.*, 1993). Further studies have also shown LDL receptor immunoreactivity in oligodendrocytes, microglia and brain capillary endothelial cells (Meresse *et al.*, 1989; Jordan *et al.*, 1991; Jung-Testas *et al.*, 1992; Dehouck *et al.*, 1994; Beffert *et al.*, 1998). Despite the presence of the LDL receptor in the brain, clinical and experimental evidence in humans and animals has thus far failed to uncover a critical role for this receptor in the nervous system (*for review see Herz and Bock, 2002*). For example, mice deficient for the LDL receptor do not appear to display neurological dysfunction (Ishibashi *et al.*, 1993) suggesting that other mechanisms or lipoprotein receptors can compensate in the absence of the LDL receptor. To date, no functions other than in lipoprotein metabolism have been shown for this receptor.

1.2.5.2 Low density lipoprotein receptor-related protein

The LDL receptor-related protein (LRP) was the second member of the LDL-receptor family to be identified (Herz *et al.*, 1988). Although located in tissues throughout the body, the LRP is most abundantly expressed in hepatocytes and neurons. *In vitro* studies have revealed that LRP binds apoE-containing lipoproteins and mediates their endocytosis in cultured cells (*for review see Krieger and Herz, 1994*). In the brain, LRP is highly expressed in neurons and is the principal receptor responsible for neuronal receptor-mediated endocytosis of apoE-containing lipoproteins. In the normal human brain, immunostaining was localised to neuronal cell bodies and proximal processes while other cell types were not positively stained (Wolf *et al.*, 1992; Rebeck *et al.*, 1993). Widespread expression of LRP mRNA throughout the brain (hippocampus, cerebral cortex, cerebellum and brainstem) has been demonstrated (Bu *et al.*, 1994, Lorent *et al.*, 1995). Immunohistochemical analysis has also detected substantial LRP immunoreactivity in pyramidal and granule neurons of the hippocampal formation (Bu *et al.*, 1994; Lorent *et al.*, 1995). In contrast to the LDL receptor, there is accumulating evidence that LRP is not only involved in lipoprotein metabolism but also acts as a multifunctional signalling receptor that can bind a diverse range of ligands and participate in neuronal signal transduction pathways (Willnow *et al.*, 1999; Herz and Strickland, 2001). The findings that conventional LRP-knockout mice die during gestation and display developmental abnormalities in the nervous system (Herz *et al.*, 1992) likely reflect the multifunctionality of this receptor.

1.2.5.3 ApoER2

The structure of ApoER2 is strikingly similar to the LDL receptor and can bind apoE-containing lipoproteins *in vitro* (*for review see Herz, 2001b*). Under normal conditions, ApoER2 expression is almost exclusively restricted to the brain and testes (Stockinger *et al.*, 1998; Stockinger *et al.*, 2000). In the brain, ApoER2 mRNA transcripts have been localised most strongly to the cerebellar cortex, choroid plexus, ependyma, hippocampus and olfactory bulb and to a lesser extent in the cerebral cortex (Kim *et al.*, 1996). In view of its homology to the LDL receptor and apoE-binding properties, a lipoprotein metabolism role was initially proposed for ApoER2. However, akin to LRP, there is increasing evidence that ApoER2 has important signalling functions, in particular as a key component of the Reelin signalling pathway that is involved in

neuronal migration during brain development (Hiesberger *et al.*, 1999; Trommsdorff *et al.*, 1999; Gotthardt *et al.*, 2000).

1.2.6 ApoE response to peripheral nerve injury – first indication of a role for apoE in nervous system pathology

The relative abundance of apoE and the presence of apoE receptors illustrate that the nervous system contains the major components of a lipid/cholesterol transport system. An important function for apoE in the injured nervous system was first indicated in the 1980s when a role for apoE was proposed in the redistribution of cholesterol among cells following peripheral nerve injury (Ignatius *et al.*, 1987a). First, synthesis of a 37kDa protein was found to be dramatically upregulated after rat peripheral nerve injury (Politis *et al.*, 1983; Skene and Shooter, 1983; Muller *et al.*, 1985; Muller *et al.*, 1986). This protein was subsequently identified as apoE (Ignatius *et al.*, 1986; Snipes *et al.*, 1986). After rat sciatic nerve crush injury, cells in the nerve sheath distal to the site of injury were shown to produce and secrete large quantities of apoE such that by 3 weeks post-injury apoE accumulated at the injury site where it accounted for approximately 2 – 5% of the total soluble extracellular protein in the regenerating sciatic nerve sheath (Ignatius *et al.*, 1986). Increasing levels of apoE after peripheral nerve injury were also shown to coincide with periods of axonal regeneration and peak levels were associated with the most active phase of axonal remyelination 3 weeks post-injury. Furthermore, axonal growth cones were enriched in LDL receptors during the period of axonal regeneration (Boyles *et al.*, 1989). From these experiments it was proposed that apoE synthesised in the lesion scavenges lipids/cholesterol from degenerating nerves and redistributes them to the growth cones of regenerating axons where the apoE complexes are internalised for new membrane synthesis and remyelination (Ignatius *et al.*, 1987b; Boyles *et al.*, 1989).

1.3 APOE polymorphism and human brain injury and disease

Interest in the neurobiology of apoE was further stimulated with the seminal discoveries in 1993 that possession of the *APOE* ϵ 4 allele was associated with late-onset familial and sporadic Alzheimer's disease (AD) (Corder *et al.*, 1993; Poirier *et al.*, 1993b; Rebeck *et al.*, 1993; Saunders *et al.*, 1993; Strittmatter *et al.*, 1993). Subsequently, the effects of *APOE* polymorphism have been investigated in a multitude of brain disorders, most notably traumatic brain injury and cerebral ischaemia.

1.3.1 *APOE* polymorphism and Alzheimer's disease

AD, originally described by Alois Alzheimer in 1907 (Alzheimer, 1907), is the most common age-related dementing illness, which at present is estimated to afflict 20 – 30 million individuals worldwide (Selkoe and Schenk, 2003). Clinically, AD is characterised by progressive deterioration of cognitive function that ultimately leads to a profound dementia around a decade after onset of clinical symptoms.

The *APOE* ϵ 4 allele was the second of four predisposing genetic factors for AD to be revealed. Mutations in the β -amyloid precursor protein (APP) gene and the presenilin-1 (PS1) and presenilin-2 (PS2) genes have also been shown to be associated with familial AD (Levy *et al.*, 1990; Goate *et al.*, 1991; Murrell *et al.*, 1991; Hendriks *et al.*, 1992; Mullan *et al.*, 1992; Levy-Lahad *et al.*, 1995; Rogaev *et al.*, Sherrington *et al.*, 1995). Following the linkage of late-onset familial AD to a region on chromosome 19 containing the *APOE* locus (Pericak-Vance *et al.*, 1991), inheritance of the *APOE* ϵ 4 allele was shown to be associated with both late-onset familial (Corder *et al.*, 1993; Strittmatter *et al.*, 1993) and sporadic AD (Poirier *et al.*, 1993; Rebeck *et al.*, 1993; Saunders *et al.*, 1993). The *APOE* ϵ 4 allele association with AD has now been corroborated in over 100 laboratories worldwide. Conversely, there is evidence to suggest that the *APOE* ϵ 2 allele may have a protective effect against AD (Corder *et al.*, 1994). The *APOE* ϵ 4 allele is not a causative gene but rather acts as a susceptibility factor. It is thought to be the most important genetic risk factor for development of AD with up to 50% of all cases of AD estimated to involve the ϵ 4 allele as the principal genetic factor (Roses, 1996; Selkoe and Schenk, 2003). Inheritance of the *APOE* ϵ 4 allele not only increases the risk for developing AD but also reduces the mean age of onset of the disease in a dose-dependent manner. Thus, individuals inheriting two copies of the ϵ 4 allele have an increased risk and earlier age of onset than individuals with one ϵ 4 allele (Saunders *et al.*, 1993). Likewise, individuals with one ϵ 4 allele have a greater risk and earlier onset of disease than those without an ϵ 4 allele (Corder *et al.*, 1993). Moreover, the mean age of onset for individuals with the ϵ 4/ ϵ 4 genotype is less than 70 years compared to over 90 years for individuals with the ϵ 2/ ϵ 3 genotype (Corder *et al.*, 1993). In contrast, the progression of dementia and duration of survival after clinical onset is not influenced by *APOE* genotype (Corder *et al.*, 1995; Gomez-Isla *et al.*, 1996). *APOE* genotype also appears to influence the age of onset of AD in early-onset families with APP mutations; individuals homozygous for *APOE* ϵ 4 with an

APP mutation experience an earlier onset of disease (St George-Hyslop *et al.*, 1994; Nacmias *et al.*, 1995). In contrast, a similar interaction of *APOE* genotype with age of onset is not generally evident in early-onset families with mutations in the PS1 gene (Van Broeckhoven, 1995; Lendon *et al.*, 1997; Houlden *et al.*, 1998). However, in a kindred in which AD is caused by a PS1 mutation, it has recently been shown that *APOE* ϵ 4 carriers were more likely to develop AD at an earlier age (Pastor *et al.*, 2003).

During the past five years, possible links between *APOE* promoter polymorphisms and the risk of AD have also been identified (Bullido *et al.*, 1998; Lambert *et al.*, 1998; Lambert *et al.*, 2002). Promoter polymorphisms may influence AD risk by modulating *APOE* transcriptional activity (Artiga *et al.*, 1998; Laws *et al.*, 2002; Laws *et al.*, 2003).

1.3.2 *APOE* polymorphism and traumatic brain injury

Among patients who experience a similar severity of head injury there is heterogeneity in the quality of recovery only partially explained by prognostic factors, such as age and treatment (Jennett *et al.*, 1979). This implies that additional factors, such as genetic make-up, may influence the response to TBI.

The association of *APOE* genotype with outcome after TBI has been investigated by a number of groups (Teasdale *et al.*, 1997; Friedman *et al.*, 1999; Lichtman *et al.*, 2000; Liberman *et al.*, 2002; Chiang *et al.*, 2003). In these studies, possession of the *APOE* ϵ 4 allele has been consistently associated with poorer outcome after TBI. In the first study to reveal this link, patients with at least one copy of the *APOE* ϵ 4 allele were more than twice as likely to have an unfavourable outcome (death, vegetative state or severe disability) 6 months after injury than their non- ϵ 4 counterparts (Teasdale *et al.*, 1997). An ϵ 4 allele dose effect was also indicated since all ϵ 4 homozygotes were severely disabled at 6 months post-injury compared to 30% of ϵ 4 heterozygotes and 17% of those without an ϵ 4 allele. An increased risk of post-traumatic seizures has also been reported in *APOE* ϵ 4 individuals (Diaz-Arrastia *et al.*, 2003). An association between *APOE* genotype and cognitive ability following TBI has also been shown. Patients possessing an *APOE* ϵ 4 allele demonstrated impaired learning and memory recall following TBI of similar severity, suggesting *APOE*-isoform dependent effects on hippocampal function after TBI (Crawford *et al.*, 2002). Furthermore, in high-exposure boxers who have experienced repetitive blows to the head, possession of the *APOE* ϵ 4 allele was associated with more pronounced neurological impairment (Jordan *et al.*,

1997). Similarly, in older American football players who have been exposed to repeated head trauma, *APOE* $\epsilon 4$ carriers were significantly over-represented among players with lower cognitive performance (Kutner *et al.*, 2000).

1.3.3 *APOE* polymorphism and cerebral ischaemia

1.3.3.1 Ischaemic (occlusive) stroke

Ischaemic stroke shares several risk factors with heart disease. The *APOE* $\epsilon 4$ allele is associated with increased levels of low-density lipoprotein and cholesterol (Davignon *et al.*, 1988; Larson *et al.*, 2000; Eichner *et al.*, 2002), atherosclerosis (Hixson, 1991; Karvonen *et al.*, 2002) and ischaemic heart disease (de Knijff and Havekes, 1996; Wilson *et al.*, 1996; Frikke-Schmidt *et al.*, 2000; Eichner *et al.*, 2002) suggesting that *APOE* $\epsilon 4$ may be a risk factor for ischaemic stroke. A number of case-control studies have shown over-representation of the *APOE* $\epsilon 4$ allele in ischaemic stroke patients (Pedro-Botet *et al.*, 1992; Margaglione *et al.*, 1998; Peng *et al.*, 1999; Luthra *et al.*, 2002) and a meta-analysis reported a significant association between ischaemic stroke and the $\epsilon 4$ allele (McCarron *et al.*, 1999). Recently, the *APOE* $\epsilon 4$ allele has been demonstrated to be a risk factor for recurrence of ischaemic stroke (Kim *et al.*, 2003). However, other studies have also reported over-representation of the *APOE* $\epsilon 2$ allele (Couderc *et al.*, 1993) and neutral findings (Coria *et al.*, 1995; MacLeod *et al.*, 2001; Souza *et al.*, 2003).

In humans, the association of *APOE* genotype with outcome from ischaemic stroke is inconclusive. Initial studies assessing outcome after ischaemic stroke demonstrated that *APOE* $\epsilon 4$ was not associated with a poor prognosis (McCarron *et al.*, 1998; McCarron *et al.*, 2000; MacLeod *et al.*, 2001). Recently, however, the prevalence of aphasia after ischaemic stroke was demonstrated to be significantly greater in *APOE* $\epsilon 4$ patients (Treger *et al.*, 2003). Furthermore, in a magnetic resonance imaging study, despite a smaller initial infarct in *APOE* $\epsilon 4$ patients, expansion of infarct volume by day 8 post-stroke was significantly greater in *APOE* $\epsilon 4$ carriers (Liu *et al.*, 2002). Conflicting results from clinical studies investigating outcome from ischaemic stroke may in part reflect the presence of potentially confounding factors (e.g. duration/severity of insult, pre-existing disease). Accordingly, the benefits of using experimental models of cerebral ischaemia, in which these confounding variables can be controlled, are underlined.

1.3.3.2 Haemorrhagic stroke

There is accumulating evidence to suggest that *APOE* polymorphism is associated with outcome after intracerebral haemorrhage (ICH). A number of studies have revealed an association between possession of the *APOE* $\epsilon 4$ allele and poorer outcome after ICH (Alberts *et al.*, 1995; McCarron *et al.*, 1998; McCarron *et al.*, 1999), an effect thought to be independent of haematoma volume and severity of oedema. A recent prospective study reported that presence of the *APOE* $\epsilon 4$ allele was linked to significantly reduced survival following ICH (McCarron *et al.*, 2003).

Cerebral amyloid angiopathy (CAA), a condition caused by deposition of the β -amyloid ($A\beta$) peptide in the walls of cerebral blood vessels, is an important cause of lobar ICH. Several studies have revealed that vascular $A\beta$ deposition is associated with the *APOE* $\epsilon 4$ allele (Schmechel *et al.*, 1993; Greenberg *et al.*, 1995; Olichney *et al.*, 1996; Premkumar *et al.*, 1996; Yamada, 2002; Chalmers *et al.*, 2003). Consistent with these findings, initial studies of CAA-related ICH demonstrated over-representation of the *APOE* $\epsilon 4$ allele (Greenberg *et al.*, 1995; Greenberg *et al.*, 1996; Premkumar *et al.*, 1996). Subsequently, however, a high frequency of the *APOE* $\epsilon 2$ allele was demonstrated in studies that accounted for concomitant AD (Nicoll *et al.*, 1996; Nicoll *et al.*, 1997; Greenberg *et al.*, 1998). This led to the proposal that while *APOE* $\epsilon 4$ may promote vascular $A\beta$ deposition, *APOE* $\epsilon 2$ is a risk factor for rupture of amyloid-laden blood vessels (Nicoll *et al.*, 1997).

Consistent findings have emerged from studies in patients with subarachnoid haemorrhage (SAH). An association between the *APOE* $\epsilon 4$ allele and risk of SAH was indicated (Kokubo *et al.*, 2000; Leung *et al.*, 2002). Poorer outcome after SAH in *APOE* $\epsilon 4$ carriers has been demonstrated in several studies (Niskakangas *et al.*, 2001; Leung *et al.*, 2002; Tang *et al.*, 2003), although a recent study did not find a link (Morris *et al.*, 2004).

1.3.3.3 Global ischaemia

Two studies in humans have examined the association of *APOE* genotype with outcome after cardiac arrest and have produced contrasting results. In the first study, patients with the *APOE* $\epsilon 3/3$ genotype had a significantly higher survival rate at 6 months and more favourable neurological outcome compared to non-*APOE* $\epsilon 3/3$ patients, suggesting a detrimental effect associated with the *APOE* $\epsilon 4$ allele (Schiefermeier *et al.*,

2000). However, in a recent study (Longstreth *et al.*, 2003), *APOE* genotype was not significantly related to survival or neurological outcome, although a larger and less homogeneous group was used in this study compared to that of Schiefermeier *et al.* (2000). *APOE* genotype was also not associated with the extent of hippocampal neuronal damage in a cohort of patients who died following an episode of global ischaemia due to cardiac arrest and subsequent period of reperfusion (Horsburgh *et al.*, 1999a).

1.3.4 Stroke and TBI as risk factors for dementia – association with *APOE* polymorphism

1.3.4.1 Stroke

Increasing evidence implicates ischaemic cerebrovascular disease as a major risk factor for dementia. Several studies have shown that the incidence of dementia is significantly higher in ischaemic stroke patients compared to controls (Tatemichi *et al.*, 1992; Tatemichi *et al.*, 1994; Censori *et al.*, 1996; Kokmen *et al.*, 1996; Henon *et al.*, 1997; Zhu *et al.*, 2000). A direct role for cerebrovascular disease in AD pathogenesis has also been proposed (Kalaria, 2000; de la Torre, 2002; Kalaria, 2002; de la Torre, 2004). At post-mortem, 60 – 90% of AD patients exhibit some form of cerebrovascular pathology and around one third display cerebral infarction (Gearing *et al.*, 1995a; Premkumar *et al.*, 1996). It has been suggested that stroke may be the major aetiological factor in a substantial number of AD patients (Kokmen *et al.*, 1996). The impact of cerebral infarction on AD was highlighted in a study of elderly nuns, since individuals with cerebral infarcts also showed more severe dementia (Snowdon *et al.*, 1997). A recent study showed the presence of cerebral infarction increased the odds of dementia by 2.8-fold (Schneider *et al.*, 2004). Synergistic effects of *APOE* ϵ 4 and cerebrovascular disease on cognitive decline and dementia have been reported (Kalmijn *et al.*, 1996; Skoog *et al.*, 1998), although other studies have found only additive effects (Dik *et al.*, 2000; Zhu *et al.*, 2000). The association between *APOE* polymorphism and vascular dementia is inconclusive, with several studies showing a higher frequency of the ϵ 4 allele in vascular dementia patients compared to controls (Frisoni *et al.*, 1994a; Frisoni *et al.*, 1994b; Isoe *et al.*, 1996; Yang *et al.*, 2002) and others showing no association (Stengard *et al.*, 1995; Frank *et al.*, 2002; Traykov *et al.*, 2002).

1.3.4.2 Traumatic brain injury

There is considerable evidence to suggest that a history of head injury is the most robust environmental risk factor for AD (Mortimer *et al.*, 1985; Mortimer *et al.*, 1991; Mayeux *et al.*, 1993; Guo *et al.*, 2000; Plassman *et al.*, 2000; Fleminger *et al.*, 2003). The risk of AD conferred by a previous head injury may also be modulated by *APOE* polymorphism. Mayeux *et al.* (1995) have shown that a history of previous head injury and possession of *APOE* $\epsilon 4$ allele act synergistically to increase the risk of AD; the risk of AD was increased 10-fold when head injury and the $\epsilon 4$ allele were both present compared with a two-fold increase in risk with presence of the $\epsilon 4$ allele alone (Mayeux *et al.*, 1995). Similarly, a survey of World War II veterans showed a trend toward a stronger association between TBI and AD in men with the *APOE* $\epsilon 4$ allele (Plassman *et al.*, 2000). Other studies have demonstrated additive effects of TBI and *APOE* $\epsilon 4$ on AD risk (O'Meara *et al.*, 1997; Guo *et al.*, 2000; Jellinger *et al.*, 2001).

1.4 Role of apoE in brain injury – insight from animal models and *APOE* deficient and transgenic mice

1.4.1 Cellular localisation of apoE after acute brain injury

The discovery of associations between *APOE* polymorphism and the susceptibility and outcome to acute brain injury and neurodegenerative disease stimulated efforts to further understand the function(s) of apoE in the brain. Initial studies employing *in vivo* rodent models of acute brain injury were aimed at addressing fundamental issues regarding apoE in the injured brain, in particular to determine if alterations in cellular apoE localisation occurred after injury.

In normal rodent brain, apoE immunoreactivity is localised to glial cells, predominantly astrocytes, and is not observed in neurons (Boyles *et al.*, 1985; section 1.2.3.1). However, following injury, marked changes in apoE localisation have been demonstrated. Increased neuronal apoE immunoreactivity after CNS injury was first shown in the selectively vulnerable hippocampus after cardiac arrest in the rat (Kida *et al.*, 1995) and transient forebrain ischaemia in gerbils (Hall *et al.*, 1995). In the same model, increased apoE mRNA levels were also observed after ischaemia (Ali *et al.*, 1996). In a rat model of transient global ischaemia, the temporal alterations in apoE after injury were investigated. In this study, apoE immunoreactivity was increased in astrocytes prior to evidence of neuronal damage and then subsequently localised to

ischaemic neurons, suggesting that neuronal accumulation of apoE was the result of uptake of astrocyte secreted apoE (Horsburgh and Nicoll, 1996). Neuronal apoE immunoreactivity and elevated levels of apoE were also observed after subdural haematoma in the rat (Horsburgh *et al.*, 1997) and transient global ischaemia in mice (Horsburgh *et al.*, 2000c). More recently, neuronal apoE immunoreactivity has been demonstrated in ischaemic neurons following focal cerebral ischaemia in the rat (Nishio *et al.*, 2003; Kamada *et al.*, 2003). Significantly, similar results have also been obtained in human post-mortem tissue where marked increases in apoE immunoreactivity in ischaemic neurons and elevated levels of apoE were found in patients who experienced an episode of global ischaemia (Horsburgh *et al.*, 1999a) and in patients with cerebral infarction (Aoki *et al.*, 2003). Together, these studies demonstrated that apoE levels are elevated in response to injury and indicate that localisation of apoE to neurons may enable modulation of pathophysiological processes in neurons.

1.4.2 Studies in *APOE* deficient mice

The development of *APOE* deficient mice (Piedrahita *et al.*, 1992) facilitated further investigation of the role of apoE in the brain. Studies using these mice have shown that apoE has neuroprotective effects against various types of acute brain injury. *APOE* deficient mice are more susceptible to the effects of focal ischaemia, showing a larger infarct volume than wild type mice (Laskowitz *et al.*, 1997). *APOE* deficient mice also display a poorer outcome (pathological and/or neurological) after global ischaemia (Horsburgh *et al.*, 1999b; Sheng *et al.*, 1999; Kitagawa *et al.*, 2002a; Kitagawa *et al.*, 2002b), closed head injury (Chen *et al.*, 1997) and focal brain lesions (Masliah *et al.*, 1996). The neuroprotective role of apoE was further highlighted when it was shown that the increased susceptibility of *APOE* deficient mice to global ischaemia could be ameliorated by restoring apoE. Intraventricular infusion of a physiological concentration of human plasma-derived and lipid-conjugated apoE (of mixed isoform) significantly reduced ischaemic neuronal damage after global ischaemia to a level comparable to that observed in wild-type mice (Horsburgh *et al.*, 2000b).

1.4.3 *APOE* transgenic mice

As described previously (*section 1.2.4.3*), rodents express only one form of apoE in contrast to the three isoforms found in humans. Generation of human *APOE* transgenic

mice has therefore been a vital development enabling direct and systematic *in vivo* investigation of the effects of human *APOE* in the brain. In combination with mouse models of brain injury, it is therefore possible to investigate the effects of human *APOE* polymorphism on the response to brain injury. Several populations of transgenic mice expressing the human *APOE* isoforms have been developed.

1.4.3.1 *APOE* transgenic mouse lines

In this thesis, mice expressing human *APOE* $\epsilon 3$ or *APOE* $\epsilon 4$ under the control of human regulatory elements were used (Xu *et al.*, 1996). The major utility of these mice is that they closely mirror the pattern of apoE expression in the human brain (i.e. glial and neuronal). Characterisation of these mouse lines showed that *APOE* gene transcription (analysed by northern blot) was evident in several organs, including the brain, kidney, heart and liver. Likewise, apoE protein expression was detected throughout the body, including the brain, liver, kidney, heart and serum. Levels of apoE protein content in different tissues were highly variable among transgenic lines depending on the number of gene copies that integrated into the genome. In the brain (and other tissues), apoE levels were comparable to endogenous mouse apoE levels in wild-type mice, therefore indicating physiologically relevant apoE expression in the brain. A key feature of these mice is that they display a human-like pattern of apoE immunostaining. ApoE immunoreactivity was localised to various cell types including astrocytes, microglia and ependymal cells. Notably, apoE immunoreactivity was also observed in subsets of neurons, particularly in the cerebral cortex, although to a lesser extent than glial immunoreactivity. In addition, another important feature of these mice is that plasma cholesterol levels approach that found in wild-type mice. Accordingly, of the several types of *APOE* transgenic mice developed, these mice likely provide the distribution of apoE expression most relevant to humans. Generation of these mice is described in detail in *section 2.2.2*.

Transgenic mice expressing human *APOE* $\epsilon 3$ and *APOE* $\epsilon 4$ under the control of the astrocyte-specific glial fibrillary acidic protein (GFAP) promoter have been developed (Sun *et al.*, 1998). The rationale for developing these mice was that astrocytes are the primary source of apoE in the human brain (Boyles *et al.*, 1985; Pitas *et al.*, 1987a; *section 1.2.3.1*) and so these mice would enable the *in vivo* study of human apoE isoforms expressed specifically by astrocytes. In these mice, apoE immunoreactivity

was localised to astrocytes and the neuropil with no clear immunostaining of neurons. This pattern of immunostaining was therefore similar to that observed for endogenous apoE in wild-type mice and rodents in general. ApoE levels in brain tissue samples from these mice (0.1 – 0.3µg/mg) were shown to be similar to levels in human brain tissue (0.4 – 0.5µg/mg), indicating physiologically relevant apoE expression in the brain.

In contrast to the mice described above, other lines of *APOE* transgenic mice have been developed in which *APOE* expression is restricted to neurons (Buttini *et al.*, 1999). The rationale for neuronal targeting of *APOE* expression was mainly based on observations that *APOE* mRNA and immunoreactivity could be detected in human brain (Han *et al.*, 1994b; Metzger *et al.*, 1996; Xu *et al.*, 1999; *section 1.2.3.1*) and therefore may have critical effects in neurons. In these mice, expression of human *APOE* ε3 and *APOE* ε4 is driven by the neuron specific enolase (NSE) promoter. *APOE* expression was limited to neural tissue and testes of these mice. *APOE* mRNA and protein levels in brain tissue and CSF were shown to be comparable to those found in humans. ApoE immunoreactivity was localised exclusively to neurons, confirming the neuron-specific expression of apoE in these mice. Plasma cholesterol levels in these mice are similar to those found in *APOE* deficient mice (i.e. elevated in comparison to wild-type mice), reflecting the lack of apoE in plasma.

The mouse lines described above were all generated by the pronuclear injection technique (Gordon *et al.*, 1980; Gordon and Ruddle, 1983). Human *APOE* transgenic mice have also been generated by targeted replacement of the endogenous mouse *APOE* gene (“knock-in mice”) (Sullivan *et al.*, 1997; Sullivan *et al.*, 1998; Knouff *et al.*, 1999; Hamanaka *et al.*, 2000), the major advantage of which is the ability to control the location of transgene integration. Since transgene expression in these mice is under the control of endogenous promoters, the distribution and level of *APOE* expression in all tissues, including the brain, is generally similar to that observed in wild-type mice (Sullivan *et al.*, 1997).

1.4.3.2 Studies in *APOE* transgenic mice

Studies in which animal models of acute brain injury have been applied in transgenic mice expressing human *APOE* isoforms have produced consistent findings showing poorer outcome associated with the *APOE* ε4 allele. *APOE* ε4 mice under the control of human regulatory sequences displayed significantly greater ischaemic neuronal damage

in the hippocampus after global ischaemia compared to *APOE* ϵ 3 mice (Horsburgh *et al.*, 2000c). In the same lines of mice, *APOE* ϵ 4 mice displayed a larger infarct volume than *APOE* ϵ 3 mice after transient focal ischaemia (Sheng *et al.*, 1998), although a major limitation of this study was that brain oedema was not controlled for during infarct quantification. Also in these transgenic lines, *APOE* ϵ 4 mice were more susceptible to the effects of closed head injury than *APOE* ϵ 3 mice (Sabo *et al.*, 2000). In mice expressing *APOE* under the control of the NSE promoter, *APOE* ϵ 3 mice were protected against excitotoxin-induced neurodegeneration whereas *APOE* ϵ 4 mice were not (Buttini *et al.*, 1999). Collectively, the results from experimental models add to and support the findings from the majority of clinical studies that indicate that the *APOE* ϵ 4 allele is associated with poorer outcome after acute brain injury. However, in view of the inconclusive results in focal ischaemic stroke studies in humans, and the limitations of previous work using a model of focal ischaemia in *APOE* transgenic mice, it is evident that the effects of *APOE* genotype in focal ischaemia merit further systematic investigation.

1.5 Mechanisms underlying *APOE* genotype effects

The precise mechanism(s) underlying the *APOE* genotype-dependent differences in susceptibility and outcome to brain injury and disease are not fully understood. A number of mechanisms pertinent to acute brain injury have been investigated although the relative importance of each of these is unknown.

1.5.1 ApoE and excitotoxicity

Recent evidence suggests that apoE may be capable of attenuating glutamate receptor-mediated excitotoxic damage and that there may be isoform-specific differences in this effect. Significantly, transgenic mice expressing apoE3 were shown to be protected from excitotoxin-induced neuronal damage whereas apoE4-expressing mice were not (Buttini *et al.*, 1999). *In vitro*, exposure of neuronal-glial primary cultures and a neuronal cell line to biologically relevant concentrations of recombinant apoE prior to NMDA exposure resulted in significant neuroprotection (Aono *et al.*, 2002). Peptides derived from the receptor-binding region of apoE were also demonstrated to exert a neuroprotective effect against NMDA-induced excitotoxicity (Aono *et al.*, 2003). Isoform-specific effects have also been demonstrated *in vitro*. ApoE3, but not apoE4,

was shown to prevent the neuronal calcium response and neuronal damage in response to NMDA receptor activation (Qiu *et al.*, 2003). These effects may not be due to direct NMDA receptor antagonism by apoE, but may be exerted through interactions with apoE cell surface receptors, such as LRP and apoER2 (Aono *et al.*, 2002). Ligand binding to LRP can modulate NMDA receptor-mediated calcium influx via putative interactions between LRP and the NMDA receptor (Bacsikai *et al.*, 2000; Qiu *et al.*, 2002; Qiu *et al.*, 2003). These interactions may be mediated by the postsynaptic scaffold protein, PSD-95 (Gotthardt *et al.*, 2000; Herz, 2001a). PSD-95 modifications after cerebral ischaemia have been described (Takagi *et al.*, 2000) and disruption of PSD-95-NMDA receptor interactions has been shown to suppress excitotoxicity and to improve neurological outcome and reduce the volume of ischaemic damage after focal cerebral ischaemia in the rat (Sattler *et al.*, 1999; Aarts *et al.*, 2002).

1.5.2 ApoE and oxidative stress

ApoE may possess antioxidant properties and protect against the effects of oxidative damage to neurons in an isoform-specific manner. In mice, *APOE* deficiency is associated with increased oxidative stress and an increase in the oxidant/antioxidant ratio in the brain (Ramassamy *et al.*, 2001; Shea *et al.*, 2002). Furthermore, elevated 4-HNE immunoreactivity observed after global ischaemia in *APOE*-deficient mice compared to wild-type mice was ameliorated by intraventricular infusion of lipid-conjugated apoE (Horsburgh *et al.*, 2000b). Similarly, pre-treatment of *APOE*-deficient mice with vitamin E, an antioxidant, markedly reduced neuronal damage after ischaemia (Kitagawa *et al.*, 2002b). There is also evidence of *APOE* genotype differences in the ability to modulate oxidative injury. In post-mortem AD brain, elevated levels of lipid peroxidation markers were associated with possession of the *APOE* $\epsilon 4$ allele (Montine *et al.*, 1997; Ramassamy *et al.*, 2000; Tamaoka *et al.*, 2000). *In vitro*, apoE can protect neurons from hydrogen peroxide- and A β -induced oxidative damage in an isoform-specific manner (E2 > E3 > E4) (Miyata and Smith, 1996; Lauderback *et al.*, 2002). It was also shown that apoE isoforms can bind with different affinities to 4-HNE (E2 > E3 > E4), suggesting isoform differences in the detoxifying abilities of apoE (Miyata and Smith, 1996; Pedersen *et al.*, 2000).

1.5.3 ApoE and cytoskeletal interactions

An intact cytoskeleton is an important element in maintaining the structural and functional integrity of neurons. Disruption of cytoskeletal proteins occurs after various forms of acute brain injury, including cerebral ischaemia and TBI (Fitzpatrick *et al.*, 1996; Lipton, 1999). After brain injury, apoE is markedly elevated in neurons (*section 1.4.1*), therefore providing the basis for interactions between apoE and cytoskeletal proteins. ApoE binding to microtubule associated proteins may promote cytoskeletal stability (Roses *et al.*, 1996). *In vitro*, apoE3 binds with much greater affinity to the microtubule associated protein, tau, than apoE4 (Strittmatter *et al.*, 1994a; Strittmatter *et al.*, 1994b; Fleming *et al.*, 1996). ApoE3 binding to tau may prevent its hyperphosphorylation and the formation of paired helical fragments. In support of this, expression of *APOE* ϵ 4 in transgenic mice and humans is associated with a greater load of hyperphosphorylated tau (Tesseur *et al.*, 2000; Thaker *et al.*, 2003). In addition to tau, apoE3 also shows greater affinity than apoE4 for binding to other microtubule associated proteins such as MAP2 (Huang *et al.*, 1994a) and neurofilament proteins (Fleming *et al.*, 1996). ApoE3 may therefore be the more effective isoform in promoting cytoskeletal stability. However, direct interactions between apoE and cytoskeletal components have been questioned since there is no conclusive evidence that intraneuronal apoE can escape the endosomal-lysosomal compartments and enter the cytosol (DeMattos *et al.*, 1999). In this regard, apoE may modulate cytoskeletal function via a cell surface signalling pathway mediated by LRP or apoER2 (Herz and Beffert, 2000).

1.5.4 Toxic effects of apoE

The majority of proposed mechanisms underlying *APOE* genotype differences assume a positive role for apoE that reflects the relative failure of the apoE4 isoform in performing several functions i.e. that absence of apoE3 (or apoE2) is the most important factor. However, there is also evidence that apoE (and apoE fragments) have neurotoxic properties and that apoE4 may exert dominant effects over apoE3 in this regard. A toxic role for apoE was first suggested by the observation that synthetic apoE-related peptides induced degeneration of cultured sympathetic neurons (Crutcher *et al.*, 1994). Further work demonstrated greater neurotoxic effects of truncated and full-length forms of apoE4 compared to apoE3 (Marques *et al.*, 1996; Marques *et al.*, 1997). Toxic effects of

apoE may be mediated by disruption of intracellular calcium levels since elevated levels of intracellular calcium, resembling events in excitotoxicity, have been found in cultured neurons exposed to apoE (Tolar *et al.*, 1999; Veinbergs *et al.*, 2002) with apoE4 inducing greater increases in intracellular calcium than apoE3 (Veinbergs *et al.*, 2002). Recently, it was shown that apoE can be cleaved to form bioactive carboxyl terminal fragments that induce formation of intracellular inclusions. *In vitro*, apoE4 was more susceptible to truncation and more readily induced formation of inclusions than apoE3 (Huang *et al.*, 2001). In mice expressing human apoE in neurons (NSE-apoE mice), apoE4 was more prone to truncation, and an excitotoxic challenge significantly increased apoE fragmentation in NSE-apoE4 but not NSE-apoE3 mice (Brecht *et al.*, 2004).

1.5.5 Plasma and brain apoE levels

An alternative mechanism has been proposed for *APOE* genotype differences in susceptibility to brain injury that is independent of isoform-specific properties of apoE. It has been suggested that all apoE isoforms may have similar neuroprotective actions and that the crucial factor is the amount of apoE available, with greater levels being more beneficial (Poirier, 1994; Poirier, 2000). In humans, the level of plasma apoE is *APOE* genotype-related with *APOE* ϵ 4 carriers consistently shown to have significantly lower levels than ϵ 2 and ϵ 3 carriers (Slooter *et al.*, 1998; Schiele *et al.*, 2000; Panza *et al.*, 2003). There is also some evidence that plasma apoE levels in AD patients are lower in *APOE* ϵ 4 carriers (Panza *et al.*, 2003). In addition, lower apoE levels in the brain parenchyma (Bertrand *et al.*, 1995; Beffert *et al.*, 1999) and in CSF (Yamauchi *et al.*, 1999b) have been reported in *APOE* ϵ 4 carriers with and without AD. Lower apoE levels in *APOE* ϵ 4 carriers has been suggested to underlie their increased susceptibility to AD and poorer recovery from injury (Bertrand *et al.*, 1995; Beffert *et al.*, 1999; Poirier, 2000). However, a number of other studies have reported conflicting findings, suggesting that *APOE* genotype is not associated with CSF or brain tissue apoE levels (LeFranc *et al.*, 1996; Pirttila *et al.*, 1996; Glockner *et al.*, 2002; Fukumoto *et al.*, 2003) or that significantly higher CSF apoE levels may be found in individuals (with and without AD) possessing the *APOE* ϵ 4 allele (Hesse *et al.*, 2000).

1.6 Endocytosis

The endocytic pathway is integral to the internalisation and intracellular trafficking of apoE. Since neuronal accumulation of apoE is a key feature in the response to ischaemic brain damage (*section 1.4.1*), alterations in this pathway are potential mechanisms that could contribute to *APOE* genotype effects in the injured brain. To date, however, there is limited information on endocytic pathway function in response to ischaemic damage.

1.6.1 Endocytic pathway

Endocytosis encompasses a number of highly evolved mechanisms used by mammalian cells to internalise small molecules, macromolecules and various other particles (e.g. toxins). Phagocytosis (“cell eating”), pinocytosis (“cell drinking”) and receptor-mediated endocytosis all reflect specialised modes of endocytosis. Although all of these methods share common features, with regard to this thesis, all descriptions of endocytosis refer to receptor-mediated endocytosis. Endocytosis is a common feature of all nucleated vertebrate cells (Mukherjee *et al.*, 1997) where it mediates the uptake and intracellular trafficking of nutrients, trophic factors and receptor-ligand complexes in a series of membranous compartments. In addition, in the CNS, neuronal endocytosis is intimately involved in events following neurotransmitter release, most notably the internalisation and recycling of plasma membrane receptors and their ligands.

Early, late and recycling endosomes comprise the group of membrane-bound compartments associated with endocytosis and together with lysosomes they form the central vacuolar system. Each of these compartments is morphologically and biochemically distinct with intra-membranous conditions optimised for the specific processes that are performed within each compartment; for example, the acidic environment of lysosomes is suited to the proteolytic actions that occur within these organelles. The importance of the endosomal-lysosomal system is highlighted by the consequences of aberrant functioning of this pathway. Endocytic disturbances are believed to play important pathophysiological roles in atherosclerosis and diabetes (Mukherjee *et al.*, 1997). Furthermore, there are around thirty inherited disorders involving defective handling of lysosomal enzymes that produce a severe phenotype characterised by cognitive impairment and widespread neurodegeneration (Nixon and Cataldo, 1995).

Upon internalisation by clathrin-mediated endocytosis, molecules are delivered to the first major sorting station of the endocytic pathway, the early endosome (McCaffrey *et al.*, 2001). From here, sequestered molecules have three major fates: recycling back to the plasma membrane in recycling endosomes; progression to the trans Golgi network for further sorting and distribution; or transport to late endosomes and lysosomes for proteolytic degradation (**Figure 7**). Endosomal trafficking along each of these distinct pathways is regulated by a number of proteins, such as the group of small GTPases known as the rab proteins.

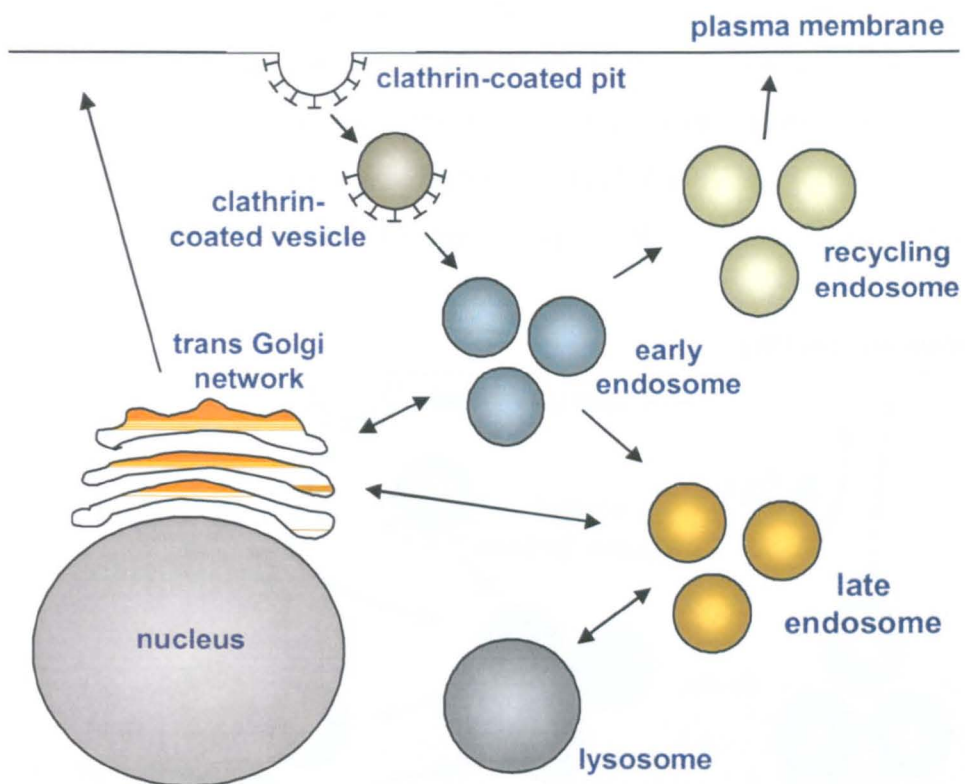


Figure 7. Schematic overview of the endocytic pathway

Internalisation occurs in clathrin-coated pits which bud from the plasma membrane to form clathrin-coated vesicles (CCVs). CCVs lose their clathrin coat and form early (sorting) endosomes. From early endosomes, internalised material may progress to late endosomes and lysosomes for degradation, to recycling endosomes for transport to the plasma membrane or to the trans Golgi network for further sorting and distribution.

1.6.2 Rab proteins

1.6.2.1 Rab proteins and regulation of endosomal trafficking

The rab family of proteins is part of the Ras superfamily of small GTPases (Stenmark and Olkkonen, 2001). Rab proteins are localised to the membranes of intracellular organelles such as endosomes, where they are thought to control vesicular docking and

fusion (Gonzalez *et al.*, 1999). Of approximately 60 members of the rab family, 12 rab proteins have been localised to the endocytic pathway in mammalian cells (Rodman *et al.*, 2000). Significantly, each of these proteins associates with particular organelles suggesting a degree of regulatory specificity (**Figure 8**). For example, rab5 is found on the membranes of early endosomes and is important for trafficking of material from internalised clathrin-coated pits to early endosomes (McLauchlan *et al.*, 1998; Rodman *et al.*, 2000). Rab4, in contrast, localises to recycling compartments where it is an important regulator of recycling activity (Daro *et al.*, 1996). Rab7, in turn, plays a critical role in regulating trafficking from early to late endosomes and lysosomes (Feng *et al.*, 1995). In order for the rab proteins to exert their regulatory effects, they must interact with specific effector proteins. One such effector whose role has been well documented is rabaptin-5, a specific effector of rab5 that is integral to early endocytic trafficking (Stenmark *et al.*, 1995; Gournier *et al.*, 1998; Gonzalez *et al.*, 1999).

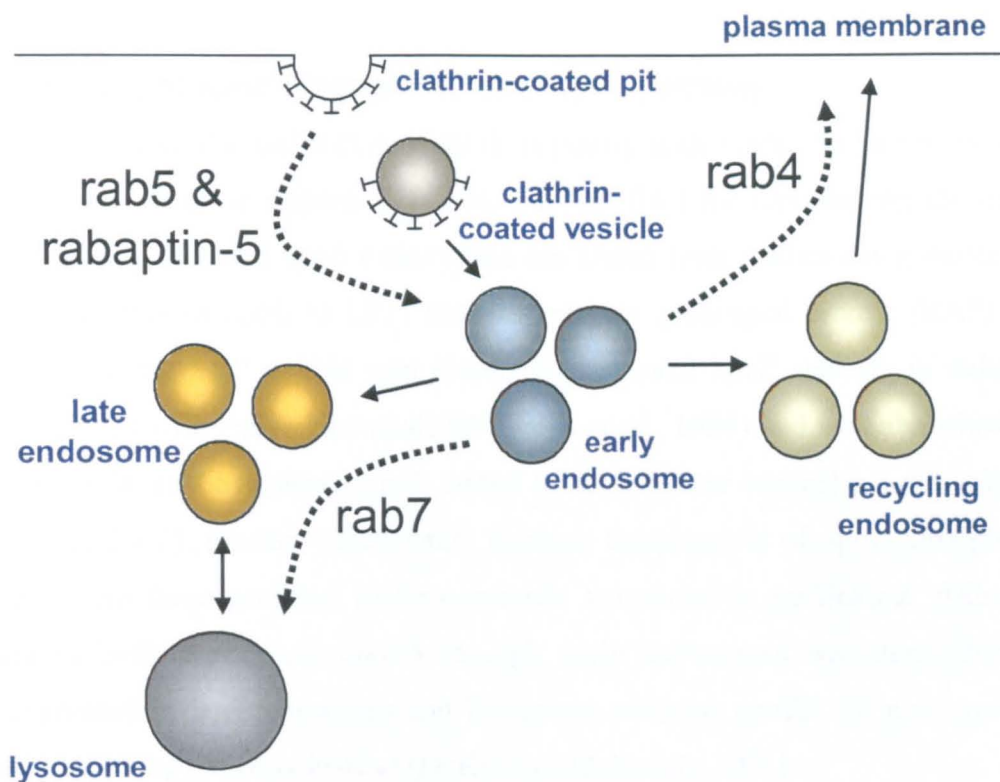


Figure 8. Role of rab proteins in endocytosis

The rab proteins are small GTPases that regulate trafficking in specific stages of the endocytic pathway. Rab5 and its effector, rabaptin-5, are important for internalisation into clathrin-coated pits and fusion with early endosomes. Rab4 regulates the direct recycling pathway from early endosomes back to the plasma membrane. Rab7 regulates transport from early to late endosomes and lysosomes.

1.6.2.2 Utility of rab proteins and effectors as endocytic markers

The specificity of rab proteins and their effectors for associating with and regulating distinct components of the endocytic pathway underlies their utility as tools to monitor activity in the various stages of endocytosis. Rab5 and rabaptin-5 are pertinent markers of internalisation/early trafficking whereas the specificity of rab4 for recycling endosomes makes it an appropriate marker of recycling activity. Overexpression of rabaptin-5 stimulates endocytic uptake whereas immunodepletion of rabaptin-5 inhibits early endosome activity (Bucci *et al.*, 1992; de Hoop *et al.*, 1994). Similarly, overexpression of rab4 promotes increased endosomal recycling (van der Sluijs *et al.*, 1992; Daro *et al.*, 1996). The level of expression of these proteins is therefore thought to be an indicator of endocytic activity in the specific pathways they regulate. Moreover, elevations in immunoreactivity of these markers have been shown to reflect increased numbers of endosomes which is indicative of enhanced activity in the relevant pathways (Cataldo *et al.*, 1997; Cataldo *et al.*, 2000).

1.6.3 Trafficking of apoE through the endocytic pathway

Although the intracellular trafficking of apoE is poorly understood, the use of *in vitro* studies has revealed some important details. Support for LRP representing the major receptor mediating neuronal apoE endocytosis has arisen from studies using molecules that prevent binding of apoE to LRP, such as receptor associated protein (RAP) and lactoferrin. Blocking LRP in this way eliminated neuronal apoE staining in cultured neurons incubated with exogenous apoE (Williams *et al.*, 1998) and also abolished the neurotrophic effects of exogenous apoE added to adult mouse cortical neuron cultures (Nathan *et al.*, 2002). Further experiments tracking the progress of apoE through the endocytic system have revealed isoform-specific variations in trafficking. Although trafficking of both apoE3 and apoE4 through early endosomes was demonstrated, apoE4 progressed to late endosomes and lysosomes whereas apoE3 did not, possibly following a recycling pathway instead (DeKroon and Armati, 2001).

1.6.4 ApoE receptors, endocytosis and signal transduction

There is accumulating evidence that the function of the LDL family of receptors, and in particular LRP, may not be restricted to the binding and internalisation of lipoproteins (Willnow *et al.*, 1999; Herz and Beffert, 2000; Herz and Strickland, 2001; Nykjaer and Willnow, 2002). The initial identification of LRP as a receptor for the protease inhibitor

α_2 -macroglobulin (Kristensen *et al.*, 1990; Strickland *et al.*, 1990) has led to the subsequent discovery of over 30 ligands that recognise LRP, including proteases, protease inhibitors and matrix metalloproteinases (Herz and Strickland, 2001). A role for LRP in signal transduction was implied by the presence of two copies of the NPxY motif in the cytoplasmic tail of LRP. Only one motif is required for mediating endocytosis suggesting that interactions with cytosolic proteins other than the endocytic machinery may be possible (Chen *et al.*, 1990; Willnow *et al.*, 1999). Two cytoplasmic adaptor proteins, disabled-1 (Dab-1) and FE65, which interact with NPxY motifs in the LRP receptor via phosphotyrosine-binding (PTB) domains have been identified (Trommsdorff *et al.*, 1998; Gotthardt *et al.*, 2000). The intracellular effects mediated by these interactions are currently unknown although studies using Dab-1 mutant mice suggest a critical role for Dab-1 in the Reelin signalling pathway (Howell *et al.*, 1997). Significantly, association of FE65 with the cytoplasmic tail of β -amyloid precursor protein (APP) has been demonstrated (Bressler *et al.*, 1996; Zambrano *et al.*, 1997; Kinoshita *et al.*, 2001), which enables interaction of LRP and APP via this adaptor protein. Additional interactions between LRP and β -APP via extracellular Kunitz-type protease inhibitor (K-PI) domains have also been shown (Kinoshita *et al.*, 2001). Together, these findings have important implications for AD pathogenesis, since they suggest mechanisms by which LRP may influence APP processing. (Ulery *et al.*, 2000; Pietrzik *et al.*, 2002). Notably, binding of apoE to LRP can modulate the interactions of LRP with APP and blocking LRP with RAP diminishes A β production (Ulery *et al.*, 2000).

In view of the integral role of NPxY domain interactions in endocytic internalisation and putative signalling pathways it is conceivable that there may be interplay between the two processes. Receptor-mediated endocytosis is a well established way of down-regulating extracellular signals and it has been proposed that assembly of receptors in clathrin-coated pits during endocytosis may displace adaptor proteins and therefore switch off cytosolic signalling capabilities (Willnow *et al.*, 1999).

1.6.5 Endocytic alterations in Alzheimer's disease

To date, there has been little investigation of endocytic pathway function in the injured brain. However, there has been increasing interest in the neuronal endosomal-lysosomal system in view of its possible importance in AD pathogenesis. Several proteins strongly

implicated in AD pathophysiology, such as apoE, APP, A β and LRP are all trafficked through the endocytic pathway and therefore the endocytic pathway, and early endosome in particular, is a key point of convergence for these molecules. The endocytic pathway is fundamental to apoE and LRP trafficking. In addition, there is evidence that APP can be processed through the endosomal-lysosomal system (Haass *et al.*, 1992; Golde *et al.*, 1992; Koo *et al.*, 1996; Yamazaki *et al.*, 1996). Furthermore, proteolytic production of A β may occur in the early endosome shortly after internalisation of APP from the cell surface (Koo *et al.*, 1994; Refolo *et al.*, 1995). Initial studies in AD post-mortem brain revealed up-regulation of neuronal lysosomal activity in affected regions (Cataldo *et al.*, 1995; Cataldo, *et al.*, 1996). Subsequently, increased endocytic activity was also shown in post-mortem AD brain which the authors speculate may induce elevated APP internalisation and A β production through increased protease delivery (Cataldo *et al.*, 1997). Enhanced endocytic uptake and recycling may represent alterations occurring during the early stages of AD since increased numbers of abnormally enlarged early and recycling endosomes were observed in post-mortem brain from individuals at pre-clinical stages of AD and in patients with Down syndrome (Cataldo *et al.*, 2000). Furthermore, possession of the *APOE* ϵ 4 allele was associated with more pronounced endocytic alterations in this study, suggesting that isoform-differences in endocytic activity may exist that could influence the processing and interactions of several putative aetiological factors in AD.

To date, the response of the endocytic pathway after cerebral ischaemia has not been investigated.

1.7 Modulation of apoE levels by *APOE* gene transfer

1.7.1 *APOE* as a candidate for gene transfer to the brain

ApoE is markedly upregulated after ischaemic brain injury and *APOE* deficient mice display a poorer outcome after cerebral ischaemia (*section 1.4*). These results suggest that the availability of apoE is a key factor that helps to protect the brain after injury. This is supported by the demonstration that restoring CSF apoE levels in *APOE* deficient mice ameliorates ischaemic damage after global ischaemia (Horsburgh *et al.*, 2000b). In this study, a physiological concentration (5 μ g/ml) of lipid-conjugated apoE was administered by intraventricular infusion and reduced the extent of ischaemic damage in *APOE* deficient mice to a level comparable with that in saline-treated wild-

type mice. In addition, there was a trend toward reduced ischaemic damage in wild-type mice infused with apoE. These data indicate that augmenting endogenous apoE levels could have beneficial effects on the response of the brain to injury.

Aside from direct administration of apoE, another approach to achieve this is by viral-vector mediated gene transfer of *APOE*. A number of studies have shown that viral vectors can be used to transfer a specific gene into the brain and mediate expression of the gene product and thus modulate levels of the targeted protein. Advantages of a viral vector-mediated gene transfer strategy to the brain include the potential for prolonged production of the protein and the ability to induce localised alterations in protein levels. Viral vector-mediated transfer of genes encoding various classes of protein (e.g. neurotrophic factors, anti-apoptotic proteins, anti-inflammatory mediators) have previously been demonstrated to have neuroprotective effects in models of cerebral ischaemia (*for review see Ooboshi et al., 2003*). To date, however, the efficacy of *APOE* gene transfer has not been investigated.

1.7.2 Viruses as vectors for gene transfer

A prerequisite for successful gene transfer is the efficient delivery of the appropriate therapeutic gene to the appropriate target tissue. Two major classes of vector system – viral and non-viral – have been developed that can mediate effective gene transfer to the CNS *in vivo*. Non-viral approaches include the use of DNA conjugates and cationic liposomes to deliver genetic material (Shi and Pardridge, 2000; Zhang *et al.*, 2003). Viral vectors, however, possess a number of properties that render them particularly suitable for gene transfer and are currently the most extensively used tools for *in vivo* gene delivery to the CNS.

Viruses are microscopic particles (10 – 50nm in diameter) composed of nucleic acid (DNA or RNA) enclosed in a protein coat (capsid) and in certain cases a membranous envelope. The key attribute of a virus that underlies its utility as a gene transfer vector is its inherent ability to infect and transfer genetic material to host cells. Viruses are therefore highly evolved natural vectors for the transfer of foreign genetic information into cells. Other properties of viral vectors that are advantageous include: the relative ease of engineering viruses to include genes of interest; increased selectivity for specific cell types (e.g. dividing/non-dividing) or tissue (e.g. brain) in comparison to non-viral vectors; and in general greater efficiency of gene transfer and stability of the foreign gene once inside the host cell. Limitations of viral vectors include the limited size of

DNA that can be transferred and the stimulation of deleterious immunological and/or inflammatory responses.

In order for viruses to be suitable for use as gene transfer vectors, they must be modified to render them replication defective and thus prevent proliferation of new viral particles and cell destruction in host tissue. Attenuation of replicative ability is achieved by removal of certain sections of the viral genome that are responsible for viral replication. Genetic manipulation of viral vectors is thus designed to retain virus infective ability but not replicative ability. Deletion of sections of the viral genome also provides a site in which the gene of interest can be inserted. A further aim of genetic modification of viral vectors is to minimise the immune/inflammatory response triggered by viral gene expression which may be achieved by removal of additional regions of the viral genome.

To date, five major classes of virus have been used extensively as viral vectors: (1) retroviruses, (2) herpes simplex viruses, (3) adenoviruses, (4) adeno-associated viruses and (5) lentiviruses. Each type of virus has its own unique properties such as the amount of DNA that can be packaged, cell tropism, efficiency and stability of transgene expression and the host immune response triggered. The most appropriate type of viral vector is therefore dependent upon a number of factors, most notably the gene of interest and the features of the target tissue/cell-type. In this thesis, an adenoviral vector was used to transfer genetic material to the brain and therefore the following section will focus on the characteristic features and utility of adenovirus as a viral vector.

1.7.3 Adenoviral vectors

Adenoviruses are linear double-stranded DNA viruses containing a genome 30 – 35kb in size that, in native form, can be pathogenic in humans causing intestinal, upper respiratory and eye infections (Kennedy *et al.*, 1997; Robbins *et al.*, 1998). Over 50 human adenoviral serotypes have been identified; serotypes 2 and 5 have been most commonly used to generate vectors. These are also the most common serotypes to which humans have been exposed and therefore pre-existing immunity may be present, a factor that may influence the efficacy of subsequent adenoviral vector administration in humans. Adenovirus serotypes 2 and 5 enter host cells through binding to the coxsackievirus-adenovirus receptor and reach the nucleus via nuclear pores where the genome remains episomal (does not integrate into the host cell genome). Four different early viral genes (E1, E2, E3 and E4) that are important for viral replication are

expressed following infection. Initial construction of attenuated adenoviral vectors (first generation vectors) involved deletion of the E1 gene, expression of which is required for induction of the E2, E3 and E4 genes and viral replication. Deletion of the E1 gene therefore produces a replication defective vector and provides a site for insertion of the therapeutic gene(s) of interest. Favourable characteristics of adenoviral vectors include their relatively large packaging capacity, relative ease of growth to high titres (up to 1×10^{13} virus particles/ml) and the ability to transduce an extensive range of cell types (dividing and non-dividing) with high efficiency, an important characteristic for gene transfer to the CNS (Akli *et al.*, 1993; Robbins *et al.*, 1998; Zou *et al.*, 2000; Kay *et al.*, 2001)

However, despite reports of sustained transgene expression for months following injection of adenovirus vectors into brain parenchyma (Byrnes *et al.*, 1996; Kajiwara *et al.*, 1997), it is widely acknowledged that a major limitation of these first generation vectors is their triggering of inflammatory and immune responses that can substantially diminish transgene expression over time (Byrnes *et al.*, 1995; Byrnes *et al.*, 1996; Tripathy *et al.*, 1996; Wood *et al.*, 1996; Kajiwara *et al.*, 1997; Kajiwara *et al.*, 2000). Immunogenicity of first generation vectors has been attributed to “leaky” expression of viral genes. For this reason, efforts were made to construct a less immunogenic adenovirus vector by deletion of additional regions of the viral genome such as the E3 and E4 genes. The result has been development of second generation vectors variously called “gutless”, “helper-dependent” or “high-capacity” adenovirus vectors that are almost devoid of viral genome (Amalfitano *et al.*, 1998; Morsy *et al.*, 1998; Gorziglia *et al.*, 1999). Attenuated immune responses and prolonged transgene expression have been demonstrated following both peripheral and intracerebral administration of these gutless adenovirus vectors in comparison to conventional first generation vectors (Morral *et al.*, 1998; O’Neal *et al.*, 1998; Thomas *et al.*, 2000; Zou *et al.*, 2000; Kochanek *et al.*, 2001b; Thomas *et al.*, 2001).

1.7.4 Adenoviral transduction and transgene expression in the brain

The cellular tropism of viral vector transduction and transgene expression in the brain is influenced by a number of factors. These include the type of virus, the cellular distribution of proteins required for entry of viral particles into host cells and the features of the promoter and associated regulatory elements driving transgene expression. Since adenovirus is capable of infecting post-mitotic cells, transduction of

neurons is feasible. Widespread distribution of the coxsackievirus-adenovirus receptor also facilitates entry of adenovirus into most cell types in the brain, including neurons and glia (Glover *et al.*, 2002). In general, therefore, adenoviral vectors transduce both neurons and non-neuronal cells (astrocytes, oligodendrocytes, microglia and endothelial cells), although transduction of non-neuronal cells probably occurs with greater efficiency (Kügler *et al.*, 2001). However, studies investigating the expression of reporter genes such as green fluorescent protein (GFP) and β -galactosidase (β -gal) have shown that the type of promoter strongly influences the cellular specificity of adenoviral transgene expression. The human cytomegalovirus (CMV) promoter is widely used to drive transgene expression in adenoviral vectors. A predominantly glial pattern of transgene expression has been reported with this promoter both *in vivo* and *in vitro* (Hermann *et al.*, 2001b; Kugler *et al.*, 2001; Kugler *et al.*, 2003). In the absence of glia, however, strong transgene expression has been demonstrated in hippocampal neurons suggesting that non-neuronal transduction and/or transgene expression may actively suppress CMV promoter activity in neurons perhaps via a cytokine-mediated mechanism (Kugler *et al.*, 2001; Kugler *et al.*, 2003). Attempts have been made to achieve neuron-restricted transgene expression through various methods including modification of the viral particle (Biermann *et al.*, 2001) and use of cell-specific promoters such as the neuron-specific enolase promoter (Navarro *et al.*, 1999; Kugler *et al.*, 2001). However, recent evidence suggests that the human synapsin 1 gene promoter may offer the most efficient and prolonged neuron-specific transgene expression *in vivo* (Kugler *et al.*, 2001; Glover *et al.*, 2003; Kugler *et al.*, 2003).

1.7.5 Adenoviral vector-mediated gene transfer and cerebral ischaemia

Reflecting their utility for CNS gene transfer, adenoviral vectors (mostly first generation) have been used in the majority of studies investigating the efficacy of gene transfer strategies in cerebral ischaemia. Delivery of adenoviral vectors containing a variety of “therapeutic” genes have been shown to protect against ischaemic brain damage (Ooboshi *et al.*, 2003). These include genes encoding neurotrophic factors (Kitagawa *et al.*, 1999; Yagi *et al.*, 2000; Hermann *et al.*, 2001b; Zhang *et al.*, 2002), anti-apoptotic proteins (Kilic *et al.*, 2002) and anti-inflammatory mediators (Betz *et al.*, 1995; Yang *et al.*, 1997b; Yang *et al.*, 1999). These data indicate that adenoviral vector-

mediated delivery is a feasible strategy for investigating the effects of *APOE* gene transfer in cerebral ischaemia.

1.8 Hypotheses and aims of thesis

In view of previous work described in this introduction, the overall objective of this thesis was to further investigate the role of *APOE* in cerebral ischaemia. To achieve this objective, three main hypotheses were tested:

1. *APOE* ϵ 4 is associated with poorer outcome after transient focal ischaemia
2. *APOE* genotype-dependent alterations in the endocytic pathway occur after cerebral ischaemia
3. Adenoviral vector-mediated gene transfer of *APOE* reduces ischaemic brain damage after transient focal ischaemia

To test the above hypotheses, a number of aims were established which were to:

1. Determine, in human post-mortem temporal lobe tissue, if *APOE* genotype-dependent alterations in the endocytic pathway occur after global ischaemia
2. Establish and characterise the intraluminal filament model of transient focal ischaemia in the mouse
3. Determine if *APOE* genotype is associated with differences in outcome after transient focal ischaemia in the mouse
4. Determine if *APOE* genotype-dependent alterations in apoE and the endocytic pathway occur after transient focal ischaemia in the mouse
5. Determine if intracerebral adenoviral vector-mediated gene transfer of *APOE* is neuroprotective in a mouse model of transient focal ischaemia

Chapter 2

Materials and Methods

2.1 Human post-mortem brain tissue

All experiments using human post-mortem tissue were approved by the ethics committee of the Southern General Hospital, Glasgow.

2.1.1 Tissue processing and selection

Paraffin-embedded sections of medial temporal lobe from patients who died after an episode of global ischaemia due to cardio-respiratory arrest and control patients (*see below*) were selected from the archives of the Department of Neuropathology, Southern General Hospital, Glasgow. Archival tissue was derived from material originally referred to the Department of Neuropathology from 1984 – 1996 for standard neuropathological examination. Tissue used in this thesis was from a systematically selected cohort of patients with detailed case histories identified by Prof James Nicoll and Dr Karen Horsburgh for a previous study (*see below*).

Whole brains were immersion-fixed in 10% formal saline for up to 3 weeks. Brains were then cut in a standard fashion for neuropathological examination; 1cm coronal slices of the cerebral hemispheres, 1cm slices of the cerebellar hemispheres at right angles to the surface markings of the folia and 0.5cm horizontal slices of the brainstem were cut. After general observations were made, regions of interest (including the medial temporal lobe) were identified and blocks were dissected from the cerebral hemispheres for paraffin processing and embedding. Thereafter, 8µm sections were cut and mounted on poly-*L*-lysine coated glass slides. Sections were routinely stained with haematoxylin and eosin and luxol fast blue/cresyl violet for histological examination.

For a previous study (Horsburgh *et al.*, 1999a), histological examination of medial temporal lobe sections from patients who died after cardio-respiratory arrest and from patients who died from other causes was performed by Prof James Nicoll and Dr Karen Horsburgh to identify suitable global ischaemia case and control material. For control material, case and post-mortem reports were consulted and tissue from patients without clinical or neuropathological evidence of neurological/psychiatric impairment or cardiovascular disease was selected. For global ischaemia material, case and post-mortem reports were consulted and patients who had experienced cardio-respiratory arrest with subsequent resuscitation and a defined period of reperfusion (survival) were identified. Tissue used in this thesis was from this carefully selected cohort of cardio-respiratory arrest and control individuals (*see Appendix C for clinical details*).

2.1.2 APOE genotyping

This procedure was performed by Mrs Janice Stewart at the Department of Neuropathology, Southern General Hospital. *APOE* genotype was determined using a polymerase chain reaction (PCR) method that was optimised for archival formalin-fixed paraffin-embedded tissue and has been described previously (Nicoll *et al.*, 1997).

For each case, one 8µm tissue section was placed in a sterile Eppendorf tube and 1ml xylene was added. Tubes were vortexed for 1min and then centrifuged at 13,000rpm for 5min. Xylene was decanted, 1ml ethanol was added and tubes were vortexed for 1min and then centrifuged at 13,000rpm for 5min. Ethanol was decanted and 1ml fresh ethanol was added and vortexing and centrifuging was repeated. Ethanol was decanted and residual ethanol was removed by placing tubes on a dry heat block (55 - 60°C) for 1h.

The dried tissue sample was resuspended in a proteinase K digest reaction mix containing 4µl proteinase K (200µg/ml), 20µl PCR buffer (Perkin Elmer Amplitaq Gold containing 15mM MgCl₂) and 176µl water (Sigma). The solutions were overlaid with 5 – 6 drops of mineral oil (Sigma) and incubated at 56°C (waterbath) overnight. Samples were then incubated at 95°C for 10min to inactivate proteinase K. Samples containing target DNA were stored at -20°C or -80°C until PCR amplification.

PCR reactions took place in a total volume of 15µl comprising 14.2µl master mix and 0.8µl target DNA solution. Master mix contained 9.025µl Analar water, 1.5µl PCR buffer (Amplitaq Gold), 1.5µl dNTP solution (containing 2mM each of dATP, dCTP, dGTP and dTTP), 1.5µl dimethyl sulphoxide (DMSO), and 0.3µl of each primer (10µM). Left and right primers were described previously (Wenham *et al.*, 1991). Sequences are as follows:

Left 5'-ACAGAATTCGCCCCGGCCTGGTACACTGCCA-3'

Right 5'-TCCAAGGAGCTGCAGGCGGCGCA-3'

14.2µl master mix was pipetted into an Eppendorf tube and was overlaid with one drop mineral oil and then 0.8µl target DNA solution was added. Tubes were then transferred to a thermal cycler (Techne Genius) which was programmed to cycle through a series of temperature changes as follows:

1. 35°C (to preheat lid)
2. 94°C – 9min (to denature target DNA and activate DNA polymerase)
then 40 cycles of

3. 94°C – 1min (to denature target DNA)
4. 65°C – 1min (to anneal primers)
5. 72°C – 2min (to extend DNA)

Hha1 Restriction endonuclease (1.2µl) was added to 15µl of PCR reaction product and incubated at 37°C overnight. The Hha1 restriction endonuclease cleaves at GCGC sites in the DNA sequence, which corresponds to arginine residues in the protein sequence. ApoE isoform differences in amino acid sequence result from substitutions at positions 112 and 158 of the 299 amino acid protein (*see section 1.2.4.2*). Hha1 digestion of the target DNA will therefore produce fragments of varying lengths depending on *APOE* isoform. These fragments can be separated and identified by gel electrophoresis.

A 10% polyacrilamide gel was used. 4µl of gel loading solution was added to 15µl of PCR product and mixed thoroughly before samples were loaded into the gel wells. A DNA ladder was also prepared: 0.5µl Hinf 1 marker was added to 24µl distilled water and then 4µl of gel loading solution was added and mixed thoroughly before loading on to the gel. The gel was run at 200volts/0.06amps for approximately 40min. Gels were then removed from the assembly, stained with ethidium bromide solution (10mg/ml) for 4min, viewed on an ultraviolet light box and photographed.

2.2 Mice

Upon arrival, all mice were housed in an animal housing facility. At both the Wellcome Surgical Institute (WSI), University of Glasgow, and Division of Neuroscience, University of Edinburgh, mice were housed in barrier-controlled units screened every 3 months for pathogens. Units were on a 12h light/dark cycle with regulated environment (temperature, humidity). All mice were given access to food and water *ad libitum* upon arrival in each facility. A summary of mouse numbers used in each study is given in **Appendix B**.

2.2.1 C57Bl/6J mice

C57Bl/6J mice were obtained from Charles-River, UK. C57Bl/6J is the most widely used inbred strain and most commonly used background strain for generation of transgenic mice (including *APOE* transgenic mice used in this thesis). An inbred strain is defined as one which has been maintained by sibling (brother x sister) matings for 20

or more consecutive generations. Aside from sex difference, mice from an inbred strain are as genetically alike as possible, being homozygous at virtually all loci.

2.2.2 APOE transgenic mice

2.2.2.1 Production of transgenic mice by pronuclear injection

There are essentially three methods of generating transgenic mice: (1) retroviral integration of foreign DNA into an early developing embryo; (2) direct microinjection of foreign DNA into the pronucleus of a newly fertilised egg; (3) genetic manipulation of embryonic stem cells. The *APOE* transgenic mice used in this thesis were generated using the pronuclear injection technique (Xu *et al.*, 1996).

The technique of producing transgenic mice by pronuclear microinjection of DNA was pioneered over 20 years ago (Gordon *et al.*, 1980; Gordon and Ruddle, 1983) and has since become the most extensively used technique. A major advantage of this technique is that large fragments of DNA can be injected into the pronucleus, thus allowing complete genes and their regulatory elements to integrate into the genome (Evans, 1994). This technique is also remarkably efficient; approximately 80% of founder mice are true transgenics (every cell contains the integrated transgene), indicating that DNA integration occurred at the one-cell embryo stage (Brinster *et al.*, 1985; Evans, 1994). A disadvantage of this technique, however, is that foreign DNA typically integrates into the genome by non-homologous recombination and therefore can integrate randomly at multiple sites and cause DNA rearrangement (Reventos and Gordon, 1990). The site of integration in the genome can affect transgene expression, so that different founder mice with different integration sites often demonstrate different levels of expression (Evans, 1994).

2.2.2.2 Generation of transgenic mice expressing human APOE

APOE transgenic mice were obtained through collaboration with Dr Allen Roses (GlaxoSmithKline, USA). *APOE* $\epsilon 3$ and $\epsilon 4$ transgenic mice expressing human *APOE* under control of human regulatory sequences were used. These lines were initially produced and characterised at Duke University, USA, and have been described in detail previously (Xu *et al.*, 1996). *APOE* knockout mice were generated by inactivating the endogenous *APOE* gene by gene targeting in embryonic stem cells (Piedrahita *et al.*, 1992). Cosmid libraries were constructed from lymphoblasts of humans who were

verified to be homozygous carriers for the *APOE* ϵ 3 and ϵ 4 alleles. Fragments containing human regulatory sequences and the coding sequences for human *APOE* (ϵ 3 and ϵ 4) were isolated, purified and injected into single-celled embryos from homozygous *APOE*-deficient mice and transferred to female recipients (a cross of C57Bl/6J x DBA/2J) to produce founder transgenic mice. Founder mice were backbred to *APOE* knockout mice to generate animals hemizygous for human *APOE* transgenes and homozygous for inactivated mouse *APOE* gene. Animals were bred to homozygosity for human *APOE* transgenes and backbred into *APOE* knockout strains to remove the genetic influence of DBA/2J background strains. The presence of human *APOE* was confirmed by polymerase chain reaction (PCR). The mice were backcrossed at least six times to C57Bl/6J mice in the USA before transport to the UK and thereafter several backcrosses to C57Bl/6J mice were made at GlaxoSmithKline, UK. For the *APOE* transgenic study in this thesis, the *APOE* ϵ 3-437 and *APOE* ϵ 4-81 lines were used which carry two copies of the respective transgenes. These lines were best matched for apoE levels from the original lines bred. The mice were transferred from GlaxoSmithKline, UK to the Wellcome Surgical Institute, where surgical procedures were performed.

2.2.2.3 *APOE* genotyping

Tail tissue samples were used to confirm the *APOE* genotype of mice bred in-house. Each mouse was briefly anaesthetised with 3% halothane in a mixture of 30% oxygen and 70% nitrous oxide. A tail-tip tissue sample was collected by removing a small portion from the tail-end using aseptic technique. The tail was cauterised to prevent bleeding and the mouse was returned to its cage. Tissue was placed in a sterile DNA/RNA-free eppendorf tube containing ethanol and stored at 4°C. Tail samples were transported at 4°C to the Southern General Hospital where *APOE* genotype was determined by Mrs Janice Stewart. After decanting ethanol, samples were dried and DNA extracted as described previously (*section 2.1.2*) except a proteinase K concentration of 100 μ g/ml was used. PCR and gel electrophoresis (**Figure 9**) was performed as previously described (*section 2.1.2*)

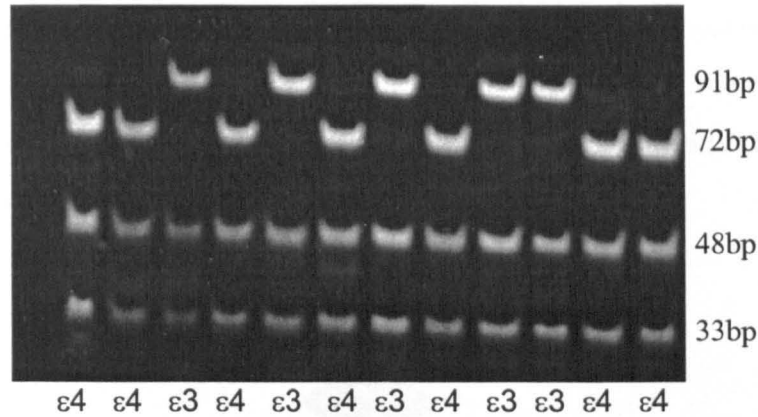


Figure 9. Genotyping of *APOE* transgenic mice

10% polyacrilamide gel stained with ethidium bromide showing the specific DNA fragments associated with the *APOE* ϵ 3 and ϵ 4 genotype. Image courtesy of Mrs Janice Stewart.

2.3 Surgical procedures

All animal procedures were carried out under appropriate Home Office Personal (60/8182) and Project Licences (60/2023, 60/2942, 60/3043) and adhered to regulations as specified in the Animals (Scientific Procedures) Act (1986). Upon arrival in the animal unit, a period of at least one week elapsed prior to surgical procedures to allow acclimatisation. Adult male mice were used for all surgical procedures.

2.3.1 Stereotaxic injection

Stereotaxic injections were performed by Dr Karen Horsburgh at the Division of Neuroscience, University of Edinburgh. Each mouse was placed in a perspex chamber and anaesthesia was induced with 3% halothane in a mixture of 30% oxygen and 70% nitrous oxide. Each mouse was then placed onto a stereotaxic frame and mechanically ventilated (125 breaths per minute). Anaesthesia was maintained with approximately 2% halothane in the same mixture of oxygen and nitrous oxide for the duration of surgery. A skin incision was made above the parietal skull and a burr hole was carefully drilled through the bone overlying the parietal cortex. Stereotaxic infusions (0.5 μ l over 5min) were made in the dorsolateral caudate nucleus (2.5mm lateral to midline at bregma level and 3mm from the cortical surface) (**Figure 10**). After infusion, the needle was left in place for 10min to prevent diffusion along the needle tract. The needle was then withdrawn and the wound sutured. Anaesthesia was discontinued and mice were allowed to regain consciousness before being transferred to a temperature-controlled (30°C) incubator for 2h. Subsequently, mice were returned to the animal recovery room

where they were housed singly and given free access to food and water. Soft food was provided during recovery to aid post-surgery feeding. Throughout the recovery period, the condition of the mice was regularly monitored (at least twice daily) and recorded on an animal recovery form.

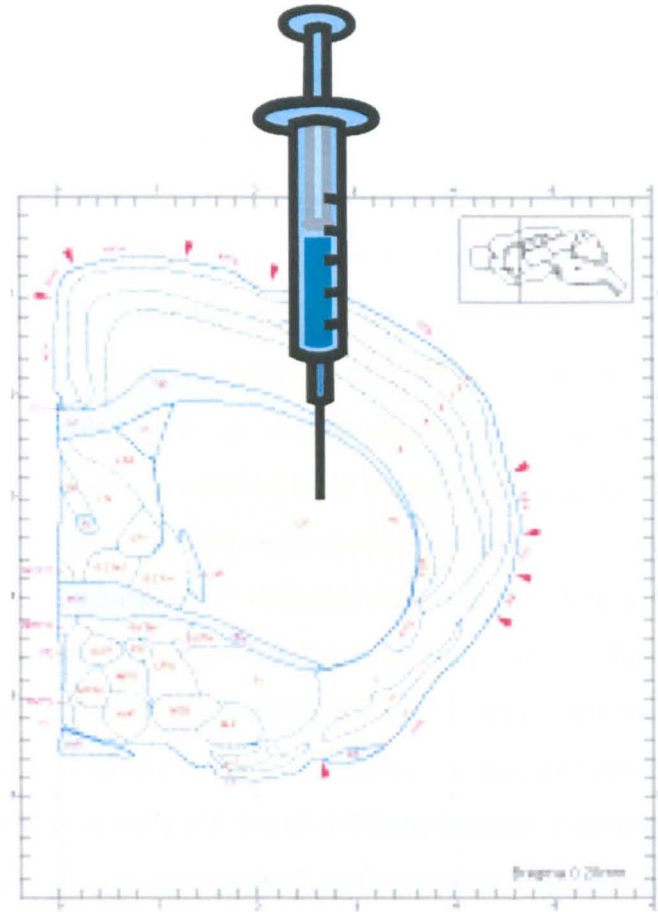


Figure 10. Location of stereotaxic injections

Injections were made in the dorsolateral caudate nucleus (2.5mm lateral to midline at bregma level and 3mm from the cortical surface).

2.3.2 Intraluminal filament occlusion

Two models of intraluminal occlusion were used in this thesis. A sustained anaesthesia (during occlusion) model was fully characterised and used in studies (*chapters 4 and 5*) performed at the Wellcome Surgical Institute, Glasgow. A recovery (during occlusion) from anaesthesia model was used in the viral vector study (*chapter 6*) performed at the Division of Neuroscience, Edinburgh.

2.3.2.1 Sustained anaesthesia model

Intraluminal filament occlusion in the mouse had not previously been performed at the Wellcome Surgical Institute and therefore, development of and gaining competence in the surgical technique was necessary prior to use of the model in studies described in this thesis. During the initial development of the technique, competence was gained in general surgical protocols, such as inducing/maintaining an appropriate level of anaesthesia, aseptic technique, control of body temperature and suturing. The technique first described by Longa *et al.* (1989) was used as the basis for optimising the surgical approach. At the outset, a number of technical issues were addressed, for example, the most appropriate approach for tissue dissection and exposure of the carotid vessels and the approximate distance to insert the filament. It was particularly important to establish the most appropriate size of occluding filament to use (*see section 4.3.1.1*) as previous studies reported the use of both a 5-0 and 6-0 heat-blunted filament. Accordingly, this preliminary work led to the intraluminal occlusion technique described below being established.

Each mouse was placed in a Perspex chamber and anaesthesia was induced with 3% halothane in a mixture of 30% oxygen and 70% nitrous oxide. The mouse was then transferred to the operating surface where anaesthesia was maintained for the duration of surgery with 1.5% halothane in the same mixture delivered by a face mask. Core temperature was monitored with a rectal probe and maintained at 37 ± 0.5 °C using a heat lamp.

Intraluminal filament occlusion was produced using a modification of the method previously described by Longa *et al.* (1989). A midline neck incision was made and the left submandibular gland freed and retracted cranially. The left carotid bifurcation was exposed and connective tissue surrounding the common carotid artery (CCA), external carotid artery (ECA), internal carotid artery (ICA) and occipital artery was cleared.

Particular care was taken to ensure that the vagus nerve was not disturbed. The occipital artery, superior thyroid artery and maxillary artery were electro-coagulated then divided. The ECA was ligated with 6-0 silk thread. 6-0 silk thread was looped loosely around the ICA proximal to the bifurcation with the pterygopalatine artery and 6-0 thread was also tied loosely around the ECA proximal to the ligature. The ECA was electro-coagulated distal to the ligature. A microvascular aneurysm clip was temporarily placed on the CCA to establish proximal control and tension was applied to the loose thread around the ICA to establish distal control. An arteriotomy was made in the ECA proximal to the ligature and distal to the loosely tied thread and then a 5-0 nylon monofilament (heat-blunted rounded tip; diameter 185 μ m) was inserted into the ECA and advanced to the carotid bifurcation. The loosely tied thread around the ECA was tightened to hold the filament in place. Tension on the thread around the proximal ICA was relieved and the ECA was divided and the stump brought in line with the ICA. The filament was advanced along the ICA (9 - 11mm distal to the carotid bifurcation) until the tip was positioned in the proximal part of the anterior cerebral artery (ACA) and therefore occluding the origin of the MCA (**Figure 11**). Sham occlusion was identical to that described above except that immediately following placement in the proximal ACA the filament was immediately withdrawn until the tip was positioned in the ECA.

In experiments requiring 24h reperfusion-recovery, the filament was withdrawn after the desired duration of occlusion to allow reperfusion through the previously occluded MCA. In mice undergoing sham occlusion, the filament was withdrawn from the ECA. The ECA stump was electro-coagulated proximal to the arteriotomy to prevent bleeding upon removal of the filament. The neck wound was then closed and sutured with 6-0 silk thread and 1ml sterile saline was administered by subcutaneous injection. Anaesthesia was discontinued and mice were allowed to regain consciousness (assisted by administration of oxygen via face mask) before being transferred to a temperature-controlled (30°C) incubator for 2h. Subsequently, mice were returned to their cages in the animal unit for the remainder of the recovery period where they were housed singly and given free access to food and water. Soft food was provided during recovery to aid post-surgery feeding. Throughout the recovery period, the condition of the mice was regularly monitored (at least 3 times daily) and recorded on an animal recovery form.

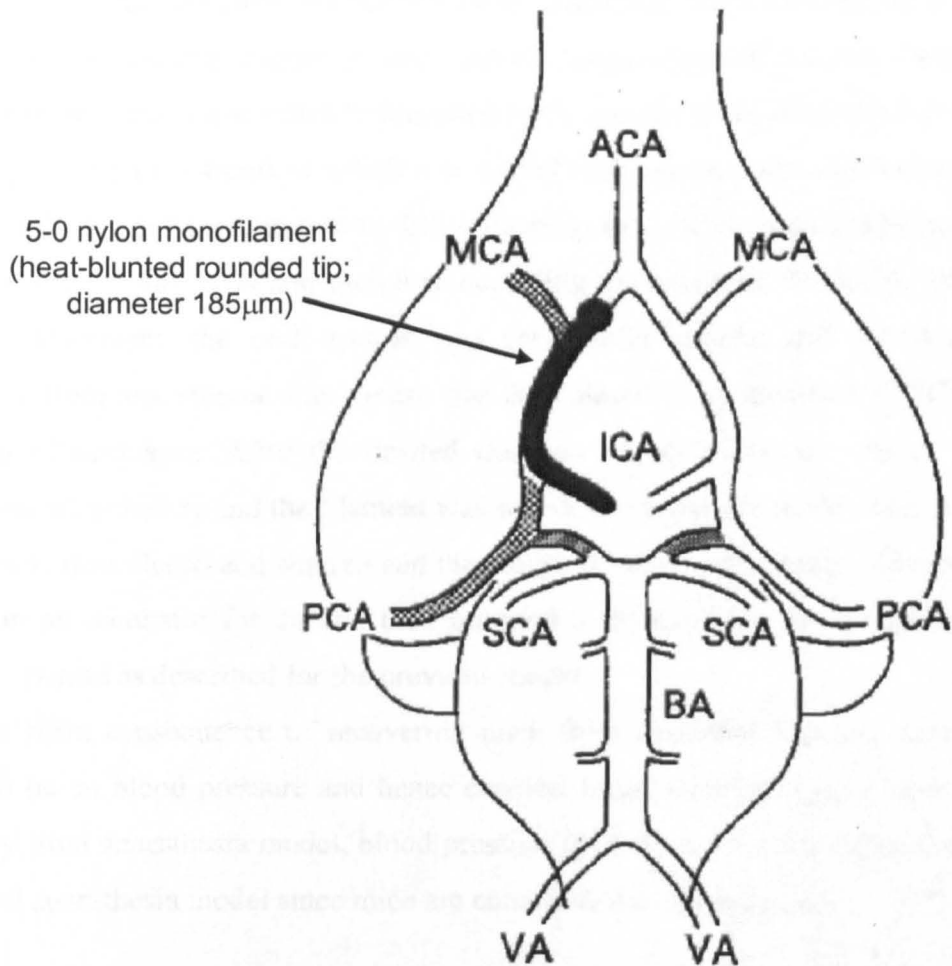


Figure 11. Intraluminal filament occlusion – surgical approach

A 5-0 filament was introduced into the ECA and advanced along the ICA 9 – 11mm distal to the carotid bifurcation. ACA – anterior cerebral artery; MCA – middle cerebral artery; ICA – internal carotid artery; PCA – posterior cerebral artery; SCA – superior cerebellar artery; BA – basilar artery; VA – vertebral artery. Figure adapted from Kitagawa *et al.*, 1998c.

2.3.2.2 Recovery from anaesthesia model

This model was previously characterised and performed by Dr Ailsa McGregor. Induction and maintenance of anaesthesia and monitoring of core temperature was achieved as described for the sustained anaesthesia model. The surgical approach was also similar to that described for the sustained anaesthesia model except for a few key differences. Following exposure and electro-coagulation of carotid vessels, an arteriotomy was made immediately proximal to the carotid bifurcation. An 8-0 filament (Ethilon), the tip (3 – 4mm) of which was coated with silicon paste was then advanced along the ICA until resistance was felt, indicating that the tip was positioned in the proximal part of the ACA and therefore occluding the origin of the MCA. Following filament placement, the neck wound was temporarily sutured and the mouse was recovered from anaesthesia. The mouse was then placed in an incubator (30°C) for the duration of occlusion. After the desired duration of occlusion, the mouse was re-anaesthetised as before and the filament was withdrawn to induce reperfusion. The neck wound was then closed and sutured and the mouse regained consciousness before being placed in an incubator for 2h and then returned to its cage for the remainder of the recovery period as described for the previous model.

The main consequence of recovering mice from anaesthesia during occlusion is likely to be on blood pressure and hence cerebral blood flow during occlusion. In the recovery from anaesthesia model, blood pressure is likely to be more stable than in the sustained anaesthesia model since mice are conscious during occlusion.

2.3.3 Monitoring of mean arterial blood pressure

Each mouse was placed in a supine position and an incision was made in the left femoral region. Connective tissue was removed to expose the femoral artery, vein and nerve. The femoral nerve was then carefully cleared from the artery and vein to provide unrestricted access to the artery. A 6-0 silk thread was tied tightly around the femoral artery and vein to establish distal control. Another 6-0 silk thread was then loosely tied around the femoral artery and vein close to the midline and tension applied to establish proximal control. Any small branches of the femoral artery which could cause potential bleeding were electro-coagulated. An arteriotomy was made in the femoral artery (in opposite side to vein) as near to the ligature as possible. A nylon cannula (internal diameter 0.50mm; external diameter 0.63mm) was then inserted into the femoral artery through the arteriotomy and glued in place. Tension was relaxed on the proximal ligature to restore blood flow through the femoral artery. The cannula was then attached to a blood pressure monitoring line and connected to a pressure transducer. Mean arterial blood pressure was monitored using a computer system receiving input from the pressure transducer.

2.3.4 Examination of cerebrovascular anatomy

The major arteries and branches of the circle of Willis were examined. Each mouse was placed in a Perspex chamber and anaesthesia was induced with 3% halothane in a mixture of 30% oxygen and 70% nitrous oxide. The mouse was then transferred to the operating surface where anaesthesia was maintained for the duration of surgery with 1.5% halothane in the same mixture delivered by a face mask. A sternotomy was performed to completely expose the heart. Approximately 20ml 0.9% saline was perfused through the vasculature via the left ventricle with an incision made in the right atrium to provide an outlet for perfused blood. A loss of colour in the liver, lungs and extremities and absence of blood from the exiting perfusate was used to indicate adequate removal of blood from the tissues. This was followed by perfusion of 5 - 10ml of carbon blue ink through the vasculature to aid visualisation of the major arteries. A change in colour of the extremities was used as an indicator to terminate perfusion. Following perfusion, the mouse was decapitated and the brain removed from the skull. Cerebrovascular anatomy was examined under a dissecting microscope and the presence or absence of posterior communicating arteries was recorded.

2.4 Assessment of neurological deficit

After 24h reperfusion and immediately prior to perfusion fixation, the neurological status of each mouse was assessed using a modification of the system described by Bederson *et al.* (1986). Neurological deficit was assessed according to a neurological grading score of increasing severity: 0 = no observable neurological deficit; 1 = failure to extend forelimb to grip cage-top; 2 = spontaneous circling; 3 = leaning/falling; 4 = no spontaneous movement.

2.5 Perfusion fixation

Mice were deeply anaesthetised with 3 - 4% halothane in a mixture of 30% oxygen and 70% nitrous oxide and a sternotomy was performed to completely expose the heart. Approximately 20ml 0.9% saline was perfused through the vasculature via the left ventricle with an incision made in the right atrium to provide an outlet for perfused blood. A loss of colour in the liver, lungs and extremities and absence of blood from the exiting perfusate was used to indicate adequate removal of blood from the tissues. This was followed by perfusion of approximately 20ml of 4% paraformaldehyde (PAM) solution through the vasculature. Rigidity of the extremities was indicative of successful fixation. Following fixation, the mice were decapitated. If fixation was considered successful, the brain was left in the skull and immersed in PAM for 24h. The brain was then removed from the skull and immersed in PAM for a further 24h after which paraformaldehyde was replaced with phosphate buffer solution. If fixation was not considered satisfactory, the brain was immediately removed from the skull and immersed in PAM for 48h followed by immersion in phosphate buffer.

2.6 Paraffin processing, embedding and cutting

2.6.1 Paraffin processing

2.6.1.1 Processing of whole brains

Paraformaldehyde-fixed brains were processed either as whole brains (Wellcome Surgical Institute, Glasgow) or as 4mm slices (Division of Neuroscience, Edinburgh). Whole brain processing was used in initial experiments involving intraluminal occlusion to enable serial sections to be cut through the entire brain and the relative positions of the eight coronal levels used for volumetric measurement to be assessed. Individual brains were placed in labelled embedding cassettes and processed in an automated processor using a protocol previously optimised for whole mouse brain processing as outlined in **Table 1**. After processing, brains were embedded in fresh paraffin, cooled and allowed to set prior to cutting.

Table 1. Paraffin processing protocol for whole brains

Station	Solution	Temp. (°C)	Duration (h)
1	70% ethanol	30	2
2	80% ethanol	30	2
3	95% ethanol	30	2
4	100% ethanol 1	30	2
5	100% ethanol 2	30	2
6	100% ethanol 3	30	2
7	100% ethanol 4	30	2
8	xylene/100% ethanol	30	2
9	xylene 1	30	2
10	xylene 2	30	2
11	paraffin 1	65	2
12	paraffin 2	65	2
13	paraffin 3	65	2

Brains were placed inside plastic processing cassettes and processed on a 26h cycle (13 stations x 2h each).

2.6.1.2 Processing of brain slices

An alternative method was used to process brains at the Division of Neuroscience, Edinburgh. Paraformaldehyde-fixed brains were placed into a mouse brain matrix and cut into two coronal blocks (4mm thick). Individual blocks were placed in labelled embedding cassettes, washed in running water and then cassettes were placed in a series of wide-bodied measuring jars containing the following solutions:

1. 70% ethanol – 2 x 30min
2. 90% ethanol – 2 x 30min
3. 100% ethanol – 2 x 30min
4. xylene – 2 x 30min
5. paraffin (65°C) – 2 x 30min
6. paraffin (65°C) – overnight

After processing, brain slices were embedded in fresh paraffin, cooled and allowed to set prior to cutting.

2.6.2 Cutting

Serial sections (6µm) were cut from paraffin-embedded whole brains or slices on a microtome. Particular care was taken to ensure sections were cut with satisfactory inter-hemispheric symmetry and ventro-dorsal alignment. Sections were stretched by surface tension on a water bath (approximately 40°C) and mounted on poly-L-lysine coated glass slides. Slides were dried on a hot-plate and then stored at room temperature in protective cases until required for staining.

2.7 Histological staining

Histological staining was used to enable observation of the general features of brain tissue (e.g. artefact, haemorrhage), examination of cell morphology and the identification of areas of ischaemic damage (*section 2.8.2*).

2.7.1 Haematoxylin and eosin

Haematoxylin and eosin (H & E) staining enables the assessment of the quality of tissue fixation/processing and identification of any artefact present. H & E is also an excellent stain for visualisation of cellular morphology and therefore differentiation of normal and ischaemic neurons is possible on the basis of morphological differences (*section*

2.8.2). Haematoxylin stains negatively-charged nucleic acids blue and is therefore primarily a nuclear stain, whereas eosin is a pink/red dye that stains acidophilic elements such as the cellular cytoplasm.

Paraffin-embedded sections (6 μ m) were de-waxed in an oven at 65°C for 20min and in xylene (10min)/HistoClear (2 x 10min) and then dehydrated in a series of alcohols: 100% (2 x 5min) → 90% (2min) → 70% (2min) before briefly rinsing in running water. Sections were immersed in haematoxylin for 30s – 3min depending on intensity required, rinsed briefly in running water and then differentiated in acid alcohol (10s) followed by a further rinse in running water (2min) and immersion in Scots Tap Water Solution (2min). Sections were then rinsed in running water (2min) before immersion in eosin (4min) and a further rinse in running water. Sections were then taken through a series of alcohols: 70% (2min) → 90% (2min) → 100% (2 x 5min). Finally, sections were cleared in xylene/HistoClear and covered with glass cover-slips.

2.7.2 Thionin

Thionin is a deep blue Nissl dye and therefore imparts a deep blue colour to basophilic components of the cell, particularly the nucleus, nucleoli and Nissl bodies found in the rough endoplasmic reticulum of the cytoplasm. Thionin staining demonstrates the grouping of nerve cell bodies into nuclei or layers, and gives information on the size of cell bodies and density of cell packing. Areas of ischaemic damage appear as areas of pallor on thionin stained tissue due to the shrinkage of the cell body and nucleus in ischaemic neurons.

Paraffin-embedded sections (6 μ m) were de-waxed in an oven at 65°C for 20min and in xylene (10min)/HistoClear (2 x 10min) and then dehydrated in a series of alcohols: 100% (2 x 5min) → 90% (2min) → 70% (2min) before briefly rinsing in running water. Sections were immersed in thionin for 20min and differentiated in 1% acetic acid (10s). Sections were then taken through a series of alcohols: 70% (2min) → 90% (2min) → 100% (2 x 5min). Finally, sections were cleared in xylene/HistoClear and covered with glass cover-slips.

2.8 Volumetric measurement of ischaemic damage

Volumetric measurement of ischaemic damage was carried out using a modification of a previously established technique that was developed and characterised in the laboratory for volumetric measurement of ischaemic damage after electro-coagulation of the MCA in rats (Osborne *et al.*, 1987). The major principles of this technique are (1) the use of thin coronal sections cut from paraffin-embedded brain, (2) histological staining of sections at anatomically defined stereotaxic levels through the brain, (3) transcription of areas of ischaemic damage on to scale diagrams representing the stereotaxic levels, (4) measurement and integration of areas of damage to calculate the volume of damage. Since intraluminal occlusion in the mouse was the model of focal ischaemia used in this thesis some modifications were necessary, most notably the use of scale diagrams derived from a stereotaxic mouse atlas.

2.8.1 Selection of sections at eight coronal levels

Eight coronal levels were selected from the stereotaxic mouse (C57Bl/6J) atlas of Hof *et al.* (2000) (1.6, 1.1, 0.2, -0.5, -1.1, -2.1, -3.6, -4.4mm with respect to bregma) (**Figure 12**). These levels were chosen based on the previous report by Osborne *et al.* (1987) demonstrating that area measurements at eight coronal levels were adequate to accurately calculate the volume of ischaemic damage. Sections (6µm) corresponding to the eight coronal levels were selected and stained with H & E. Distinct neuroanatomical landmarks defined which sections were chosen for each level (**Table 2**).

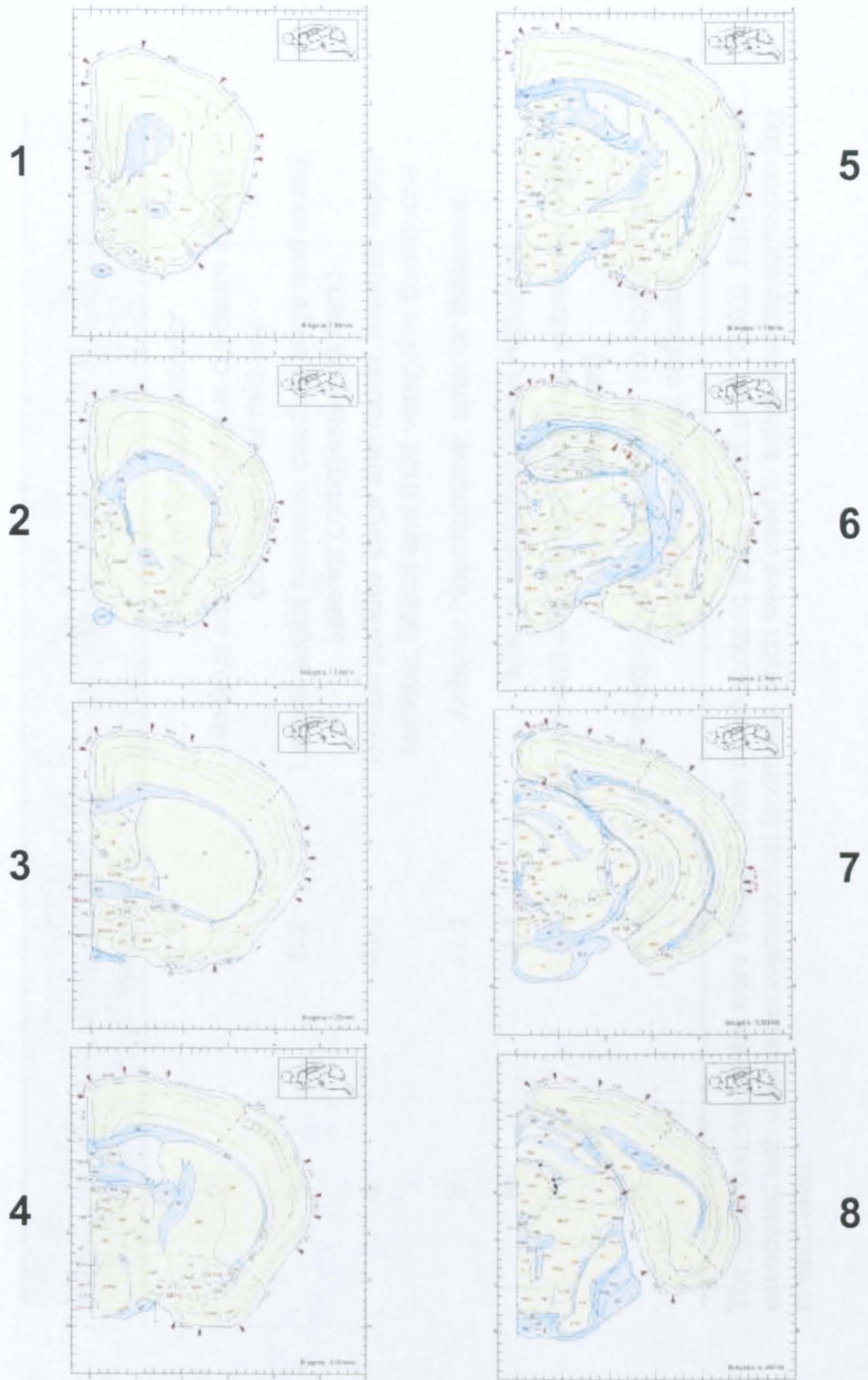


Figure 12. Coronal levels for quantification of ischaemic damage

Sections corresponding to the eight coronal levels were selected for haematoxylin and eosin staining. Areas of ischaemic damage were delineated at each coronal level and integrated with the distance between levels to calculate a volume of ischaemic damage. Diagrams of coronal levels are from the stereotaxic atlas of Hof *et al.*, (2000).

Table 2. Coronal levels and their neuroanatomical landmarks

Coronal level	Stereotaxic co-ordinates (relative to bregma) (mm)	Neuroanatomical landmarks
1	1.6	End of forceps anterior
2	1.1	Nucleus accumbens; corpus callosum almost continuous at mid-line
3	0.2	Lateral septal nucleus; caudate large and round; anterior commissure as band
4	-0.5	Globus pallidus large and round; minimal septal nucleus; lateral and third ventricles continuous
5	-1.1	Anterior hippocampus; anterior thalamus
6	-2.1	Medial habenula; lateral habenula
7	-3.6	Temporal and full hippocampus; substantia nigra (pars compacta)
8	-4.4	Peri-aqueductal grey matter, no hippocampus; subiculum; superior colliculus

The eight coronal levels were selected from the stereotaxic atlas of Hof *et al.* (2000). Each level is associated with distinct neuroanatomical landmarks which were used to select sections corresponding to each level.

2.8.2 Identification of areas of ischaemic damage

Areas of ischaemic damage were readily identifiable on H & E stained sections on account of characteristic cell morphology and tissue changes (**Figure 13**). Notably, areas of ischaemic damage contain neurons that typically display a shrunken and triangular cell body and nucleus and intensely eosinophilic cytoplasm. Pallor and vacuolation of the neuropil are also observed in areas of ischaemic damage. In contrast, undamaged tissue is composed of compact neuropil and contains neurons that typically display a large, round nucleus and cell body. Accordingly, boundaries between areas of ischaemic damage and morphologically normal tissue could be delineated.

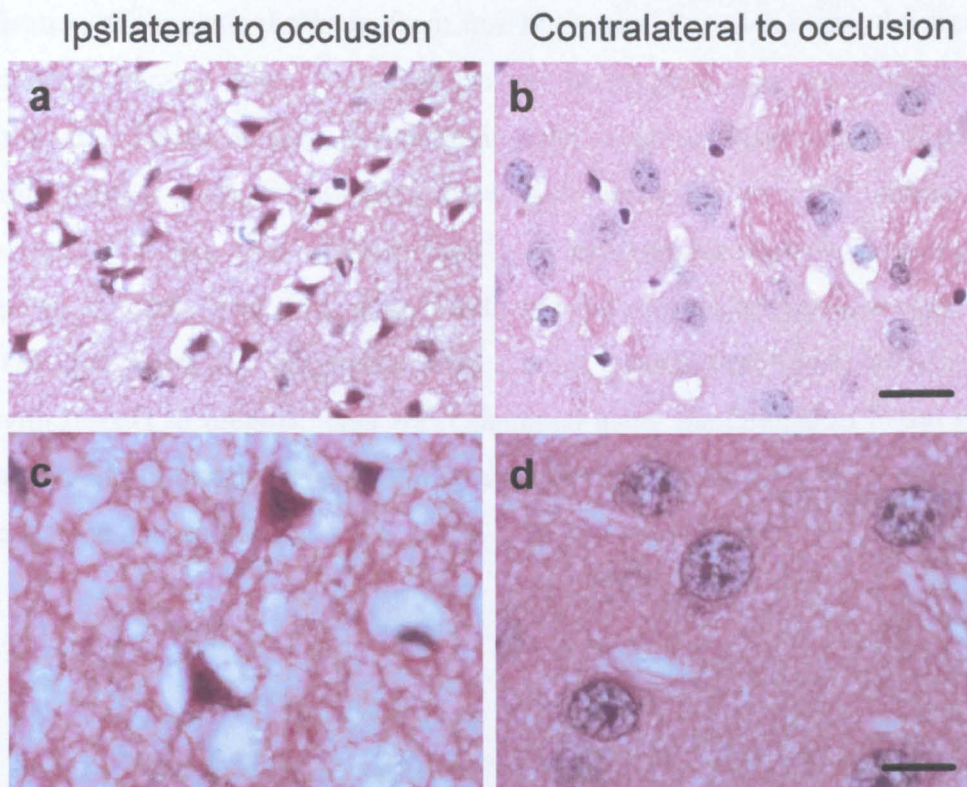


Figure 13. Identification of areas of ischaemic damage

Areas of ischaemic damage (a,c) are characterised by shrunken, eosinophilic neurons surrounded by a vacuolated neuropil. In contrast, undamaged tissue (b,d) is composed of compact neuropil and contains neurons with large, round cell bodies and thin cytoplasm. Scale bar (a,b), 25 μ m; (c,d), 10 μ m.

2.8.3 Calculation of volume of ischaemic damage

Scale diagrams representing the eight coronal levels were reproduced from the stereotaxic atlas of Hof *et al.* (2000) at 35% original size (x9 actual size of mouse brain) and arranged on an A4 sheet. A master copy was kept from which all copies were made using the same photocopier to ensure reproducibility. Areas of ischaemic damage were identified as described above and delineated on to the scale diagrams representing the eight coronal levels. The scale diagrams were placed on a light box, covered with a Perspex block to prevent paper curl and then digitised on an MCID image analysis system. The scale diagrams were superimposed on a stereotaxic grid which enabled direct calibration of distance from the digitised images and therefore accounted for the magnification of the scale diagrams from true brain size. For each brain, the area of the hemisphere at coronal level 3 (0.2mm rostral to bregma) was measured to verify reproducibility of scale diagram photocopying and image analyser set-up. The areas of ischaemic damage were then transcribed and measured at each coronal level. Approximation of the total volume (mm^3) of hemispheric ischaemic damage was achieved by integration of areas (mm^2) with the distance (mm) between each coronal level. The end points for integration were 2.9mm (rostral limit) and -4.9mm (caudal limit) with respect to bregma. This was calculated using the GraphPad Prism software package which computes the area under a curve representing the area of ischaemic damage at each coronal level.

2.9 Immunohistochemistry

2.9.1 Antibodies

Initial characterisation of primary antibodies was performed to determine the concentrations which produced optimal immunostaining in different tissues as outlined in **Table 3**. The species that the primary antibody was raised in determined the type of secondary antibody used which in turn determined the species of normal sera used in blocking solution to prevent non-specific binding of the secondary antibody (**Table 3**). For each antibody, control for the specificity of immunostaining was achieved by omission of primary antibody.

2.9.2 Avidin-biotin (ABC) method of immunohistochemistry

The “ABC” method of immunohistochemistry was used for all peroxidase-based staining procedures (Hsu *et al.*, 1981) (**Figure 14**). The extremely high affinity binding of avidin to biotin underlies this method. (1) The first step of the procedure is to incubate the section with primary antibody raised against the antigenic site(s) of interest. (2) A biotin-conjugated secondary antibody is then added which binds to the primary antibody and introduces many biotin molecules localised to the site of the antigen. (3a) An enzyme complex is formed consisting of avidin and the biotinylated enzyme peroxidase (Vectastain ABC kit). (4a) This complex is added to the section where it binds to the biotin on the secondary antibody localised at the antigenic site(s) thus amplifying the original signal. The final stage is the addition of an enzyme substrate (diaminobenzidine) which the peroxidase converts to a readily visible brown deposit that can be viewed using conventional light microscopy. Advantages of using this protocol include increased sensitivity and lower background staining. To amplify the signal further, a Vectastain ABC Elite kit can be used to form the avidin-biotinylated peroxidase complex. The Elite complex provides a stronger signal since the biotinylated peroxidase enzyme contains a greater number of peroxidase molecules.

The high affinity binding of avidin and biotin also underlies the method used for fluorescent immunohistochemistry. However, at step (3) (**Figure 14**), an avidin-conjugated fluorochrome (3b) is added so that fluorochrome is localised at the antigenic site(s) through binding of avidin to the biotin on the secondary antibody (4b). The fluorochrome can then be visualised using a fluorescent microscope.

Table 3. Primary antibodies, optimised concentrations and their corresponding secondary antibodies and blocking serum

Primary Antibody	Supplier	Species raised in	Concentration			Secondary antibody	Species raised in	Normal serum in blocking solution
			Mouse		Human			
			DAB	Fluorescence	DAB			
ApoE	Chemicon	Goat	1:5000	1:1000		Anti-goat	Horse	NHS
GFAP	Chemicon	Mouse		1:100		Anti-mouse	Horse	NHS
Neu-N	Chemicon	Mouse		1:100		Anti-mouse	Horse	NHS
Rabaptin-5	Santa Cruz	Goat	1:100E	1:50	1:50E	Anti-goat	Horse	NHS
Rab4	Santa Cruz	Rabbit	1:200E	1:50	1:50E	Anti-rabbit	Goat	NGS

The concentration of each primary antibody was optimised for the specific staining method (peroxidase-DAB or fluorescence) and the type of tissue (mouse or human). A specific species of blocking serum was used for each primary (and corresponding secondary) antibody to prevent non-specific binding of the secondary antibody. E, Vectastain Elite ABC kit used; NHS, normal horse serum; NGS, normal goat serum.

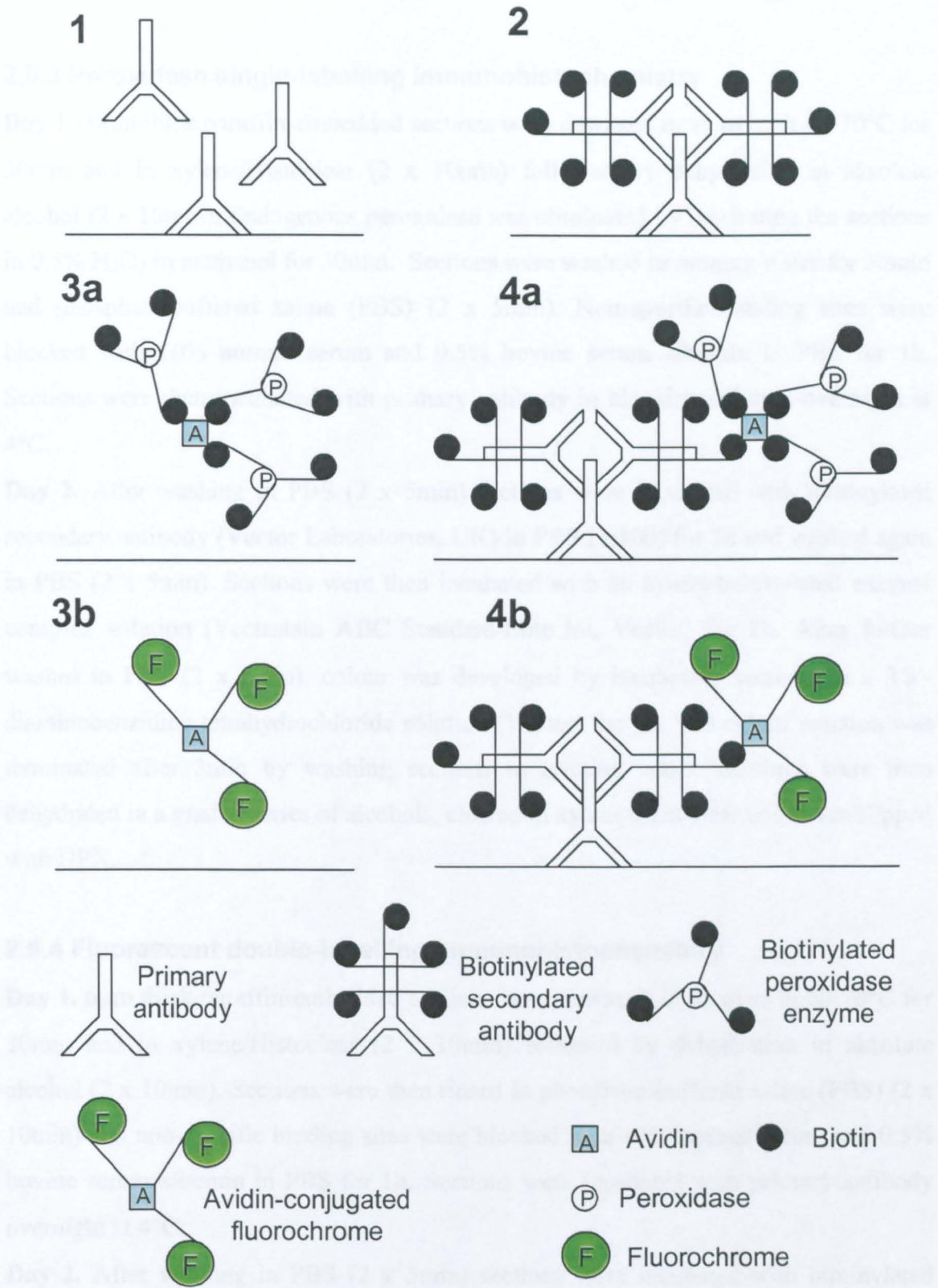


Figure 14. "ABC" immunohistochemistry method

(1) Tissue is incubated with primary antibody which binds to the antigen of interest. (2) A biotinylated secondary antibody is added which binds to the primary antibody. (3a) An avidin-biotinylated peroxidase complex is formed and added to the section where (4a) the avidin binds to the biotinylated secondary antibody. A chromogenic enzyme substrate (e.g. DAB) is then added that is converted to a readily visible deposit by the peroxidase. (3b) The procedure is similar for fluorescent immunostaining except an avidin-conjugated fluorochrome (e.g. fluorescein) is added which binds to the secondary antibody (4b).

2.9.3 Peroxidase single-labelling immunohistochemistry

Day 1. 6µm thick paraffin-embedded sections were dewaxed in an oven at 60-70°C for 30min and in xylene/Histoclear (2 x 10min) followed by dehydration in absolute alcohol (2 x 10min). Endogenous peroxidase was eliminated by incubating the sections in 0.5% H₂O₂ in methanol for 30min. Sections were washed in running water for 30min and phosphate-buffered saline (PBS) (2 x 5min). Non-specific binding sites were blocked with 10% normal serum and 0.5% bovine serum albumin in PBS for 1h. Sections were then incubated with primary antibody in blocking solution overnight at 4°C.

Day 2. After washing in PBS (2 x 5min) sections were incubated with biotinylated secondary antibody (Vector Laboratories, UK) in PBS (1:100) for 1h and washed again in PBS (2 x 5min). Sections were then incubated with an avidin-biotinylated enzyme complex solution (Vectastain ABC Standard/Elite kit, Vector) for 1h. After further washes in PBS (2 x 5min), colour was developed by incubating sections in a 3'3'-diaminobenzidine tetrahydrochloride solution (Vector) for 1h. The colour reaction was terminated after 3min by washing sections in running water. Sections were then dehydrated in a graded series of alcohols, cleared in xylene/Histoclear and cover-slipped with DPX.

2.9.4 Fluorescent double-labelling immunohistochemistry

Day 1. 6µm thick paraffin-embedded sections were dewaxed in an oven at 60-70°C for 30min and in xylene/Histoclear (2 x 10min) followed by dehydration in absolute alcohol (2 x 10min). Sections were then rinsed in phosphate-buffered saline (PBS) (2 x 10min) and non-specific binding sites were blocked with 10% normal serum and 0.5% bovine serum albumin in PBS for 1h. Sections were incubated with primary antibody overnight at 4°C.

Day 2. After washing in PBS (2 x 5min) sections were incubated with biotinylated secondary antibody in PBS (1:100) for 1h and washed again in PBS (2 x 5min). Sections were then incubated with fluorochrome-conjugated avidin D (Vector) (1:100 in PBS) for 1h. For the previous stage and for the remainder of the protocol sections were covered with aluminium foil to prevent bleaching of the fluorochrome. Sections were further washed in PBS (2 x 10min) before non-specific binding sites were blocked with 10% normal serum (relevant for species biotinylated secondary antibody is raised in)

and 0.5% bovine serum albumin in PBS for 1h. Blocker was drained off and sections were incubated with the second primary antibody overnight at 4°C.

Day 3. After washing in PBS (2 x 5min) sections were incubated with biotinylated secondary antibody in PBS (1:100) for 1h and washed again in PBS (2 x 5min). Sections were then incubated with fluorochrome-conjugated avidin D (1:100 in PBS) for 1h. The fluorochrome chosen at this stage possessed different excitation and emission wavelengths than the fluorochrome used to label the first primary antibody. For example, if fluorescein was used to label the first primary antibody, Texas red was used as the fluorochrome to label the second primary antibody. This produces the double-labelling effect whereby sites localised with each primary antibody emit a different wavelength and hence colour of light when viewed with a fluorescent microscope. Sections were then thoroughly washed in PBS (3 x 5min), cover-slipped with non-fading aqueous mounting medium and stored in the dark at 4°C.

2.9.5 GFP fluorescence

In tissue containing green fluorescent protein (GFP) derived from adenoviral vector injection, 6µm paraffin-embedded sections were de-waxed in xylene (2 x 10min) and cover-slipped with non-fading aqueous mounting medium.

2.9.6 Quantification of immunostaining

2.9.6.1 Volumetric measurement of immunoreactivity

The volume of immunoreactivity was quantified similarly to volumetric assessment of ischaemic neuronal damage (*section 2.8.3*). Clearly defined areas of immunoreactivity with identifiable boundaries were delineated on to scale diagrams (x9 actual size) from the stereotaxic mouse atlas of Hof *et al.* (2000), representing the eight coronal levels previously described (*section 2.8.1*). Scale diagrams were then digitised on an MCID image analysis system and approximation of the total volume of immunoreactivity was achieved by integration of areas with the distance between each coronal level.

2.9.6.2 Semi-quantitative assessment of immunoreactivity

The degree of immunoreactivity in a defined region was classified using a scoring system as follows: 0 = no cellular staining; 1 = <35% cells stained; 2 = 35% - 70% cells stained; 3 = >70% cells stained.

2.10 Measurement of apoE levels

An enzyme-linked immunosorbent assay (ELISA) technique was used to determine the brain tissue levels of apoE following stereotaxic injections of adenoviral vector or vehicle. This assay is based on the antibody sandwich principle (**Figure 15**). First, a capture antibody raised against the protein of interest is bound to a microtiter plate to create the solid phase. Samples and standards are then incubated with the solid phase antibody, which captures the protein. A detection antibody is then added that recognises a different epitope of the protein and completes the sandwich. Addition of a conjugated secondary antibody (e.g. HRP-conjugated) is then followed by incubation with a substrate solution such that colour develops in proportion to the amount of bound protein. Colour development is then stopped and the intensity of the colour is measured. The major advantage of the sandwich ELISA technique is its high sensitivity to detect even very low levels of protein.

Procedures using tissue from adenoviral-treated mice were performed in a fume hood. 1% Virkon and 100% alcohol were available to hand at all times.

2.10.1 Tissue harvesting

Each mouse was deeply anaesthetised with 3 - 4% halothane in a mixture of 30% oxygen and 70% nitrous oxide and a sternotomy was performed to completely expose the heart. Approximately 20ml of cold (4°C) 0.9% saline was perfused through the vasculature via the left ventricle with an incision made in the right atrium to provide an outlet for perfused blood. A loss of colour in the liver, lungs and extremities and absence of blood from the exiting perfusate was used to indicate adequate removal of blood from the tissues. The brain was removed from the skull, placed in a mouse brain matrix and a 3mm coronal slice of tissue was cut containing the bilateral injection tracts. In the 3mm slice, tissue surrounding each injection tract was then dissected out on ice and each tissue sample was then frozen in liquid nitrogen and stored at -80°C until homogenisation.

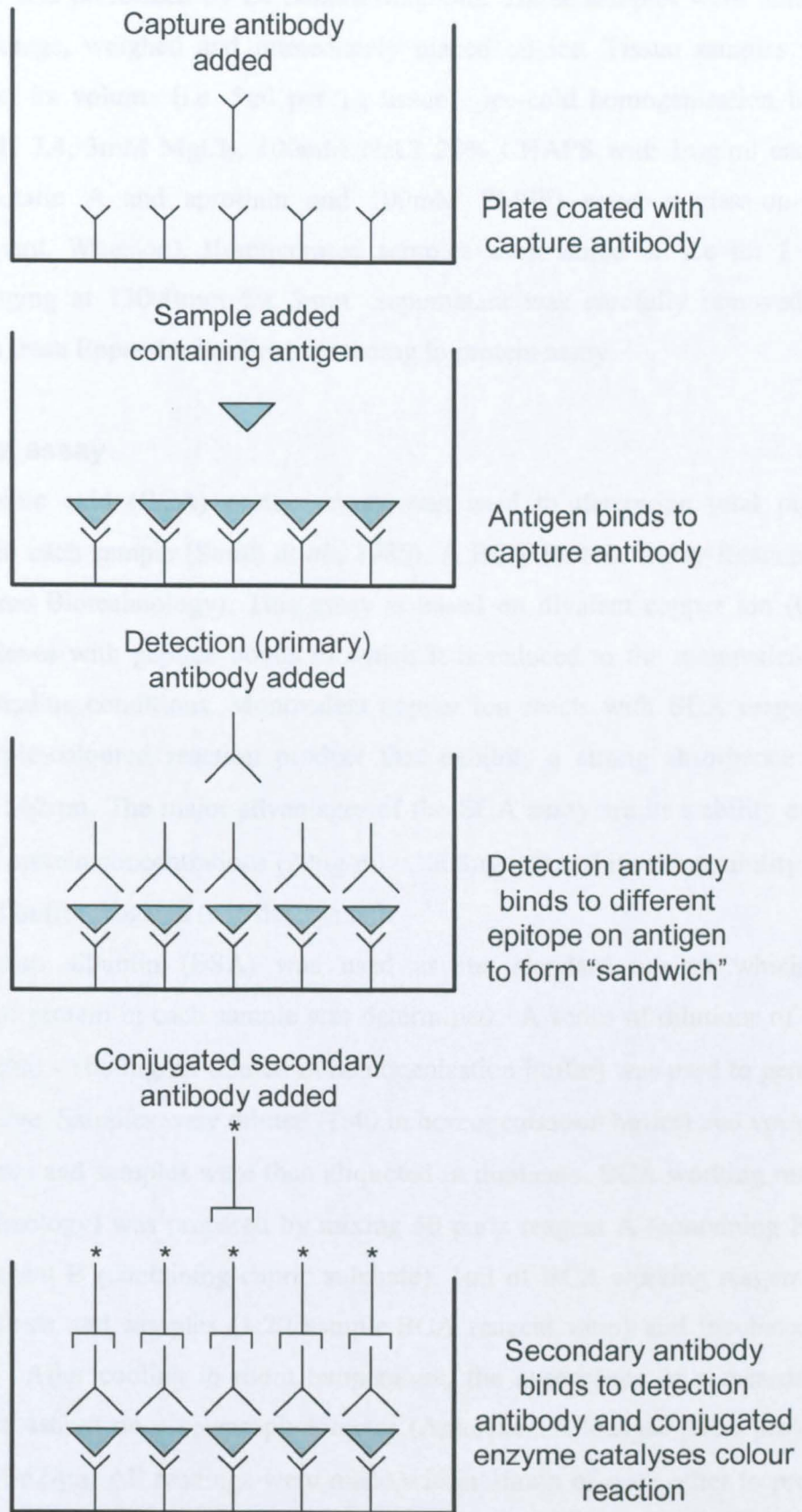


Figure 15. Sandwich ELISA method

2.10.2 Sample homogenisation and protein extraction

This procedure was performed by Dr Sandra Magnoni. Tissue samples were removed from -80°C storage, weighed and immediately placed on ice. Tissue samples were homogenised in 5x volume (i.e. 5ml per 1g tissue) ice-cold homogenisation buffer (25mM Tris pH 7.4, 3mM MgCl₂, 100mM NaCl, 20% CHAPS with 1mg/ml each of leupeptin, pepstatin A and aprotinin and 100mM PMSF) using a glass-on-glass homogeniser (1ml, Wheaton). Homogenised samples were stored on ice for 1 hour before centrifuging at 13000rpm for 5min. Supernatant was carefully removed and transferred to a fresh Eppendorf before proceeding to protein assay.

2.10.3 Protein assay

The bicinchoninic acid (BCA) protein assay was used to determine total protein concentration in each sample (Smith *et al.*, 1985). A BCA Protein Assay Reagent Kit was used (Pierce Biotechnology). This assay is based on divalent copper ion (Cu²⁺) forming complexes with peptide bonds in which it is reduced to the monovalent ion (Cu⁺) under alkaline conditions. Monovalent copper ion reacts with BCA reagent to produce a purple-coloured reaction product that exhibits a strong absorbance at a wavelength of 562nm. The major advantages of the BCA assay are its stability over a broad range of protein concentrations (20µg/ml - 2000µg/ml) and its compatibility with a wide range of buffer reagents (e.g. detergents).

Bovine serum albumin (BSA) was used as the standard against which the concentration of protein in each sample was determined. A series of dilutions of BSA standard (50µg/ml - 1000µg/ml diluted in homogenisation buffer) was used to generate the standard curve. Samples were diluted (1:40 in homogenisation buffer) and vortexed. 50µl of standards and samples were then aliquoted in duplicate. BCA working reagent (Pierce Biotechnology) was prepared by mixing 50 parts reagent A (containing BCA) with 1 part reagent B (containing cupric sulphate). 1ml of BCA working reagent was added to standards and samples (1:20 sample:BCA reagent ratio) and incubated for 30min at 37°C. After cooling to room temperature, the absorbance of standards and samples was measured on a spectrophotometer (Amersham Ultraspec 3100 pro) at a wavelength of 562nm. All readings were made within 10min of each other to prevent error due to continuing colour development.

To determine the protein concentration of each sample, a standard curve was prepared by plotting the mean absorbance at 562nm of each BSA standard against its concentration. The standard curve was used to determine the protein concentration of each unknown sample. As each sample was run in duplicate, the protein concentration for each sample was calculated by determining the protein concentration of each replicate from the standard curve and computing the mean of the duplicates.

2.10.4 ELISA

This procedure was performed by Mr Andrew Wong. A 96-well plate (Nunc Maxisorp) was first coated (100 μ L/well) with the capture antibody (rabbit anti-human apolipoprotein E (1:5000), Dako, diluted in 16mM carbonate/34mM bicarbonate buffer pH 9.6) and incubated overnight (>17h) at 4°C. Following washes (x3) with phosphate buffered saline (PBS), blocking solution (2% bovine serum albumin (BSA) in PBS) was added (150 μ l/well) and the plate incubated for 1h at 37°C. After 3 washes in 1% PBS-Tween 20 (PBST), apoE standard (recombinant human apolipoprotein E3, Chemicon) was diluted (0.25ng/ml – 40ng/ml in sample diluent [1% BSA in PBS]) and added to five columns of wells (100 μ l/well). Frozen samples were thawed on ice, diluted in sample diluent and plated in triplicate (100 μ l/well). The plate was then sealed and incubated for 2h at 37°C. The detection antibody (goat polyclonal anti-apolipoprotein E, Chemicon, 1:2000 in sample diluent) was added (100 μ l/well) after further washes in PBST (x3) and the plate incubated for 1h at 37°C. Washes in PBST (x3) were then followed by addition (100 μ l/well) of horse radish peroxidase conjugated secondary antibody (rabbit anti-goat HRP conjugated IgG, Dako, 1:5000 in sample diluent) and the plate incubated for 1h at 37°C. After washes in PBST (x4) and PBS (x2), the chromogen o-phenylenediaminedihydrochloride (OPD) was added (100 μ l/well) at room temperature. The colour reaction was terminated after 10min by addition of 1M sulphuric acid (100 μ l/well). Absorbance was read at a wavelength of 492nm on a plate reader.

To calculate the apoE concentrations in each of the samples a standard curve was generated by plotting the absorbance of each apoE standard against its concentration. The apoE concentration of the unknown samples was then derived from the standard curve. As each sample was run in triplicate, the apoE concentration for each sample was calculated from the three replicates by determining the apoE concentration of each replicate from the standard curve and computing the mean of these values. Knowledge

of the total protein concentration of the sample (determined in protein assay above) then enabled apoE concentration for each sample to be expressed as ng apoE/mg total protein.

2.11 Measurement of local cerebral blood flow

2.11.1 Utility of ^{14}C -iodoantipyrine as a radioactive tracer

Carbon-14 labelled iodoantipyrine (^{14}C -IAP) was used as a radioactive tracer. There are several properties of this particular isotope which confer its suitability for use in measuring cerebral blood flow:

1. high lipid solubility – facilitates diffusion across blood brain barrier
2. blood-tissue partition co-efficient is uniform throughout the brain
3. slowly metabolised by the liver (6% per hour) therefore remains stable over the experimental period
4. solubility in blood does not vary with the haematocrit
5. non-volatile
6. ^{14}C has a very long half-life (5730 years) – facilitates preparation of permanent autoradiograms
7. commercially available

2.11.2 Administration of ^{14}C -IAP

^{14}C -IAP was administered by intraperitoneal injection. Intraperitoneal administration of ^{14}C -IAP results in a linear increase in the arterial concentration of ^{14}C -IAP with time, at least until 2min after injection (Maeda *et al.*, 2000) (**Figure 16**). This represents an excellent ramp delivery of tracer and therefore eliminates the unwanted effects of equilibration of rapidly perfused tissue with the blood compartment. In consideration of the above, $15\mu\text{Ci}$ ^{14}C -IAP in 0.15ml physiological saline was injected into the intraperitoneal cavity and allowed to circulate for 2min. The injection was given in the right side of the supine mouse to minimise the risk of puncturing the bladder and a gauze pad was placed under the mouse to aid uptake of isotope into the peritoneal vessels and prevent reflux through the injection site. Heart rate and respiratory rate were monitored closely immediately prior to ^{14}C -IAP administration since the degree of sympathetic activity is likely to influence the dynamics of isotope uptake.

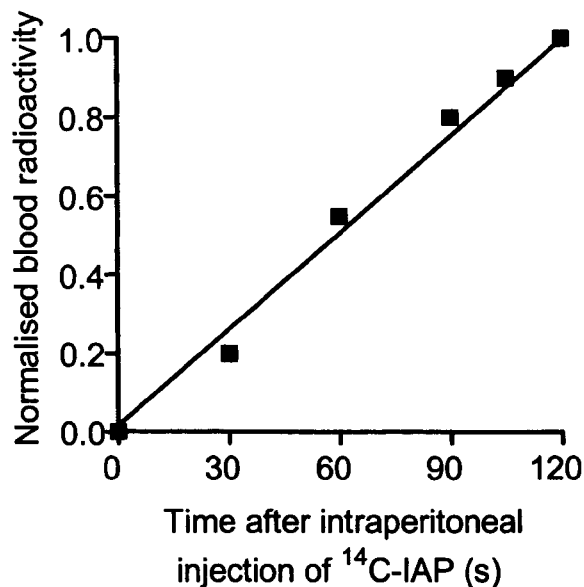


Figure 16. Representative time course of arterial ¹⁴C radioactivity after intraperitoneal injection of ¹⁴C-IAP

Intraperitoneal injection of 15 μ Ci ¹⁴C-IAP results in a linear increase in ¹⁴C radioactivity in arterial blood at least until 2min after administration of the tracer. Adapted from Maeda *et al.*, 2000.

2.11.3 Measurement of terminal heart blood sample ¹⁴C-IAP concentration

Exactly 2min after administration of ¹⁴C-IAP, the experiment was terminated by decapitation and the torso was immediately immersed in liquid nitrogen. The torso was then slightly thawed in a water bath (37°C) and a vertical incision was cut in the chest wall to expose the heart. An incision was made in the left ventricle of the heart and 3 samples of frozen blood were collected on to pre-weighed filter paper discs placed inside glass scintillation vials. The glass vials containing the filter paper discs with heart blood samples were then re-weighed to determine the exact weight of the blood sample. Colour was bleached from the blood sample by addition of 0.4ml hydrogen peroxide directly on to the filter disc. 1ml distilled water was similarly added and the vial left at room temperature overnight. The following day, 10ml scintillant (EcoScint) was added to the vial and left to stand at room temperature for at least 2h. To determine ¹⁴C activity in the blood sample, the vial was placed in a liquid scintillation counter and the number of disintegrations per minute (dpm) was counted during a 10min period. This was repeated twice and the mean number of dpm was calculated from the three measurements of ¹⁴C radioactivity. The activity of the blood sample can be expressed in standard units (Curie, Ci) using the following conversion:

$$1\text{nCi} = 2220\text{dpm}$$

The concentration of ^{14}C -IAP (nCi/ml) in the terminal blood sample was then calculated by dividing the activity of the blood sample by its volume (calculated from the weight of the blood sample by assuming a specific gravity of 1.05g/ml for blood).

2.11.4 Measurement of local brain tissue ^{14}C -IAP concentration

2.11.4.1 ^{14}C autoradiography

Upon termination of the experiment by decapitation, the brain was immediately removed from the skull and immersed in chilled isopentane (-42°C) for 2min. Concurrently, the torso was immersed in liquid nitrogen (*section 2.11.3*). The frozen brain was then embedded in cryomatrix and covered with a thin film of cryoprotectant. $20\mu\text{m}$ coronal brain sections were cut on a cryostat at -22°C . Three of every ten sections were mounted on glass coverslips and dried on a hot plate at 60°C . Sections were then enclosed in an X-ray cassette along with a set of 13 pre-calibrated ^{14}C plastic resin standards with increasing ^{14}C concentration. Autoradiograms of the plastic standards and coronal brain sections were generated by exposure to ^{14}C sensitive X-ray film (Kodak Biomax MR1 film) for 5 days. Following 5 days exposure, autoradiograms were developed in a dark room using an automated processor.

2.11.4.2 Densitometric analysis of autoradiograms

Measurement of ^{14}C -IAP concentration in discrete brain regions was carried out on an MCID image analysis system. An autoradiogram was placed on a light box with stable light intensity, covered with a Perspex block to prevent curling and a digitised image was produced on screen. A standard curve was then generated by measuring the relative optical densities (RODs) of each of the ^{14}C plastic standards. Additionally, the ROD of a background area of the film was measured; essentially acting as standard zero (i.e. the ROD reading when the concentration of ^{14}C is zero). In general, the concentration of standard 1 was too low to darken the X-ray film during a 5 day exposure period and therefore was not used to generate the standard curve. Furthermore, the typical range of ^{14}C concentrations in the mouse brain was between those represented by standards 2 to 5 (44 – 271nCi/g). Consequently, the standard curve was generated from the ROD measurements of film background and ^{14}C standards 2 to 5 (**Figure 17**). Linear interpolation was used to fit a line to the standard curve.

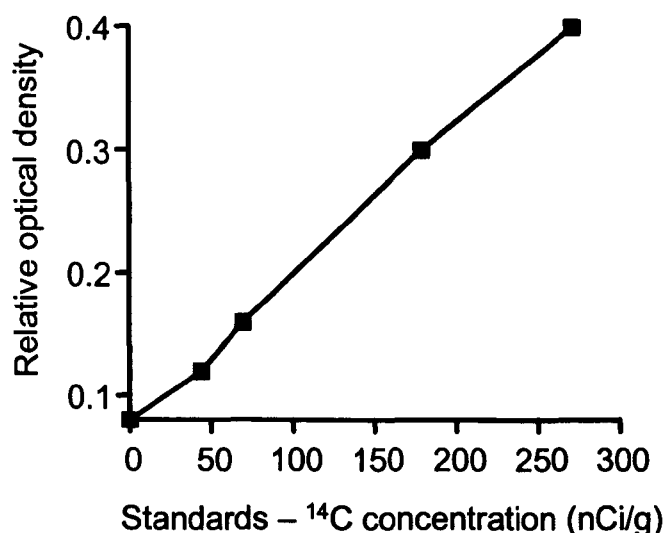


Figure 17. Representative standard curve of relative optical density readings from ¹⁴C standards

The standard curve was generated from a background reading and standards 2 to 5 (44, 70, 179 and 271 nCi/g respectively).

Local tissue concentrations of ¹⁴C-IAP were determined from ROD measurements in 12 neuroanatomically-defined regions: frontal cortex; motor cortex; somatosensory cortex; insular cortex; dorsolateral caudate; ventromedial caudate; hippocampus (CA1); dorsolateral thalamus; ventromedial thalamus; hypothalamus; auditory cortex; and cerebellum. RODs were determined in the 12 regions of interest ipsilateral and contralateral to occlusion by computing the mean of the measurements from 6 adjacent coronal sections at each anatomical locus.

2.11.5 Calculation of local cerebral blood flow

Calculation of local cerebral blood flow (LCBF) using the ¹⁴C-IAP method requires the determination of three variables:

1. brain tissue:blood partition coefficient for ¹⁴C-IAP (0.8) (Sakurada *et al.*, 1978)
2. local brain tissue ¹⁴C-IAP concentration at the end of the experiment
3. profile of ¹⁴C-IAP concentration in arterial blood during the experiment

Determination of the second of the above variables is relatively straight-forward and is achieved as described previously (*section 2.11.4*). However, in the mouse, ascertaining the history of ¹⁴C-IAP arterial blood concentration is more challenging. In larger animals, such as rats and cats, cannulation of blood vessels for intravenous infusion of ¹⁴C-IAP and repeated arterial blood sampling during the experimental period is

practicable. In the mouse, however, cannulation of multiple vessels is technically very demanding and substantially extends the period of anaesthesia. Furthermore, due to the small blood volume of the mouse, repeated arterial blood sampling may initiate inadvertent systemic hypotension. To avoid these difficulties, Maeda *et al.* (2000) described a method that combined intraperitoneal administration of ^{14}C -IAP with sampling of arterial heart blood at the end of the experiment. Using this method, the concentration of ^{14}C -IAP in the heart sample did not differ significantly from that measured from the terminal arterial blood sample obtained by repeated sampling. Since arterial blood ^{14}C -IAP concentration rises linearly during the experiment, knowledge of terminal arterial blood ^{14}C -IAP concentration can be used to construct a time-course of ^{14}C -IAP concentration in arterial blood during the experiment.

Absolute values of local cerebral blood flow were computed by MCID image analysis software based on the operational equation (Figure 18). An arterial input curve was generated using the known ^{14}C -IAP radioactivities (in dpm) in blood at the beginning (0s) and end (120s) of the experiment and assuming that concentration of ^{14}C -IAP at 60s was half that measured at 120s.

Generation of an arterial input curve followed by determination of local brain tissue ^{14}C -IAP concentrations (section 2.11.4) then enabled calculation of local cerebral blood flow (ml/100g/min) using the operational equation (Sakurada *et al.*, 1978) (Figure 18).

$$C_i(T) = \lambda K \int_0^T C_a(t) e^{-K(T-t)} dt$$

Figure 18. Operational equation for calculation of cerebral blood flow

Operational equation as described by Sakurada *et al.* (1978) for determination of the rate of cerebral blood flow. $C_i(T)$ is the tissue concentration of tracer at time T after administration of the tracer; λ is the brain tissue:blood partition coefficient; K is a constant equal to $f/m/\lambda W$ where f/W is the flow rate f (ml/min) divided by the tissue mass W (g) and m is a constant equal to 1 that reflects unrestricted diffusion of tracer from the blood compartment to brain tissue compartment. t is the variable time. The rate of cerebral blood flow per unit mass of tissue (f/W) is calculated from the local brain tissue concentration of tracer at time T [$C_i(T)$] determined from densitometric analysis of autoradiograms, the concentration of tracer in arterial blood from times 0 – T , and the brain tissue:blood partition coefficient for the tracer (0.8 for ^{14}C -IAP).

2.12 Adenoviral vectors

Procedures involving adenoviral vectors were approved by the Health and Safety Executive and had local approval from the Advisory Committee on genetically modified work. Second generation recombinant adenoviral vectors containing the gene encoding human apolipoprotein E3 (Ad-*APOE*) or the gene encoding green fluorescent protein (GFP) (Ad-GFP) were obtained through collaboration with Dr Andy Baker (University of Glasgow, UK) and Dr George Dickson (Royal Holloway University, UK). Vectors were constructed at Royal Holloway and have been described in detail previously (Harris *et al.*, 2002). These second generation viral vectors were generated using adenovirus serotype 5 and had the E1 and E3 regions of the viral genome and the adenovirus DNA polymerase (E2b) gene deleted. Deletion of these viral elements underlies the principal advantage of second generation (E1⁻, E3⁻, polymerase⁻) vectors compared to conventional first generation vectors, which is the reduced potential for viral gene expression and diminished risk of an immune response. The transgene was located in the E1 region and expression was driven by the full human cytomegalovirus (CMV) promoter/early enhancer (**Figure 19**). Adenoviral vectors were stored in viral storage buffer (10% glycerol in PBS) at -80°C until use when they were thawed on ice prior to injection.

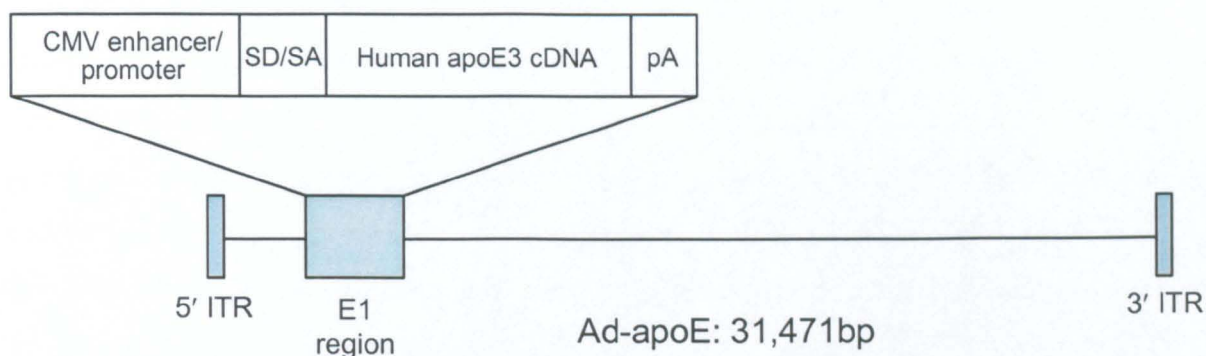


Figure 19. Schematic representation of adenoviral vector containing *APOE* gene
The transgene expression cassette is located in the E1 region of the viral genome and contains the human CMV promoter/early enhancer driving expression of the human apoE cDNA followed by an SV40 polyadenylation signal (pA). Figure adapted from Harris *et al.*, 2002.

2.13 Statistical analysis

Details of statistical tests used are given in individual results chapters.

Chapter 3

Endocytic pathway alterations in human temporal lobe after global cerebral ischaemia and association with *APOE* genotype

3.1 Introduction and aims

Endocytosis is integral to the cellular uptake and trafficking of apoE. Endocytic pathway alterations may be central to mechanisms which could mediate *APOE* genotype-dependent differences in susceptibility to acute brain injury. The specific aims of the present study were to determine, in human post-mortem temporal lobe brain sections, if:

1. alterations in the endocytic pathway occur after global ischaemia
2. there is an association between differences in endocytic pathway alterations and *APOE* genotype after global ischaemia

3.2 Materials and methods

This study was carried out at the Wellcome Surgical Institute, University of Glasgow. All experiments were performed unaware of control or global ischaemia status and *APOE* genotype.

3.2.1 Post-mortem human brain tissue

Paraffin-embedded sections of medial temporal lobe (*section 2.1*) from 43 patients who died after an episode of global ischaemia (and subsequent reperfusion) due to cardio-respiratory arrest and from 38 control patients, were studied. Cohort clinical details are given in **Appendix C**. The control and global ischaemia groups were matched for age and male/female ratio: control patients (25 males, 13 females; mean age 51 years); global ischaemia patients (27 males, 16 females; mean age 50 years). In the global ischaemia group, the survival period after the initial ischaemic episode (cardiac arrest) ranged from 11h to 3 months. *APOE* genotype of controls and global ischaemia cases was determined from paraffin-embedded sections as described in *section 2.1.2*.

3.2.2 Immunohistochemistry

Adjacent sections were immunostained (peroxidase protocol) with rabaptin-5 and rab4 antibodies (*section 2.9.3*).

3.2.2.1 Semi-quantification of rabaptin-5 and rab4 immunostaining

Semi-quantitative assessment of rabaptin-5 and rab4 immunoreactivity within specific regions of the hippocampus and neocortex of the temporal lobe was performed at x200

magnification. The degree of neuronal rabaptin-5 and rab4 immunoreactivity was graded according to a scoring system (*section 2.9.6.2*) in five regions of the temporal lobe (hippocampus CA1 sector, hippocampus CA2 sector, hippocampus CA3/4 sector, dentate gyrus and neocortex). The degree of glial rabaptin-5 and rab4 immunoreactivity in the same regions was similarly scored. An average degree of neuronal and glial rabaptin-5 and rab4 immunoreactivity for the temporal lobe in each control and global ischaemia case was calculated from the sum of the degree of neuronal/glial immunoreactivity in CA1 + CA2 + CA3/4 + dentate gyrus + neocortex divided by 5. Reproducibility of semi-quantitative assessment was tested (**Appendix D**).

3.2.2.2 β -amyloid deposition and neurofibrillary tangles

All controls and global ischaemia cases were screened for the presence of β -amyloid (A β) deposits (diffuse and neuritic) and neurofibrillary tangles in paraffin-embedded sections previously immunostained by Dr Karen Horsburgh with anti-A β (to detect A β deposits) and anti-tau (to detect neurofibrillary tangles) antibodies. In each case, the presence or absence of diffuse A β deposits and neuritic plaques and neurofibrillary tangles was determined.

3.2.3 Ischaemic neuronal damage

Semi-quantification (as above) of the degree of ischaemic neuronal damage in the five regions had previously been performed in haematoxylin and eosin-stained sections adjacent to those immunostained with rabaptin-5 and rab4 by Dr Karen Horsburgh (Horsburgh *et al.*, 1999a). An average degree of ischaemic neuronal damage for the temporal lobe in each control and global ischaemia case was previously calculated as above.

3.2.4 Statistical analysis

Mann-Whitney *U*-statistic was used to assess statistical differences in the degree of neuronal and glial rabaptin-5 and rab4 immunoreactivity and ischaemic damage in each area within the temporal lobe between the control and global ischaemia groups. Spearman Rank correlation analysis was used to assess the association between the average degree of neuronal rabaptin-5 or rab4 immunoreactivity and the average degree of ischaemic neuronal damage. In the global ischaemia group, Spearman Rank

correlation analysis was used to assess the association between the average degree of neuronal rabaptin-5 and rab4 immunoreactivity and also to assess the association between neuronal rabaptin-5 or rab4 immunoreactivity and patient survival time.

Two-way analysis of variance (ANOVA) was used to assess the association between *APOE* genotype and the average degree of neuronal rabaptin-5 or rab4 immunoreactivity in response to global ischaemia. Two-way ANOVA tested for an interaction between the effects of possession of an *APOE* $\epsilon 4$ allele and of an episode of global ischaemia on the average degree of neuronal immunoreactivity of the endocytic markers. Use of two-way ANOVA assumes a normal distribution of data. Assumption of normality was reasonable when the average response per subject was calculated (Kolmogorov-Smirnov test, $P > 0.05$). Fisher's exact test was used to assess the association between *APOE* genotype and A β deposition. All data are presented as mean \pm SEM.

3.3 Results

3.3.1 Ischaemic neuronal damage

Cardio-respiratory arrest is the most common cause of global ischaemia, which induces neuronal damage in selectively vulnerable regions of the brain (*see section 1.1.2.2*). In the present cohort of individuals, ischaemic damage was previously assessed by Dr Karen Horsburgh (Horsburgh *et al.*, 1999a). There was extensive neuronal damage in the hippocampus and neocortex after global ischaemia whereas there was minimal neuronal damage in controls. In global ischaemia cases, there was a characteristic pattern of selective neuronal damage in vulnerable regions of the temporal lobe. In affected areas, neurons were shrunken with densely stained nuclei and intensely eosinophilic cytoplasm (**Figure 20**). The degree of neuronal damage was significantly greater in global ischaemia cases compared to controls ($P < 0.0005$) in all regions of the temporal lobe (**Figure 20**).

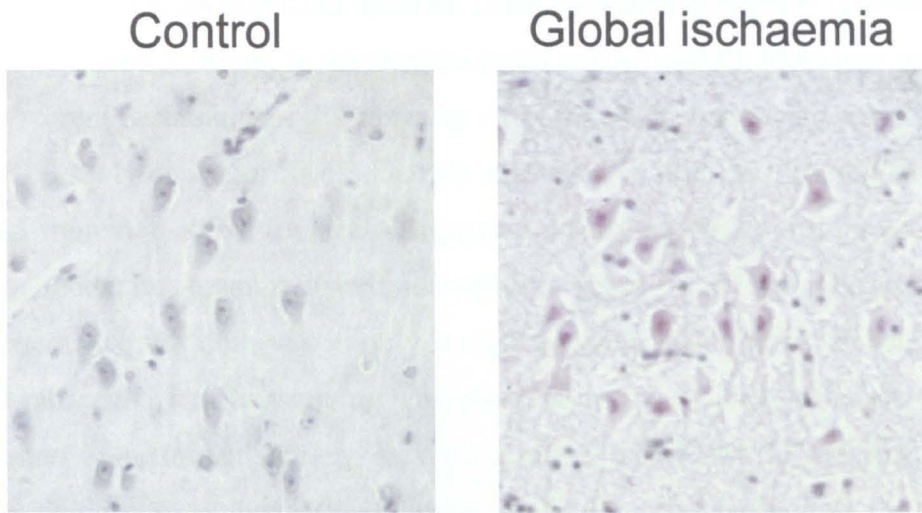
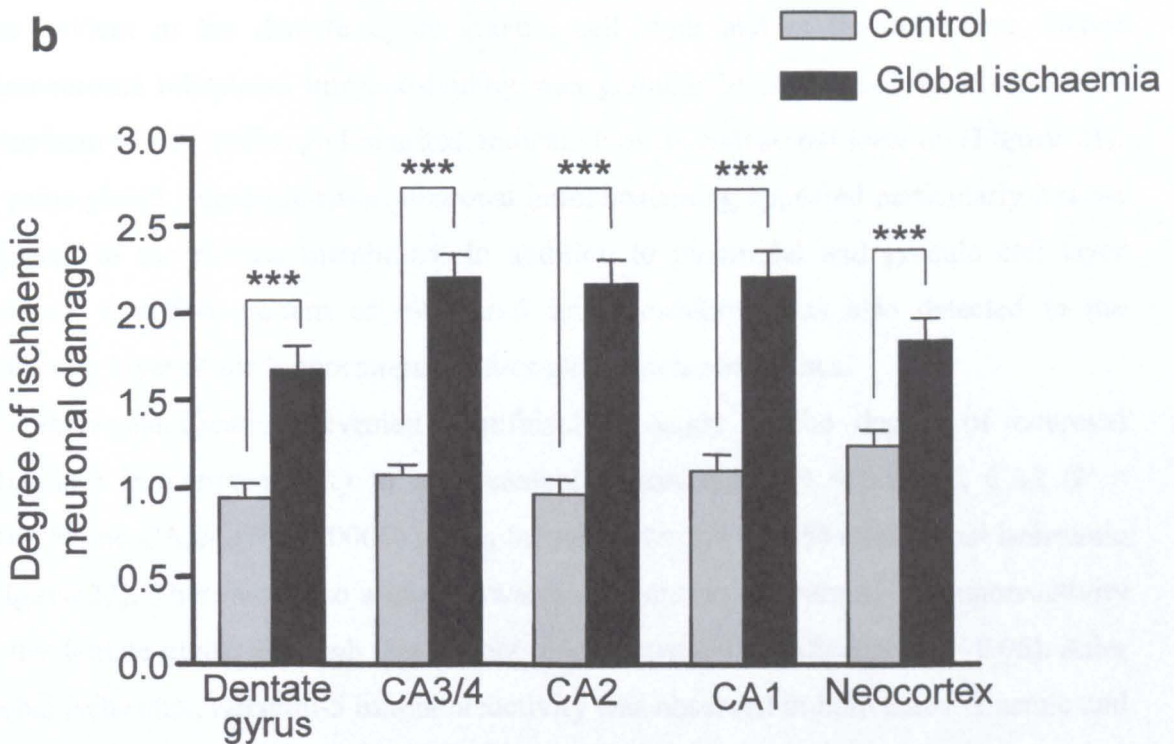
a**b**

Figure 20. Ischaemic neuronal damage after global ischaemia

Ischaemic damage was assessed previously by Dr Karen Horsburgh (Horsburgh *et al.*, 1999a). (a) Example of ischaemic neuronal damage in a control individual and a patient who died after an episode of global ischaemia. Neuronal damage is absent in the control whereas neurons displaying the histological features of ischaemic cell change are evident in the global ischaemia patient. Photomicrographs are from the hippocampal CA1 sector. (b) There was a significant increase in the degree of neuronal damage after global ischaemia compared to controls in each region of the temporal lobe examined. *** $P < 0.0005$, Mann-Whitney U -statistic. $n = 38$ (control); $n = 43$ (global ischaemia). Data are presented as mean \pm SEM.

3.3.2 Rabaptin-5 immunostaining

3.3.2.1 Neuronal immunostaining

The majority of controls displayed minimal (semi-quantitative score = 1) or no neuronal rabaptin-5 immunoreactivity. In the dentate gyrus and neocortex, there was no neuronal rabaptin-5 immunostaining in the majority of controls. In hippocampus sectors CA1, CA2 and CA3/4 the majority of controls displayed a minimal amount of neuronal rabaptin-5 immunoreactivity which was predominantly confined to the pyramidal cell layer. A moderate amount (semi-quantitative score = 2) of dense rabaptin-5 immunoreactivity was observed in only 3 of 38 controls. After global ischaemia, dense neuronal rabaptin-5 immunostaining was observed in the majority of cases; there was no evidence of neuronal staining in only 2 of 43 cases. As in controls, neuronal immunostaining after global ischaemia was predominantly confined to the pyramidal cell layer of hippocampus sectors CA1, CA2 and CA3/4, in particular CA1, but was also evident in the dentate gyrus granule cell layer and in the neocortex. Dense intraneuronal rabaptin-5 immunostaining was granular in nature and localised to the cytoplasm of cell bodies and neurites, indicative of its endosomal location (**Figure 21**). In some global ischaemia cases, neuronal immunostaining appeared particularly intense adjacent to the plasma membrane. In addition to pyramidal and granule cell layer staining, a diffuse pattern of rabaptin-5 immunostaining was also detected in the molecular layer of the hippocampus in four global ischaemia cases.

Semi-quantification revealed significant increases in the degree of neuronal rabaptin-5 immunoreactivity in hippocampal sectors CA1 ($P < 0.0005$), CA2 ($P < 0.0005$) and CA3/4 ($P < 0.0005$) and in the neocortex ($P < 0.05$) after global ischaemia (**Figure 22**). There was also a trend towards an increase in neuronal immunoreactivity in the dentate gyrus, although this did not reach statistical significance ($P > 0.05$). After global ischaemia, rabaptin-5 immunoreactivity was observed in both non-ischaemic and ischaemic neurons. There was a weak correlation between the average degree of neuronal rabaptin-5 immunoreactivity and the average degree of ischaemic neuronal damage in the temporal lobe ($P = 0.024$, $r = 0.34$) (**Figure 23**). There was no correlation between neuronal rabaptin-5 immunoreactivity and ischaemic neuronal damage in controls ($P > 0.05$). There was also no association between the extent of neuronal rabaptin-5 immunoreactivity and survival time after the global ischaemic episode ($P > 0.05$) (**Figure 24**).

3.3.2.2 Glial immunostaining

Glial rabaptin-5 immunostaining was detected in both controls and after global ischaemia. In both groups, the degree of immunoreactivity was less than that observed in neurons. The majority of controls displayed only minimal or no glial rabaptin-5 immunostaining and, when present, immunostaining was predominantly confined to the neocortex. After global ischaemia, only 7 of 43 cases showed a moderate or greater level of glial rabaptin-5 immunoreactivity. As in controls, glial immunostaining was primarily observed in the neocortex, but in addition, was also observed in the hippocampal CA3/4 sector. In the hippocampus, glial immunostaining displayed a less laminar pattern than the neuronal staining.

Semi-quantification revealed a significant increase in the degree of glial rabaptin-5 immunoreactivity in only the CA3/4 sector of the hippocampus ($P < 0.05$) after global ischaemia compared to controls (**Figure 22**).

Control



Global Ischaemia

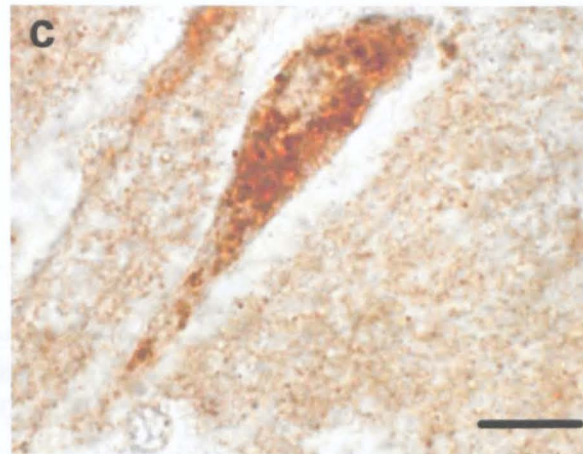
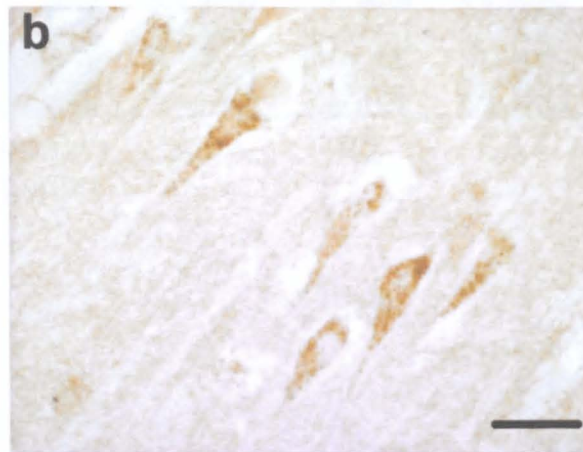


Figure 21. Rabaptin-5 immunostaining

Representative examples of neuronal rabaptin-5 immunoreactivity from a patient who experienced an episode of global ischaemia (b,c) and a control individual (a). In the control (a), there is minimal neuronal rabaptin-5 immunoreactivity. After global ischaemia (b,c), there is markedly increased neuronal rabaptin-5 immunoreactivity in neurons displaying the features of ischaemic cell change. Photomicrographs are from the hippocampal CA1 sector. Scale bar (a,b), 25 μ m; (c,e), 10 μ m.

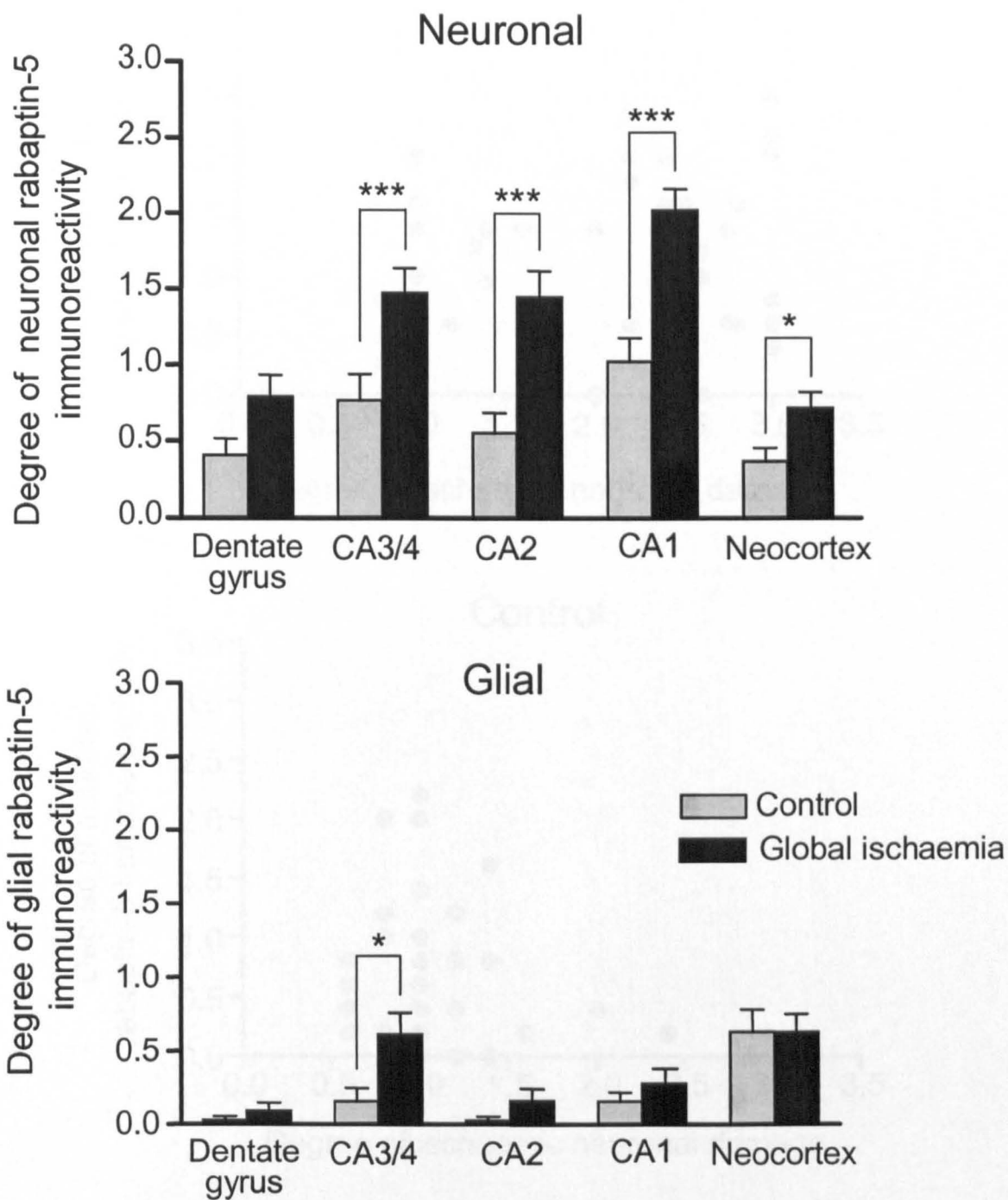


Figure 22. Semi-quantitative assessment of rabaptin-5 immunoreactivity

There was a significant increase in the degree of neuronal rabaptin-5 immunoreactivity after global ischaemia compared with controls in all regions examined except the dentate gyrus. Only in CA3/4 was there a significant change in the degree of glial rabaptin-5 immunoreactivity after global ischaemia. * $P < 0.05$, *** $P < 0.0005$, Mann-Whitney U -statistic. $n = 38$ (control); $n = 43$ (global ischaemia). Data are presented as mean \pm SEM.

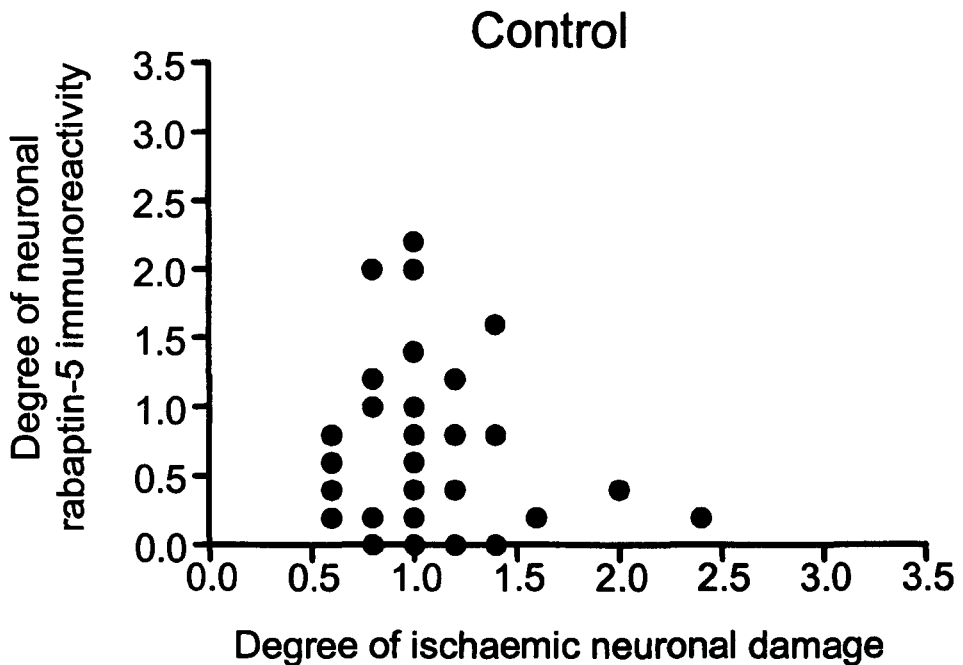
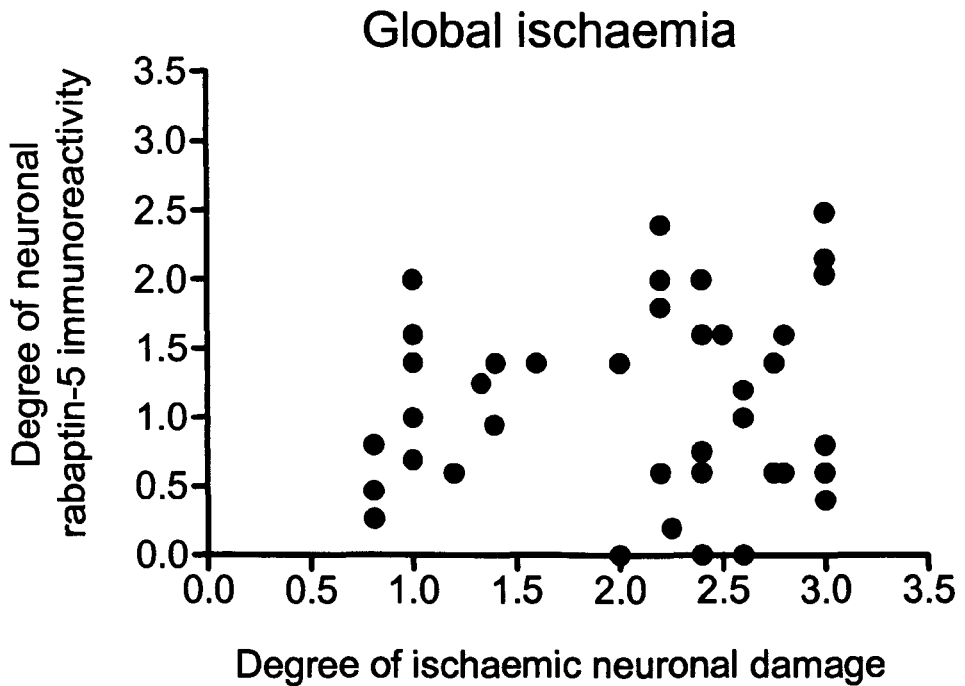


Figure 23. Association between ischaemic neuronal damage and neuronal rabaptin-5 immunoreactivity

There was a significant correlation between the average degree of ischaemic neuronal damage and the average degree of neuronal rabaptin-5 immunoreactivity in temporal lobe after global ischaemia ($P = 0.024$; $r = 0.34$, Spearman Rank). There was no correlation in controls ($P > 0.05$, Spearman Rank).

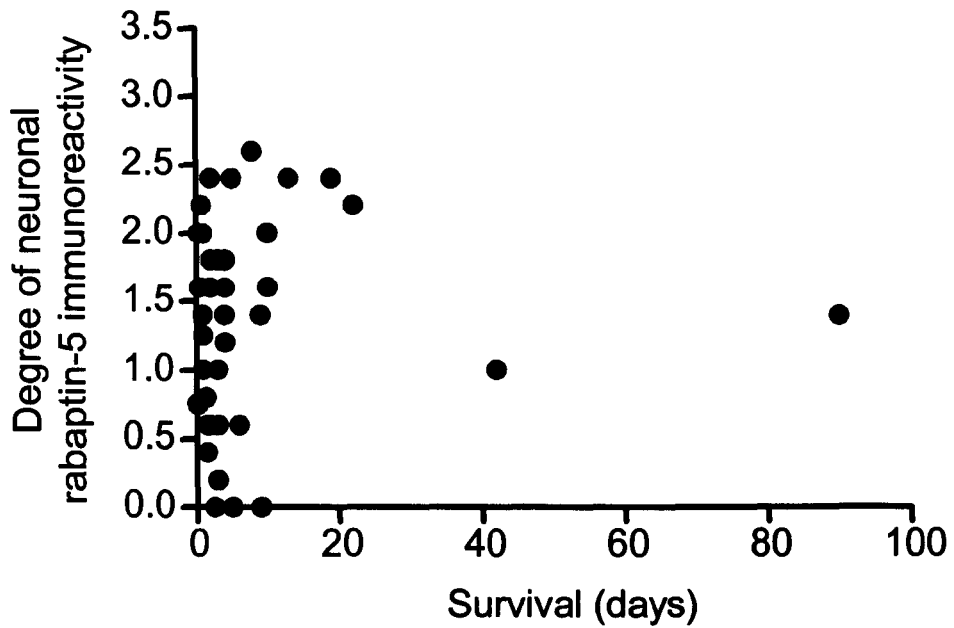


Figure 24. Association between survival time after global ischaemia and neuronal rabaptin-5 immunoreactivity
 There was no correlation between survival time after an episode of global ischaemia and the average degree of neuronal rabaptin-5 immunoreactivity in temporal lobe ($P > 0.05$, Spearman Rank).

3.3.3 Rab4 immunostaining

3.3.3.1 Neuronal immunostaining

Neuronal rab4 immunoreactivity (**Figure 25**) was detected in both controls and after global ischaemia. In both groups, immunostaining was observed throughout the temporal lobe, although was most prominent in the hippocampus, in particular the CA1 sector. In the hippocampus and dentate gyrus, neuronal rab4 immunostaining was primarily restricted to the pyramidal cell layer and granule cell layer respectively. The majority of controls displayed a minimal (score = 1) degree of neuronal rab4 immunoreactivity, however, in 8 of 38 controls there was a moderate (score = 2) or greater (score = 3) degree of neuronal immunoreactivity, particularly in the hippocampus. It was noted that the level of neuronal rab4 immunoreactivity in controls was greater than the level of neuronal rabaptin-5 immunoreactivity in all regions of the temporal lobe. In the majority of global ischaemia cases, the greatest extent of neuronal rab4 immunoreactivity was observed in the hippocampal sectors whereas in the dentate gyrus and neocortex, a minimal and moderate level, respectively, were observed most frequently. Neuronal rab4 immunoreactivity was evident in all global ischaemia cases. Similar to rabaptin-5, intraneuronal rab4 immunostaining was localised to the cytoplasm of cell bodies and proximal neurites, however, a diffuse pattern of rab4 immunostaining in the neuropil was not observed in any controls or global ischaemia cases.

Semi-quantification revealed significant increases in the degree of neuronal rab4 immunoreactivity after global ischaemia in hippocampal sectors CA1 ($P < 0.05$), CA2 ($P < 0.05$), CA3/4 ($P < 0.05$) and in the dentate gyrus ($P < 0.05$) and neocortex ($P < 0.005$) (**Figure 26**). As observed with rabaptin-5, rab4 immunoreactivity was evident in both non-ischaemic and ischaemic neurons after global ischaemia. However, correlation analysis showed that there was no association between the average degree of neuronal rab4 immunoreactivity in temporal lobe and the degree of ischaemic neuronal damage after global ischaemia ($P > 0.05$) (**Figure 27**). There was also no association between neuronal rab4 immunoreactivity and neuronal damage in controls ($P > 0.05$) (**Figure 27**). In addition, there was no association between neuronal rab4 immunoreactivity and survival time after global ischaemia ($P > 0.05$) (**Figure 28**).

3.3.3.2 Correlation between neuronal rab4 and rabaptin-5 immunostaining

In adjacent sections immunostained for rab4 and rabaptin-5 it was evident that similar areas were immunoreactive for both antibodies after global ischaemia. It was also noted that the average degree of neuronal rab4 and rabaptin-5 immunoreactivity were similar after global ischaemia. Correlation analysis indicated a moderate association between the average degree of neuronal rab4 and rabaptin-5 immunoreactivity in temporal lobe after global ischaemia ($P = 0.003$, $r = 0.48$) but no association in controls ($P > 0.05$) (Figure 29).

3.3.3.3 Glial immunostaining

As observed in neurons, glial rab4 immunoreactivity was evident in both controls and after global ischaemia. However, in both groups, the degree of immunoreactivity was less than that observed in neurons. Minimal (score = 1) or no (score = 0) glial rab4 immunoreactivity was observed in the majority of controls in the hippocampus and neocortex; in the dentate gyrus there was almost complete absence of glial rab4 immunostaining. After global ischaemia, minimal or moderate (score = 2) levels of glial rab4 immunoreactivity were predominantly detected in the hippocampus and neocortex although as in controls, glial rab4 immunostaining was generally not observed in the dentate gyrus.

Semi-quantification revealed a significant increase in the degree of glial rab4 immunoreactivity after global ischaemia in only the CA2 sector of the hippocampus ($P < 0.05$) (Figure 26). It was noted that, in both controls and after global ischaemia, the degree of glial rab4 immunoreactivity was greater than the degree of glial rabaptin-5 immunoreactivity.

Control



Global Ischaemia

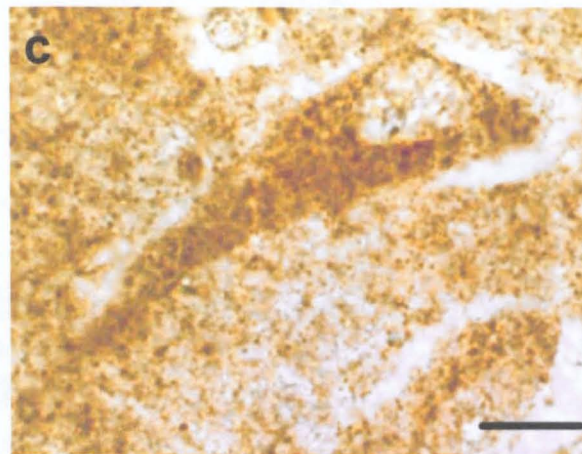
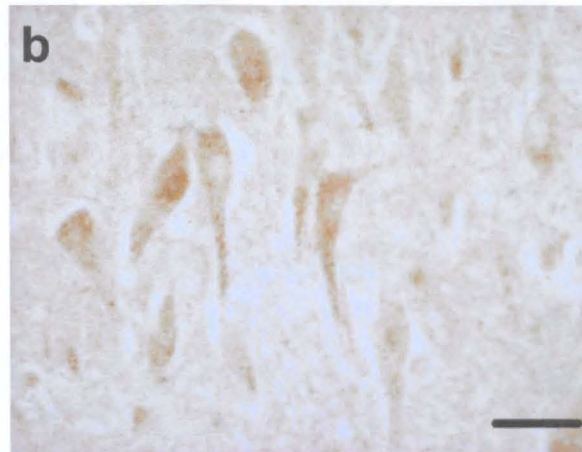


Figure 25. Rab4 immunostaining

Representative examples of neuronal rab4 immunoreactivity from a patient who experienced an episode of global ischaemia (b,c) and a control individual (a). In the control (a), there is minimal neuronal rab4 immunoreactivity. After global ischaemia (b,c), there is markedly increased neuronal rab4 immunoreactivity in neurons displaying the features of ischaemic cell change. Photomicrographs are from the hippocampal CA1 sector. Scale bar (a,b), 25 μ m; (c,e), 10 μ m.

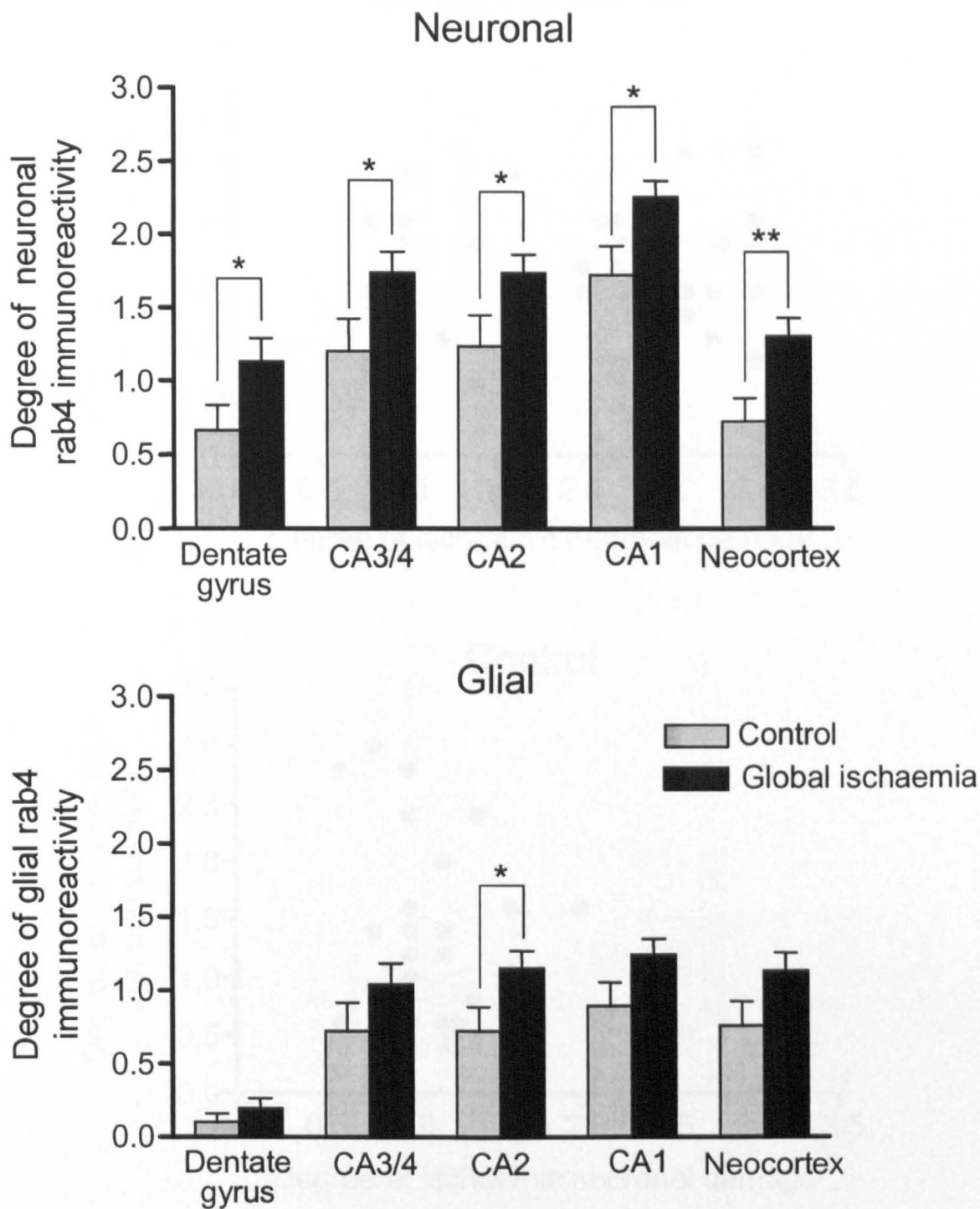


Figure 26. Semi-quantitative assessment of rab4 immunoreactivity

There were significant increases in the degree of neuronal rab4 immunoreactivity after global ischaemia in all regions of temporal lobe examined. A trend toward an increased degree of glial rab4 immunoreactivity was revealed in all regions after global ischaemia, however, only in the hippocampal CA2 sector did the increase reach statistical significance. * $P < 0.05$, ** $P < 0.005$, Mann-Whitney U -statistic. $n = 38$ (control); $n = 43$ (global ischaemia). Data are presented as mean \pm SEM.

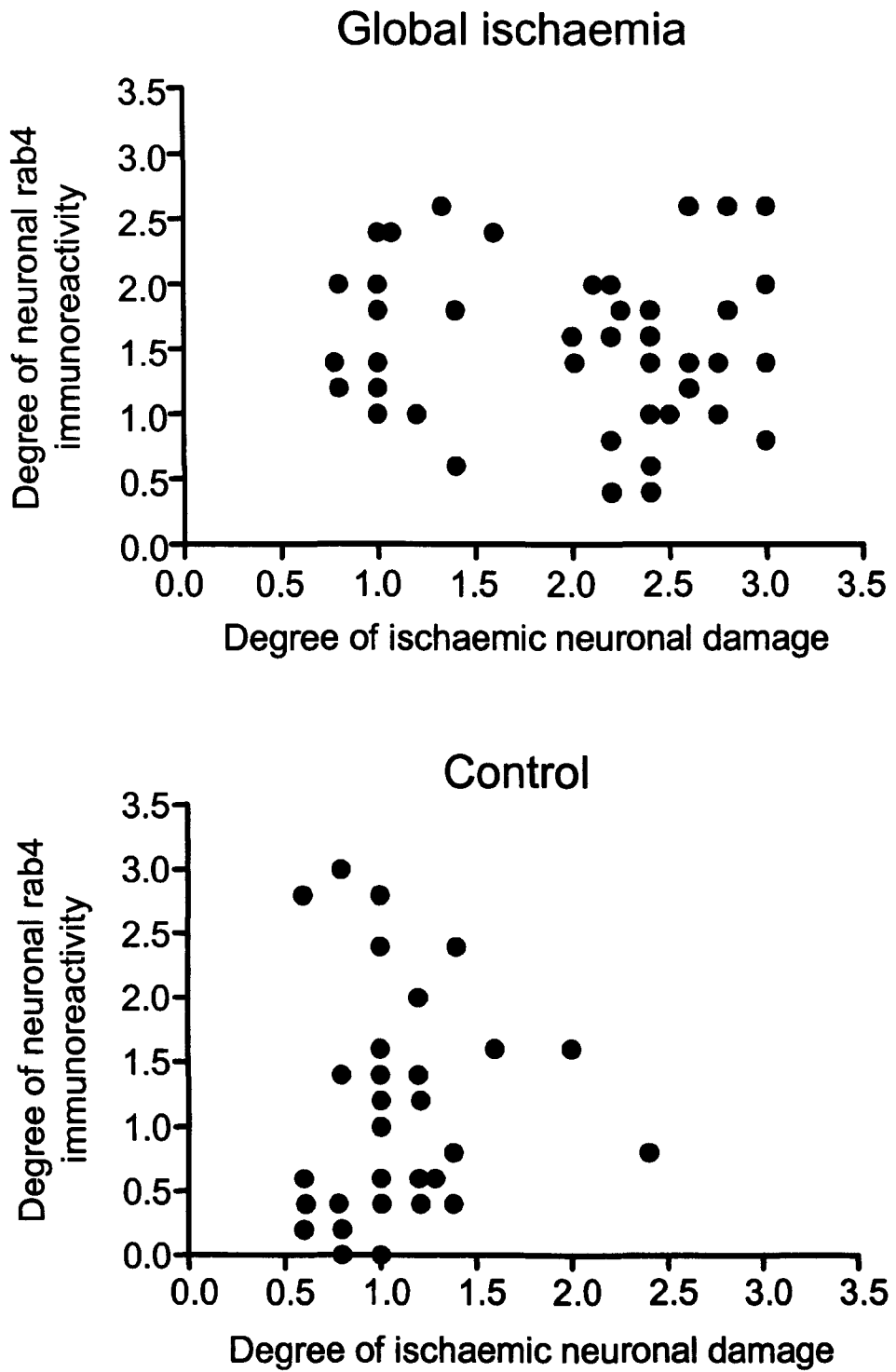


Figure 27. Association between ischaemic neuronal damage and neuronal rab4 immunoreactivity

There were no correlations between the average degree of ischaemic neuronal damage and the average degree of neuronal rab4 immunoreactivity in temporal lobe after global ischaemia ($P > 0.05$, Spearman Rank) or in controls ($P > 0.05$, Spearman Rank).

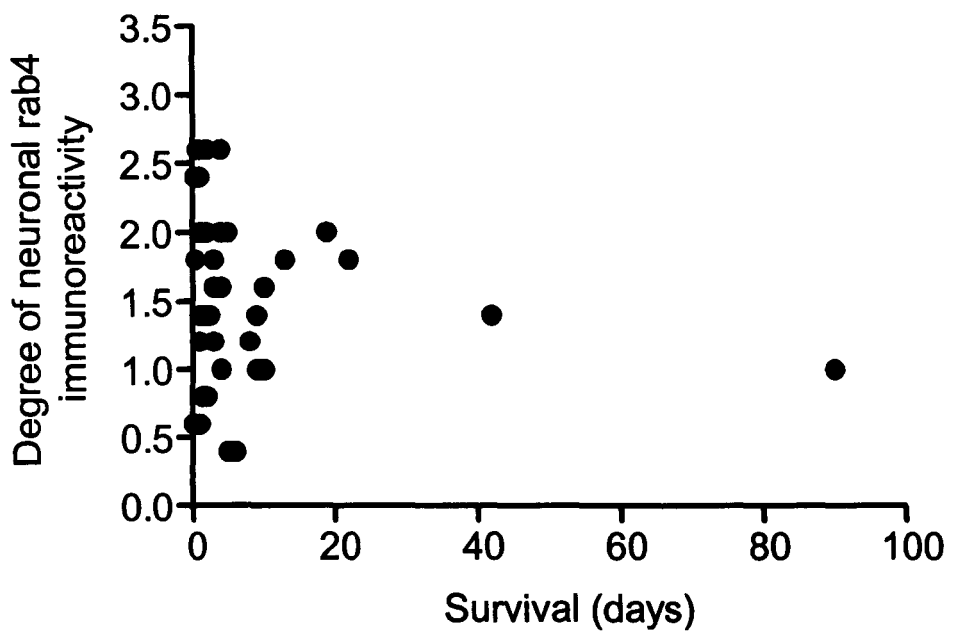


Figure 28. Association between survival time after global ischaemia and neuronal rab4 immunoreactivity

There was no correlation between survival time after an episode of global ischaemia and the average degree of neuronal rab4 immunoreactivity in temporal lobe ($P > 0.05$, Spearman Rank).

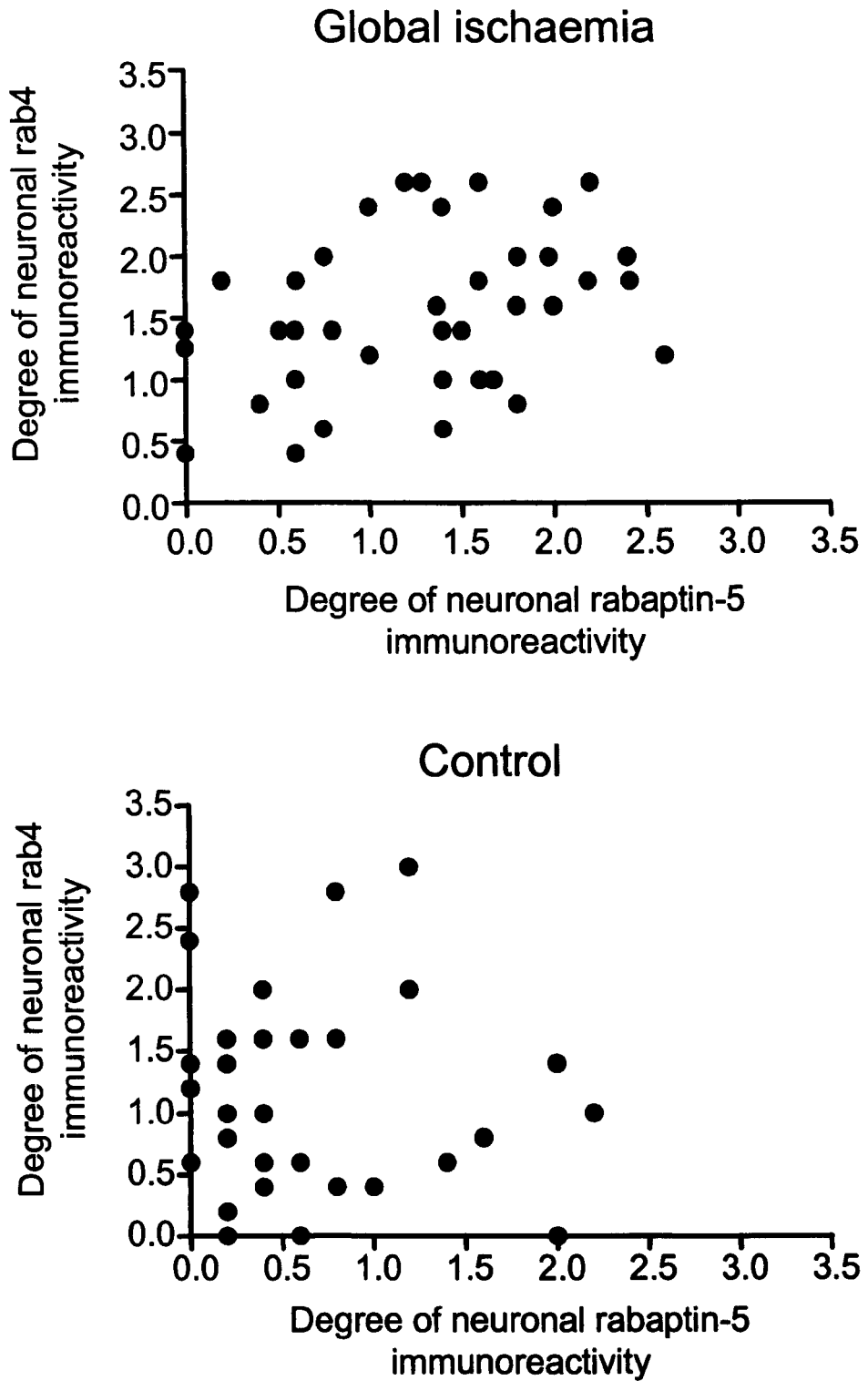


Figure 29. Association between neuronal rabaptin-5 and rab4 immunoreactivity
 There was a significant correlation between the average degree of neuronal rabaptin-5 and rab4 immunoreactivity after global ischaemia ($P = 0.003$; $r = 0.48$, Spearman Rank). There was no association in controls ($P > 0.05$, Spearman Rank).

3.3.4 Association between *APOE* genotype and alterations in neuronal rabaptin-5 and rab4 immunostaining after global ischaemia

To determine if *APOE* genotype was associated with alterations in the degree of neuronal rabaptin-5 and rab4 immunoreactivity after global ischaemia, controls and global ischaemia cases were separated according to those individuals who possessed at least one *APOE* $\epsilon 4$ allele and those without an $\epsilon 4$ allele. The success rate for determination of *APOE* genotype was high; *APOE* genotype was undetermined in only three control patients. Consequently, 35 controls were used for *APOE* genotype analysis. The frequency of the *APOE* $\epsilon 4$ allele was similar in the control and global ischaemia groups. In the control group, 11 individuals possessed at least one *APOE* $\epsilon 4$ allele (7 males, 4 females; mean age 49 years) and 24 individuals were without an $\epsilon 4$ allele (18 males, 6 females; mean age 52 years). In the global ischaemia group, 15 patients possessed at least one *APOE* $\epsilon 4$ allele (9 males, 6 females; mean age 49 years) and 28 patients were without an $\epsilon 4$ allele (18 males, 10 females; mean age 52 years). The number of individuals homozygous for the *APOE* $\epsilon 4$ allele was too low to evaluate if the effects of this genotype (two controls and two global ischaemia cases were *APOE* $\epsilon 4$ homozygotes). Likewise, the frequency of the *APOE* $\epsilon 2$ allele was too low to determine any impact of this genotype (two controls and three global ischaemia cases possessed one *APOE* $\epsilon 2$ allele; there were no controls or global ischaemia patients homozygous for the $\epsilon 2$ allele). An average degree of neuronal rabaptin-5 and rab4 immunoreactivity for the temporal lobe was calculated from the individual scores in each of the five regions - hippocampal sectors CA1, CA2, CA3/4, the dentate gyrus and neocortex.

Two-way ANOVA showed that the average degree of neuronal rabaptin-5 immunoreactivity was not significantly different between the *APOE* $\epsilon 4$ and non-*APOE* $\epsilon 4$ groups ($P > 0.05$) but was significantly greater after global ischaemia compared to control ($P = 0.001$). There was no significant interaction between possession of the *APOE* $\epsilon 4$ allele and an episode of global ischaemia ($P > 0.05$) (Figure 30). Two-way ANOVA revealed that the average degree of rab4 immunoreactivity was not significantly different between the *APOE* $\epsilon 4$ and non-*APOE* $\epsilon 4$ groups ($P > 0.05$) and was also not significantly different after global ischaemia compared to control ($P > 0.05$). However, there was a significant interaction between possession of the *APOE* $\epsilon 4$ allele and an episode of global ischaemia ($P = 0.017$) (Figure 31). The mean increase in

the average degree of neuronal rab4 immunoreactivity after global ischaemia was 0.9 units lower on the semi-quantitative score in *APOE* ϵ 4 carriers than in individuals without an *APOE* ϵ 4 allele (95% confidence interval of 0.2 to 1.6 units lower).

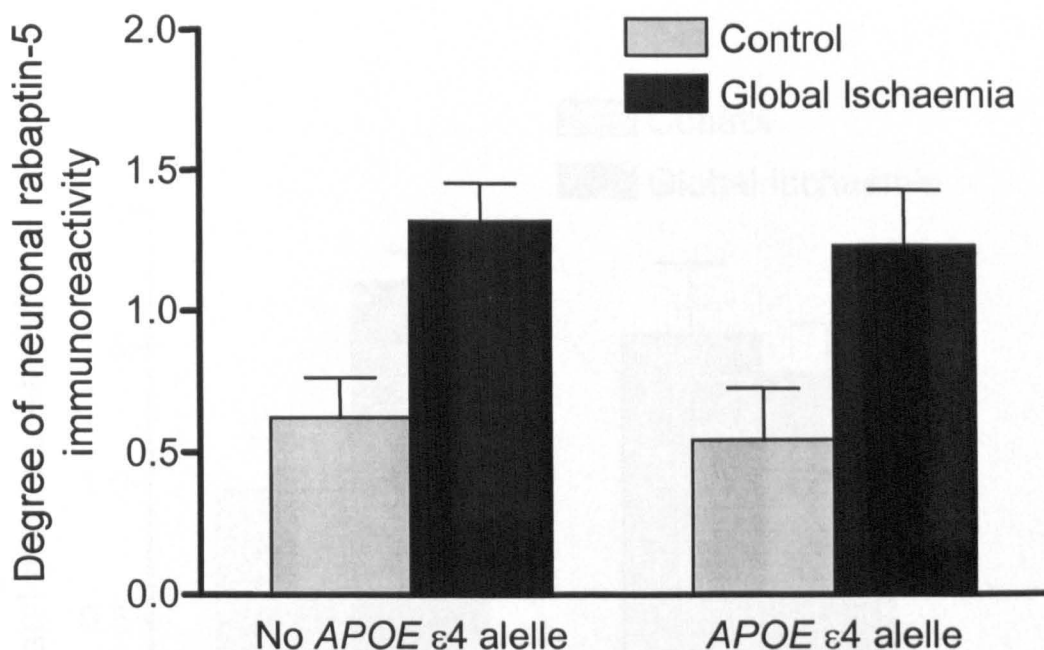


Figure 30. Effect of *APOE* genotype on alterations in neuronal rabaptin-5 immunoreactivity after global ischaemia

The average degree of neuronal rabaptin-5 immunoreactivity in temporal lobe was not significantly different between the *APOE* ϵ 4 and non-*APOE* ϵ 4 groups ($P > 0.05$, two-way ANOVA) but was significantly greater after global ischaemia compared to control ($P = 0.001$, two-way ANOVA). There was no interaction between possession of an *APOE* ϵ 4 allele and an episode of global ischaemia ($P > 0.05$, two-way ANOVA). $n = 24$ (control without ϵ 4); $n = 11$ (control with ϵ 4); $n = 28$ (global ischaemia without ϵ 4); $n = 15$ (global ischaemia with ϵ 4). Data are presented as mean \pm SEM.

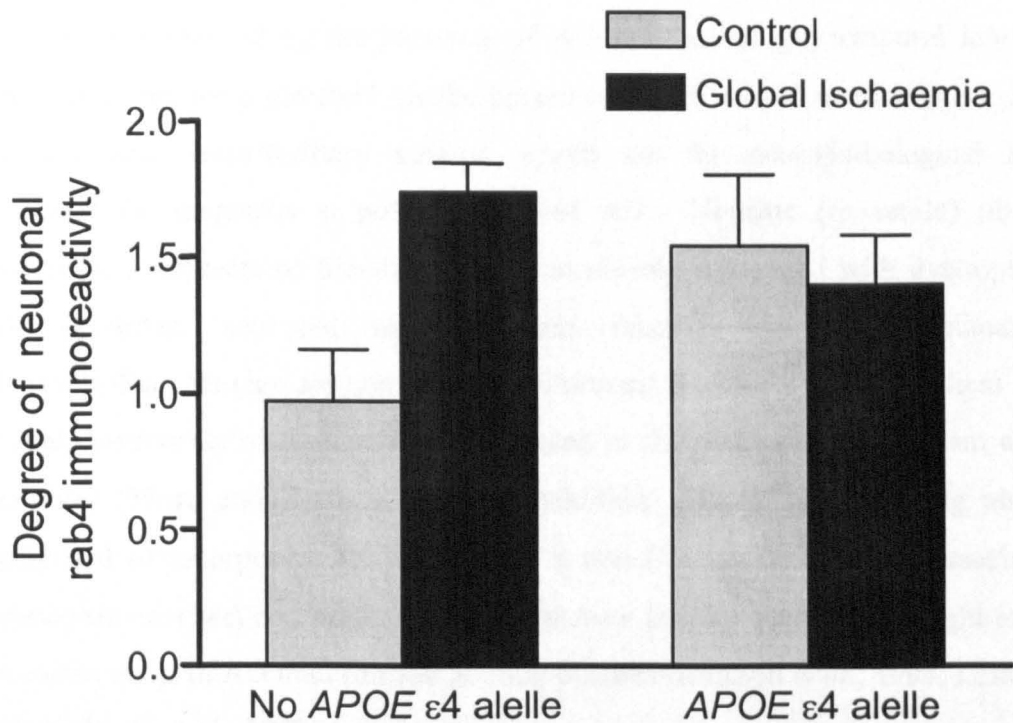


Figure 31. Effect of APOE genotype on alterations in neuronal rab4 immunoreactivity after global ischaemia

The average degree of neuronal rab4 immunoreactivity in temporal lobe was not significantly different between the APOE ϵ 4 and non-APOE ϵ 4 groups ($P > 0.05$, two-way ANOVA) and was also not significantly different after global ischaemia compared to control ($P > 0.05$, two-way ANOVA). There was a significant interaction between possession of an APOE ϵ 4 allele and an episode of global ischaemia on the average degree of neuronal rab4 immunoreactivity ($P = 0.017$, two-way ANOVA). $n = 24$ (control without ϵ 4); $n = 11$ (control with ϵ 4); $n = 28$ (global ischaemia without ϵ 4); $n = 15$ (global ischaemia with ϵ 4). Data are presented as mean \pm SEM.

3.3.5 β -amyloid deposition and neurofibrillary tangles

Previous studies have shown that there are marked alterations in the endocytic pathway in individuals with AD and also in patients with Down syndrome (with early AD) (Cataldo *et al.*, 1997; Cataldo *et al.*, 2000). The present work clearly indicated that there were marked endocytic pathway alterations in response to global cerebral ischaemia and that these were *APOE* genotype-dependent. In order to assess if these alterations may have been influenced by the presence of AD-type pathology, temporal lobe sections from all brains were screened for the presence of diffuse and neuritic β -amyloid ($A\beta$) deposits and neurofibrillary tangles, which are the neuropathological hallmarks (required for diagnosis at post-mortem) of AD. Neuritic (or senile) plaques are extracellular deposits of fibrillar $A\beta$ protein closely associated with dystrophic axons and dendrites, activated microglia and reactive astrocytes (Selkoe, 1991). Neurofibrillary tangles are composed of abnormal bundles of paired helical filaments (hyperphosphorylated tau) most often located in the perinuclear cytoplasm and apical dendrites (Mirra and Hyman, 2002). In addition, diffuse $A\beta$ -containing plaques are composed of amorphous $A\beta$ which is in a non-fibrillar state (rarely associated with dystrophic neurites) and may represent immature lesions which are thought to occur at an earlier stage in AD than fibrillar neuritic plaques (Dickson *et al.*, 1995; Lemere *et al.*, 1996; Morris *et al.*, 1996).

A minority of controls and global ischaemia cases displayed $A\beta$ deposits and neurofibrillary tangles. $A\beta$ deposits were present in 3 of 38 controls (one with diffuse plaques and two with neuritic and diffuse plaques) and 5 of 43 global ischaemia cases (four with diffuse plaques only and one with neuritic and diffuse plaques). Only 1 of 38 control and 2 of 43 global ischaemia cases displayed neuritic plaques and neurofibrillary tangles (indicative of AD), therefore suggesting that endocytic alterations after global ischaemia were unlikely to be the result of AD-type pathological processes.

The *APOE* $\epsilon 4$ allele is associated with increased susceptibility to AD and a greater number of $A\beta$ -containing plaques in AD patients (Berr *et al.*, 1994; Gearing *et al.*, 1995b; Polvikoski *et al.*, 1995; Marz *et al.*, 1996; Kraszpulski *et al.*, 2001). In the present study, $A\beta$ deposition was not associated with possession of an *APOE* $\epsilon 4$ allele in the control or global ischaemia groups ($P > 0.05$). $A\beta$ deposits were present in 1 of 11 controls with an *APOE* $\epsilon 4$ allele and 3 of 24 controls without an *APOE* $\epsilon 4$ allele. In the global ischaemia group, $A\beta$ deposits were present in 3 of 15 individuals with an

APOE ϵ 4 allele and 4 of 28 individuals without an *APOE* ϵ 4 allele. Thus, *APOE*-genotype dependent alterations in endocytic pathway alterations after global ischaemia are unlikely to be the result of genotype-related differences in susceptibility to AD.

3.4 Discussion

The results from the present study demonstrate alterations in the endocytic pathway in human hippocampus and neocortex after global ischaemia. Immunoreactivity of the endocytic pathway markers, rabaptin-5 and rab4, was markedly increased in neurons and to a lesser degree in glia of patients who had experienced an episode of global ischaemia compared to controls, indicative of an up-regulation of endocytic pathway function. Furthermore, *APOE* genotype-dependent differences in endocytic pathway alterations after global ischaemia were also demonstrated.

3.4.1 Global ischaemia and ischaemic neuronal damage

The patients in this study experienced an episode of global cerebral ischaemia caused by cardio-respiratory arrest. Patients were subsequently resuscitated and, accordingly, the ischaemic episode was followed by a defined period of reperfusion (survival). In humans, and in animal models, an episode of global ischaemia with subsequent reperfusion produces a relatively stereotyped pathology in which there is selective and delayed neuronal damage in selectively vulnerable areas of the brain, including the hippocampus, cerebral cortex and striatum (Auer and Sutherland, 2002). Within each region, a hierarchy of vulnerability also exists. For example, in the hippocampus of the human brain, the pyramidal neurons of the CA1 sector are particularly susceptible to ischaemic injury (Auer and Sutherland, 2002). It is pertinent to note that individuals included in the control group may also have experienced some degree of terminal hypoxia and/or hypotension since cardiac arrest is an inevitable consequence of death, although this would also be true of the global ischaemia cases. Crucially, however, control individuals would not have experienced any cerebral reperfusion. In a previous study using the present cohort, the extent of neuronal damage throughout the temporal lobe was markedly increased after global ischaemia compared to controls, with only minimal neuronal damage in control brain (Horsburgh *et al.*, 1999a). It is likely, therefore, that controls did not experience a significant level of ischaemic insult to the brain.

3.4.2 Endocytic pathway alterations

Alterations in the neuronal endocytic pathway have previously been observed in post-mortem brain from patients with Alzheimer's disease (AD) (Cataldo *et al.*, 1997; Cataldo *et al.*, 2000). Akin to global ischaemia, selective neuronal damage in vulnerable regions of the brain (e.g. hippocampus, entorhinal cortex) is a predominant feature of AD. This suggests that the cascade of events associated with neuronal damage may include changes in intracellular trafficking activity through the endocytic system. In post-mortem AD brain, early endosomal volume in cortical pyramidal neurons was significantly increased as detected with antibodies to rab5 and rabaptin-5 (Cataldo *et al.*, 2000). In addition, elevated rab4 immunoreactivity was also observed in cortical pyramidal neurons. These observations are believed to indicate an increase in endocytic pathway activity since overexpression of rab5, rabaptin-5 and rab4 have all been shown to promote increased endocytosis (Bucci *et al.*, 1992; van der Sluijs *et al.*, 1992; de Hoop *et al.*, 1994; Daro *et al.*, 1996). In the present study, neuronal rabaptin-5 and rab4 immunoreactivity was markedly increased in all regions of temporal lobe examined in global ischaemia patients. It is interesting to note that, in controls and global ischaemia cases, highest levels of neuronal rabaptin-5 and rab4 immunoreactivity were observed in the hippocampal CA1 sector, the most susceptible area to ischaemic damage in humans. These data suggest that ischaemic neuronal damage caused by an episode of global ischaemia may induce increases in endocytic pathway activity similar to the alterations previously described in AD. In support of this, there was a significant association between the extent of ischaemic damage and the degree of neuronal rabaptin-5 immunoreactivity after global ischaemia, although no association was evident between ischaemic neuronal damage and rab4 immunoreactivity. Minimal neuronal rabaptin-5 and rab4 immunoreactivity was detected in control brain. It is possible that some controls may have experienced a mild ischaemic insult for reasons discussed above and that this may have affected the endocytic pathway, although there was no correlation between the extent of ischaemic neuronal damage and neuronal rabaptin-5 or rab4 immunoreactivity in controls. Intense rabaptin-5 and rab4 immunoreactivity was observed extensively in neurons displaying the characteristic morphological features of ischaemic damage in global ischaemia cases, which is consistent with the theory that endocytic pathway alterations are involved in the response to ischaemic neuronal damage. In addition, intense rabaptin-5 and rab4 immunoreactivity was also observed in some morphologically "normal" neurons. A possible explanation for these observations

is that rabaptin-5 and rab4 in morphologically normal neurons reflect endocytic pathway alterations involved in the early response of the neuron to an ischaemic insult and prior to the appearance of morphological evidence of ischaemic damage. Similar findings were found previously in this cohort with 4-hydroxynonenal (4-HNE), a marker of oxidative stress-induced lipid peroxidation. 4-HNE immunoreactivity was also present in morphologically normal and ischaemic neurons after global ischaemia and it was proposed that 4-HNE in normal neurons indicated the early effects of free radical damage on lipids that would likely culminate in neuronal damage (McCracken *et al.*, 2001). In addition, neuronal endosomal alterations have been observed in post-mortem brain from young individuals with Down syndrome (Cataldo *et al.*, 2000). Individuals with Down syndrome invariably develop AD by age 50, and therefore these endocytic pathway changes precede other classic neuropathological markers of AD such as neuronal damage and loss, amyloid deposition and neurofibrillary tangle formation. It is conceivable, therefore, that endocytic pathway alterations may occur at an early stage in response to a neuronal insult but prior to the appearance of morphological evidence of damage.

The results from this study suggest that overall endocytic pathway activity is increased after global ischaemia. Furthermore, the two distinct stages of endocytosis that rabaptin-5 and rab4 are involved in enable separation of the response of these two phases of endocytosis after global ischaemia. Rabaptin-5 is specifically localised to early endosomes where it participates in their fusion during endocytic internalisation. Accordingly, an increase in neuronal rabaptin-5 immunoreactivity is indicative of elevated internalisation and trafficking of material from the plasma membrane to early endosomes. In contrast, rab4 is explicitly localised to recycling endosomes that are returning to the plasma membrane. Consequently, elevated neuronal rab4 immunoreactivity after global ischaemia implies that endosomal recycling and transport of material back to the plasma membrane is also enhanced after global ischaemia. Therefore, in the present study there is evidence of a parallel response of the internalisation/early trafficking and recycling stages of endocytosis in neurons after global ischaemia. This is supported by the present finding of a significant association between neuronal rabaptin-5 and rab4 immunoreactivity in global ischaemia cases.

3.4.3 *APOE* genotype and endocytic pathway alterations

When individuals were separated into groups according to *APOE* genotype (with or without an *APOE* $\epsilon 4$ allele), there were two notable findings. First, there was a significant interaction between the effects of *APOE* genotype and an episode of global ischaemia on the alterations in degree of neuronal rab4 immunoreactivity in response to global ischaemia. In contrast, there was no interaction between the effects of *APOE* genotype and an episode of global ischaemia on alterations in the degree of neuronal rabaptin-5 immunoreactivity. These data indicate that there is a differential response of the internalisation/early trafficking and recycling phases of endocytosis in *APOE* $\epsilon 4$ carriers and individuals without an *APOE* $\epsilon 4$ allele after global ischaemia. Rabaptin-5 immunoreactivity was similarly increased in both *APOE* genotype groups after global ischaemia, reflecting comparable increases in endocytic internalisation/early trafficking. In contrast, there was a trend toward increased rab4 immunoreactivity in response to global ischaemia in individuals without an *APOE* $\epsilon 4$ allele, whereas an opposite trend was evident in *APOE* $\epsilon 4$ carriers. These data suggest an increase in the number of endosomes following a recycling route back to the plasma membrane after global ischaemia in non-*APOE* $\epsilon 4$ individuals compared to *APOE* $\epsilon 4$ carriers in which there may be a reduction in the number of endosomes trafficked along the recycling pathway. Second, the data indicate marked *APOE* genotype differences in the degree of neuronal rab4 immunoreactivity in control brain. The degree of neuronal rab4 immunoreactivity was approximately 50% greater (not statistically significant) in *APOE* $\epsilon 4$ controls suggestive of underlying differences in endocytic pathway activity in non-ischaemic control brain. Since endocytic activation has previously been demonstrated in AD and in view of the association between *APOE* $\epsilon 4$ and development of AD, elevated endosomal recycling activity in *APOE* $\epsilon 4$ controls may be related to the presence of early AD in some individuals. This is unlikely, however, since all brains were screened for the presence of A β deposits and neurofibrillary tangles which were only evident in a minority of controls and global ischaemia cases. Furthermore, the presence of A β deposits and/or tangles was not associated with *APOE* genotype. Significantly, in the control group, one *APOE* $\epsilon 4$ individual displayed neuritic and diffuse A β deposits and tangles but only minimal rabaptin-5 and rab4 immunoreactivity. Thus, it is possible that greater rab4 immunoreactivity in the control *APOE* $\epsilon 4$ group may reflect *APOE* genotype specific intrinsic differences in endosomal trafficking in uninjured brain.

Previously, *APOE* genotype has been associated with differences in aspects of general brain function in uninjured brain, such as cerebral blood flow and glucose metabolism (Small *et al.*, 1995; Scarmeas *et al.*, 2003). *In vitro* studies have shown isoform-specific differences in endocytic trafficking and localisation of apoE in uninjured neurons (DeKroon and Armati, 2001) and apoE3 and apoE4 have been shown to accumulate in different parts of cultured neurons (Nathan *et al.*, 1994; Nathan *et al.*, 2002). Isoform-specific effects influencing neuronal physiology in normal brain may therefore underlie the discrepancy in endocytic recycling activity between the *APOE* ϵ 4 and non-*APOE* ϵ 4 control groups.

In a previous study using this cohort of individuals, there was no association between the degree of neuronal damage after global ischaemia and *APOE* genotype (Figure 32) (Horsburgh *et al.*, 1999a). Therefore, in this cohort, *APOE* genotype-dependent differences in the endocytic response to global ischaemia are not linked to differences in pathological outcome. However, inability to control for important variables such as the duration and severity of the ischaemic insult in human subjects may preclude the detection of *APOE* genotype differences in neuronal damage. In addition, as discussed earlier, endocytic pathway alterations may reflect changes occurring early in the cascade of cellular processes triggered by the ischaemic insult. The majority of global ischaemia cases survived for 3 days or less and in view of the involvement of delayed neuronal damage in global ischaemia it is unclear if ischaemic damage matures further beyond this time-point. Thus, it is conceivable that *APOE* genotype differences in endocytic alterations could precede pathological differences.

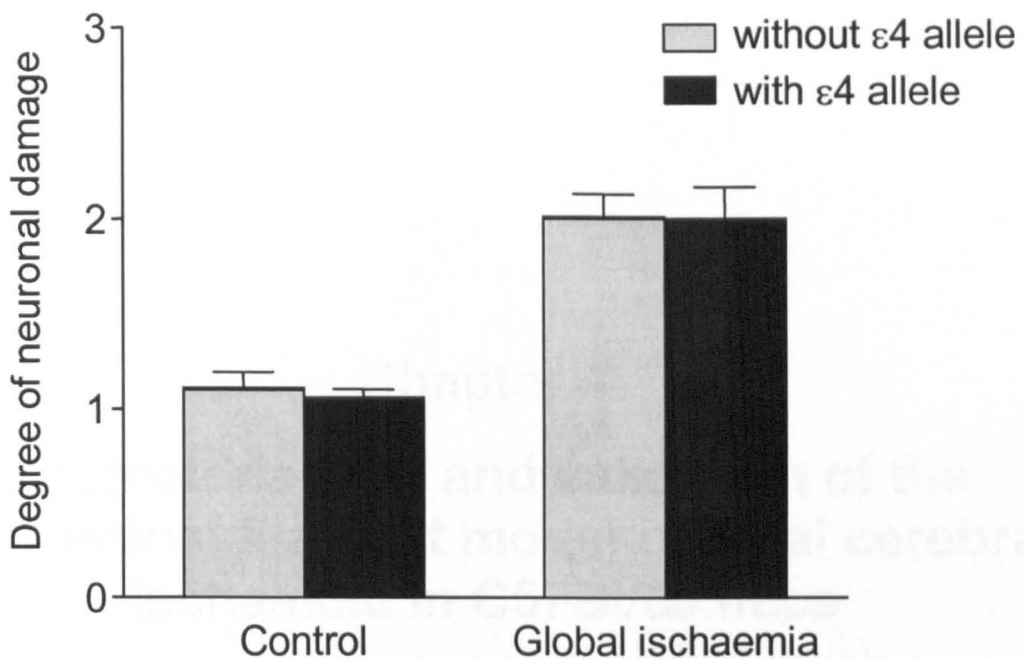


Figure 32. Effect of *APOE* genotype on ischaemic neuronal damage

Ischaemic damage was assessed previously by Dr Karen Horsburgh (Horsburgh *et al.*, 1999a). There was no significant difference in the degree of neuronal damage in individuals with and without an *APOE* $\epsilon 4$ allele in controls or after global ischaemia. $P > 0.05$, Mann-Whitney *U*-statistic. $n = 24$ (control without $\epsilon 4$); $n = 11$ (control with $\epsilon 4$); $n = 28$ (global ischaemia without $\epsilon 4$); $n = 15$ (global ischaemia with $\epsilon 4$). Data are presented as mean \pm SEM.

The *APOE* genotype dependent differences in endocytic pathway alterations after global ischaemia evident in the present study raise the possibility that differences in the response of this pathway may contribute to the mechanisms underlying *APOE* genotype differences in susceptibility to acute brain injury shown previously. Since the endocytic pathway is integral to intracellular processing of apoE, these results suggest that there may be isoform-specific differences in the way that apoE (and other molecules) is trafficked through neurons after injury. The potential importance of interactions between the endocytic pathway, apoE trafficking and other processes involved in the response to cerebral ischaemia are discussed later (*sections 5.4.6 and 5.4.7*).

3.4.4 Conclusions

In summary, the aims stated at the outset of this study have been achieved:

1. upregulation of endocytic activity was evident in human post-mortem temporal lobe tissue after an episode of global ischaemia
2. *APOE* genotype was associated with differences in endocytic pathway alterations after global ischaemia

Chapter 4

Characterisation and validation of the intraluminal filament model of focal cerebral ischaemia in C57Bl/6J mice

4.1 Introduction and aims

The intraluminal filament occlusion (sustained anaesthesia) model of focal ischaemia was established and characterised to enable further evaluation of the roles of *APOE* genotype and endocytic pathway alterations in the response to cerebral ischemia. The model was established in C57Bl/6J mice, the background strain of *APOE* transgenic mice used in the following study (*chapter 5*). The specific aims of the present study were to:

1. establish and validate the reproducibility of an intraluminal occlusion model of focal cerebral ischaemia in the mouse
2. determine the occlusion-duration effects of intraluminal occlusion on the extent and distribution of ischaemic damage and local cerebral blood flow
3. determine the effects of focal cerebral ischaemia on the response of the endocytic pathway

4.2 Materials and methods

This study was carried out at the Wellcome Surgical Institute, University of Glasgow. Measurement of ischaemic damage and local cerebral blood flow was performed unaware of occlusion duration.

4.2.1 Mice

Adult male C57Bl/6J strain mice obtained from Charles River, UK, were used.

4.2.2 Development of model

4.2.2.1 Development of surgical technique

Prior to characterising the model, preliminary work was required to gain competence in general surgical protocols and to establish the best surgical approach for intraluminal occlusion (*section 2.3.2.1*).

4.2.2.2 Comparison of 5-0 and 6-0 filament

Previous reports of focal cerebral ischaemia induced by a heat-blunted filament employed either a 5-0 or thinner 6-0 nylon monofilament. Once competence was gained in the surgical approach, experiments were performed to establish the most suitable size of filament to use. Cerebral blood flow was assessed qualitatively using the ^{14}C

autoradiography technique (*section 2.11.2*) after 15min intraluminal occlusion induced with either a 5-0 or 6-0 filament (n = 5 in each group). ^{14}C -IAP was administered 2min prior to the end of occlusion (i.e. at 13min). Clear evidence of hypoperfusion in core MCA territory (*see section 4.3.1.1*) ipsilateral to occlusion indicates a successful occlusion. Therefore, autoradiograms were assessed to determine if hypoperfusion (relative to the contralateral hemisphere) was present in two core MCA regions: (1) dorsolateral caudate nucleus, and (2) somatosensory cortex.

4.2.2.3 Measurement of ischaemic damage – validation of method

An adaptation of the technique developed by Osborne *et al.* (1987) was used for volumetric measurement of ischaemic damage as described (*section 2.8*). As the present study was the first to use the adapted technique, it was also necessary to test and verify the accuracy of the technique prior to full volumetric analysis. Two important features distinguished the adapted method from the original: (1) the modified technique used scale diagrams derived from a stereotaxic mouse atlas (Hof *et al.*, 2000) compared to scale drawings of rat stereotaxic levels in the original technique, (2) mouse scale diagrams are overlaid on a stereotaxic grid which allows direct calibration of distance on the MCID image analyser and accounts for magnification from actual brain size; in contrast, the rat scale drawings are not on a stereotaxic grid therefore indirect calibration using a graticule and incorporation of a known magnification factor is required during volumetric calculations to account for enlargement of scale drawings from actual brain size.

To test the accuracy of the adapted technique, the volume of ischaemic damage was compared in five mice using direct calibration of distance from the stereotaxic grid with that obtained using the previously established system of indirect calibration of distance using a graticule with incorporation of a magnification correction factor (as in original Osborne technique).

4.2.3 Characterisation of model

4.2.3.1 Effect of occlusion duration on ischaemic damage

To assess the effects of occlusion duration on the volume of ischaemic damage, mice ($29 \pm 0.9\text{g}$) were randomly assigned to one of three groups: 15min occlusion (n = 8); 30min occlusion (n = 8); 60min occlusion (n = 7). After the appropriate duration of occlusion, the filament was withdrawn to allow reperfusion for 24h at which point mice

were anaesthetised and sacrificed by trans-cardiac perfusion fixation. Sections (6µm) were cut from paraffin embedded brain and the volume of ischaemic damage was measured as described (*section 2.8*). For brains to be included for volumetric analysis the following criteria had to be met: (1) clear evidence of ischaemic damage in the striatum, and (2) absence of haemorrhage as observed in haematoxylin and eosin-stained tissue. Reproducibility of measurement of ischaemic damage was tested (**Appendix E**).

4.2.3.2 Effect of occlusion duration on cerebral blood flow

The occlusion-duration effects of intraluminal occlusion on local cerebral blood flow (LCBF) were assessed in groups of mice undergoing 15min (n = 6) or 60min intraluminal filament occlusion (n = 6) and 15min (n = 4) or 60min (n = 4) sham occlusion. LCBF was measured as described (*section 2.11*). ¹⁴C-IAP was administered 2min prior to the end of occlusion (at 13min or 58min). Reproducibility of LCBF measurement was tested (**Appendix F**).

4.2.3.3 Effect of occlusion duration on blood pressure

The temporal profile of mean arterial blood pressure (MABP) during intraluminal occlusion was monitored in separate groups of mice subjected to 60min intraluminal filament occlusion (n = 8) or 60min sham occlusion (n = 6) as described (*section 2.3.3*). MABP was recorded at 5 minute intervals until the animal was sacrificed.

4.2.4 Examination of cerebrovascular anatomy

In a separate group of mice (n = 10), the major arteries of the circle of Willis were examined as described (*section 2.3.4*).

4.2.5 Operational definition of MCA territory

In order to assess the spatial distribution of ischaemic damage, an independent definition of “MCA territory” was required. The operational definition of MCA territory used in the present study was derived from a series of detailed and systematic experiments by Scremin examining the rodent cerebral vascular system (Scremin, 1995). At normal levels of perfusion pressure and in the absence of vascular abnormalities, the MCA and its major branches supply the striatum and the majority of

the cerebral cortex (including motor, somatosensory, piriform, auditory cortex). The hippocampus and thalamus do not receive their blood supply from the MCA or its collaterals; these structures derive their blood supply from the posterior cerebral artery and its major branches and therefore lie outside MCA territory.

4.2.6 Immunohistochemistry

To assess the effects of focal ischaemia on the endocytic pathway, paraffin-embedded sections (6µm) were immunostained (peroxidase protocol) with antibodies to rabaptin-5 and rab4 (*section 2.9.3*).

4.2.7 Statistical analysis

One-way analysis of variance (ANOVA) followed by Student's unpaired *t*-test (incorporating Bonferroni correction factor of 3) was used to assess statistical differences in the volume of ischaemic damage among the three occlusion groups. Student's unpaired *t*-test was used to assess statistical differences in LCBF between the 15min occlusion and 60min occlusion groups. Student's unpaired *t*-test was used to assess statistical differences in MABP after 60min occlusion between sham occlusion and intraluminal occlusion groups. All data are presented as mean ± SEM.

4.3 Results

4.3.1 Development of model

4.3.1.1 Comparison of 5-0 and 6-0 filament

To determine the most appropriate type of filament to use for occlusion in the full study, the pattern of cerebral blood flow was assessed on ^{14}C autoradiograms following occlusion with either a 5-0 (thicker) or 6-0 (thinner) filament (**Table 4** and **Figure 33**). Hypoperfusion (relative to contralateral hemisphere) was observed in the dorsolateral caudate nucleus in 2 of 5 mice after occlusion with a 6-0 filament and in 4 of 5 mice after occlusion with a 5-0 filament. In the somatosensory cortex, hypoperfusion was observed in 1 of 5 mice after occlusion with a 6-0 filament and in 3 of 5 mice after occlusion with a 5-0 filament. Since clear hypoperfusion in MCA core territory (particularly the dorsolateral caudate nucleus) reflects a successful occlusion, these results demonstrate that a successful occlusion was achieved more consistently with a 5-0 filament. In addition, the 5-0 filament moved along the lumen of the carotid vessels more smoothly and was more easily manipulated and directed. Accordingly, less time was required to correctly place the 5-0 filament, an important factor in the application of this technique. In consideration of the above findings, the 5-0 filament was chosen as the more suitable for this model and was used subsequently for all occlusions.

Table 4. Hypoperfusion associated with intraluminal occlusion with a 5-0 and thinner 6-0 filament

Filament size	No. of mice with hypoperfusion in MCA territory	
	Dorsolateral caudate nucleus	Somatosensory cortex
5-0	4 of 5	3 of 5
6-0	2 of 5	1 of 5

More consistent hypoperfusion in core MCA regions was produced by occlusion with the 5-0 filament indicating that this filament size was more suitable for achieving successful occlusion.

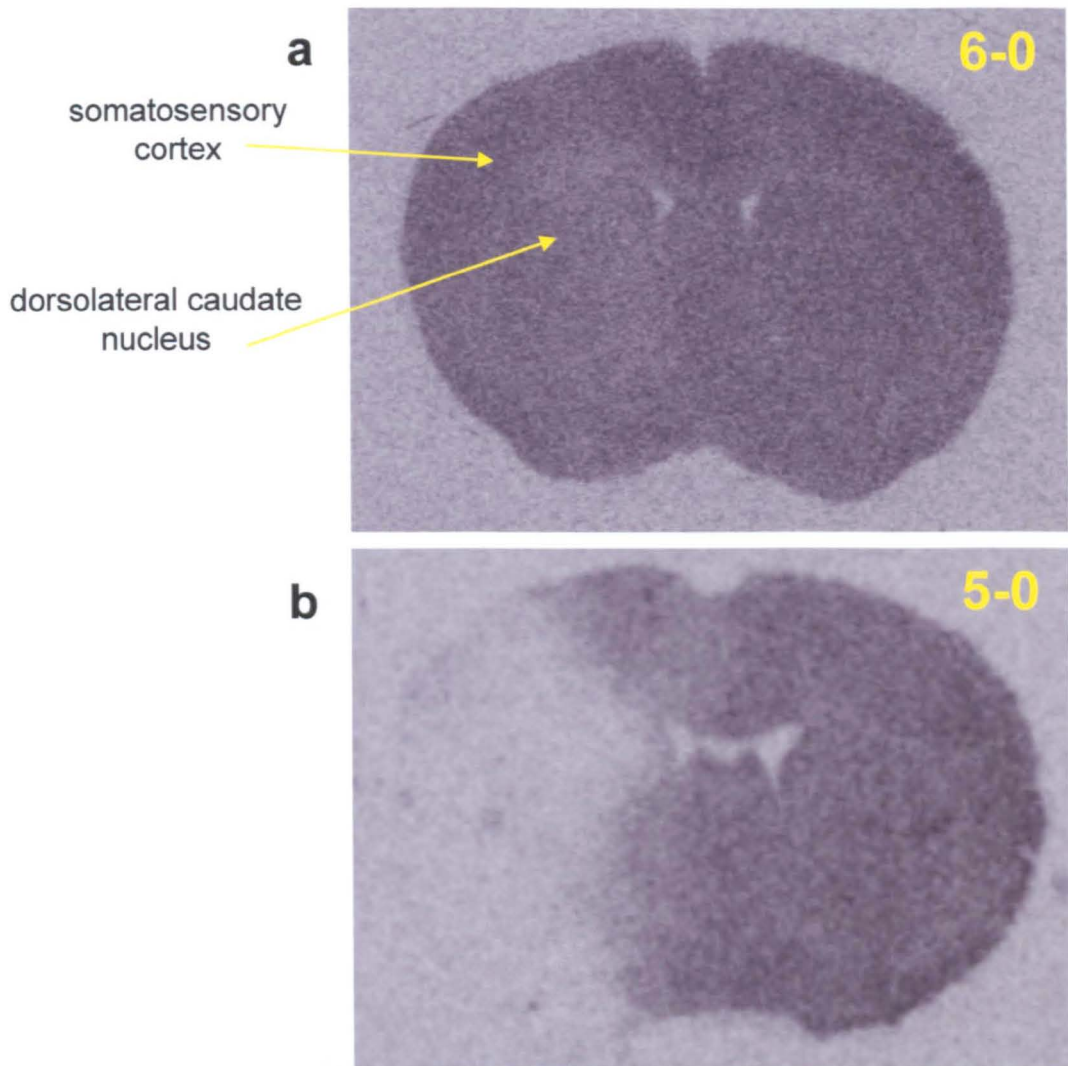


Figure 33. Effect of filament size on hypoperfusion in MCA territory

Representative autoradiograms illustrating (a) absence of hypoperfusion in MCA territory after occlusion with a 6-0 filament, indicating an unsuccessful occlusion, and (b) illustrating clear hypoperfusion (relative to contralateral hemisphere) in core MCA territory of occluded hemisphere after occlusion with a 5-0 filament, indicating a successful occlusion.

4.3.1.2 Measurement of ischaemic damage – validation of method

To confirm the accuracy of the method adapted for use in mice, the volume of ischaemic damage was compared in a group of mice ($n=5$) using either direct (from mouse atlas stereotaxic grid) or indirect (from graticule with magnification correction) calibration of distance. Linear magnification of the mouse scale diagrams was measured under a dissecting microscope and determined to be 9.25. The results shown in **Figure 34** demonstrate that the adapted method of volumetric measurement of ischaemic damage using direct distance calibration produced values that strongly correlated with those obtained using indirect distance calibration from a graticule ($P = 0.0003$, $r^2 = 0.98$). This confirmed the accuracy of the adapted technique adapted for measuring the volume of ischaemic damage after intraluminal occlusion in mice.

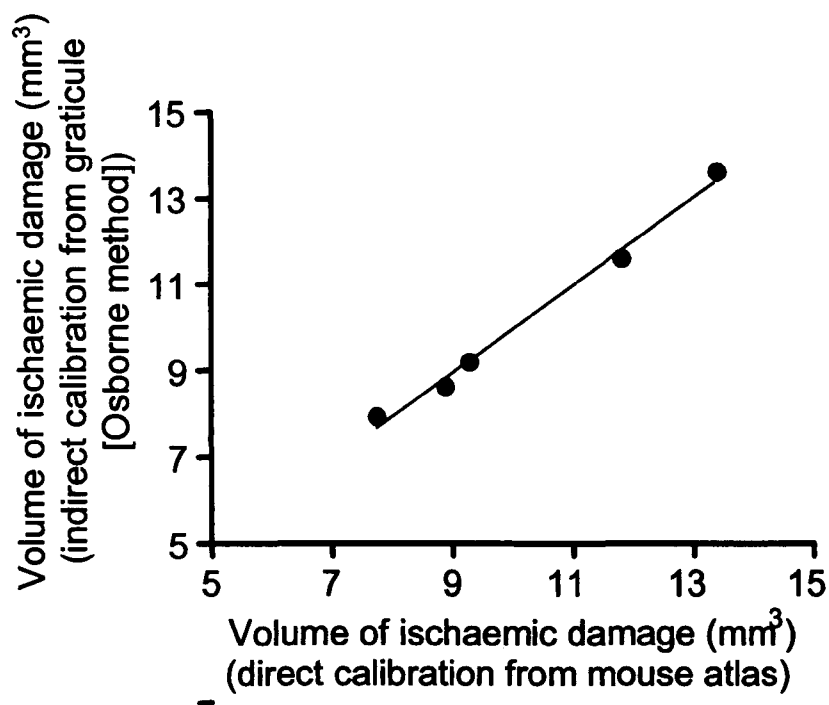


Figure 34. Validation of adapted method for measurement of ischaemic damage
The volumes of ischaemic damage obtained with the adapted method (direct calibration of distance from mouse atlas) strongly correlated ($P = 0.003$, $r^2 = 0.98$) with volumes obtained using a previously characterised method (Osborne *et al.*, 1987) involving indirect calibration from a graticule.

4.3.2 Characterisation of model

4.3.2.1 Post-operative recovery

Post-operative recovery was closely monitored in mice undergoing 24h reperfusion. In general, animals adopted a hunched posture and displayed a reduction in normal exploratory behaviour throughout the recovery period. Circling (during spontaneous movement) and/or leaning (at rest) to one side were observed regardless of occlusion duration. In mice that experienced 15min occlusion, mobility and grooming behaviour was largely preserved. In contrast, minimal spontaneous movement was generally noted in mice that experienced 30min or 60min occlusion, although the response to tactile stimulation was not diminished. Normal grooming behaviour was generally absent in these mice. Sporadic episodes of spinning (barrel-rolling) were observed infrequently irrespective of occlusion duration. Subsequent histological analysis revealed that, in all mice, barrel-rolling during recovery corresponded to the presence of an intracranial haemorrhage. In addition, normal feeding was absent in all mice during the recovery period.

4.3.2.2 Haemorrhage rate, mortality rate and absence of ischaemic damage

Prior to full neuropathological analysis, haematoxylin and eosin-stained tissue from each brain was examined to determine if the criteria for proceeding to analysis were met (Table 5).

Table 5. Mice excluded prior to measurement of ischaemic damage

Duration of occlusion (min)	Number of mice excluded		
	Mortality	Haemorrhage	No ischaemic damage
15 (n = 8)	0	1 (12.5%)	1 (12.5%)
30 (n = 8)	1 (12.5%)	1 (12.5%)	1 (12.5%)
60 (n = 7)	2 (28%)	0	0
Combined (n = 23)	3 (13%)	2 (9%)	2 (9%)

Criteria for inclusion included 24h recovery, absence of haemorrhage and clear histological evidence of ischaemic damage.

4.3.2.3 *Effect of occlusion duration on ischaemic damage*

Areas of tissue displaying ischaemic pathology were identified on coronal haematoxylin and eosin-stained sections. With 15min occlusion, areas of ischaemic pathology were characterised by ischaemic damage to neurons and glial cells. There was minimal damage to vascular cells. Pallor and vacuolation of the neuropil were also features of these areas of ischaemic damage. With 30min occlusion and 60min occlusion, areas of ischaemic damage displayed similar pathology to that observed with 15min occlusion, although vascular pathology was more marked with these durations of occlusion.

The volume of ischaemic damage increased markedly with increasing duration of occlusion: 15min occlusion ($9 \pm 2\text{mm}^3$); 30min occlusion ($56 \pm 6\text{mm}^3$); 60min occlusion ($69 \pm 2\text{mm}^3$) and was highly reproducible in all groups (co-efficient of variance, 3% with 60min occlusion) (**Figure 35**).

The spatial distribution of ischaemic damage was highly sensitive to the duration of occlusion (**Table 6**). With 15min occlusion, ischaemic damage was restricted to MCA territory (striatum and cortex). Increasing the duration of occlusion beyond 15min resulted in ischaemic damage both within and outside (e.g. hippocampus, thalamus) MCA territory.

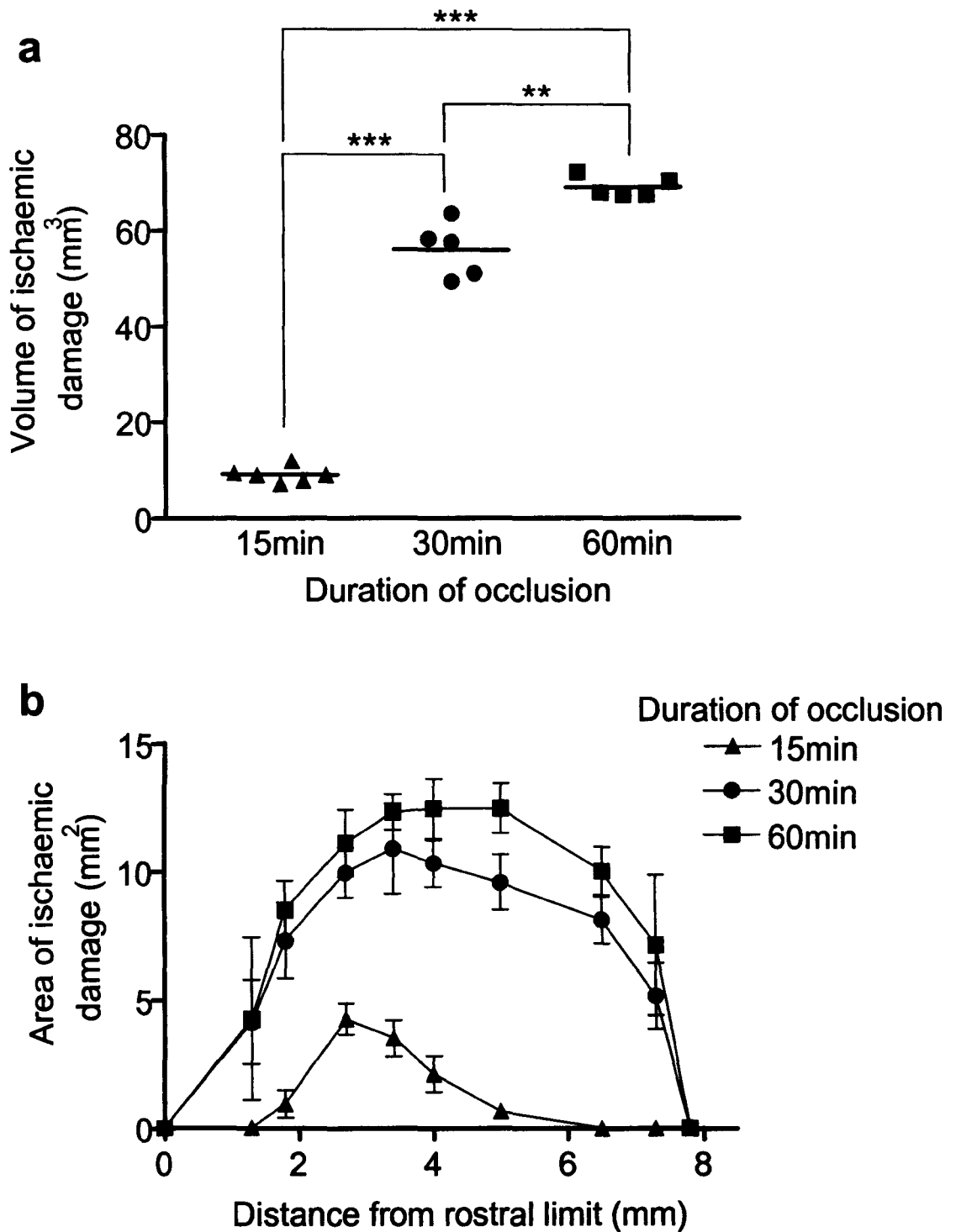


Figure 35. Effect of occlusion duration on ischaemic damage

(a) There were significant increases in the volume of ischaemic damage with increasing duration of occlusion. Bars show mean. (b) The area of ischaemic damage at each coronal level was markedly increased when occlusion duration was increased beyond 15min. $**P < 0.01$; $***P < 0.001$, one-way ANOVA followed by Student's unpaired *t*-test with Bonferroni correction factor. 15min (n=6); 30min (n = 5); 60min (n = 5). Data are presented as mean \pm SEM.

Table 6. Frequency of ischaemic damage in specific brain regions

Duration of occlusion (min)	Number of mice with ischaemic damage in specific brain regions				
	Striatum	Cerebral cortex	Hippocampus	Thalamus	Hypothalamus
15	6 of 6	1 of 6	0 of 6	0 of 6	0 of 6
30	5 of 5	5 of 5	5 of 5	4 of 5	1 of 5
60	5 of 5	5 of 5	5 of 5	5 of 5	5 of 5

Ischaemic damage was confined to MCA territory (striatum, cortex) after 15min occlusion. Increasing the duration of occlusion to 30min resulted in consistent involvement of regions outside MCA territory including the hippocampus and thalamus but only infrequent involvement of the hypothalamus. 60min occlusion produced a similar pattern of ischaemic damage to 30min occlusion but with more frequent involvement of the hypothalamus.

4.3.2.4 Effect of occlusion duration on cerebral blood flow

To assess the effects of increasing the duration of occlusion on cerebral hypoperfusion, local cerebral blood flow (LCBF) was measured in distinct neuroanatomical loci within and outside MCA territory and in an area exempt from the ischaemic insult (cerebellum). In sham-occluded mice, LCBF could not be measured fully quantitatively as the values were above the measurable limit of the image analysis system (2000ml/100g/min). The potential reasons for the excessively high values are discussed later (*section 4.4.1.3*). Therefore, in sham animals, the local tissue concentration of ^{14}C -IAP at each anatomical locus was normalised to the concentration of ^{14}C -IAP in the cerebellum, an area exempt from the ischaemic insult. The normalised values were used as indices of cerebral blood flow in each locus. There were no hemispheric asymmetries in local brain tissue ^{14}C concentration observed after sham occlusion indicating that surgical manipulation did not contribute to hypoperfusion in the occluded hemisphere (**Figure 36**). There were no significant differences in relative ^{14}C -IAP concentration after 60min occlusion compared to 15min occlusion in any anatomical locus suggesting that surgical manipulation did not contribute to the more severe hypoperfusion observed in some areas after 60min occlusion (**Table 7**).

LCBF was reduced after both 15min occlusion and 60min occlusion in the occluded hemisphere (**Figure 37**). However, the severity of hypoperfusion was significantly different in these two groups. In 9 of 12 regions examined LCBF was significantly lower after 60min occlusion compared to 15min occlusion ($P < 0.05$) (**Table 8** and **Figure 38**). In core MCA territory, such as the dorsolateral caudate nucleus, there was marked hypoperfusion after both 15min occlusion and 60min occlusion. In contrast, outside the territory of the MCA (e.g., hippocampus, dorsolateral thalamus, hypothalamus), marked hypoperfusion was apparent after 60min occlusion but not 15min occlusion. LCBF was not significantly different in the cerebellum, motor cortex and ventromedial thalamus after 60min occlusion compared to 15min occlusion ($P > 0.05$) (**Figure 39**).

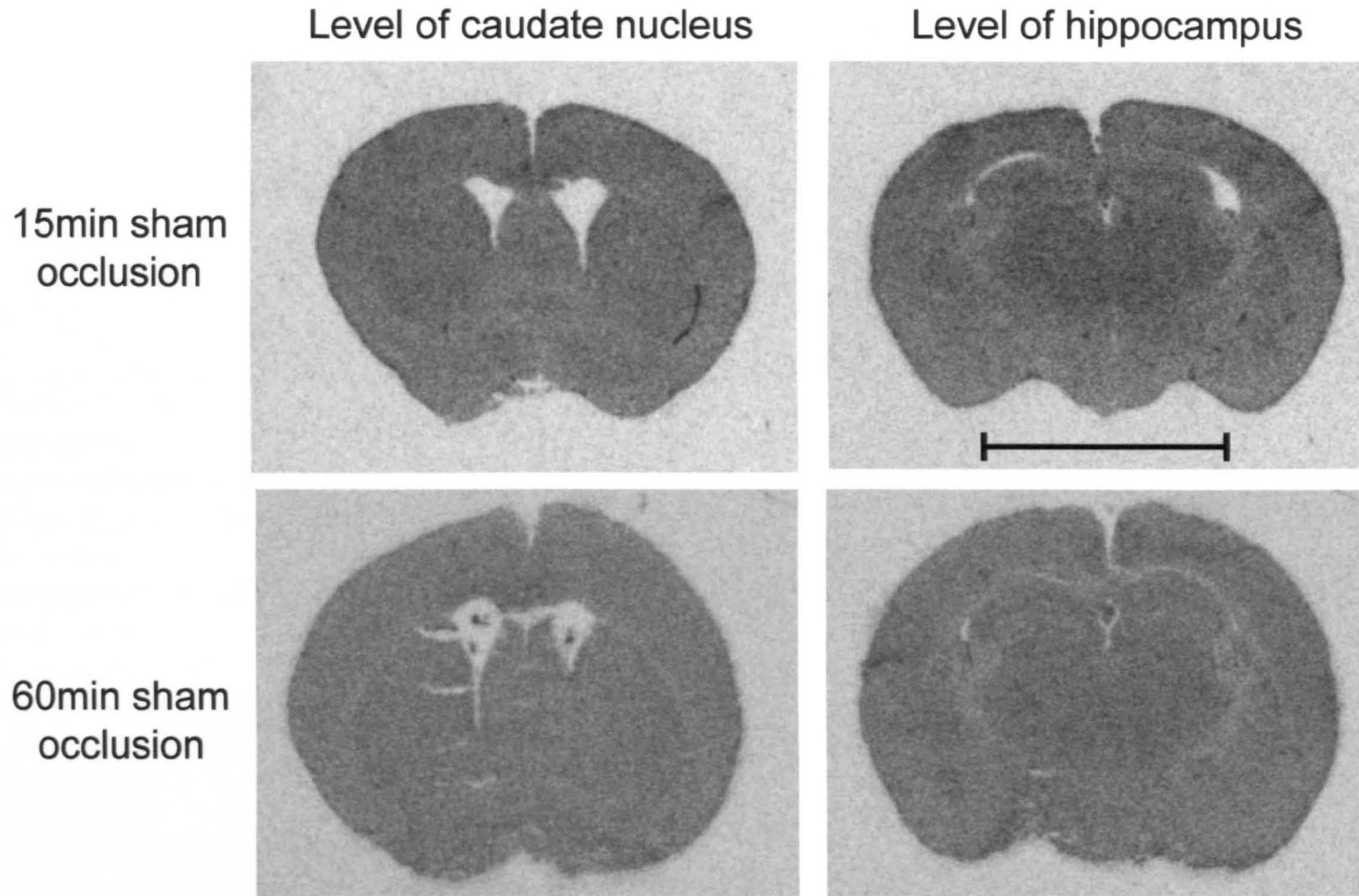


Figure 36. Representative ^{14}C -IAP autoradiograms after 15min and 60min sham occlusion

Visual inspection of autoradiograms revealed that sham occlusion did not result in any hemispheric asymmetries in local brain tissue ^{14}C concentration indicating that sham surgery did not result in cerebral hypoperfusion in the ipsilateral hemisphere. This observation was made after both 15min and 60min occlusion. Scale bar, 5mm.

Table 7. Effect of sham occlusion duration on local brain tissue ^{14}C concentration

	Local tissue concentration of ^{14}C -IAP (normalised to cerebellum)			
	<i>Ipsilateral to occlusion</i>		<i>Contralateral to occlusion</i>	
	15min Occ.	60min Occ.	15min Occ.	60min Occ.
Cerebellum (cortex)	1.00	1.00	1.00	1.00
Frontal cortex	1.06 ± 0.03	1.05 ± 0.03	1.05 ± 0.03	1.00 ± 0.02
Caudate nucleus (dorsolateral)	1.07 ± 0.05	1.09 ± 0.10	1.08 ± 0.04	1.07 ± 0.06
Caudate nucleus (ventromedial)	1.02 ± 0.04	1.07 ± 0.11	1.04 ± 0.04	1.03 ± 0.11
Motor cortex	1.06 ± 0.04	1.02 ± 0.09	1.07 ± 0.04	1.04 ± 0.06
Somatosensory cortex	1.09 ± 0.05	1.08 ± 0.08	1.09 ± 0.04	1.04 ± 0.08
Insular cortex	1.04 ± 0.06	1.08 ± 0.07	1.05 ± 0.04	1.03 ± 0.01
Hippocampus (CA1)	1.03 ± 0.05	1.05 ± 0.05	1.05 ± 0.04	1.03 ± 0.06
Thalamus (dorsolateral)	1.12 ± 0.05	1.18 ± 0.03	1.12 ± 0.03	1.16 ± 0.01
Thalamus (ventromedial)	1.14 ± 0.03	1.18 ± 0.01	1.15 ± 0.03	1.17 ± 0.02
Hypothalamus	0.90 ± 0.04	1.01 ± 0.05	0.88 ± 0.04	1.04 ± 0.03
Auditory cortex	1.00 ± 0.04	1.04 ± 0.04	1.00 ± 0.04	1.01 ± 0.02

The local tissue concentration of ^{14}C -IAP at each anatomical locus was normalised to the concentration of ^{14}C -IAP in the cerebellum, an area exempt from the ischaemic insult, and used as an index of LCBF. There were no significant differences in the normalised ^{14}C concentrations after 60min occlusion compared to 15min occlusion in any locus examined ($P > 0.05$). Unpaired Student's *t*-test for the comparison between 60min occlusion and 15min occlusion. Occ. (occlusion). $n = 4$ (each group). Data are presented as mean ± SEM.

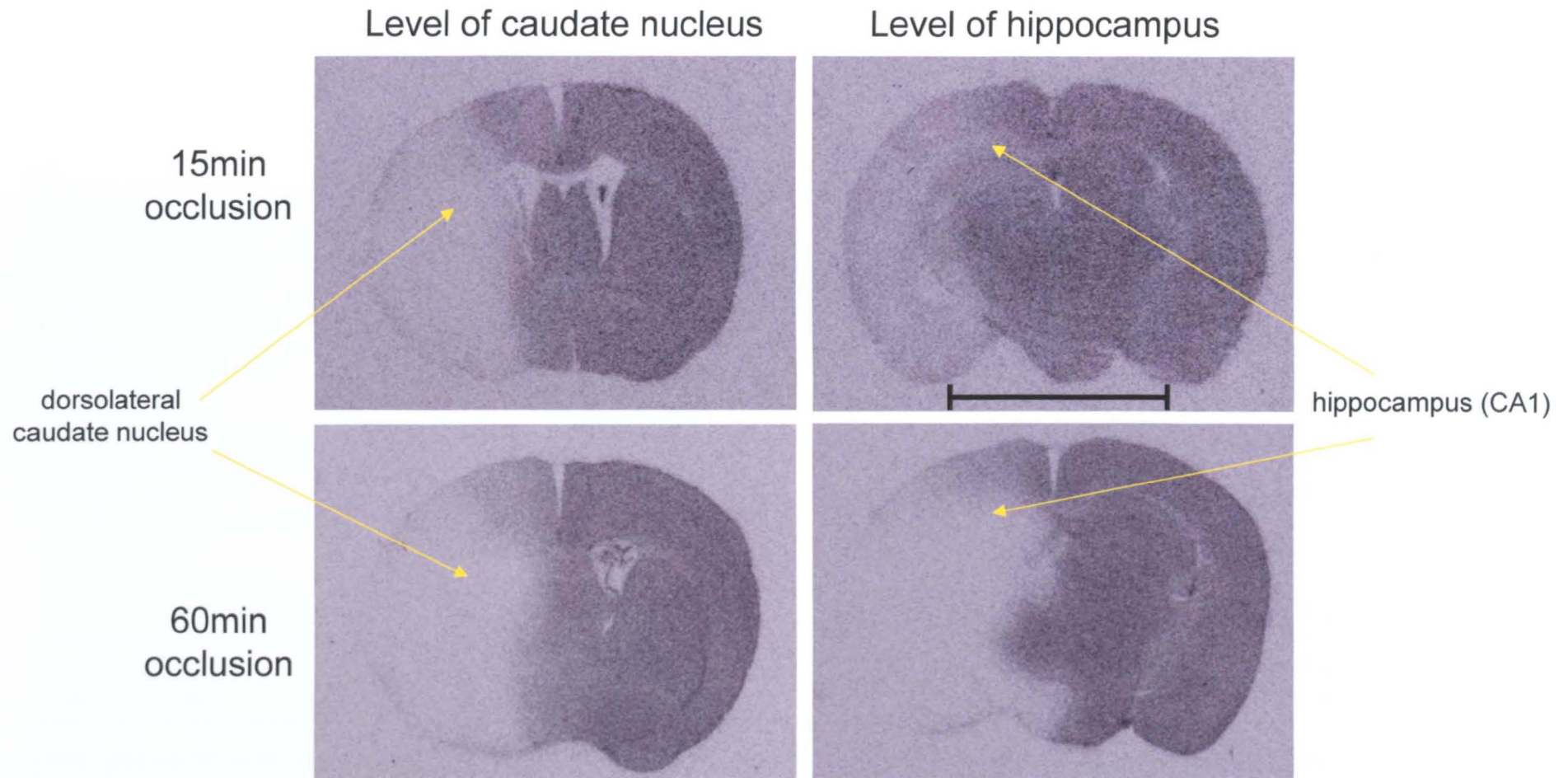


Figure 37. Representative ^{14}C -IAP autoradiograms after 15min and 60min intraluminal occlusion
 After 15min occlusion, marked cerebral hypoperfusion was restricted to MCA core territory (e.g. dorsolateral caudate nucleus). After 60min occlusion, in addition to core MCA areas, marked cerebral hypoperfusion was observed in regions outside MCA territory such as hippocampus and dorsolateral thalamus. Scale bar, 5mm.

Table 8. Effect of intraluminal filament occlusion duration on local cerebral blood flow

	Local cerebral blood flow (ml/100g/min)			
	<i>Ipsilateral to occlusion</i>		<i>Contralateral to occlusion</i>	
	15min Occ. (% contralateral)	60min Occ. (% contralateral)	15min Occ.	60min Occ.
Cerebellum (cortex)	123 ± 6 (103%)	115 ± 3 (97%)	121 ± 5	119 ± 3
Frontal cortex	57 ± 9 (41%)	14 ± 4** (11%)	138 ± 12	122 ± 6
Caudate nucleus (dorsolateral)	33 ± 5 (26%)	9 ± 2*** (8%)	127 ± 6	119 ± 7
Caudate nucleus (ventromedial)	51 ± 7 (43%)	12 ± 2*** (11%)	119 ± 7	109 ± 7
Motor cortex	57 ± 8 (45%)	36 ± 6 (32%)	128 ± 14	114 ± 5
Somatosensory cortex	46 ± 8 (32%)	12 ± 2** (9%)	143 ± 8	128 ± 6
Insular cortex	45 ± 10 (36%)	12 ± 3* (10%)	124 ± 11	116 ± 7
Hippocampus (CA1)	61 ± 7 (55%)	16 ± 6*** (16%)	111 ± 3	103 ± 5
Thalamus (dorsolateral)	64 ± 12 (48%)	23 ± 8* (17%)	133 ± 6	133 ± 4
Thalamus (ventromedial)	119 ± 11 (84%)	86 ± 17 (60%)	141 ± 8	143 ± 6
Hypothalamus	68 ± 7 (70%)	36 ± 10* (37%)	97 ± 7	98 ± 5
Auditory cortex	43 ± 11 (39%)	8 ± 3* (7%)	111 ± 6	109 ± 4

LCBF was significantly lower after 60min intraluminal filament occlusion compared to 15min occlusion in 9 of 12 anatomical loci examined in the occluded hemisphere. There were no statistically significant differences in LCBF between 60min and 15min occlusion at any loci examined contralateral to the occluded hemisphere. * $P < 0.05$; ** $P < 0.01$; *** $P < 0.001$, unpaired Student's *t*-test for the comparison between 60min occlusion and 15min occlusion. Occ. (occlusion). $n = 6$ (each group). Data are presented as mean ± SEM.

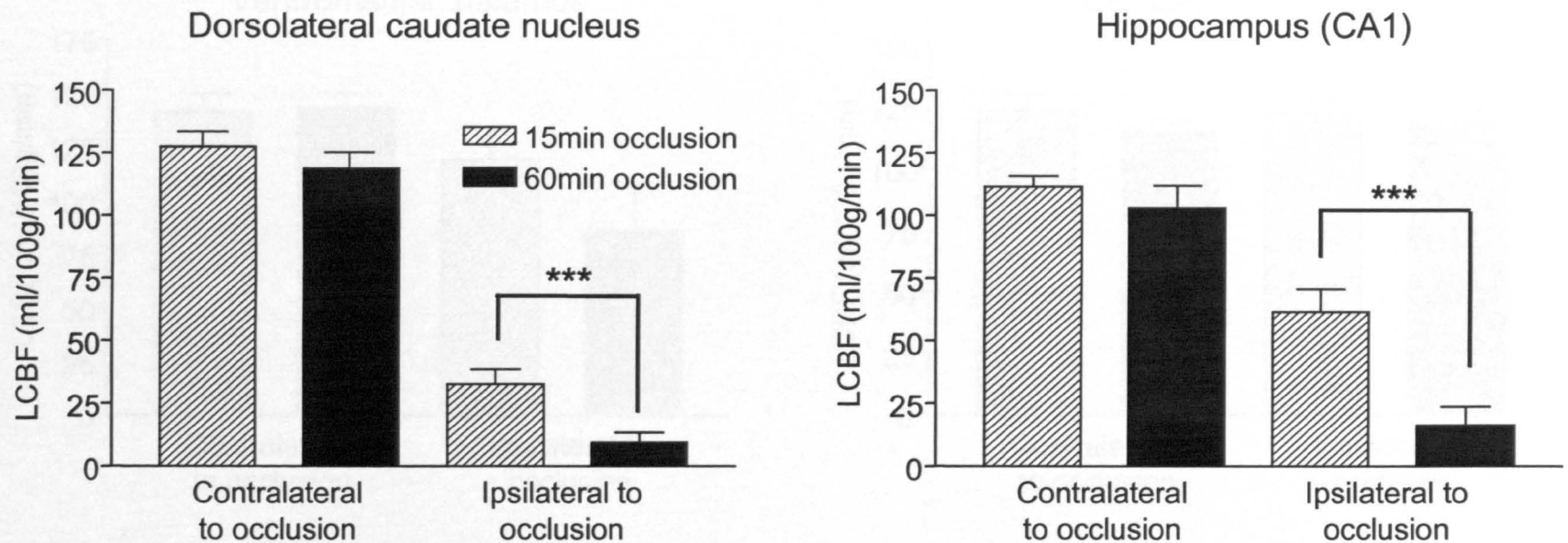


Figure 38. Effect of occlusion duration on local cerebral blood flow in the dorsolateral caudate nucleus and hippocampus (CA1)
 LCBF was significantly lower after 60min occlusion compared to 15min occlusion in the dorsolateral caudate nucleus (MCA core territory) and in the CA1 region of the hippocampus (outside MCA territory). There were no statistical differences in LCBF in either region in the contralateral hemisphere after 60min occlusion compared to 15min occlusion. Data extracted from Table 1. *** $P < 0.001$, unpaired Student's t -test. $n = 6$ (each group). Data are presented as mean \pm SEM.

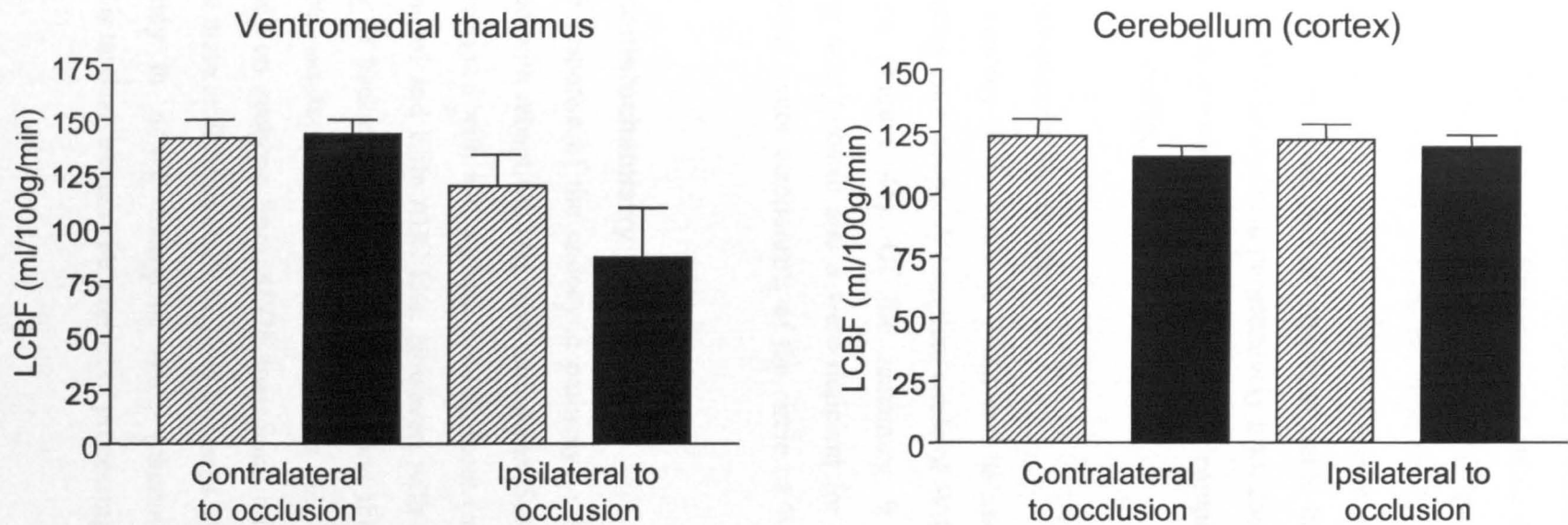


Figure 39. Effect of occlusion duration on local cerebral blood flow in the ventromedial thalamus and cerebellum

In the hemisphere ipsilateral to occlusion, significant reductions in LCBF were not observed in all loci examined. For example in the ventromedial thalamus, LCBF was reduced after 60min compared to 15min occlusion, however, this did not reach statistical significance ($P > 0.05$). In the cerebellum, which is exempt from the direct ischaemic episode, LCBF was similar after 60min and 15min occlusion both ipsilateral and contralateral to occlusion suggesting that general physiological decline was not responsible for more severe cerebral hypoperfusion in other areas after 60min occlusion. Unpaired Student's *t*-test for the comparison between 60min occlusion and 15min occlusion. $n = 6$ (each group). Data are presented as mean \pm SEM.

4.3.2.5 Effect of occlusion duration on blood pressure

Mean arterial blood pressure (MABP) remained stable during surgical manipulation in both the sham and intraluminal occlusion groups (**Figure 40**). Immediately following placement of the filament tip, a transient increase in MABP was observed in both groups, followed by a return to pre-occlusion levels at which blood pressure stabilised. In the sham occlusion group, MABP remained stable throughout the occlusion. In the occlusion group, MABP declined progressively from 25min after the onset of occlusion and was significantly lower after 60min occlusion compared to sham occlusion (61 ± 2 mmHg vs. 77 ± 2 mmHg, $P < 0.0001$).

4.3.3 Cerebrovascular anatomy

The vascular anatomy of the circle of Willis and its associated arteries was examined under a dissecting microscope. A complete circle of Willis was present in only 1 of 10 mice examined (**Figure 41**). Of the remaining 9 mice, 6 had one posterior communicating artery absent and 3 were deficient for both posterior communicating arteries. All other major components of the circle of Willis appeared normal in these mice.

4.3.4 Immunohistochemistry

To assess the response of the endocytic pathway to focal ischaemia, sections were immunostained with rabaptin-5 and rab4 antibodies. Several concentrations of primary antibodies were used with and without pre-treatment (microwaving, pepsin treatment) and with Standard and Elite ABC kits. However, with all combinations, staining was weak (mainly of background) and non-specific and therefore the endocytic response could not be assessed after focal ischaemia in C57Bl/6J mice. Preliminary immunostaining on sections from *APOE* transgenic mice produced specific staining, indicating that these antibodies could be used to assess endocytic pathway activity in the following study in *APOE* transgenic mice (*chapter 5*). The reason for these discrepancies is unclear, but may be a result of processing of brains at different times.

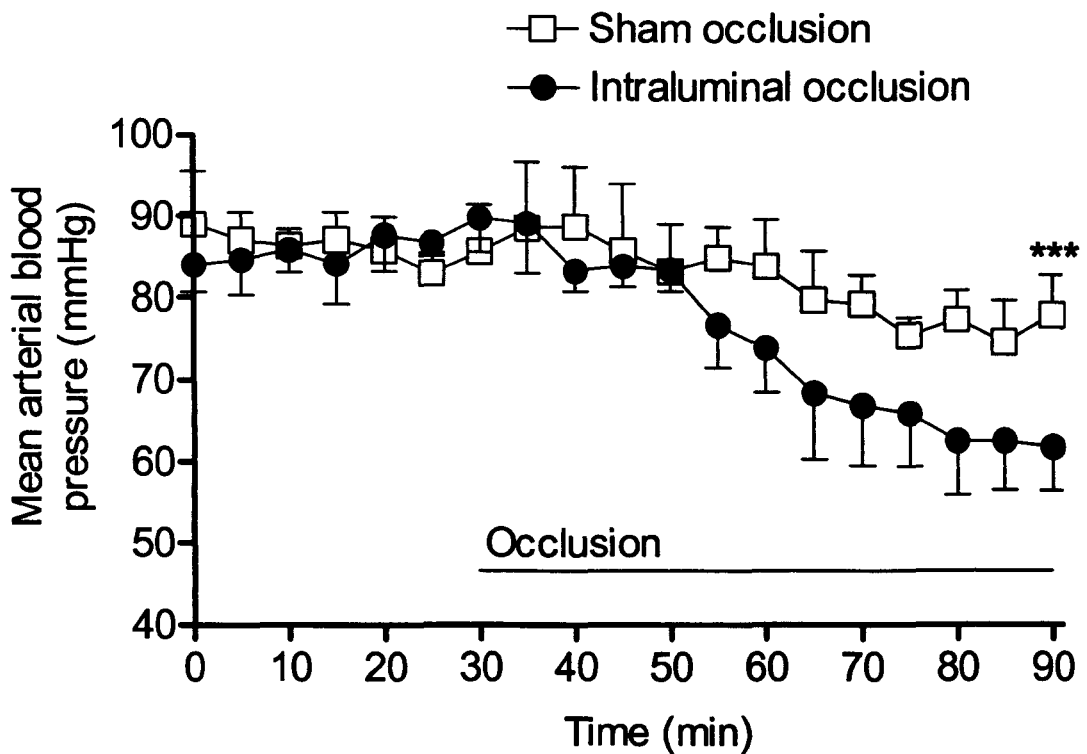


Figure 40. Mean arterial blood pressure during 60min occlusion

Mean arterial blood pressure (MABP) remained stable during the surgical procedure. In the sham occlusion group, MABP remained relatively stable throughout the entire procedure with only a small decline evident 45min after sham occlusion. In the occlusion group, a progressive decline in MABP was noted 25min after occlusion onset and MABP was significantly lower after 60min occlusion compared to sham occlusion. MABP recorded every 5min throughout the procedure. $***P < 0.0001$, Student's unpaired *t*-test. $n = 6$ (sham occlusion); $n = 8$ (intraluminal occlusion). Data are presented as mean \pm SEM.

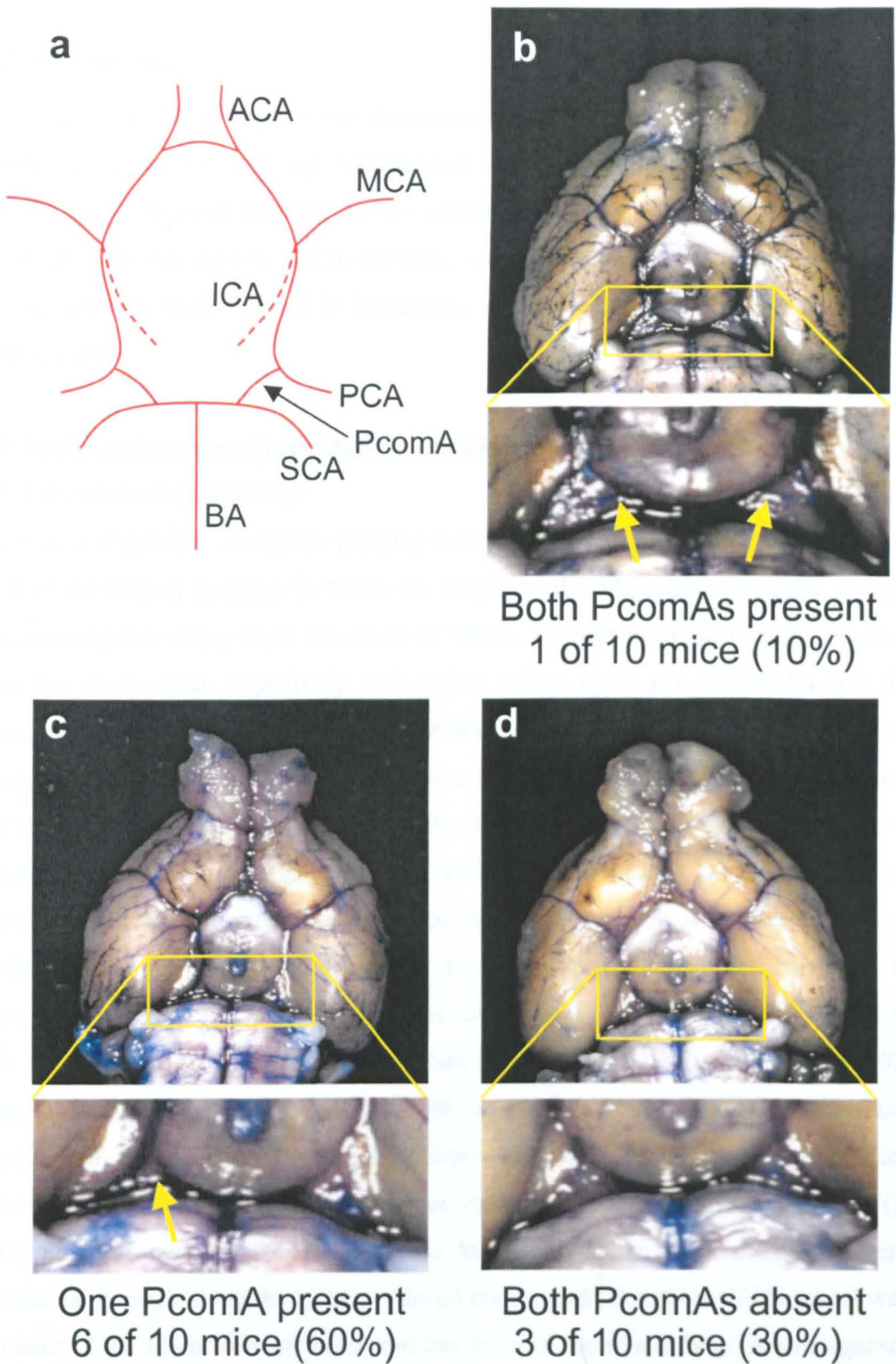


Figure 41. Integrity of the circle of Willis in C57Bl/6J mice

(a) Diagram of major arteries in a complete circle of Willis. (b) 1 of 10 mice had a complete circle of Willis containing both PcomAs (arrows). (c) 6 of 10 mice had one PcomA present (arrow) and (d) 3 of 10 mice had both PcomAs absent. ACA (anterior cerebral artery); MCA (middle cerebral artery); PCA (posterior cerebral artery); PcomA (posterior communicating artery); SCA (superior cerebellar artery); BA (basilar artery); ICA (internal carotid artery).

4.4 Discussion

The results from the present study demonstrate that a reproducible model of focal cerebral ischaemia induced by intraluminal filament occlusion was achieved in C57Bl/6J mice. A steep increase in the extent of ischaemic damage, that included recruitment of tissue outside MCA territory, was observed with increasing occlusion duration and was likely related to increasing severity of hypoperfusion and PcomA hypoplasticity.

4.4.1 Technical and methodological considerations

4.4.1.1 Intraluminal occlusion

Successful intraluminal occlusion requires that the tip of the intraluminal filament is placed at the correct position to block the origin of the MCA and therefore prevent blood entering this artery from the circle of Willis. Correct placement of the filament cannot be determined objectively but rather relies upon (1) knowledge of the approximate distance from the carotid bifurcation to insert the filament so that the tip reaches the origin of the MCA, and (2) resistance felt while gently pushing the filament along the internal carotid artery indicating that the tip is lodged in the proximal part of the anterior cerebral artery and therefore occluding the MCA. During preliminary experiments to learn and refine the technique, resistance was felt after advancement of the filament approximately 10mm distal to the carotid bifurcation. This was in agreement with previous studies describing intraluminal occlusion in the mouse in which the filament was inserted 9 – 11.5mm (Clark *et al.*, 1997; Hata *et al.*, 1998; Kitagawa *et al.*, 1998c; Belayev *et al.*, 1999; Mao *et al.*, 1999). There are two major consequences arising from failure to achieve correct filament placement that are characteristic of the intraluminal occlusion technique in both mice and rats: (1) inadequate obstruction of the origin of the MCA caused by the filament not being advanced far enough along the internal carotid artery, and (2) rupture of the vessel wall as a result of the filament being advanced too far/with too much force. A consequence of the first of the above complications is absence of cerebral hypoperfusion and ischaemic pathology (Schmid-Elsaesser *et al.*, 1998) whereas the latter is associated with bleeding from the punctured vessel and subarachnoid haemorrhage (Garcia, 1993; Clark *et al.*, 1997; Tsuchiya *et al.*, 2003a). Previous studies have reported exclusion rates due to intracranial haemorrhage of up to 30% (Matsuo *et al.*, 1994; Clark *et al.*,

1997; Yanaka *et al.*, 1997; Tsuchiya *et al.*, 2003a). Perhaps related to the incidence of intracranial haemorrhage, high mortality rates (up to 80%) have also been reported following intraluminal occlusion in the mouse (Kitagawa *et al.*, 1998c; Connolly *et al.*, 1996; Clark *et al.*, 1997). In the present study, mortality rate and incidence of intracranial haemorrhage were both less than 15% and therefore within the range previously reported. The occurrence of intracranial haemorrhage did not appear to be associated with increasing duration of occlusion. This is not unexpected since haemorrhage is likely to occur due to incorrect filament placement regardless of occlusion duration. Examination of brains revealed that deaths during recovery were not due to intracranial haemorrhage. A particularly severe ischaemic insult may be the underlying cause since deaths occurred only after longer periods of occlusion (30min and 60min), consistent with previous reports (Connolly *et al.*, 1996; Kitagawa *et al.*, 1998c).

4.4.1.2 Measurement of ischaemic damage – validation of method

The studies described in this thesis involved occlusion of the MCA in mice with an intraluminal filament. A rigorously tested method for volumetric assessment of ischaemic damage following focal cerebral ischaemia had previously been established and used extensively in the laboratory (Osborne *et al.*, 1987). However, this method was set up in order to measure infarct volumes in rats following electro-coagulation of the MCA (Tamura *et al.*, 1981) and therefore volume calculation was derived from area measurements on scale diagrams of the rat brain. It was necessary, therefore, to establish and validate the accuracy and reproducibility of a modified version of the Osborne method that would be pertinent to the mouse intraluminal occlusion model. Volumes of damage calculated from area measurements at eight coronal levels had been shown previously to provide a close approximation of the true infarct volume in rats (Osborne *et al.*, 1987). Therefore, eight coronal levels for area measurement were chosen from a stereotaxic mouse atlas (Hof *et al.*, 2000). Areas of ischaemic damage were delineated on to scale diagrams derived from the stereotaxic atlas representing the eight coronal levels. An advantage of the mouse scale diagrams was their superimposition on a stereotaxic grid which enabled direct calibration of distance from the grid for area measurements and accounted for magnification of the diagrams from true brain size. Previously, indirect calibration from a graticule measurement and subsequent use of a magnification factor was required with the rat scale diagrams. In the

present study, volumetric measurement of ischaemic damage using direct distance calibration from the mouse stereotaxic diagrams produced comparable values to those generated from indirect graticule distance calibration as used in the Osborne method. This confirmed that the adapted method using direct distance calibration from mouse atlas scale diagrams produced accurate measurements of the volume of ischaemic damage.

It was also important to validate the reproducibility of volumetric measurement as there are a number of potential sources of error during the measurement process. These include selection of the appropriate sections for each coronal level, identification of areas of ischaemic damage, delineation of areas of damage on to scale diagrams and area measurement on the image analysis system. In the present study, measurement of the volume of ischaemic damage in two different sessions was highly reproducible (**Appendix E**) and therefore errors arising from the above sources were minimal. Overall, the refined technique for volumetric assessment of ischaemic damage in mice was considered to provide accurate and reproducible measurements.

4.4.1.3 Measurement of local cerebral blood flow

In the present study, LCBF was measured quantitatively using a modification of the method first described and validated by Maeda *et al.* (2000). This method was used to avoid some of the complications associated with LCBF measurement in mice using techniques originally developed and tailored for use in larger species that involve multiple blood vessel cannulations (Reivich *et al.*, 1969; Sakurada *et al.*, 1978). In small rodents, such as mice, cannulation of multiple blood vessels for ^{14}C -IAP infusion and arterial blood sampling is less practicable. Extensive and precise surgery under prolonged general anaesthesia is required. In addition, blood loss during repeated sampling of arterial blood may lead to systemic hypotension on account of the relatively small blood volume in the mouse. In the present study, these complications were avoided by intraperitoneal administration of ^{14}C -IAP in conjunction with a single sampling of heart blood upon termination of the experiment. Sampling of blood samples from the frozen heart was readily attainable.

A possible source of error in LCBF measurement, particularly applicable to the mouse, arises from the post-mortem diffusion of ^{14}C -IAP. During the time required to remove the brain from the skull and freeze in isopentane, the tracer can diffuse from more highly perfused areas to tissue with lower levels of perfusion resulting in

distortion of autoradiograms. In larger species, such as the cat and rat, this may not present a major problem due to the relatively large structures and greater diffusion distances. However, in the mouse, structures are smaller and more tightly packed and diffusion distances are greatly reduced. Therefore, underestimation of LCBF in high-flow areas and overestimation in low-flow areas may result. To minimise post-mortem diffusion of tracer it is necessary therefore to avoid any delay in removal and freezing of the brain. In the present study, it was possible to transfer the brain to the freezing medium (isopentane) 30 – 40s after decapitation. It has been shown previously that removal and freezing of the brain 1 - 2min following decapitation results in the loss of normal contrasts in optical densities among various structures observed on autoradiograms. Freezing of the brain in 30s, however, gave rise to structural heterogeneity approaching that observed in the rat although it was proposed that some degree of tracer diffusion still occurred (Jay *et al.*, 1988). In the present study, structural heterogeneity was also observed although to a lesser extent than that observed in rat studies previously conducted in the department and elsewhere. It is likely, therefore, that some degree of tracer diffusion occurred in this study and that the magnitude of LCBF may be underestimated in high-flow areas and overestimated in low-flow areas.

A further consideration in LCBF measurement is the exponential relationship that exists between local brain tissue ^{14}C concentration and absolute CBF. At lower ^{14}C tissue concentrations, the curve is linear and therefore a small change in ^{14}C concentration will produce a proportional change in CBF. At higher concentrations of ^{14}C , however, the slope of the curve increases rapidly. In this region, a small increase in tissue ^{14}C concentration would be reflected by a much larger increase in CBF. A consequence of this relationship is that in highly perfused areas (with high ^{14}C concentrations), LCBF may be overestimated. This is in contrast to the effect discussed above in which underestimation of LCBF in high-flow areas may occur due to tracer diffusion. In the present study, such overestimation of LCBF is more likely to occur in the hemisphere contralateral to occlusion, particularly in high-flow areas which included somatosensory cortex and dorsolateral thalamus. In contrast, in ischaemic territory (ipsilateral to occlusion) tissue ^{14}C concentration is relatively low and therefore LCBF measurement is less prone to overestimation.

4.4.2 Ischaemic damage after intraluminal occlusion

4.4.2.1 Reproducibility of ischaemic damage

In the present study it was important to establish if reproducible volumes of ischaemic damage were attainable using this model as previous reports in both mice and rats suggested that a significant limitation of the intraluminal occlusion model is variability in extent of ischaemic damage (Laing *et al.*, 1993; Kuge *et al.*, 1995; Connolly *et al.*, 1996; Clark *et al.*, 1997; Takano *et al.*, 1997). The inherent variability of the model may be partly attributable to some of the technical complications described in *section 4.4.1.1*. In the present study, the volume of ischaemic damage was highly reproducible after 15min, 30min or 60min intraluminal occlusion.

Previously, strategies to minimise variability have included coating of the filament end with either silicon resin (Koizumi *et al.*, 1986; Takano *et al.*, 1997; Hata *et al.*, 1998) or poly-L-lysine (Belayev *et al.*, 1996; Belayev *et al.*, 1999). The rationale behind these approaches is that coating the filament increases the adhesive forces between the filament and the vascular endothelium and so minimises the chances of residual flow past the filament. Although reproducibility has been demonstrated with these coated filaments, limitations include possible direct toxic effects of the coating substance on the endothelium and increased risk of haemorrhage as a result of excessive adhesion (Huang *et al.*, 1998). In the present study, use of a heat-blunted uncoated filament produced a high level of reproducibility. Several important factors may underlie this consistency. First, mice within a narrow weight-range ($29 \pm 0.9\text{g}$) were used. It has been shown previously that the size of filament is an important determinant of a successful occlusion and that the appropriate diameter of filament varies with the animal's weight (Connolly *et al.* 1996; Hata *et al.*, 1998). Consequently, if a uniform thickness of filament is employed, using mice within a narrow weight range should improve reproducibility. In the present study, the diameter of the heat-blunted filament tip was measured microscopically and therefore both filament size and animal weight were rigorously controlled. Second, to occlude the MCA, a technique that does not require interference with the pterygopalatine artery, a branch of the internal carotid artery (ICA), was used. In many studies, the pterygopalatine artery is ligated or electrocoagulated. However, due to its small size, deep-lying position and proximity to the vagus nerve, gaining access to this artery may produce inadvertent damage to the vagus nerve or one of its smaller branches with detrimental effects on the cardiovascular

and/or respiratory system(s) during the surgical procedure. Third, to assess the volume of ischaemic damage, a well-established and characterised technique developed in rats (Osborne *et al.*, 1987) was optimised and validated for use in mice. This method involves light microscopic examination of thin sections stained with haematoxylin and eosin to delineate areas of ischaemic damage at multiple coronal levels. Such a system affords greater accuracy and sensitivity of measurement than the frequently-employed 2,3,5-triphenyltetrazoline chloride method in which relatively fewer and thicker tissue blocks are used to differentiate areas of viable and damaged tissue (Liszcak *et al.*, 1984; Park *et al.*, 1988a).

4.4.2.2 *Effects of occlusion duration on extent and spatial distribution of ischaemic damage*

Increasing the duration of occlusion resulted in progressively larger volumes of ischaemic damage. However, the increase in volume of damage was disproportionately steep, in particular between 15min and 30min occlusion; the volume of ischaemic damage with 30min occlusion was 5-fold greater than with 15min occlusion. The steepness of the relationship between duration of occlusion and volume of ischaemic damage differs from that described in other species (Jones *et al.*, 1981) where the volume of damage increases markedly between 1 – 3h of occlusion (Kaplan *et al.*, 1991). In the present study in the mouse, this relationship was somewhat compressed with the occlusion-duration effect on extent of ischaemic damage most pronounced between 15min and 30min occlusion.

Expansion of the ischaemic lesion from 15min to 30min occlusion groups was in part due to development of damage in MCA territory (e.g. cerebral cortex) but also to the involvement of regions of the brain outside MCA territory, such as the hippocampus and thalamus. This finding is in agreement with previous reports of the susceptibility of the C57Bl/6J mouse to the effects of focal cerebral ischaemia. Using MAP2 immunoreactivity as a marker of viable neurons, Kitagawa *et al.* (1998c) demonstrated the loss of MAP2-immunoreactive neurons in the caudoputamen, cerebral cortex and hippocampus after intraluminal filament occlusion, reflecting areas of damage extending outside MCA territory. Belayev *et al.* (1999) also observed ischaemic damage in areas outside MCA territory such as the hippocampus and thalamus. Additionally, Hata *et al.* (1998) reported that the incidence of infarction in regions such as the hippocampus, thalamus and hypothalamus may be up to 75% after intraluminal filament

occlusion. In contrast, in other strains of mice such as CBA and DBA/2 the ischaemic lesion was confined to the caudoputamen and cerebral cortex with hippocampal neurons remaining intact (Kitagawa *et al.*, 1998c). The spatial distribution of damage in the C57Bl/6J mouse also appears to differ from that previously observed in the rat as structures not consistently damaged in rat (e.g. hippocampus, thalamus) are consistently involved in the mouse (Belayev *et al.*, 1999). This suggests that PcomA deficiency in C57Bl/6J mice, as observed in this and previous studies (Kitagawa *et al.*, 1998c; Kelly *et al.*, 2001b), may be a contributory factor in damage observed outside MCA territory since rats and the CBA and DBA/2 mouse strains have an intact circle of Willis (Kitagawa *et al.*, 1998c). Recently in the rat, however, cellular alterations indicative of direct ischaemic damage were observed in areas outside MCA territory following intraluminal occlusion but not electrocoagulation of the MCA prompting the authors to propose that this technique should not be viewed as a model of pure MCA occlusion (Kanemitsu *et al.*, 2002). Thus, strain- and model-specific factors may underlie the distinctive spatial pattern of ischaemic damage induced by intraluminal occlusion and are likely mediated through effects on cerebral blood flow.

The sensitivity of lesion volume/spatial distribution to intraluminal occlusion duration in the C57Bl/6J mouse has important practical implications, most notably the need for precise control over the duration of occlusion in order to minimise inter-animal variability.

4.4.3 Cerebral blood flow during intraluminal occlusion

In the present study, the intensity of ischaemia was most dense in the dorsolateral caudate nucleus and somatosensory cortex (e.g. 8 – 9% of contralateral value after 60min occlusion). There is little published LCBF data in mouse models of focal cerebral ischaemia, although systematic measurement of LCBF has been previously reported in rats following intraluminal occlusion (Memezawa *et al.*, 1992; Belayev *et al.*, 1997). The topographical pattern of severity of CBF deficit in the present study is consistent with these previous reports using the same model in which ischaemia was also demonstrated to be most intense in the somatosensory cortex and lateral caudoputamen. These areas represent core MCA territory and therefore would be expected to be most severely affected by occlusion. In the hemisphere contralateral to occlusion, a gradient of LCBF was observed declining from high-flow areas such as the ventromedial thalamus through areas with intermediate flow (e.g. caudate nucleus) to

the relatively modestly perfused hypothalamus. This spectrum of LCBF is also in agreement with previous studies that have quantitatively measured LCBF in non-occluded mice (Jay *et al.*, 1988; Maeda *et al.*, 2000).

Increasing the duration of occlusion was associated with increases in the severity of cerebral hypoperfusion in the hemisphere ipsilateral to occlusion. The lower levels of CBF observed after 60min occlusion (compared to 15min occlusion) may be a reflection of the progressive decline in blood pressure and neurochemical events associated with cerebral ischaemia (e.g. release of vasoconstrictor substances such as endothelins, increase in tissue pressure and platelet aggregation obstructing collateral vessels). The hypotension observed with 60min occlusion in the mouse is likely to exacerbate the ischaemic insult as a result of autoregulatory disturbances. Cerebral autoregulation is the physiological regulatory mechanism that maintains constant blood flow in the face of changes in perfusion pressure (Paulson *et al.*, 1990). Failure of this mechanism is a feature of cerebral ischaemia (Dirnagl and Pulsinelli, 1990). Consequently, when blood pressure declines, CBF will fall accordingly and will likely impact on the extent of ischemic damage. For example, after occlusion in the rat, transient hypotension of 40mmHg increased the volume of ischaemic damage by 45% (Osborne *et al.*, 1987). In the present study, in mice, blood pressure declined by 25mmHg after 60min occlusion. Bilateral common carotid artery occlusion (BCCAO) also induced reductions in MABP in C57Bl/6J mice but not MF1 mice (Kelly *et al.*, 2001b) suggesting a strain-specific effect perhaps linked to lack of PcomA integrity. Regions of the brain involved in the regulation of blood pressure, in particular the hypothalamus (Talman, 1985; Fontes *et al.*, 2001; Dampney *et al.*, 2002), experience ischaemia during intraluminal filament occlusion or BCCAO when there is absence of a PcomA.

With durations of occlusion in excess of 30min, hypoperfusion and ischaemic damage were consistently observed in the hippocampus, thalamus and hypothalamus. The blood supply of these areas is not derived from the MCA (Scremin, 1995). In rats, intraluminal filament placement occludes the anterior choroidal artery in addition to the MCA leading to ischaemic damage in the hypothalamus. A similar mechanism may be responsible for hypothalamic damage in the C57Bl/6J mouse after intraluminal filament occlusion. Cerebral hypoperfusion and ischaemic damage observed in the hippocampus and thalamus in C57Bl/6J mice may be a reflection of abnormalities observed in the posterior portion of the circle of Willis in this and other studies (Kitagawa *et al.*, 1998c;

Kelly *et al.*, 2001b). Absence or inadequacy of collateral supply via the PcomA when an intraluminal filament is introduced into the internal carotid artery and directed towards the anterior portion of the circle of Willis will also be exacerbated by hypotension.

There have been few previous studies examining the temporal-spatial progression of CBF deficits during occlusion in ischaemia models, particularly in the mouse. However, there is some evidence to suggest that the severe decline in CBF observed in the present study may be specific to intraluminal occlusion in the C57Bl/6J mouse. Kitagawa *et al.* (1998c) observed cerebral hypoperfusion in areas outside MCA territory in C57Bl/6 mice but not DBA/2 mice indicating a possible C57Bl/6 strain-specific effect, however, this study did not examine the temporal profile of CBF deficits. In the rat, there is minimal evidence of cerebral hypoperfusion in areas outside MCA territory following electro-coagulation (Hakim *et al.*, 1992) and clip occlusion (Takagi *et al.*, 1995) of the MCA. Most recently, in a thorough study using intraluminal occlusion, LCBF in areas outside MCA territory (hippocampus, thalamus) of the occluded hemisphere was not significantly different from levels in the non-occluded control hemisphere (Belayev *et al.*, 1997). The temporal profile of CBF deficits in rats has also been studied and has shown that the degree of hypoperfusion remains relatively stable with increasing occlusion duration (Hakim *et al.*, 1992; Memezawa *et al.*, 1992). Of particular relevance to the present study is the previous demonstration in rats experiencing intraluminal occlusion that CBF deficits in the occluded hemisphere remain constant after 20, 60 and 120min of occlusion (Memezawa *et al.*, 1992). The current findings, which show a severe decline in CBF with increasing occlusion duration, are therefore in contrast to these previous studies. Thus, although distant changes in CBF have been reported in other rodent species, the magnitude, distribution and extreme duration-dependence are not in accord with the present report. Furthermore, the species/strain specific effects of intraluminal occlusion on the temporal-spatial pattern of CBF deficits parallels the pathological observations discussed above. Consequently, results from the previous studies outlined above in association with the present findings collectively suggest that intraluminal occlusion in the C57Bl/6 mouse produces a distinctive occlusion duration-dependent pattern of CBF deficits and ensuing ischaemic pathology that is not observed in other species (e.g. rat) or other strains of mice (e.g. DBA/2).

4.4.4 Implications for utility of model in further studies

Elucidation of the above features of the intraluminal occlusion model has important implications for its application. In particular, the choice of occlusion duration requires particular consideration. Reproducibility was demonstrated after each occlusion duration and therefore 15min, 30min or 60min occlusion are all vindicated on the basis of acceptable inter-animal variability. However, 30min and 60min occlusion were associated with declining blood pressure and widespread hypoperfusion, factors that produce massive volumes of ischaemic tissue (approximately 60% of hemisphere after 60min occlusion). Such large volumes of damage may represent the upper limit of damage and therefore are not appropriate for investigation of factors that may modulate the amount of ischaemic damage (e.g. genetics, pharmacotherapy). In addition, 30min and 60min occlusion were associated with greater mortality rate compared to 15min occlusion. Therefore, in view of the low mortality rate, high degree of reproducibility and avoidance of the effects of declining systemic blood pressure and widespread cerebral hypoperfusion, 15min occlusion was considered to be the most suitable occlusion duration for investigating the influence of *APOE* genotype on outcome and endocytic pathway activity in response to focal cerebral ischaemia as described in the following chapter.

4.4.5 Conclusions

In summary, the major objective of the present study - to characterise the intraluminal filament occlusion model of focal cerebral ischaemia in C57Bl/6J mice – has been accomplished. The aims stated at the outset of this study have been achieved:

1. an intraluminal occlusion model was developed in C57Bl/6J mice and the reproducibility of ischaemic damage validated after three different durations (15min, 30min and 60min) of occlusion
2. increasing the duration of occlusion resulted in a steep increase in the extent of ischaemic damage and widespread increases in the severity of cerebral hypoperfusion

However, rabaptin-5 and rab4 immunostaining was unsuccessful in C57Bl/6J paraffin-processed tissue after focal ischaemia. Thus, it was not possible to define if there were alterations in the endocytic pathway in response to focal ischaemia in C57Bl/6J mice.

Chapter 5

Association between *APOE* genotype and differences in outcome and endocytic pathway alterations after focal cerebral ischaemia in mice

5.1 Introduction and aims

APOE transgenic mice expressing human *APOE* isoforms have been developed that display a human-like pattern of *APOE* expression and apoE immunoreactivity (Xu *et al.*, 1996). The effects of *APOE* genotype on outcome and apoE and endocytic pathway alterations after focal ischaemia were investigated in these mice. The specific aims of the present study were to determine, in a mouse model of transient focal ischaemia, if:

1. *APOE* genotype is associated with differences in outcome
2. there are alterations in apoE that are *APOE* genotype-dependent
3. there are endocytic pathway alterations that are *APOE* genotype-dependent

5.2 Materials and methods

This study was carried out at the Wellcome Surgical Institute, Glasgow. All experiments were performed unaware of *APOE* genotype.

5.2.1 Mice

Adult male human *APOE* transgenic mice ($33 \pm 1.8\text{g}$), were used (*section 2.2.2*).

5.2.2 Focal ischaemia and evaluation of neurological deficit

Transient focal ischaemia (15min) was induced by intraluminal filament occlusion (sustained anaesthesia model) in *APOE* $\epsilon 3$ ($n = 17$) and *APOE* $\epsilon 4$ ($n = 20$) as described (*section 2.3.2.1*). After 15min occlusion, the filament was withdrawn to allow reperfusion for 24h. After 24h reperfusion, mice were assigned a neurological deficit score of 0 to 4 as described (*section 2.4*). Following neurological evaluation, mice were perfused transcardially (*section 2.5*) and paraffin-processed (*section 2.6.1.1*). Paraffin embedded brains were cut into $6\mu\text{m}$ sections (*section 2.6.2*) which were used for histological and immunohistochemical analysis.

5.2.3 Measurement of ischaemic damage

The volume of ischaemic damage was measured in haematoxylin and eosin-stained tissue as described (*section 2.8*). Criteria for inclusion were: (1) clear evidence of ischaemic damage in the striatum, and (2) absence of intracranial haemorrhage as observed in haematoxylin and eosin-stained tissue.

5.2.4 Immunohistochemistry

Adjacent sections (6µm) were immunostained (peroxidase protocol) with apoE, rabaptin-5 and rab4 antibodies as described (*section 2.9.3*). Fluorescent double-labelling immunostaining was performed on selected sections as described (*section 2.9.4*).

5.2.4.1 Volumetric measurement of apoE immunostaining

Boundaries between areas of tissue containing numerous intensely stained apoE-positive cells and areas with few and faintly stained cells (normally outside the ischaemic territory) could be defined. The distribution of clearly defined areas of apoE immunostaining could therefore be delineated at eight coronal levels. Areas were then integrated with the distance between each coronal level to calculate a volume in the same way as for ischaemic damage (*section 2.9.6.1*). Reproducibility of volumetric measurement was tested (**Appendix G**).

5.2.4.2 Semi-quantification of apoE, rabaptin-5 and rab4 immunoreactivity

Semi-quantification of apoE, rabaptin-5 and rab4 immunoreactivity was performed at the level of the caudate nucleus (coronal level 3, 0.2mm anterior to bregma). In the hemisphere ipsilateral to occlusion, the degree of cellular immunoreactivity in the ischaemic caudate nucleus was semi-quantified in six fields, using a 10mm² grid at x400 magnification, according to a scoring system as described (*section 2.9.6.2*). The average degree of immunoreactivity was then calculated. Reproducibility of semi-quantification was tested (**Appendix H**).

5.2.5 Statistical analysis

All statistical comparisons were made between the *APOE* ε3 and *APOE* ε4 groups. Student's unpaired *t*-test was used to assess statistical significance of differences in the volume of ischaemic damage. Mann-Whitney *U*-statistic was used to assess statistical significance of differences in neurological deficit. Student's unpaired *t*-test was used to assess statistical significance of differences in the volume of apoE immunostaining. Pearson correlation was used to assess statistical significance of the association between the volume of ischaemic damage and the volume of apoE immunostaining. Mann-Whitney *U*-statistic was used to assess statistical significance of differences in the degree of apoE, rabaptin-5 and rab4 immunoreactivity. Spearman correlation was used

to assess statistical significance of the association between the degree of apoE immunoreactivity and the degree of rabaptin-5 or rab4 immunoreactivity. All data are presented as mean \pm SEM

5.3 Results

5.3.1 Mortality rate, haemorrhage rate and absence of ischaemic damage

Prior to volumetric measurement of ischaemic damage, haematoxylin and eosin-stained tissue from each brain was examined to determine if the criteria for proceeding to analysis were met (**Table 9**).

It was noted that mortality rate (11%) and the percentage of brains without evidence of ischaemic damage (14%) in the present study were similar to the frequencies observed in the previous study (*chapter 4*) in C57Bl/6J mice. In contrast, the haemorrhage rate in the present study was considerably higher in *APOE* transgenic mice (38%) than that observed in the previous study in C57Bl/6J mice (9%). Putative reasons for this discrepancy are discussed later (*section 5.4.1*). There were no apparent differences between *APOE* ϵ 3 and *APOE* ϵ 4 mice in mortality rate (12% vs 10%), haemorrhage rate (35% vs 40%) or the percentage of mice with no ischaemic damage (12% vs 15%).

Table 9. Mice excluded prior to measurement of ischaemic damage

Genotype	Number of mice excluded		
	Deaths	Haemorrhage	No ischaemic damage
<i>APOE</i> ϵ 3 (n = 17)	2 (12%)	6 (35%)	2 (12%)
<i>APOE</i> ϵ 4 (n = 20)	2 (10%)	8 (40%)	3 (15%)
Combined (n = 37)	4 (11%)	14 (38%)	5 (14%)

Criteria for inclusion included 24h recovery, absence of haemorrhage and clear histological evidence of ischaemic damage. A high exclusion rate due to intracranial haemorrhage was evident in both *APOE* ϵ 3 and *APOE* ϵ 4 mice. Mortality rate and the number of mice without histological evidence of ischaemic damage were relatively low and similar in both groups.

5.3.2 Effect of *APOE* genotype on Ischaemic damage

The volume of ischaemic damage was significantly greater in *APOE* ϵ 4 compared to *APOE* ϵ 3 mice ($9 \pm 1\text{mm}^3$ vs. $7 \pm 1\text{mm}^3$, $P = 0.006$). The volume of ischaemic damage was also highly reproducible in both the *APOE* ϵ 3 and *APOE* ϵ 4 groups (**Figure 42**).

The spatial distribution of ischaemic damage was similar in both the *APOE* ϵ 3 and *APOE* ϵ 4 groups (**Table 10**) and in general was restricted to the striatum. Thus, the distribution of ischaemic damage was similar to that observed after the same duration of occlusion in the previous study in C57Bl/6J mice (*chapter 4*). In the hemisphere ipsilateral to occlusion, ischaemic damage was observed in the striatum in all mice. Ischaemic damage extended outside the striatum infrequently to include small areas of the somatosensory cortex overlying the striatum and the dorsolateral thalamus. No ischaemic damage was observed in the hippocampus and hypothalamus of any mice. In the hemisphere contralateral to occlusion, there was no evidence of ischaemic damage.

Table 10. Frequency of ischaemic damage in specific brain regions

Genotype	Number of mice with ischaemic damage		
	Striatum	Cortex	Thalamus
<i>APOE</i> ϵ 3	7 of 7	2 of 7	1 of 7
<i>APOE</i> ϵ 4	7 of 7	2 of 7	1 of 7

In general, 15min occlusion produced ischaemic damage restricted to the striatum with only infrequent involvement of cerebral cortex (somatosensory) and the thalamus (dorsolateral). The distribution of ischaemic damage was not related to *APOE* genotype.

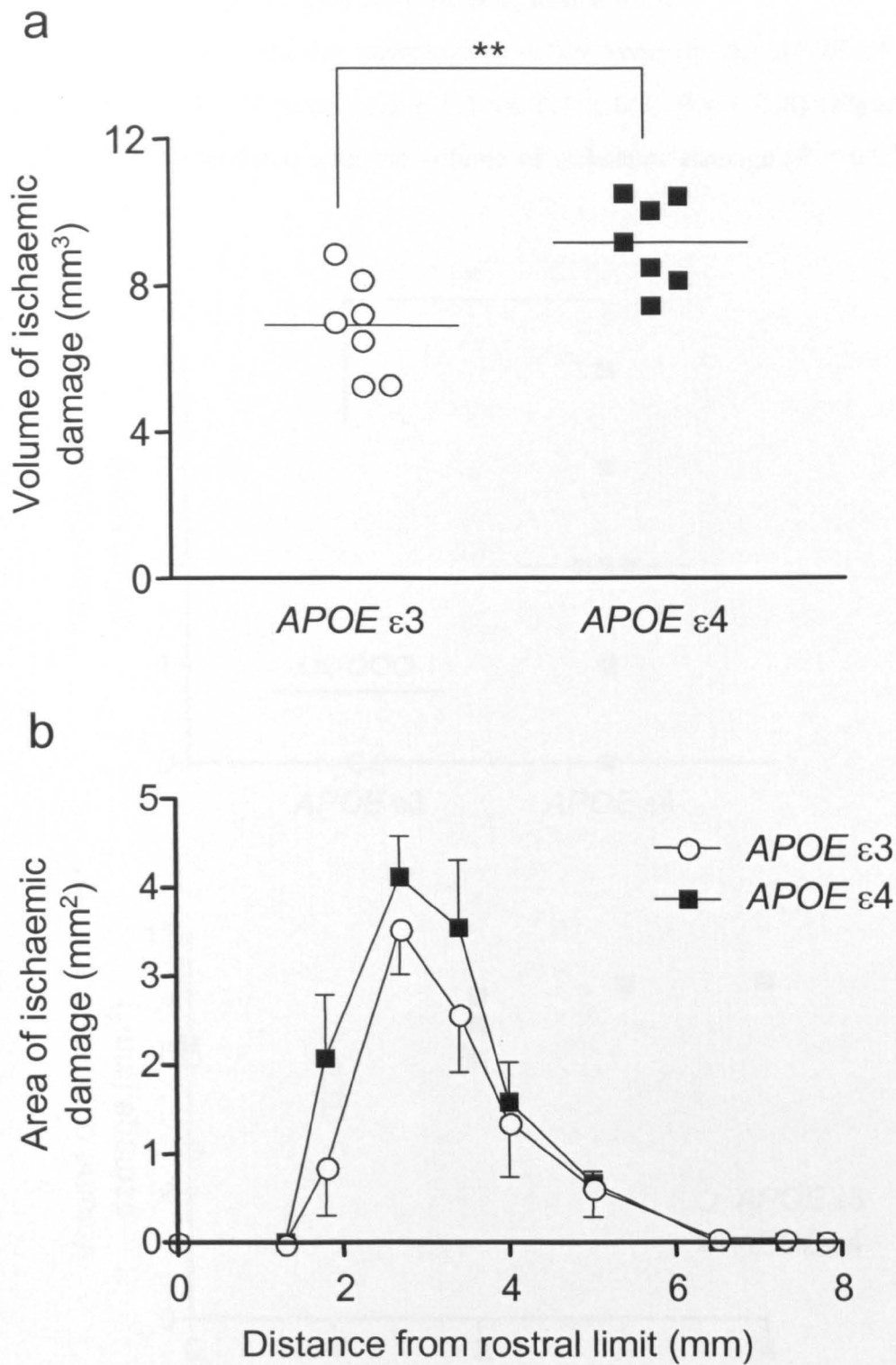


Figure 42. Effect of *APOE* genotype on volume of ischaemic damage

(a) The volume of ischaemic damage was significantly greater in *APOE* ϵ 4 mice. Bars show mean. (b) There was a trend toward larger areas of damage at coronal levels in *APOE* ϵ 4 mice. $**P < 0.01$, Student's unpaired *t*-test. $n = 7$ (each group). Data are presented as mean \pm SEM.

5.3.3 Effect of *APOE* genotype on neurological deficit

There was a significantly greater neurological deficit score in the *APOE* $\epsilon 4$ group compared to the *APOE* $\epsilon 3$ group (2.0 ± 1.3 vs. 0.7 ± 0.5 , $P = 0.038$) (Figure 43). Neurological deficit correlated with the volume of ischaemic damage ($P = 0.034$, $r = 0.82$) (Figure 43).

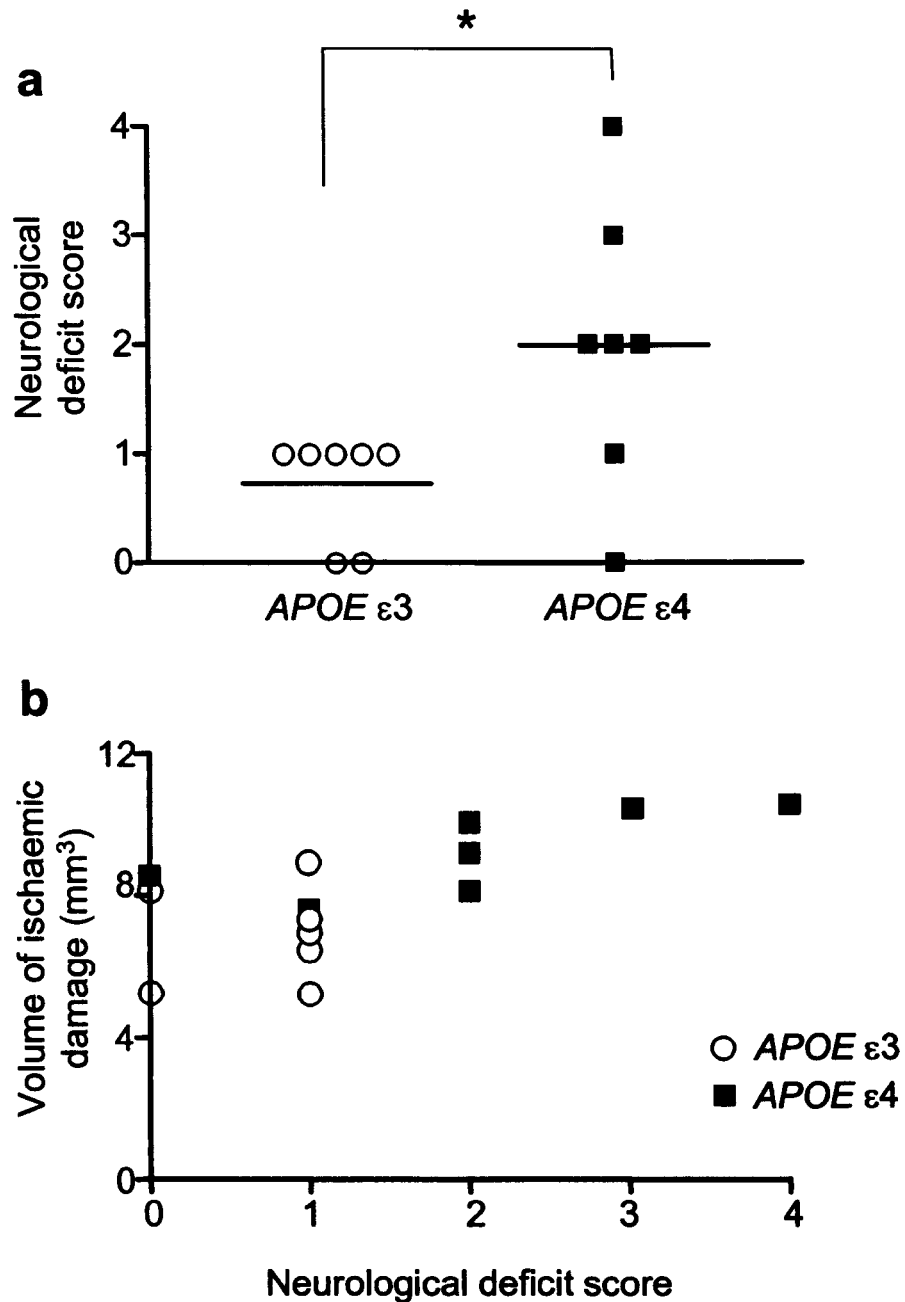


Figure 43. Effect of *APOE* genotype on neurological deficit

(a) Significantly greater neurological deficits were observed in *APOE* $\epsilon 4$ mice. Bars show mean. (b) There was a significant correlation between the neurological deficit score and the volume of ischaemic damage ($P = 0.03$; $r = 0.82$, Spearman Rank correlation co-efficient). * $P < 0.05$, Mann-Whitney *U*-statistic. $n = 7$ (each group).

5.3.4 ApoE immunostaining

5.3.4.1 Control immunostaining in the non-ischaemic hemisphere

In both *APOE* $\epsilon 3$ and *APOE* $\epsilon 4$ mice, faint apoE immunostaining of the neuropil was observed throughout the hemisphere. ApoE immunostaining of glial cells was also observed, most notably in cells displaying astrocytic morphology in the caudate nucleus (**Figure 44**). There was minimal evidence of neuronal apoE immunostaining in the caudate nucleus, thalamus and hippocampus, but in the cerebral cortex, neuronal apoE immunostaining was more readily observed, particularly in the parietal cortex. Glial apoE immunostaining was also observed in white matter tracts, including the internal capsule and corpus callosum. In the internal capsule, cells displayed small, spherical nuclei and cell bodies and in some areas were arranged in rows and orientated along the plane of the fibre tracts, characteristic of oligodendrocytes. In the corpus callosum, cellular staining appeared to be predominantly astrocytic. There were no observable differences in apoE immunostaining between *APOE* $\epsilon 3$ and *APOE* $\epsilon 4$ mice in the hemisphere contralateral to occlusion.

5.3.4.2 Alterations in the ischaemic hemisphere

In both *APOE* $\epsilon 3$ and *APOE* $\epsilon 4$ mice, marked alterations in the cellular localisation and intensity of apoE immunostaining were observed in areas of tissue displaying ischaemic damage in the occluded hemisphere (**Figure 45**). Most noticeably, there was a marked increase in neuronal apoE immunoreactivity compared to the non-ischaemic contralateral hemisphere. Intensely apoE-immunoreactive neurons exhibited the morphological features of ischaemic cell change (e.g. shrunken, triangular cell body). There were no observable differences in apoE immunoreactivity in ischaemic neurons between *APOE* $\epsilon 3$ and *APOE* $\epsilon 4$ mice. Double-labelling (apoE and neu-N antibodies) was performed, however, high background fluorescence and non-specific apoE immunoreactivity in areas of ischaemic damage precluded the detection of apoE/neu-N co-localisation. Increased apoE immunoreactivity in glial cells was also observed in areas of ischaemic damage, although the intensity of immunostaining was less than that observed in neurons. To a lesser extent, apoE immunostaining of the neuropil was increased compared to the contralateral hemisphere.

In areas outside the ischaemic territory, (e.g. undamaged cerebral cortex) apoE immunostaining was similar to that observed in the non-ischaemic contralateral

hemisphere. However, faint apoE immunostaining of a few pyramidal neurons in the CA3 sector of the hippocampus was observed infrequently in both *APOE* ϵ 3 (1 of 7) and *APOE* ϵ 4 (1 of 7) mice in the occluded hemisphere. These neurons appeared morphologically normal. A similar pattern of glial apoE immunoreactivity in the internal capsule was observed to that detected in the contralateral hemisphere in both *APOE* ϵ 3 and *APOE* ϵ 4 mice.

5.3.4.3 Volumetric measurement of apoE immunostaining

As described above, in the ischaemic hemisphere, increased apoE immunoreactivity (compared to the non-ischaemic hemisphere) was localised to areas of ischaemic damage. Areas of tissue containing numerous intensely apoE-immunoreactive cells could be demarcated from tissue containing minimal apoE immunostaining. Thus, areas and volumes of tissue containing increased apoE immunoreactivity could be determined. The volume of tissue displaying increased apoE immunoreactivity was significantly greater in *APOE* ϵ 4 compared to *APOE* ϵ 3 mice ($8 \pm 1\text{mm}^3$ vs. $6 \pm 1\text{mm}^3$, $P = 0.013$) and was similar to the volume of ischaemic damage [*APOE* ϵ 3 mice (6mm^3 vs. 7mm^3); *APOE* ϵ 4 mice (8mm^3 vs. 9mm^3)]. There was a significant correlation between the volume of apoE immunoreactivity and the volume of ischaemic damage ($P = 0.007$, $r^2 = 0.89$) (**Figure 46**).

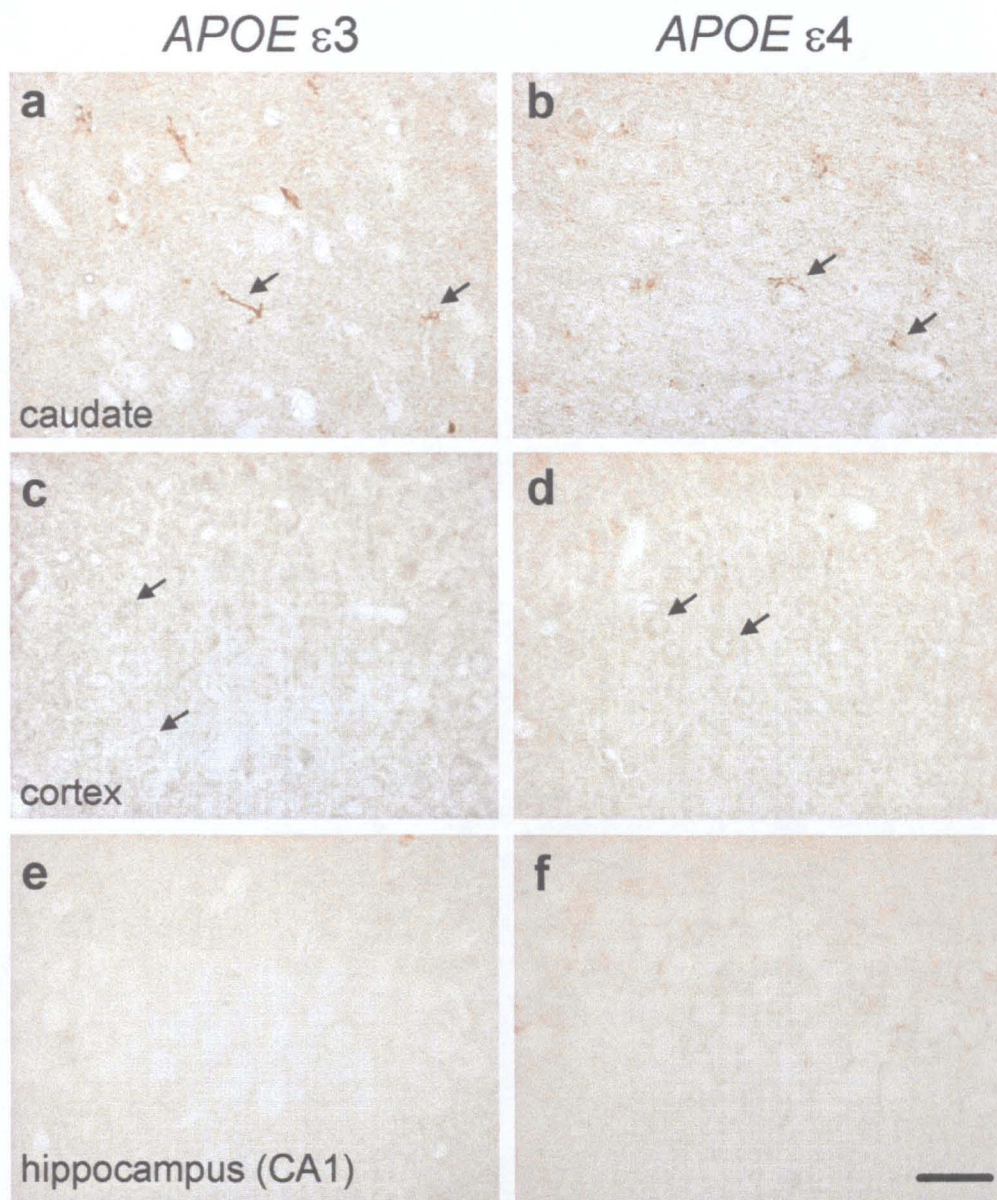


Figure 44. Control apoE immunostaining in the non-ischaemic hemisphere

In general, minimal glial and neuronal apoE immunostaining was observed in the non-ischaemic hemisphere contralateral to occlusion of both *APOE* ϵ 3 and *APOE* ϵ 4 mice. (a,b) Glial apoE immunostaining (arrows) was predominantly observed in the caudate nucleus. (c,d) Faint neuronal apoE immunostaining (arrows) was detected in the cerebral cortex but was minimal in other areas including the caudate nucleus (a,b), and hippocampus (e,f). Scale bar, 25 μ m.

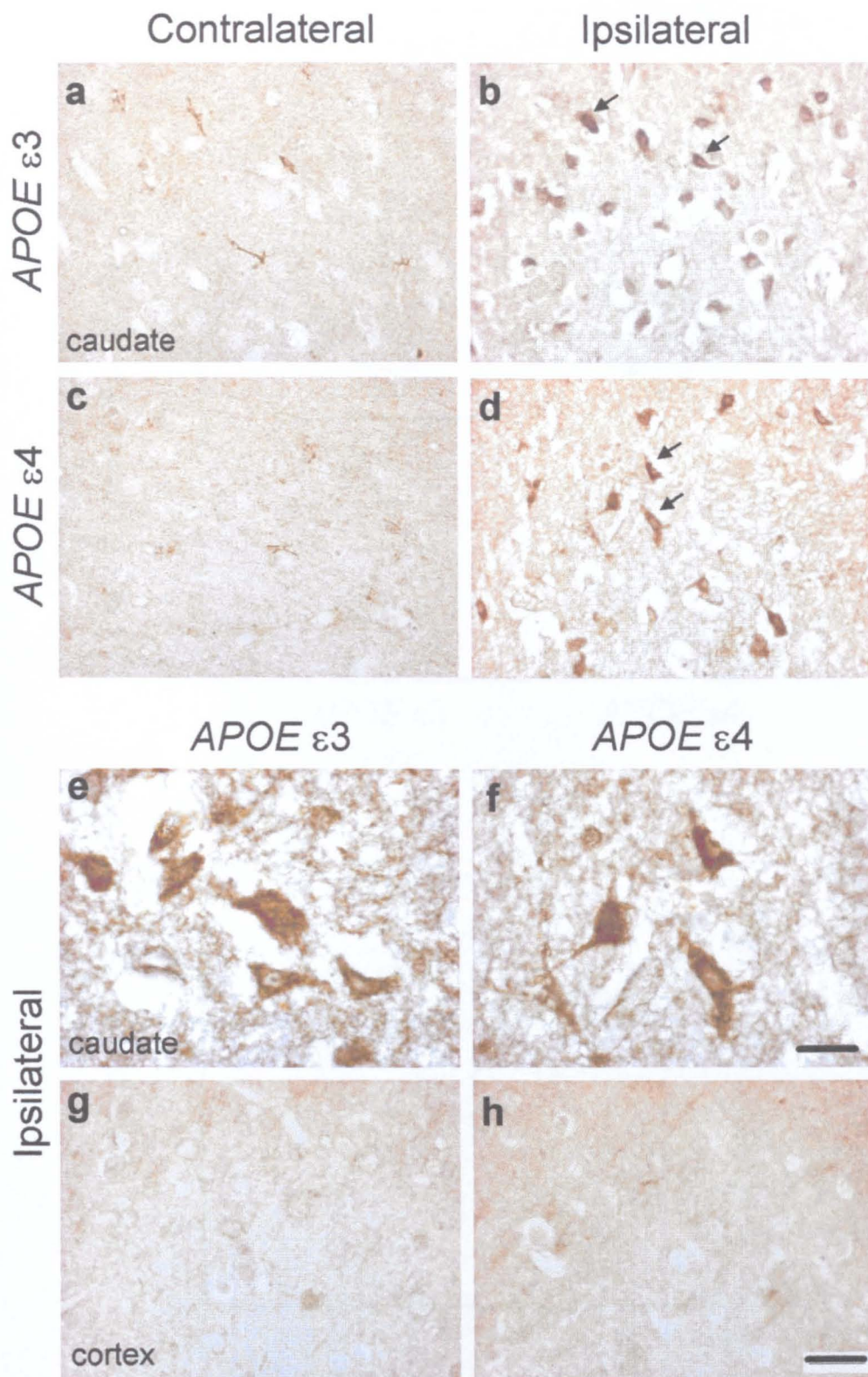


Figure 45. Alterations in apoE immunostaining in the ischaemic hemisphere

Alterations in the intensity and cellular localisation of apoE immunostaining were observed in both *APOE* ϵ 3 and *APOE* ϵ 4 mice in the ischaemic hemisphere ipsilateral to occlusion. In ischaemic areas (e.g. caudate nucleus shown), intense apoE-immunoreactive cells were observed (b,d). Neurons with ischaemic morphology were strongly immunoreactive for apoE (arrows). Glial apoE immunostaining in the contralateral hemisphere is shown for comparison (a,c). High-magnification photomicrographs illustrate the dense apoE immunostaining in the cytoplasm of ischaemic neurons (e,f). In contrast, areas outside the ischaemic territory ipsilateral to occlusion (e.g. cerebral cortex shown) displayed only minimal glial and neuronal apoE immunostaining (g,h). Scale bar (a-d, g,h), 25 μ m; (e,f), 10 μ m.

5.3.4.4 Semi-quantification of apoE immunoreactivity

Semi-quantification of apoE immunostaining was carried out in the caudate nucleus in the hemisphere ipsilateral to occlusion and thus provided an index of the degree of apoE in response to ischaemic damage induced by intraluminal occlusion. Semi-quantification revealed that the degree of apoE immunoreactivity was similar in both *APOE* ϵ 3 and *APOE* ϵ 4 mice (2.04 ± 0.52 vs. 2.14 ± 0.50 , $P > 0.05$) (Figure 47).

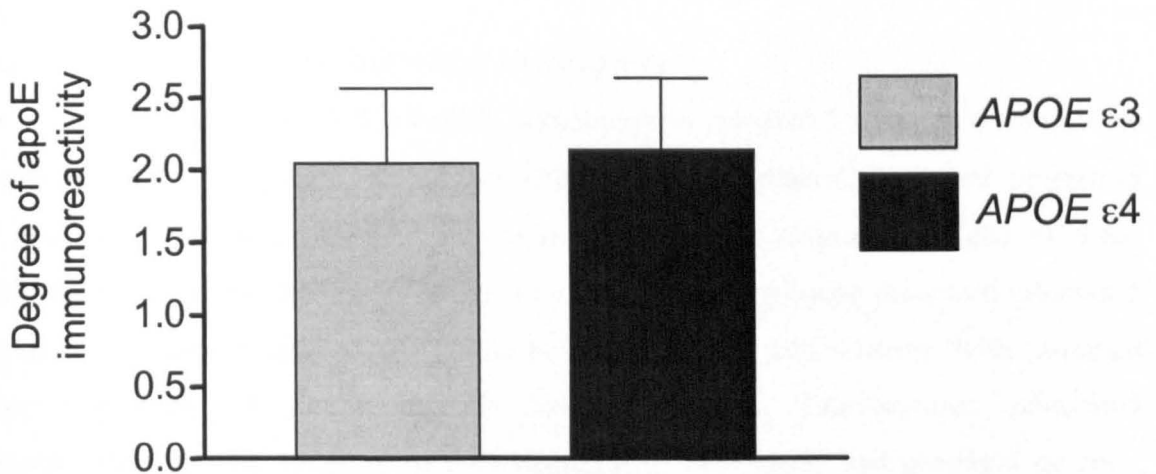


Figure 47. Semi-quantification of apoE immunoreactivity

Semi-quantification was carried out in the caudate nucleus of the ischaemic hemisphere (ipsilateral to occlusion). The degree of apoE immunoreactivity was similar in both *APOE* ϵ 3 and *APOE* ϵ 4 mice ($P > 0.05$, Mann-Whitney *U*-statistic). $n = 7$ (each group). Data are presented as mean \pm SEM.

5.3.5 Rabaptin-5 immunostaining

5.3.5.1 Control immunostaining in the non-ischaemic hemisphere

In both *APOE* ϵ 3 and *APOE* ϵ 4 mice, faint rabaptin-5 immunostaining of the neuropil was observed. Minimal rabaptin-5 immunostaining of neurons and glial cells was also observed in the non-ischaemic hemisphere in both *APOE* ϵ 3 and *APOE* ϵ 4 mice (**Figure 48**). Cellular rabaptin-5 immunostaining was distributed throughout the hemisphere, including the caudate nucleus, cerebral cortex, hippocampus and thalamus.

5.3.5.2 Alterations in the ischaemic hemisphere

In both *APOE* ϵ 3 and *APOE* ϵ 4 mice, alterations in rabaptin-5 immunostaining were observed in the ischaemic hemisphere (**Figure 48**). In general, increased rabaptin-5 immunoreactivity was observed in the neuropil and in neurons and glia of areas displaying ischaemic damage. The majority of neurons displaying increased rabaptin-5 immunoreactivity exhibited the features of ischaemic cell change with minimal immunostaining of morphologically normal neurons. Intraneuronal rabaptin-5 immunostaining was localised to the cytoplasm of cell bodies and proximal neurites, indicative of its endosomal location. Most intense rabaptin-5 immunostaining was observed adjacent to the plasma membrane. Glial cells with the morphology of reactive astrocytes occasionally exhibited increased rabaptin-5 immunoreactivity in ischaemic areas.

Rabaptin-5 immunostaining in areas outside the ischaemic territory (e.g. undamaged cerebral cortex, hippocampus) was similar to that observed in the non-ischaemic contralateral hemisphere in both *APOE* ϵ 3 and *APOE* ϵ 4 mice.

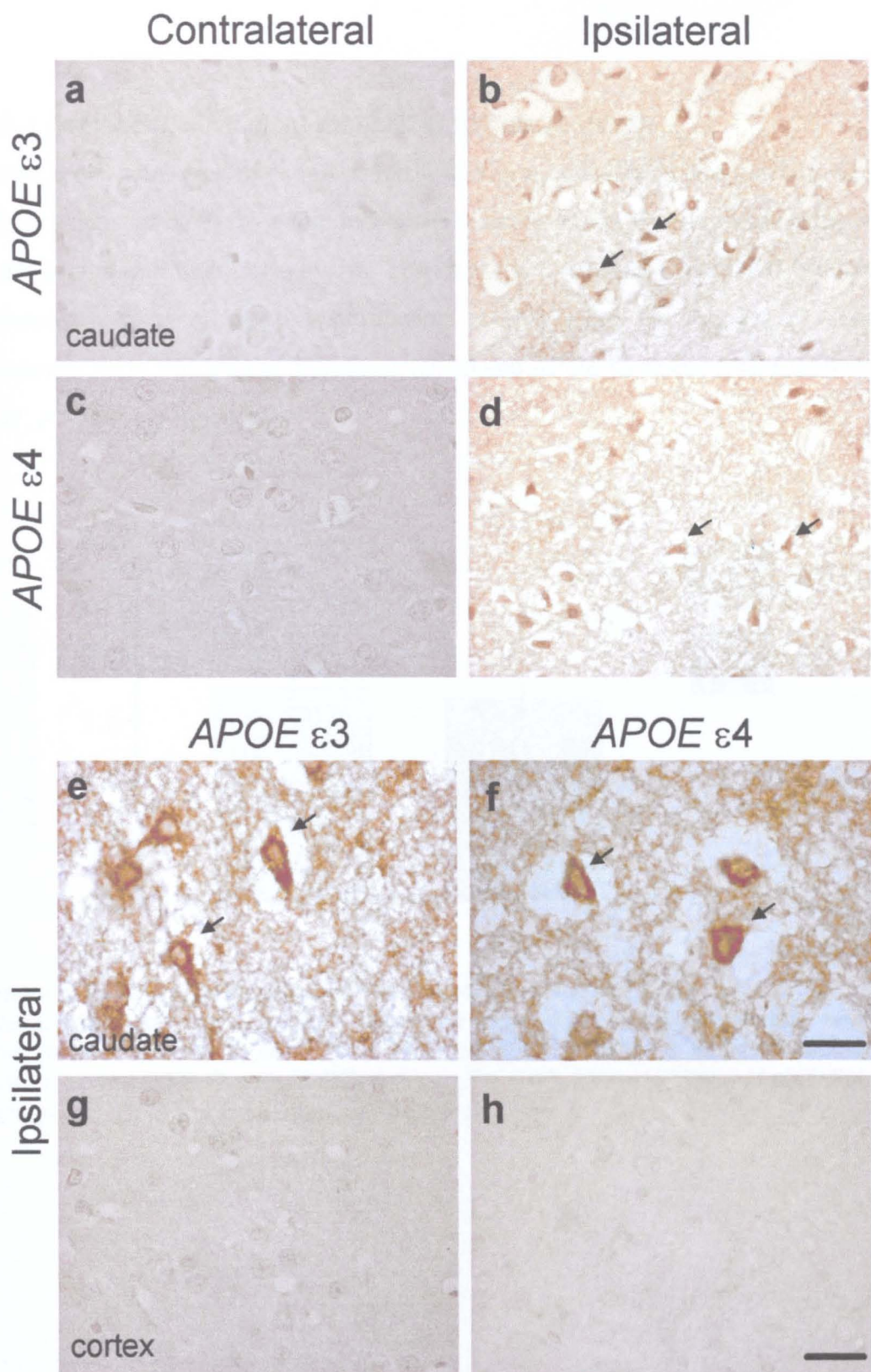


Figure 48. Rabaptin-5 immunostaining

Throughout the non-ischaemic hemisphere contralateral to occlusion (e.g. caudate nucleus shown), minimal neuronal and glial rabaptin-5 immunoreactivity was observed (a,c). In ischaemic areas of the occluded hemisphere (caudate nucleus shown), increased neuropil and cellular rabaptin-5 immunoreactivity was observed (b,d). These included cells with the morphology of ischaemic neurons (arrows). High-magnification photomicrographs (e,f) illustrate rabaptin-5 immunostaining in the cytoplasm of ischaemic neurons (arrows). Areas outside the ischaemic territory in the hemisphere ipsilateral to occlusion (e.g. cerebral cortex shown) displayed faint neuronal and glial rabaptin-5 immunoreactivity. Scale bar (a-d, g,h), 25 μ m; (e,f), 10 μ m.

5.3.5.3 Semi-quantification of rabaptin-5 immunoreactivity

As with apoE, semi-quantification of rabaptin-5 immunostaining was carried out in the caudate nucleus in the hemisphere ipsilateral to occlusion to give an index of the degree of rabaptin-5 immunoreactivity in response to ischaemic damage induced by intraluminal occlusion. Semi-quantification revealed that the degree of rabaptin-5 immunoreactivity was similar in both *APOE* ϵ 3 and *APOE* ϵ 4 mice (1.76 ± 0.74 vs. 1.67 ± 0.47 , $P > 0.05$) (Figure 49).

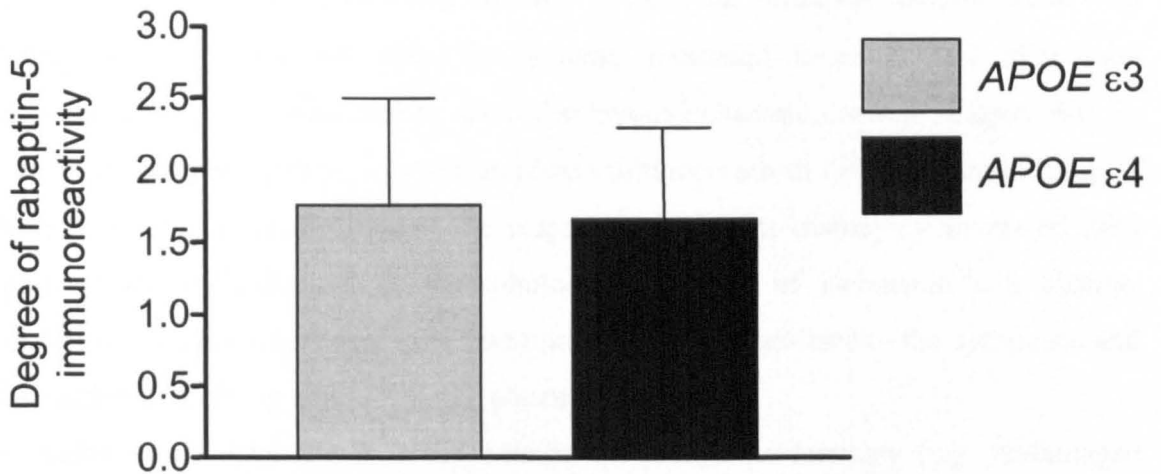


Figure 49. Semi-quantification of rabaptin-5 immunoreactivity

Semi-quantification was carried out in the caudate nucleus of the ischaemic hemisphere (ipsilateral to occlusion). The degree of rabaptin-5 immunoreactivity was similar in both *APOE* ϵ 3 and *APOE* ϵ 4 mice ($P > 0.05$, Mann-Whitney *U*-statistic). $n = 7$ (each group). Data are presented as mean \pm SEM.

5.3.6 Rab4 immunostaining

5.3.6.1 Control immunostaining in the non-ischaemic hemisphere

Similar to rabaptin-5, minimal rab4 immunostaining of the neuropil, neurons and glia was observed in both *APOE* ϵ 3 and *APOE* ϵ 4 mice (**Figure 50**). Cellular immunostaining was distributed throughout the hemisphere, including the caudate nucleus, cerebral cortex, hippocampus and thalamus.

5.3.6.2 Alterations in the ischaemic hemisphere

Alterations in rab4 immunostaining were observed in the ischaemic hemisphere in both *APOE* ϵ 3 and *APOE* ϵ 4 mice. In general, increased neuronal and glial rab4 immunoreactivity was observed in areas displaying ischaemic damage (**Figure 50**). In contrast to rabaptin-5, there was not an observable increase in rab4 immunostaining of the neuropil in ischaemic tissue. The majority of neurons displaying increased rab4 immunoreactivity exhibited the morphological features of ischaemic cell change. Similar to rabaptin-5, neuronal rab4 immunostaining was localised to the cytoplasm and was particularly strong adjacent to the plasma membrane.

Rab4 immunostaining in areas outside the ischaemic territory (e.g. undamaged cerebral cortex) was similar to that observed in the non-ischaemic contralateral hemisphere in both *APOE* ϵ 3 and *APOE* ϵ 4 mice.

Figure 50. Rab4 immunostaining (overleaf)

Throughout the non-ischaemic hemisphere contralateral to occlusion (e.g. caudate nucleus shown), minimal neuronal and glial rab4 immunoreactivity was observed in both *APOE* ϵ 3 and *APOE* ϵ 4 mice (a,c). In ischaemic areas of the hemisphere ipsilateral to occlusion (caudate nucleus shown), increased cellular rab4 immunoreactivity was observed (b,d). These included cells with the morphology of ischaemic neurons (arrows). The extent of rab4 immunoreactivity was markedly greater in *APOE* ϵ 3 mice (b) compared to *APOE* ϵ 4 mice (d). High-magnification photomicrographs illustrate intense rab4 immunoreactivity in the cytoplasm of ischaemic neurons (arrows) in a representative *APOE* ϵ 3 mouse brain and faint rab4 immunoreactivity in a representative *APOE* ϵ 4 mouse brain. Areas outside the ischaemic territory in the hemisphere ipsilateral to occlusion (e.g. cerebral cortex shown) displayed minimal neuronal and glial rabaptin-5 immunoreactivity in both *APOE* ϵ 3 and *APOE* ϵ 4 mice. Scale bar (a-d, g,h), 25 μ m; (e,f), 10 μ m.

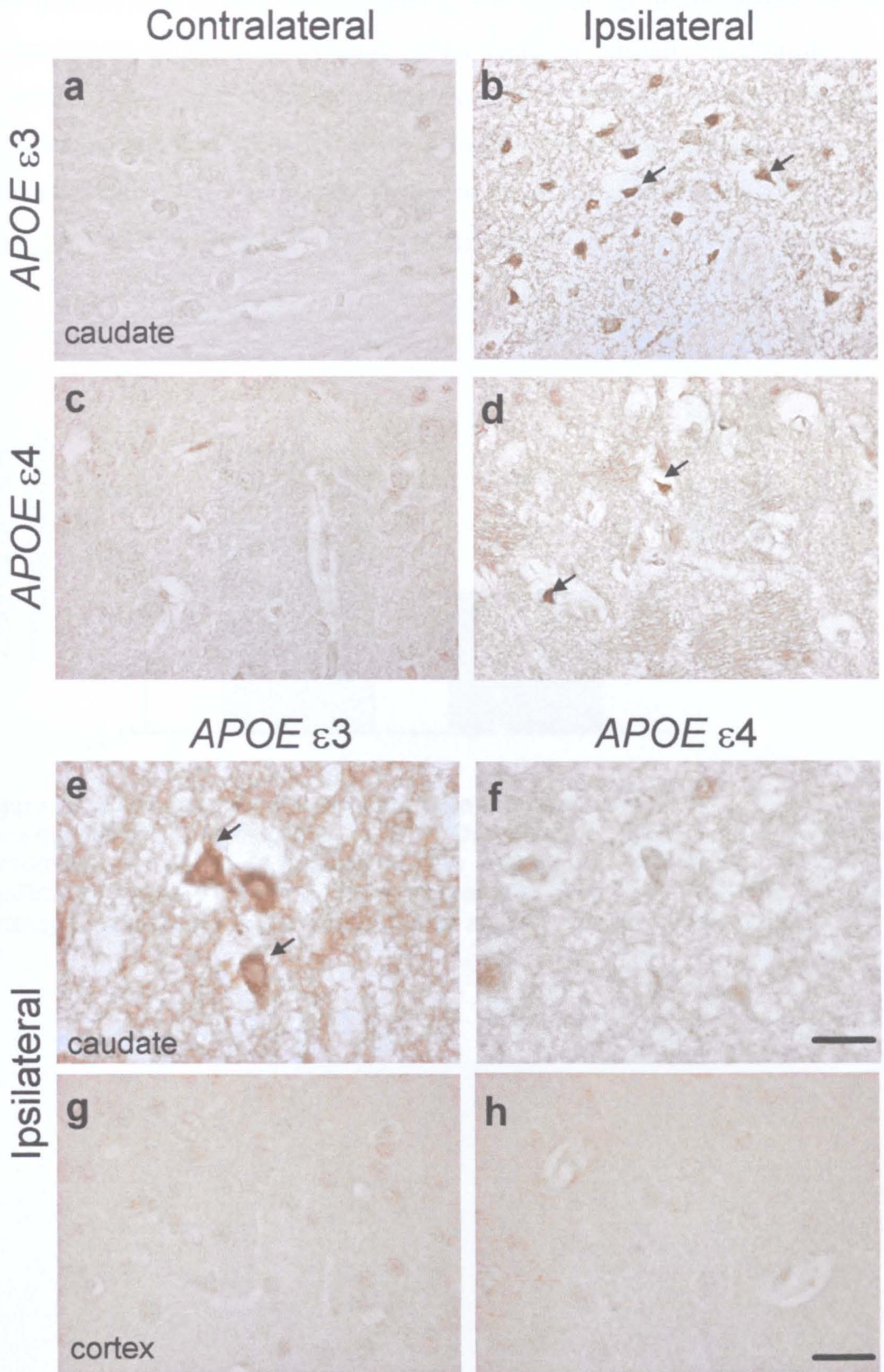


Figure 50. Rab4 immunostaining (legend on previous page)

5.3.6.3 Semi-quantification of rab4 immunoreactivity

Semi-quantification of rab4 immunostaining was carried out in the caudate nucleus in the hemisphere ipsilateral to occlusion (as for apoE and rabaptin-5 previously) to give an index of the degree of rab4 immunoreactivity in response to ischaemic damage induced by intraluminal occlusion. Semi-quantification revealed that the degree of rab4 immunoreactivity was significantly greater in *APOE* ϵ 3 compared to *APOE* ϵ 4 mice (2.38 ± 0.76 vs. 1.19 ± 0.92 , $P = 0.021$) (Figure 51).

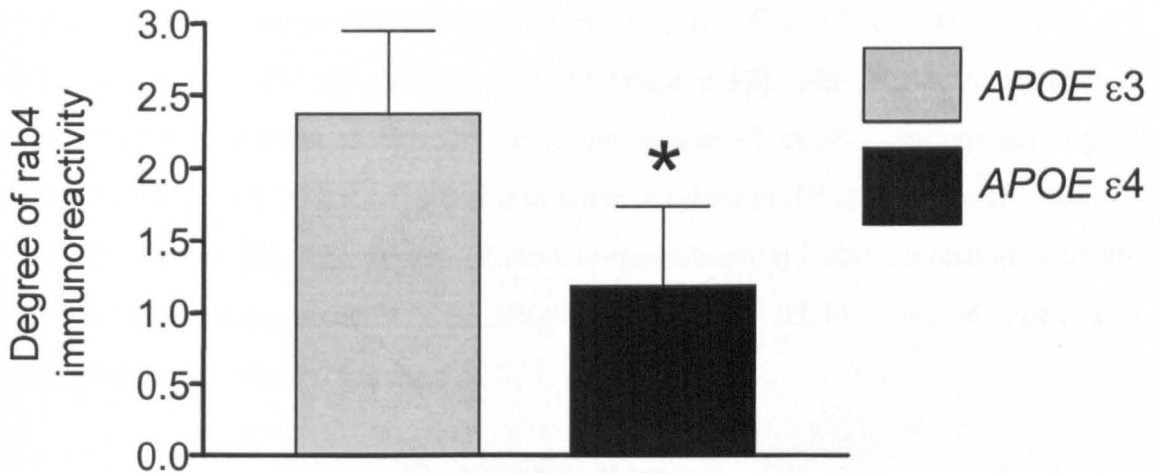


Figure 51. Semi-quantification of rab4 immunoreactivity

Semi-quantification was carried out in the caudate nucleus of the ischaemic hemisphere (ipsilateral to occlusion). The degree of rab4 immunoreactivity was significantly greater in *APOE* ϵ 3 mice compared to *APOE* ϵ 4 mice. * $P < 0.05$, Mann-Whitney U -statistic. $n = 7$ (each group). Data are presented as mean \pm SEM.

5.3.7 Correlations of apoE, rabaptin-5 and apoE immunoreactivity

Rabaptin-5 (internalisation) and rab4 (recycling) are markers of two different stages of the endocytic pathway. Correlation analysis of rabaptin-5 and rab4 immunoreactivity was performed to determine if there was a parallel response of these two endocytic processes to ischaemic damage. Endocytosis is integral to apoE trafficking, and may therefore be involved in the apoE response to ischaemic damage. Correlation analysis of apoE and rabptin-5 or rab4 immunoreactivity was also performed to determine if there was an association between the apoE and endocytic responses to ischaemic damage.

Correlation analysis revealed that the degree of rabaptin-5 immunoreactivity correlated with the degree of rab4 immunoreactivity in *APOE* ϵ 3 mice ($P = 0.029$, $r = 0.80$) but not in *APOE* ϵ 4 mice ($P > 0.05$) (Figure 52). The degree of rabaptin-5 immunoreactivity correlated strongly with the degree of apoE immunoreactivity in *APOE* ϵ 3 mice ($P = 0.008$, $r = 0.89$) and to a lesser extent in *APOE* ϵ 4 mice ($P = 0.047$, $r = 0.76$) (Figure 53). The degree of rab4 immunoreactivity also correlated with the degree of apoE immunoreactivity in *APOE* ϵ 3 mice ($P = 0.045$, $r = 0.76$) but not in *APOE* ϵ 4 mice ($P > 0.05$) (Figure 53).

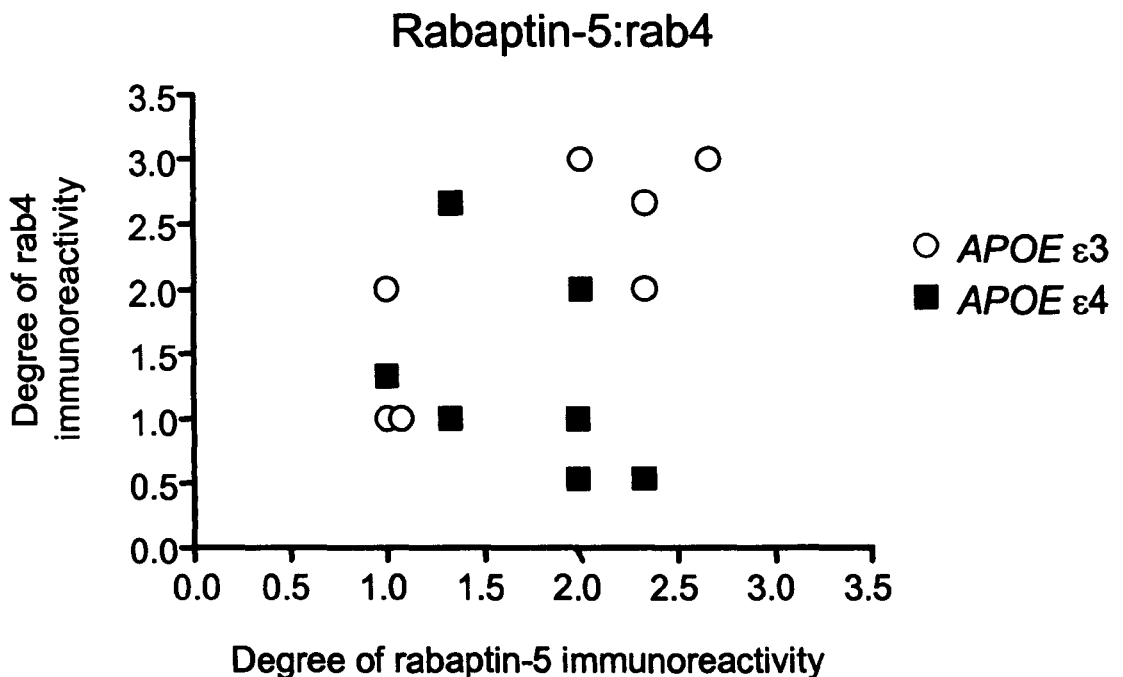


Figure 52. Association between rabaptin-5 and rab4 immunoreactivity

The degree of rabaptin-5 immunoreactivity correlated with the degree of rab4 immunoreactivity in *APOE* ϵ 3 mice ($P = 0.029$, $r = 0.80$) but not in *APOE* ϵ 4 mice ($P > 0.05$, Spearman Rank correlation co-efficient).

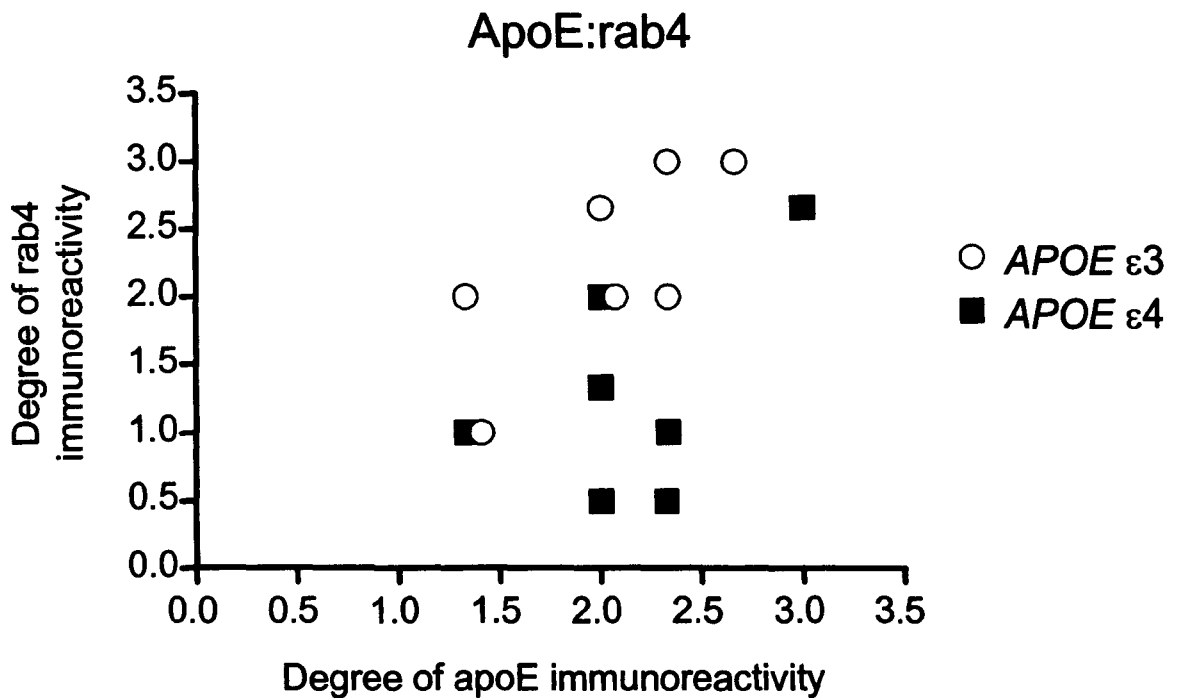
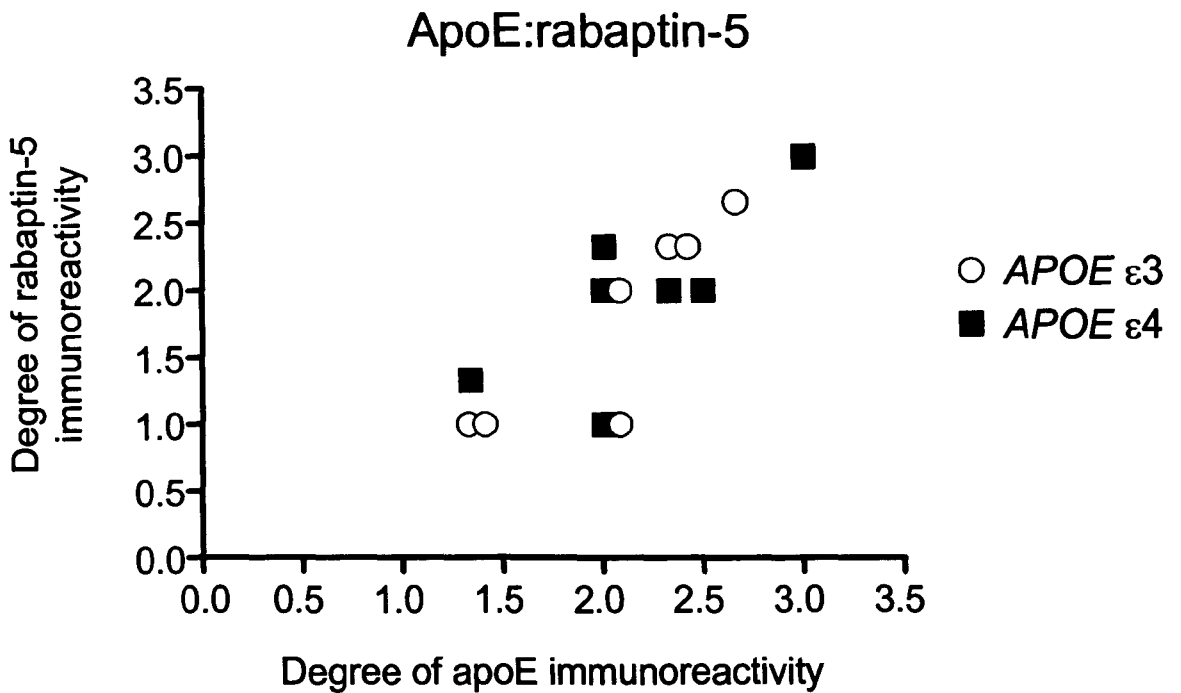


Figure 53. Association between apoE and rabaptin-5 or rab4 immunoreactivity
 The degree of rabaptin-5 immunoreactivity correlated with the degree of apoE immunoreactivity in both *APOE* ε3 ($P = 0.008$, $r = 0.89$) and *APOE* ε4 mice ($P = 0.047$, $r = 0.76$, Spearman Rank correlation co-efficient). The degree of rab4 immunoreactivity correlated with the degree of apoE immunoreactivity in *APOE* ε3 mice ($P = 0.045$, $r = 0.76$) but not in *APOE* ε4 mice ($P > 0.05$, Spearman Rank correlation co-efficient).

5.4 Discussion

The results from this study have demonstrated that transgenic mice expressing the human *APOE* $\epsilon 4$ allele show a poorer pathological (greater volume of ischaemic damage) and neurological (greater neurological deficit score) outcome compared to mice expressing human *APOE* $\epsilon 3$ after transient focal cerebral ischaemia. In both groups, ischaemic damage was closely associated with alterations in apoE immunostaining, most notably an increase in neuronal apoE immunoreactivity in comparison to non-ischaemic tissue. In addition, alterations in immunostaining of the endocytic pathway markers, rabaptin-5 and rab4, were also associated with ischaemic damage and, furthermore, the nature of these alterations was dependent on *APOE* genotype.

5.4.1 *APOE* genotype and outcome after focal ischaemia

The present data indicate that the *APOE* $\epsilon 4$ allele is associated with a poorer outcome in a mouse model of focal cerebral ischaemia. To date, studies investigating the influence of *APOE* genotype on outcome after focal ischaemic stroke in humans have produced conflicting results. Some studies did not find an association between *APOE* genotype and outcome (McCarron *et al.*, 1998; McCarron *et al.*, 1999; MacLeod *et al.*, 2001) whereas others have suggested a poorer prognosis in *APOE* $\epsilon 4$ carriers after stroke (Liu *et al.*, 2002; Treger *et al.*, 2003). Conflicting findings may, in part, be related to the heterogeneity of human stroke and the inability to control for underlying confounding factors, such as pre-existing disease and lifestyle factors (e.g. smoking) and the location, severity and duration of the ischaemic insult, in human studies. For example, in one study which did not detect an *APOE* genotype-related difference in outcome, there was substantial variability in the location of the ischaemic lesion (MacLeod *et al.*, 2001). Only 24% of patients demonstrated a subcortical lesion with others displaying lesions in various other regions such as the cerebellum and brainstem. In contrast, in another study which analysed a more homogenous sample of stroke patients (infarcts limited to MCA territory), a poorer prognosis was indicated in *APOE* $\epsilon 4$ carriers (Liu *et al.*, 2002). Such confounding variables can be overcome in animal models of cerebral ischaemia, as in the present study which incorporated a stringently controlled duration of focal ischaemia and reperfusion. A brief duration (15min) of occlusion followed by 24h

reperfusion produced a highly reproducible volume and distribution of ischaemic damage in both *APOE* ϵ 3 and *APOE* ϵ 4 mice.

The findings that the extent of ischaemic damage and the neurological deficit were significantly greater in *APOE* ϵ 4 mice are consistent with and expand upon previous studies investigating the effects of *APOE* genotype on outcome in animal models of focal cerebral ischaemia. Using a similar transient focal ischaemia model, but with a substantially longer occlusion duration (60min) than in the present study (15min), Sheng *et al.* (1998) found that mice expressing human *APOE* ϵ 4 displayed a larger total infarct volume than *APOE* ϵ 3 mice. However, in the study by Sheng *et al.*, the effects of brain oedema on measurements of ischaemic damage were not controlled for. In a recent study in which brain oedema was controlled for, Mori *et al.* (2003) reported that total infarct volume was greater in *APOE* ϵ 4/4 knock-in mice compared to ϵ 3/3 and ϵ 2/2 mice after 24h permanent focal ischaemia. In view of the primarily striatal distribution of ischaemic damage in the present study, it is of note that Sheng *et al.* (1998) also found that the subcortical infarct volume was significantly greater in *APOE* ϵ 4 mice. This suggests that *APOE* genotype can influence the extent of ischaemic damage after focal ischaemia throughout the hemisphere. In the present study, the severity of the neurological deficit was greater in *APOE* ϵ 4 mice and neurological score also correlated with the volume of ischaemic damage. These data suggest that differences in the extent of ischaemic damage translate to varying degrees of functional impairment and that the more severe neurological deficit in *APOE* ϵ 4 mice is linked to the greater amount of ischaemic damage in this group. These data are also consistent with previous studies that reported more severe neurological deficits in *APOE* ϵ 4 mice (Sheng *et al.*, 1998; Mori *et al.*, 2003). In these studies, differences in functional outcome likely relate to variation in the extent of cortical and subcortical/striatal damage rather than striatal damage alone as in the current study. The present data and previous findings therefore demonstrate a consistent association between the *APOE* ϵ 4 allele and poorer outcome in animal models of focal ischaemia, which may reflect the ability to control important experimental conditions in such studies. In addition, poorer outcome in *APOE* ϵ 4 mice has been demonstrated in other models of acute brain injury, including global ischaemia, closed head injury and excitotoxic damage (Buttini *et al.*, 1999; Buttini *et al.*, 2000; Horsburgh *et al.*, 2000c; Sabo *et al.*, 2000), suggesting that the *APOE* ϵ 4

allele may have common (detrimental) effects on the response to various types of acute brain injury.

Previous studies have not found any differences in gross brain morphology in *APOE* transgenic mice at the ages (2 – 3 months) used in this study (Xu *et al.*, 1996) and so gross neuroanatomical differences are unlikely to account for the differences in outcome observed in the present study. However, it is pertinent to consider that the C57BL/6J strain provided the genetic background for these *APOE* transgenic mice. Cerebrovascular anatomical discrepancies in the circle of Willis, in particular hypoplasticity of the posterior communicating artery (PcomA), are an inherent feature of the C57BL/6J mouse and are associated with increased susceptibility to ischaemic damage in this strain (*chapter 4 in this thesis*; Barone *et al.*, 1993; Connolly *et al.*, 1996; Fujii *et al.*, 1997; Yang *et al.*, 1997a; Kitagawa *et al.*, 1998c; Kelly *et al.*, 2001b; Majid *et al.*, 2001). The previous study in this thesis (*chapter 4*) demonstrated that PcomA hypoplasticity is likely associated with important downstream effects on blood pressure and cerebral blood flow that impact upon the distribution and extent of ischaemic damage. However, in this study a brief duration of occlusion (15min) was used, which was previously determined to be exempt from the synergistic effects of PcomA hypoplasticity and declining blood pressure and cerebral blood flow (*chapter 4*). Assessment of histology in the present study revealed that ischaemic damage was absent in the hippocampus of all mice, which also suggests that PcomA hypoplasticity did not contribute to the differences in outcome. It is unclear, however, if the volume of tissue at risk of ischaemic damage was similar in both the *APOE* ϵ 3 and *APOE* ϵ 4 mice. Thorough analysis of cerebral blood flow would be required to provide such information. Previously, it was shown that the severity of blood flow reduction during focal ischaemia and vascular anomalies in the circle of Willis were similar in *APOE*-deficient and wild-type mice (Bart *et al.*, 1998).

Transgenic mice used in this study were back-bred to a common genetic background (C57BL/6J) at least six times in the USA before transport to the UK where several further back-crosses were carried out. These steps ensure that a level of homology in genetic background approaching 100% was achieved. In addition, the *APOE* ϵ 3 and *APOE* ϵ 4 lines selected from the original lines generated (Xu *et al.*, 1996) were matched for the number of copies of the *APOE* gene (two copies). Differences in outcome are therefore not related to the *APOE* gene copy number. However, the sites of

APOE gene integration could differ in each line and affect other coding regions of the genome. Thus, subtle genetic differences may still exist between the *APOE* $\epsilon 3$ and *APOE* $\epsilon 4$ mouse lines. The extent to which such slight differences, if present, would impact upon the response to ischaemia is unknown.

5.4.2 ApoE alterations after focal ischaemia

The mechanism(s) underlying the association between *APOE* genotype and differences in outcome after focal ischaemia and other forms of acute brain injury are currently unclear. A role for apoE in modulating the neuronal response to damage in an isoform-specific manner after acute brain injury has been proposed. Key to this proposal has been the demonstration that apoE is markedly upregulated and can accumulate in neurons under pathological conditions, thus providing a basis for putative interactions with pathways involved in neuronal death and/or survival. Previously, increased neuronal apoE has been observed following global ischaemia in rodents (Hall *et al.*, 1995; Kida *et al.*, 1995; Ali *et al.*, 1996; Horsburgh and Nicoll, 1996; Ishimaru *et al.*, 1996; Horsburgh *et al.*, 2000c) and humans (Horsburgh *et al.*, 1999a), focal ischaemia (Kitagawa *et al.*, 2001; Kamada *et al.*, 2003; Nishio *et al.*, 2003) and subdural haematoma (Horsburgh *et al.*, 1997) in rats, spinal cord injury in the mouse (Haasdijk *et al.*, 2002; Seitz *et al.*, 2003), excitotoxin-induced injury in the mouse (Grootendorst *et al.*, 2000), and after stroke in humans (Aoki *et al.*, 2003). However, at the outset of this thesis, there was little information regarding the spatial distribution and cellular localisation of apoE following focal ischaemia in *APOE* transgenic mice.

In the present study, marked increases in cellular (including neuronal) apoE immunoreactivity were observed in ischaemic tissue. Analysis of the distribution of elevated apoE immunoreactivity in the occluded hemisphere revealed that the volume of apoE immunoreactivity strongly correlated with the volume of ischaemic damage, suggesting an important role for apoE in the response to ischaemic damage. The close spatial relationship between ischaemic damage and increased apoE immunostaining may underlie the larger volume of apoE immunoreactivity observed in *APOE* $\epsilon 4$ mice, since this group also displayed a greater volume of ischaemic damage. This pattern parallels that previously reported in a global ischaemia model in which increased neuronal apoE immunoreactivity was associated with increased ischaemic neuronal damage in the hippocampus of *APOE* $\epsilon 4$ compared to *APOE* $\epsilon 3$ mice after 17min global

ischaemia (Horsburgh *et al.*, 2000c). However, although the distribution of apoE immunoreactivity was significantly greater in *APOE* ϵ 4 mice in the present study, within the ischaemic territory, semi-quantitative assessment revealed no difference in the degree of apoE immunoreactivity between *APOE* ϵ 3 and *APOE* ϵ 4 mice. This is particularly interesting in view of previous studies which have shown baseline differences in apoE levels in the same lines of *APOE* ϵ 3 and *APOE* ϵ 4 mice as used in the present study. Western blot analyses showed that apoE levels in the brain were approximately 50% lower in *APOE* ϵ 3 mice (Sheng *et al.*, 1998; Horsburgh *et al.*, 2000c). This difference was maintained after global ischaemia, although to a lesser magnitude (approximately 15% lower in *APOE* ϵ 3 mice) (Figure 54). It was not

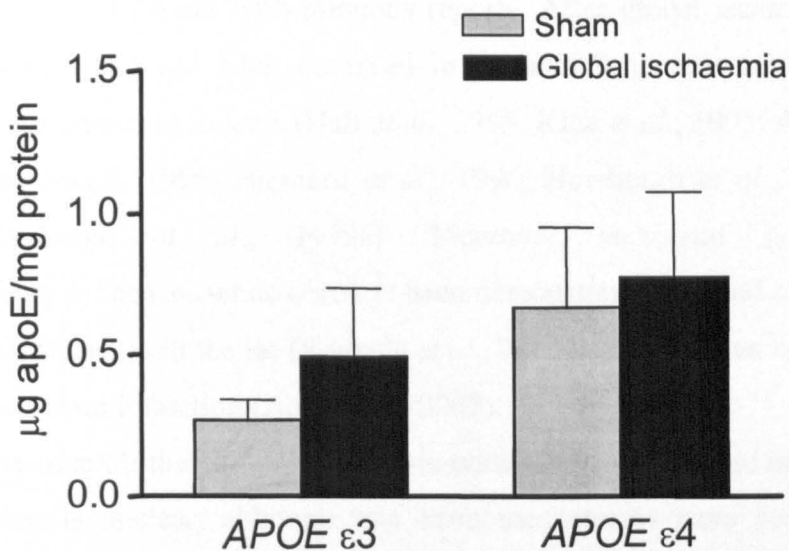


Figure 54. ApoE levels in *APOE* ϵ 3-437 and *APOE* ϵ 4-81 lines of mice

In the lines of transgenic mice used in the present study, it was shown previously (Horsburgh *et al.*, 2000) that there were greater levels of apoE in *APOE* ϵ 4 mice after sham treatment and after global ischaemia (BCCAo), although differences were not significantly different. $P > 0.05$. Figure courtesy of Dr Karen Horsburgh.

possible to assay apoE levels in the present cohort of mice, although since the same transgenic mouse lines were used as before, it may be speculated that baseline levels were greater in *APOE* ϵ 4 mice. Thus, it might be expected that the degree of apoE immunoreactivity in ischaemic tissue in the present study would be greater in *APOE* ϵ 4 mice given the greater amount of apoE available in these mice. It could be proposed that the mice used in the present were better matched for apoE levels than previously, although this is unknown since apoE levels could not be determined and would appear

unlikely based on the consistent findings in two previous studies (Sheng *et al.*, 1998; Horsburgh *et al.*, 2000c). A more plausible explanation is that the focal ischaemic insult was both of similar and sufficient severity in *APOE* ϵ 3 and *APOE* ϵ 4 mice to induce a similar, possibly maximal, upregulation of apoE and therefore preclude detection of genotype-dependent differences in the apoE response to ischaemic damage. The similar degree of apoE immunoreactivity in both *APOE* transgenic groups may therefore reflect this uniformity in severity of ischaemic damage.

Within ischaemic areas, intense apoE immunoreactivity was evident in glial cells and ischaemic neurons. In addition to an upregulation of apoE, these observations also indicate an apparent redistribution of apoE in ischaemic tissue since minimal and predominantly glial apoE immunoreactivity was observed in non-ischaemic tissue. These findings are consistent with previous reports. After global ischaemia increased apoE immunoreactivity has been observed in pyramidal neurons of the selectively vulnerable hippocampus in rodents (Hall *et al.*, 1995; Kida *et al.*, 1995; Ali *et al.*, 1996; Horsburgh and Nicoll, 1996; Ishimaru *et al.*, 1996; Horsburgh *et al.*, 2000c) and in humans (Horsburgh *et al.*, 1999a). Moreover, increased neuronal apoE immunoreactivity in the ischaemic core has been demonstrated 24h and seven days after transient focal ischaemia in the rat (Kamada *et al.*, 2003) and in human brain associated with areas of cerebral infarction (Aoki *et al.*, 2003).

The source of apoE that accumulates in neurons after an ischaemic insult in this and previous studies is unclear, although two main mechanisms have been proposed – uptake of glial-derived apoE and/or neuronal synthesis of apoE. Since neurons express several receptors of the low density lipoprotein receptor family, notably the low density lipoprotein receptor-related protein (LRP), that are capable of internalising apoE-containing lipoproteins, it is possible that neuronal apoE is derived from uptake of apoE from the extracellular space. Astrocytes are believed to be the predominant source of apoE in the brain (Boyles *et al.*, 1985; Pitas *et al.*, 1987a) and it has been speculated that neuronal apoE is derived from internalisation of astrocyte-secreted apoE. Recently, Nishio *et al.* (2003) observed increased apoE immunoreactivity in astrocytes, neurons and macrophages after focal ischaemia in the rat. In contrast, *APOE* mRNA was expressed in astrocytes and macrophages but not in neurons and is therefore compatible with an astrocytic origin for neuronal apoE. In the present study, increased glial apoE immunoreactivity was evident in ischaemic tissue. It is possible that apoE could initially

be upregulated in glial cells and subsequently sequestered by ischaemic neurons. Horsburgh and Nicoll (1996) demonstrated that after transient global ischaemia in the rat, apoE immunoreactivity was initially increased in astrocytes 24h after ischaemia and prior to evidence of neuronal damage and subsequent localisation of apoE to damaged neurons 72h after ischaemia. It is worth noting, however, that the development of neuronal damage follows a different time-course in focal and global ischaemia. Whether the temporal pattern of apoE redistribution observed after global ischaemia can occur within 24h after focal ischaemia is unclear. After acute subdural haematoma in the rat, neuronal accumulation of apoE was visible 30min after injury without evidence of increased glial apoE, suggesting a non-glial origin for apoE, such as from the circulation due to blood-brain barrier breakdown after injury (Horsburgh *et al.*, 1997). Another possibility is that apoE is produced within neurons. In contrast to the uninjured rodent brain, neuronal apoE immunoreactivity has been demonstrated in humans (Han *et al.*, 1994a; Han *et al.*, 1994b; Metzger *et al.*, 1996; Xu *et al.*, 1999) and apoE mRNA transcripts have also been localised to human brain neurons (Xu *et al.*, 1999), thus providing evidence that apoE can be synthesised locally within neurons. In the present study, transgenic mice expressing human *APOE* under the control of the human promoter were used. Accordingly, these mice display a human-like pattern of glial and neuronal apoE immunoreactivity in the uninjured brain (Xu *et al.*, 1996). Detection of apoE immunostaining in some cortical neurons of morphologically normal tissue in this study is consistent with previous work and is suggestive of neuronal synthesis of apoE since this pattern of apoE immunostaining is not observed in wild-type mice (Xu *et al.*, 1996). Neuronal accumulation of apoE was demonstrated to occur in a neuroblastoma cell line in the absence of glial cells after an oxidative challenge, indicating upregulation of neuronal apoE synthesis (Aoki *et al.*, 2003). In addition, increased *APOE* mRNA was observed in hippocampal neurons following kainic acid induced excitotoxicity (Boschert *et al.*, 1999). Thus, the evidence described above suggests that neuronal uptake of glial-derived apoE is an important mechanism contributing to the accumulation of apoE in neurons after acute brain injury and that this may be augmented by increased synthesis of apoE within neurons.

5.4.3 ApoE and mechanisms of neuroprotection in acute brain injury

Marked upregulation of apoE after ischaemic brain injury suggests a role for apoE as an injury-response protein. A protective role for apoE in acute brain injury has been

highlighted by studies showing a poorer outcome in *APOE* deficient mice after focal ischaemia (Laskowitz *et al.*, 1997), closed head injury (Chen *et al.*, 1997) and global ischaemia (Horsburgh *et al.*, 1999; Sheng *et al.*, 1999; Kitagawa *et al.*, 2002a; Kitagawa *et al.*, 2002b). It has been proposed that apoE scavenges and redistributes cholesterol and lipids to damaged neurons where they are internalised by receptor-mediated endocytosis and used to promote neuronal survival and repair (Ignatius *et al.*, 1987a; Poirier *et al.*, 1993a; Poirier, 1994; Vance *et al.*, 2000). Neuronal accumulation of apoE after injury may reflect this process. In addition, a number of mechanisms pertinent to cerebral ischaemia, that may be independent of the lipid transport-delivery properties of apoE, have been suggested to underlie the neuroprotective effects of apoE.

ApoE and apoE-derived peptides can attenuate NMDA-mediated excitotoxicity in cell culture (Aono *et al.*, 2002; Aono *et al.*, 2003). Significantly, there is evidence that apoE3 provides more potent protection against excitotoxic injury than apoE4 (Buttini *et al.*, 1999; Qiu *et al.*, 2003). These differences may contribute to the worse outcome in *APOE* ϵ 4 mice in the acute phase (e.g. 24h after ischaemia). Putative interactions between the major neuronal apoE receptor, LRP, and the NMDA receptor via adaptor proteins such as PSD-95 have been described (Bacsikai *et al.*, 2000; Gotthardt *et al.*, 2000; Herz, 2001a), and may provide a pathway through which apoE could alter glutamate receptor function and excitotoxic damage. Antioxidant properties of apoE have been shown *in vitro* (Lee *et al.*, 2004) and *in vivo*, in the uninjured brain (Ramassamy *et al.*, 2001; Shea *et al.*, 2002) and after global ischaemia (Horsburgh *et al.*, 2000b). Furthermore, apoE3 (and apoE2) has been shown to provide greater neuroprotection against oxidative insults than apoE4 (Miyata and Smith, 1996; Pedersen *et al.*, 2000; Lauderback *et al.*, 2002). Thus, an impaired ability to counteract oxidative stress may also contribute to poorer outcome in *APOE* ϵ 4 mice. Similarly, relative neuroprotection in *APOE* ϵ 3 mice may result from a greater ability to attenuate the acute inflammatory response (Lynch *et al.*, 2003) and apoptotic cell death (DeKroon *et al.*, 2003). ApoE3 also binds with greater affinity to various cytoskeletal components, such as neurofilament proteins and the microtubule associated proteins, tau and MAP2 (Huang *et al.*, 1994; Strittmatter *et al.*, 1994a; Strittmatter *et al.*, 1994b; Fleming *et al.*, 1996). This may promote greater cytoskeletal stability and neuronal survival after injury. In addition, evidence is accumulating of neurotoxic effects of apoE, in particular truncated apoE4 fragments, which can cause intracellular inclusions and elevations in

intracellular calcium levels as occurs during excitotoxicity (Tolar *et al.*, 1999; Huang *et al.*, 2001; Veinbergs *et al.*, 2002; Brecht *et al.*, 2004). However, the existence of toxic apoE fragments after cerebral ischaemia has not been investigated to date. In this regard, it is interesting to note that, in the present study, the volume of ischaemic damage in *APOE* ϵ 4 mice ($9 \pm 1\text{mm}^3$) was similar to that observed previously (*chapter 4*) in C57Bl/6J mice ($9 \pm 2\text{mm}^3$), whereas the volume of damage in *APOE* ϵ 3 mice was reduced ($7 \pm 1\text{mm}^3$). This suggests that the difference in extent of ischaemic damage in the present study is related to protective effects of apoE3 rather than toxic effects of apoE4 relative to endogenous mouse apoE.

In addition to the above putative mechanisms for the effects of *APOE* genotype on outcome to cerebral ischaemia, results from the present study raise the possibility that endocytic pathway alterations may contribute to the effects of *APOE* genotype on the outcome to cerebral ischaemia.

5.4.4 Endocytic pathway alterations after focal ischaemia

Marked increases in rabaptin-5 and rab4 immunostaining were observed in areas of tissue displaying ischaemic damage in comparison to non-ischaemic areas such as the contralateral hemisphere and undamaged cerebral cortex of the ipsilateral hemisphere. Rabaptin-5 and rab4 are proteins integral to endocytic pathway function and the level of expression/immunoreactivity of these molecules has been shown to reflect endocytic pathway activity (*see section 1.6.2.2*). The observations in the present study would therefore indicate up-regulation of endocytosis in response to focal cerebral ischaemia. Moreover, rabaptin-5 and rab4 are involved in two distinct stages of the endocytic pathway and therefore enable separation of the response of these two phases of endocytic trafficking. Rabaptin-5 localises to early endosomes, and therefore an increase in rabaptin-5 immunoreactivity is indicative of elevated trafficking of material from the plasma membrane through coated vesicles that subsequently form early endosomes. In contrast, rab4 localises to recycling endosomes that are returning to the plasma membrane and, consequently, an increase in rab4 immunostaining suggests an increase in recycling activity.

5.4.5 *APOE* genotype-dependent differences in endocytic pathway alterations after focal ischaemia

In the present study, *APOE* genotype was associated with differences in the extent of immunostaining of the endocytic recycling marker rab4 in ischaemic tissue. Although the degree of rabaptin-5 immunoreactivity was similar in both *APOE* ϵ 3 and *APOE* ϵ 4 mice, the degree of rab4 immunoreactivity was significantly greater in *APOE* ϵ 3 mice. In view of the specific roles of rabaptin-5 and rab4 in distinct stages of endocytosis, these data suggest that there is a differential response of the internalisation/early trafficking and recycling phases of endocytosis in response to focal cerebral ischaemia in *APOE* ϵ 3 and *APOE* ϵ 4 mice (**Figure 55**). A similar degree of rabaptin-5 immunoreactivity would indicate that endocytic internalisation and trafficking to early (sorting) endosomes was comparable in both transgenic groups. However, a greater level of rab4 immunoreactivity in *APOE* ϵ 3 mice suggests that endocytic recycling activity was markedly increased in comparison to *APOE* ϵ 4 mice. Interestingly, there was a correlation between the degree of rabaptin-5 and rab4 immunoreactivity in *APOE* ϵ 3 mice but not in *APOE* ϵ 4 mice. These results suggest that there may be a parallel response of the internalisation and recycling phases of endocytosis to ischaemic damage in *APOE* ϵ 3 mice whereas there may be uncoupling of these two processes in *APOE* ϵ 4 mice.

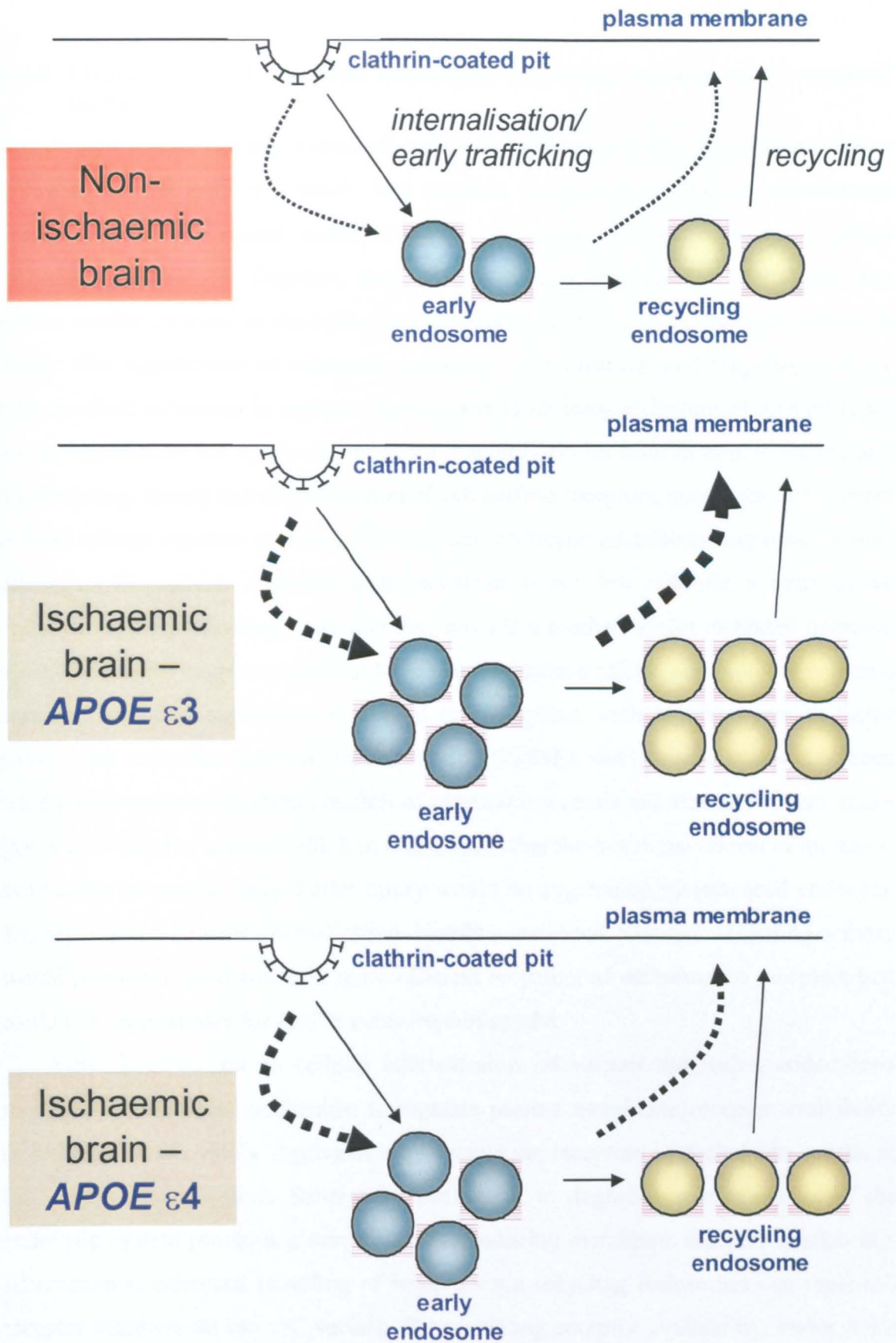


Figure 55. APOE genotype-dependent differences in the response of the endocytic pathway to cerebral ischaemia
 Solid arrows denote direction of transport. Thickness of broken arrows denote extent of activity in the particular phase of endocytosis.

5.4.6 Implications of elevated endocytic pathway activity after cerebral ischaemia

The present results indicate enhanced endocytic pathway activity in ischaemic tissue following a focal ischaemic insult. This parallels the findings in human post-mortem tissue, in which increased endocytosis was observed after an episode of global ischaemia (*chapter 3*). Together, these results suggest that cerebral ischaemia may induce similar changes in the endocytic pathway irrespective of the type of ischaemic insult. The significance of enhanced endocytic internalisation and recycling activity after cerebral ischaemia is unclear. Endocytosis is an integral feature of all cell types and is essential for the uptake of important macromolecules such as trophic factors and nutrients (e.g. lipids) and internalisation of cell surface receptors, processes that support normal cellular function and integrity. As such, endocytic alterations may have various effects on the cellular response to an ischaemic insult. For example, a more active endocytic system following ischaemia may provide a mechanism for increased neuronal uptake of various neurotrophins that have neuroprotective effects and promote neuronal survival. Increased expression of several neurotrophins, such as nerve growth factor (NGF) and brain-derived neurotrophic factor (BDNF) and their receptors has been widely demonstrated in animal models of cerebral ischaemia and traumatic brain injury (*for review see Abe et al., 2000*). It is conceivable that the beneficial effects of increased availability of growth factors after injury would be augmented by enhanced endocytic activity to promote their internalisation. Notably, increased endocytic recycling activity would provide a mechanism for more efficient recycling of neurotrophin receptors that could then be available for further neurotrophin uptake.

Aside from its role in cellular internalisation of various molecules, endocytosis provides an important mechanism to regulate plasma membrane receptor availability (Mukherjee *et al.*, 1997). Aggregation of membrane receptors in coated pits results in their rapid internalisation. Subsequent trafficking to degradative components of the endocytic system provides a mechanism for reducing membrane receptor availability. Alternatively, enhanced recycling of receptors via recycling endosomes can replenish receptor numbers on the cell surface. By regulating receptor availability, endocytosis can influence extracellular signalling pathways that are mediated by binding of ligands to plasma membrane receptors and endocytosis has been shown to be a well established way of down-regulating extracellular signals (Willnow *et al.*, 1999). Endocytic activation after cerebral ischaemia may therefore enable modulation of signalling

pathways associated with the response to ischaemia. For example, enhanced endocytosis may promote internalisation of ionotropic glutamate receptors and provide a mechanism for attenuating excitotoxic pathways. Previously, glutamate receptor endocytosis has been demonstrated to be an important factor in the modulation of synaptic strength in neural plasticity paradigms (*for reviews see Carroll et al., 2001; Malinow and Malenka, 2002; Gomes et al., 2003; Malenka, 2003*).

5.4.7 Alterations in the endocytic pathway - possible mechanism underlying *APOE* genotype differences in outcome to acute brain injury

The present data indicate that the endocytic recycling response after focal ischaemia is attenuated in *APOE* $\epsilon 4$ mice in comparison to *APOE* $\epsilon 3$ mice. These findings are similar to those obtained in human post-mortem tissue in which an attenuated recycling response was evident in *APOE* $\epsilon 4$ carriers after an episode of global ischaemia. A different response of the endocytic pathway provides a novel mechanism that may contribute to the *APOE* genotype-dependent differences in outcome to acute brain injury. Accumulation of apoE in ischaemic neurons was observed in this and previous studies and it has been proposed that apoE acts as a transport protein to deliver lipids/cholesterol to injured neurons for membrane repair and synaptic reorganisation. Endocytosis of apoE-containing lipoprotein particles via apoE receptors (e.g. LRP) is likely to be an important facet of neuronal accumulation of apoE after injury and therefore up-regulation of the endocytic pathway, as observed in this study, will enhance uptake of apoE and associated lipids. Following internalisation, components of the lipoprotein-receptor complex dissociate and apoE and receptors can be directed to lysosomes for degradation or be recycled to the cell surface. Results from this study suggest that endocytic recycling is more active in *APOE* $\epsilon 3$ mice after cerebral ischaemia. Accordingly, it is conceivable that recycling of apoE and its receptors are enhanced in *APOE* $\epsilon 3$ mice. Significantly, this would replenish the pool of apoE available for mobilising lipids to injured neurons and would restore apoE receptors to the cell surface, processes that are likely to further promote neuronal uptake of apoE and allied lipids. Thus, the relative neuroprotective effects associated with the *APOE* $\epsilon 3$ allele may result from more pronounced endocytic recycling that in turn enhances apoE-mediated delivery of vital cellular components (lipids, cholesterol) required for neuronal survival and repair. In this scenario, it may be expected that neuronal apoE

accumulation would be greater in *APOE* $\epsilon 3$ mice, however, in the present study, the degree of apoE immunoreactivity in ischaemic tissue was similar in both *APOE* $\epsilon 3$ and *APOE* $\epsilon 4$ mice. There were also no observable differences in intensity of apoE immunoreactivity between *APOE* $\epsilon 3$ and *APOE* $\epsilon 4$ mice. A possible explanation for these findings is that the extent of endocytic internalisation and early trafficking (as indicated by rabaptin-5 immunoreactivity) was similar in both transgenic groups and that this stage of endocytosis is the principal determinant of apoE uptake. Subsequently, apoE may be trafficked along different routes with a recycling path more prominent in *APOE* $\epsilon 3$ mice. Enhanced apoE recycling in *APOE* $\epsilon 3$ mice may promote greater turnover of apoE such that the extent of neuronal apoE accumulation is similar in *APOE* $\epsilon 3$ and *APOE* $\epsilon 4$ mice at a given time. However, lipid/cholesterol delivery will be more efficient in *APOE* $\epsilon 3$ mice due to the continued replenishing of the pool of apoE available for lipid/cholesterol delivery and uptake.

Previous studies have provided evidence that apoE can escape lysosomal degradation and be recycled and re-secreted following internalisation. *In vitro*, incubating cells with apoE-containing lipoproteins resulted in their rapid internalisation and after 4h the release of significant amounts of endocytosed apoE (retroendocytosis) but not lipoprotein-derived cholesterol, suggesting that apoE escaped degradation (Rensen *et al.*, 2000). Similar results were obtained *in vivo*, where only 15 – 20% of endocytosed apoE was degraded in contrast to hydrolysis of 75% of associated cholesterol (Rensen *et al.*, 2000). ApoE may escape lysosomal degradation by following a recycling pathway. Pulse-chase experiments have demonstrated that approximately 80% of internalised lipoprotein-associated apoE can escape the lysosomal pathway as a result of targeting to recycling endosomes (Heeren *et al.*, 2001). Recently, it was shown that a significant proportion of internalised CSF-derived apoE is resistant to degradation and was localised to non-lysosomal vesicles (Ljungberg *et al.*, 2003). Interestingly, isoform-specific differences of endocytic trafficking of apoE in primary human neuronal cultures have been shown. Using marker proteins specific for different endocytic compartments, progression of internalised apoE3 and apoE4 through these compartments differed. Although both isoforms were similarly trafficked to early endosomes, apoE4 progressed to late endosomes/lysosomes whereas there was minimal evidence for apoE3 following this route (DeKroon and Armati, 2001). A likely explanation is that a significant proportion of apoE3 was directed to recycling

endosomes thus precluding its progression to late endosomes/lysosomes. Retroendocytosis of apoE3 would promote a continuous lipid delivery system and the finding in the present study of greater endocytic recycling activity in *APOE* ϵ 3 mice is consistent with this previous *in vitro* data.

APOE genotype-dependent differences in endocytic pathway function and endocytic trafficking of apoE may also modulate the outcome to acute brain injury via mechanisms independent of the lipid transport/delivery properties of apoE. It has been proposed that apoE3 may exert neuroprotective effects by promoting increased stability of the neuronal cytoskeleton (Strittmatter *et al.*, 1994a; Strittmatter *et al.*, 1994b). However, such a function would appear to require apoE to escape the endosomal-lysosomal system and be available in the cytosol, an event lacking in conclusive evidence (DeMattos *et al.*, 1999). Furthermore, cytosolic apoE has been shown to be cytotoxic (DeMattos *et al.*, 1999). There is evidence to suggest that rab proteins, notably rab4, can interact with the cytoskeleton, in particular microtubule components where they can direct vesicle movement (Gonzalez and Scheller, 1999; Bielli *et al.*, 2001). It may be speculated that the more prominent recycling pathway associated with apoE3 could promote interactions with the cytoskeleton via rab4, a process that would not be dependent on the release of apoE into the cytosol.

Generation of toxic apoE fragments may also be affected by endocytic pathway function. Evidence suggests that generation of truncated apoE fragments can have neurotoxic effects and that apoE4 in particular is more prone to truncation (Marques *et al.*, 1996; Marques *et al.*, 1997; Huang *et al.*, 2001; Brecht *et al.*, 2004). The lysosomal compartment is a likely location where apoE cleavage could occur in view of the proteolytic conditions that exist in these vesicles. After cerebral ischaemia the increased neuronal uptake of apoE and elevated endocytic pathway activity may accelerate the progression of apoE to the lysosomal system and promote apoE fragment production. Since previous studies have shown that apoE4 is preferentially trafficked to late endosomes/lysosomes (DeKroon and Armati, 2001), this may account for the greater tendency of apoE4 to be truncated. In contrast, apoE3 may be protected from truncation by following a recycling pathway. Lysosomal leakage has been demonstrated to be enhanced in the presence of apoE4 (Ji *et al.*, 2002), which can promote apoptosis and could allow apoE to enter the cytosol where it can exert neurotoxic properties (DeMattos *et al.*, 1999). Thus, *APOE*-dependent effects on endocytic trafficking could

modulate the propensity for apoE to develop neurotoxic properties via its fragmentation. Consequently, investigation of apoE fragmentation after cerebral ischaemia would be merited.

Lastly, *APOE*-genotype differences in endocytic pathway behaviour may modulate outcome to acute brain injury through effects on signal transduction pathways involving apoE receptors. In view of the accumulating evidence that members of the LDL receptor family, such as LRP and apoER2, can function as signalling receptors in addition to their prototypic role as cell surface endocytic receptors (Willnow *et al.*, 1999; Herz, 2001b), it is evident that these receptors lie at the “crossroads” of endocytic and signal transduction pathways. Endocytosis is an important mechanism for regulating transduction pathways elicited at the cell surface through its ability to internalise and recycle receptors or target them for degradation (Willnow *et al.*, 1999). Ligand-binding to LRP has been shown to be capable of inducing NMDA receptor-mediated calcium influx (Bacsikai *et al.*, 2000; Qiu *et al.*, 2002). It is evident that increased neuronal apoE internalisation after injury would occur at the convergence of the endocytic and signalling pathways. Thus, endocytic pathway alterations may not only influence the trafficking of apoE but could also influence apoE receptor signalling cascades pertinent to cerebral ischaemia.

5.4.8 Conclusions

In summary, the present study has demonstrated an association between *APOE* genotype and differences in outcome and endocytic pathway alterations after focal cerebral ischaemia in the mouse. The present results suggest a novel mechanism that may contribute to the deleterious effects on outcome to acute brain injury that are associated with possession of the *APOE* $\epsilon 4$ allele. The aims stated at the outset of this study have been achieved:

1. the volume of ischaemic damage and the neurological deficit score were significantly greater in *APOE* $\epsilon 4$ mice compared to *APOE* $\epsilon 3$ mice after transient focal cerebral ischaemia
2. increased apoE immunoreactivity (including neuronal) was closely associated with areas of ischaemic damage in both *APOE* $\epsilon 3$ and *APOE* $\epsilon 4$ mice. The degree of apoE immunoreactivity in the ischaemic lesion was similar in *APOE* $\epsilon 3$ and *APOE* $\epsilon 4$ mice, however, the distribution of apoE immunoreactivity was significantly greater in *APOE* $\epsilon 4$ mice

3. increased immunoreactivity of the endocytic pathway markers, rabaptin-5 and rab4, was observed in areas of ischaemic damage. The degree of rabaptin-5 immunoreactivity was similar in *APOE* ϵ 3 and *APOE* ϵ 4 mice. The degree of rab4 immunoreactivity was significantly greater in *APOE* ϵ 3 mice.

Chapter 6

**Adenoviral-mediated gene transfer of *APOE*
 ϵ 3 markedly reduces ischaemic brain
damage after transient focal cerebral
ischaemia in mice**

6.1 Introduction and aims

The previous study (*chapter 5*) demonstrated that mice expressing human *APOE* $\epsilon 3$ have an improved outcome to transient focal ischaemia compared to *APOE* $\epsilon 4$ mice. Augmenting apoE levels in the brain has also been shown to have neuroprotective effects after cerebral ischaemia in mice (Horsburgh *et al.*, 2000b). This study investigated the effects of viral vector-mediated gene transfer of *APOE* $\epsilon 3$ on outcome after transient focal ischaemia. The specific aims of the present study were to determine, in C57Bl/6J mice, if adenovirus-mediated gene transfer of *APOE* $\epsilon 3$:

1. augments endogenous apoE levels in the brain
2. attenuates ischaemic brain damage after transient focal ischaemia

6.2 Materials and methods

This study was carried out at the Division of Neuroscience, University of Edinburgh. All experiments were performed blinded to treatment.

6.2.1 Mice

Adult male C57Bl/6J strain mice obtained from Charles River, UK, were used

6.2.2 Adenoviral (Ad) vectors

Second generation adenoviral vectors (viral E1, E2b, E3 genes deleted) with the *APOE* $\epsilon 3$ cDNA (Ad-*APOE*) or GFP gene (Ad-GFP) inserted (*section 2.12*) were used.

6.2.3 Preliminary characterisation of adenoviral transduction and transgene expression

The class of adenoviral vector used in the present study (“second generation” with the viral E1, E2b and E3 gene deleted) had previously been administered to the periphery only (e.g. muscle, liver). Therefore, preliminary experiments involving stereotaxic injections of vectors (or vehicle) without subsequent focal ischaemia were performed initially, (1) to confirm that the vector transgene was expressed in the brain following intrastriatal injection, and (2) to provide an indication of the extent and distribution of transduction and tissue/cellular damage associated with vector administration.

Vectors (and vehicle) were administered via stereotaxic injection into the caudate nucleus as described (*section 2.3.1*). Three mice received injection (0.5 μ l) of Ad-*APOE*

(one each administered 3.4×10^9 vp/ml, 3.4×10^{10} vp/ml and 3.4×10^{11} vp/ml), 3 mice received injection of Ad-GFP (one each administered 3.4×10^9 vp/ml, 3.4×10^{10} vp/ml and 3.4×10^{11} vp/ml) and one mouse received injection of vehicle (10% glycerol in PBS). Three days after vehicle or vector administration, mice were sacrificed by transcardiac perfusion fixation. Adjacent sections around the level of the injection tract were stained with haematoxylin and eosin and immunostained for apoE. Sections from Ad-GFP injected mice were also mounted for inspection of GFP expression. Observations were made regarding the distribution and localisation of transgene expression, extent of tissue/cellular damage and apoE immunostaining.

6.2.4 Effects of Ad-APOE administration on outcome and apoE immunostaining after focal ischaemia

6.2.4.1 Vector and vehicle administration

Mice (28 ± 0.3 g) were randomly assigned to three groups based on their treatment with vehicle (10% PBS in glycerol) ($n = 5$), Ad-GFP ($n = 6$) or Ad-APOE ($n = 6$). Vehicle and vectors were applied by stereotaxic infusion into the caudate nucleus (*section 2.3.1*). Based on observations from the preliminary experiments (*section 6.3.1*), vectors were administered at a concentration of 3.4×10^{11} vp/ml in $0.5 \mu\text{l}$ PBS containing 10% glycerol. An equal volume of vehicle was infused in vehicle-treated mice.

6.2.4.2 Focal ischaemia and evaluation of neurological deficit

Three days after stereotaxic injections, transient focal ischaemia (60min) was induced by intraluminal occlusion (recovery from anaesthesia model) as described (*section 2.3.2.2*). This model of intraluminal occlusion was employed in the present study based on the hypothesis that application of Ad-APOE would reduce the amount of ischaemic damage. Accordingly, a model that produces a substantial volume of damage (striatal and cortical) was considered most appropriate. The results in *chapter 4* demonstrated that the sustained anaesthesia model characterised in this thesis produced extensive volumes of ischaemic damage with 30 or 60min occlusion but was associated with declining MABP and widespread reductions in CBF outside MCA territory. These factors may render the brain unreceptive to neuroprotective strategies. In the recovery from anaesthesia model, mice are conscious during occlusion which should result in more stable MABP. Previous work also demonstrated that this model produces reproducible striatal and cortical ischaemic lesions with 45min occlusion. In the present

study, 60min occlusion was chosen since it was hypothesised that stereotaxic injection through a burr hole in the cranium may attenuate the ischaemic insult by reducing intracranial pressure.

After 24h reperfusion, mice were assigned a neurological deficit score of 0 to 4 as described (*section 2.4*). Following neurological evaluation, mice were perfused transcardially (*section 2.5*) and paraffin-processed (*section 2.6.1.2*). Paraffin embedded brains were cut into 6 μ m sections (*section 2.6.2*) which were used for histological and immunohistochemical analysis.

6.2.4.4 Measurement of ischaemic damage

The volume of ischaemic damage was measured in haematoxylin and eosin-stained tissue as described (*section 2.8*). Criteria for inclusion were: (1) clear evidence of ischaemic damage in the striatum, and (2) absence of intracranial haemorrhage as observed in haematoxylin and eosin-stained tissue.

6.2.4.5 ApoE immunohistochemistry

Paraffin-embedded sections (6 μ m) were immunostained (peroxidase protocol) with anti-apoE as described (*section 2.9.3*).

Adjacent sections to those stained with haematoxylin and eosin were used to delineate the distribution of intense apoE immunostaining at eight coronal levels. Delineation of the areas of tissue displaying intense apoE immunostaining was performed at low magnification (x25). In doing so, apoE immunostaining in ischaemic neurons was not readily visible and therefore only areas of intense apoE immunostaining (mainly of neuropil) related to stereotaxic injection were quantified. Areas were then integrated with the distance between each coronal level to calculate a volume in the same way as for ischaemic damage (*section 2.9.6.1*). Reproducibility of volumetric measurement was tested (**Appendix I**).

6.2.5 Effect of Ad-APOE administration on apoE levels

ApoE levels were measured in mice receiving intrastriatal injections of vehicle, Ad-GFP or Ad-APOE without subsequent focal ischaemia. Mice were given bilateral injections (0.5 μ l) of vehicle (10% PBS in glycerol) or Ad-GFP (3.4×10^{11} vp/ml) or Ad-APOE (3.4×10^{11} vp/ml) into the caudate nucleus (n = 2 mice per treatment group). Each

hemisphere was treated as an individual data point, therefore $n = 4$ for each treatment. Three days after injection, mice were perfused transcardially and brain tissue was harvested as described (*section 2.10.1*). Tissue samples were homogenised (*section 2.10.2*) and total protein content was assayed (*section 2.10.3*). ApoE levels were then quantified by sandwich ELISA (*section 2.10.4*).

6.2.6 Statistical analysis

Two comparisons were made for areas and volumes of ischaemic damage, neurological deficit score, areas and volumes of apoE immunostaining and apoE levels: 1) vehicle vs. Ad-GFP; 2) Ad-GFP vs. Ad-*APOE*. To assess statistical differences, comparisons were performed using one-way ANOVA followed by Student's unpaired *t*-test incorporating a Bonferroni correction factor of 2. All data are presented as mean \pm SEM.

6.3 Results

6.3.1 Preliminary characterisation of adenoviral transduction and transgene expression

6.3.1.1 GFP expression

GFP expression was first examined in Ad-GFP injected mice without subsequent focal ischaemia. In all Ad-GFP injected mice, there was evidence of adenovirally transduced cells in the hemisphere ipsilateral to injection, as revealed by intense GFP fluorescence. The distribution of cells displaying intense GFP fluorescence was dependent on the concentration of Ad-GFP administered (**Figure 56**). With the lowest dose (3.4×10^9 vp/ml), the distribution of intense GFP-labelled cells was limited to a small area of tissue immediately surrounding the injection tract. Increasing the vector dose to 3.4×10^{10} vp/ml resulted in a greater distribution of adenovirally transduced cells. The number of intense GFP-labelled cells in the caudate nucleus was markedly increased in comparison to the lower dose. In addition to GFP-labelled cells adjacent to the injection tract, there were also more distant cells labelled in the caudate nucleus and a few GFP-positive cells in the external capsule. Administration of the highest dose of vector (3.4×10^{11} vp/ml) resulted in the most extensive distribution of GFP-labelled cells. The distribution of GFP-positive cells in the caudate nucleus was similar to that observed with injection of 3.4×10^{10} vp/ml vector, however with the highest dose there was also extensive expression of GFP in cells of the subcortical white matter.

The majority of intense GFP fluorescent cells in the caudate nucleus displayed large, round cell bodies with visible neurites of varying length (**Figure 57**). Many of the GFP expressing cells in subcortical white matter displayed small, elongated cell bodies and were orientated along the plane of the fibres suggesting that oligodendrocytes were the predominant cell type expressing GFP (**Figure 57**). It was not possible to confirm this, however, since a specific oligodendrocytic marker suitable for use in paraffin-embedded tissue was not available. Double-labelling with the neuronal marker, neu-N, and the astrocytic marker, GFAP, was performed and did not show any co-localisation between GFP and either marker. However, the strong GFP signal may have masked the weak neu-N and GFAP signals. It should be noted that, although GFP expression provides an indication of adenoviral transduction, it is likely to be an underestimation since there may be additional cells and/or cell types transduced that are expressing GFP at undetectable levels or not at all.

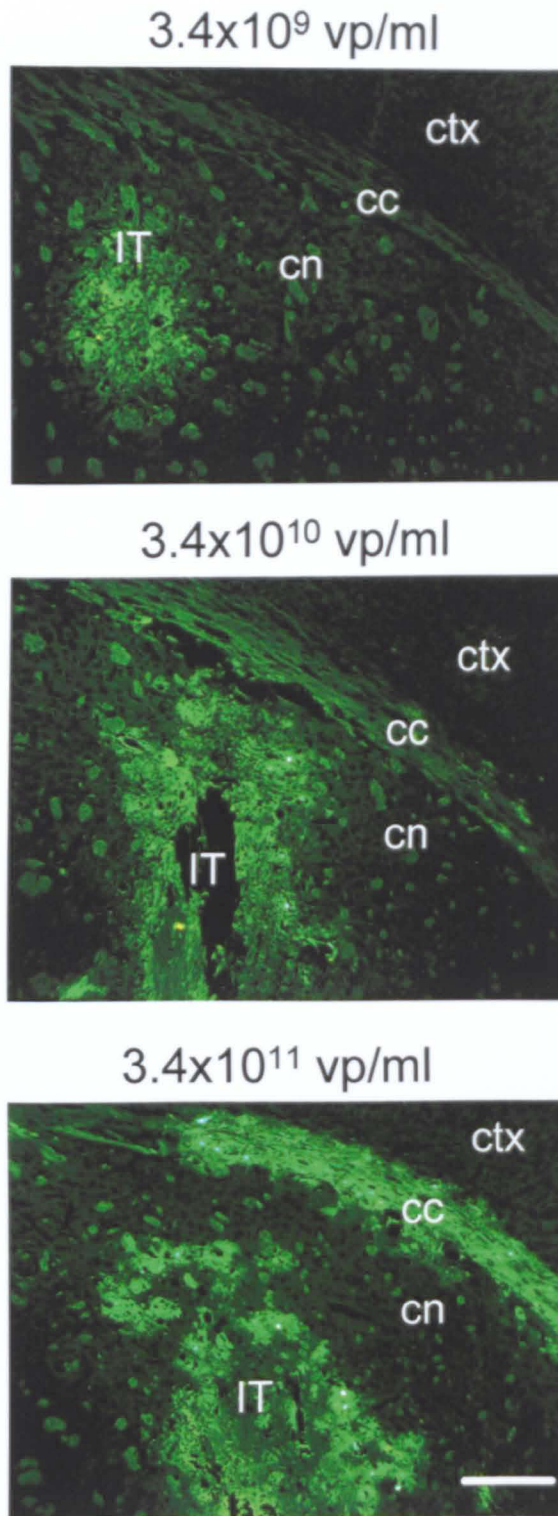


Figure 56. Effect of adenoviral vector dose on distribution of GFP expression
 Increasing the titre of Ad-GFP resulted in an increase in the number and distribution of cells expressing GFP. At the lowest dose (3.4×10^9 vp/ml) GFP-labelled cells were confined to tissue immediately surrounding the injection tract. In contrast, at the highest dose (3.4×10^{11} vp/ml) GFP labelled cells were more widely distributed in the caudate nucleus and were also observed in the corpus callosum. ctx, cerebral cortex; cc, corpus callosum; cn, caudate nucleus; IT, injection tract. Scale bar, 100 μ m.

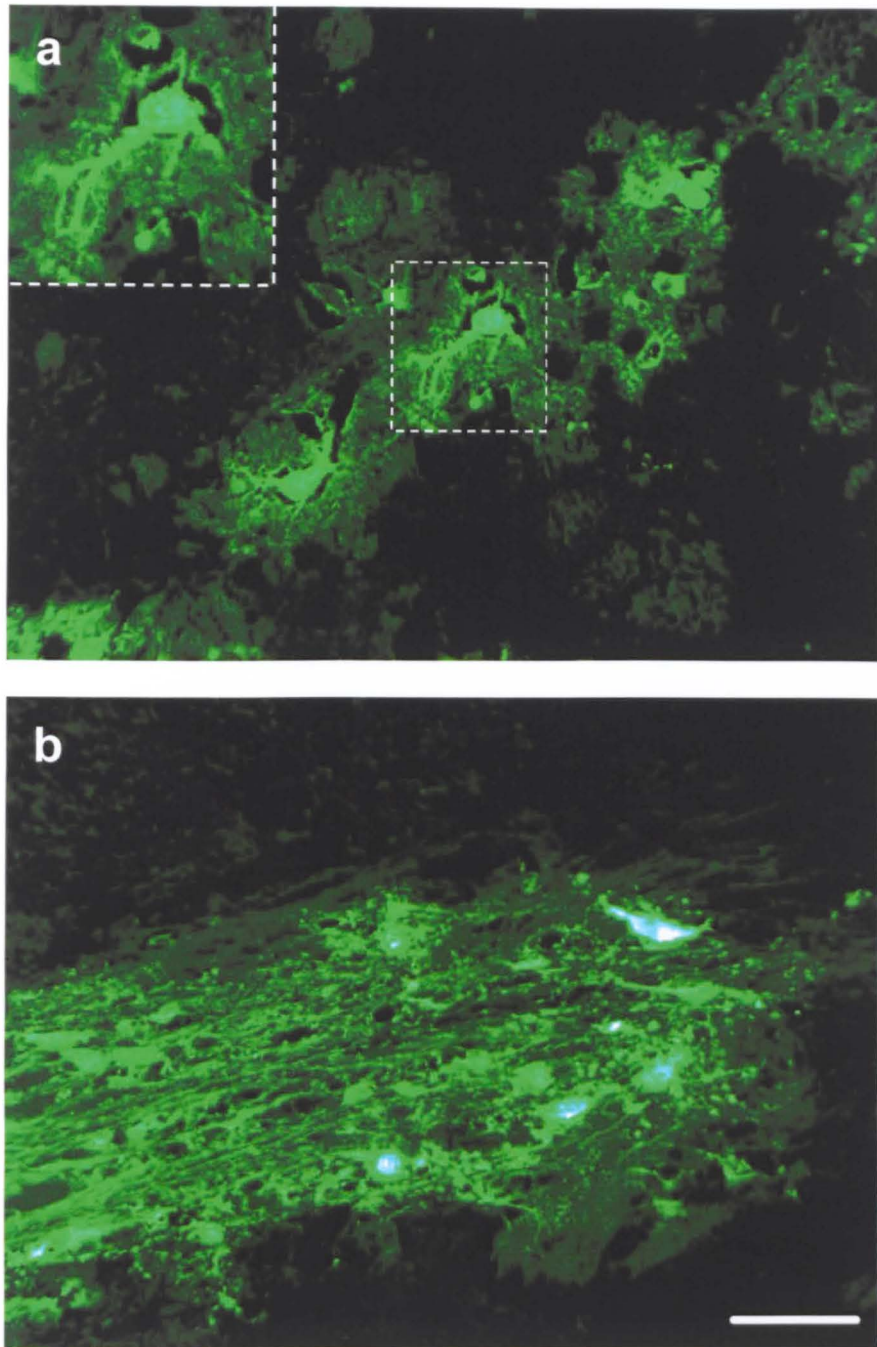


Figure 57. GFP expression in the caudate nucleus and subcortical white matter
Intense GFP fluorescence, indicative of adenoviral transduction and transgene expression, was observed in cells in (a) the caudate nucleus and (b) the corpus callosum. GFP expression appeared to be localised mainly to oligodendrocytes. Scale bar, 25µm.

6.3.1.2 Histology

Sections from mice given vehicle, Ad-GFP or Ad-*APOE* without subsequent ischaemia were stained with haematoxylin and eosin to examine histological damage associated with the injection tract and/or adenoviral transduction. In all treatments groups, injections were associated with some distortion of tissue due to mechanical damage produced by the needle. In general, this was limited to a thin strip of tissue in the cortex and caudate nucleus (**Figure 58**). Mechanical disruption of tissue was also accompanied in most cases by a small amount of bleeding localised to the injection tract. There were no apparent differences in the extent of tissue disruption or bleeding among vehicle, Ad-GFP or Ad-*APOE* treated mice. Examination of tissue at higher magnification revealed that vehicle or vector injection without subsequent ischaemia resulted in only minimal cellular damage that was localised to mechanically disrupted tissue bordering the injection tract (**Figure 58**). No differences were observed in the extent of cellular damage in vehicle, Ad-GFP and Ad-*APOE* treated mice. In addition, there were no increases observed in the extent of cellular injury with increasing dose of Ad-GFP or Ad-*APOE*. Notably, in Ad-GFP treated mice, sections stained with haematoxylin and eosin adjacent to those examined for GFP revealed that, in areas of tissue containing GFP expressing cells, there was no histological evidence of cellular injury. These observations suggest that there were no significant direct cytotoxic effects of adenoviral transduction and transgene expression and that mechanical damage was the primary factor underlying the minimal tissue and cellular injury localised to the injection tract..

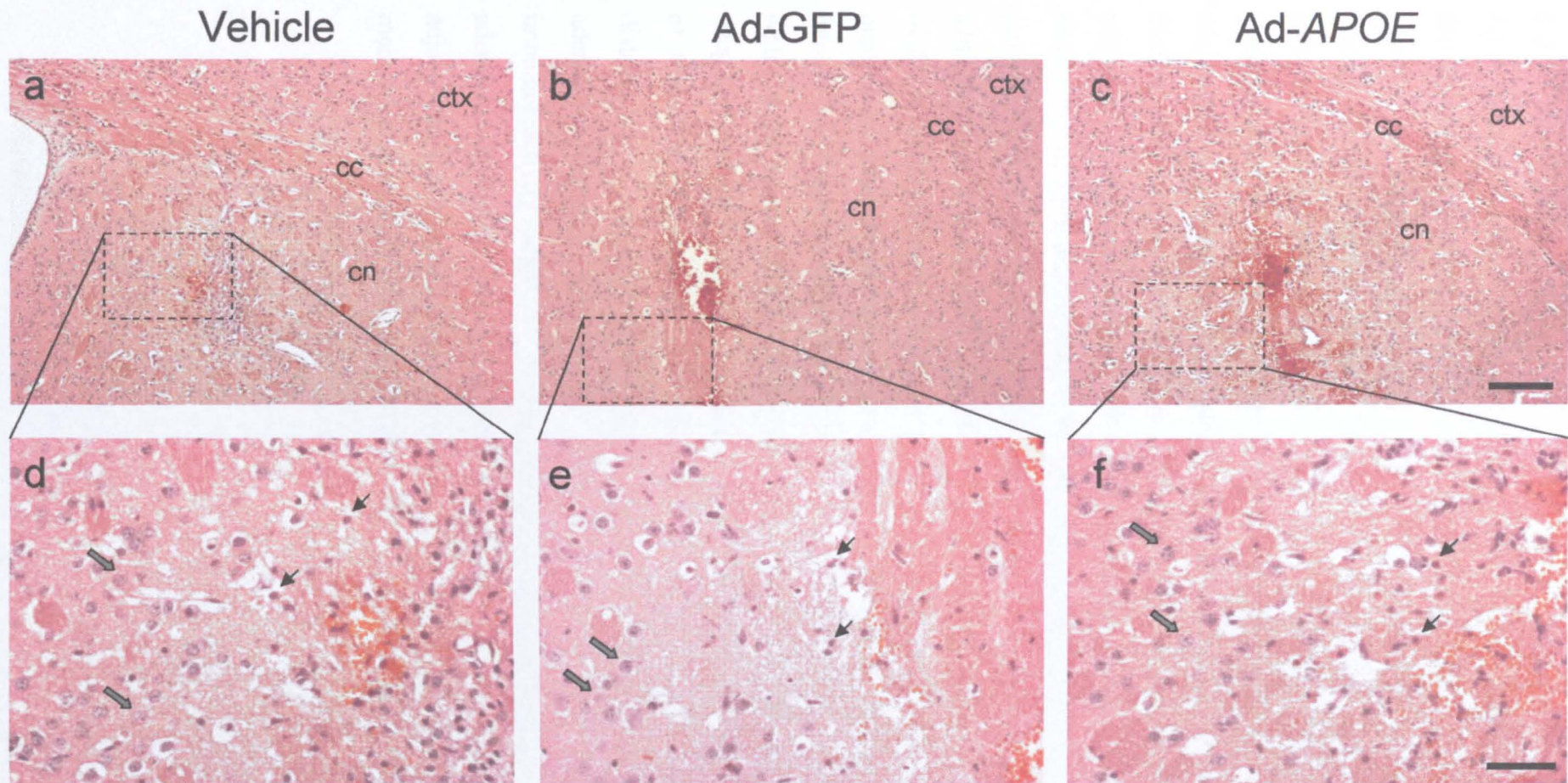


Figure 58. Tissue damage after vehicle or adenoviral vector injection

(a-c) A small amount of tissue distortion caused by mechanical needle damage was observed regardless of treatment. (d-f) In addition, cellular injury was observed locally around the injection tract (arrows), however this did not extend far from the injection tract as indicated by the appearance of normal cellular morphology (block arrows). ctx, cortex; cc, corpus callosum; cn, caudate nucleus. Scale bar (a-c), 300 μ m; (d-f), 50 μ m.

6.3.1.3 ApoE immunostaining

ApoE immunostaining was examined in vehicle, Ad-GFP and Ad-*APOE* treated mice that did not undergo focal ischaemia. ApoE immunoreactivity was observed in all mice, however, the intensity and distribution of apoE immunoreactivity varied markedly among the three groups (**Figure 59**). Faint apoE immunoreactivity of a few cells surrounding the injection tract was observed following administration of vehicle. Faintly stained cells appeared to have shrunken cell bodies and were located in the zone of damaged tissue observed in the adjacent section stained with haematoxylin and eosin. Similar observations were made in Ad-GFP treated mice regardless of the dose of vector given. Administration of Ad-*APOE* resulted in markedly greater intensity and distribution of apoE immunoreactivity. Increasing the dose of Ad-*APOE* also resulted in progressive increases in the intensity and distribution of apoE immunoreactivity. After administration of the highest dose of Ad-*APOE* (3.4×10^{11} vp/ml), extensive distribution of dense apoE immunoreactivity of the neuropil – encompassing most of the caudate nucleus and extending to the external capsule – was observed (**Figure 59**). In addition, intense apoE immunoreactivity of glial cells in the caudate nucleus and subcortical white matter was observed. Furthermore, dense neuropil apoE immunoreactivity in the deep layers of the cerebral cortex was observed after administration of the highest dose of Ad-*APOE* (**Figure 60**). These observations suggest that the greater intensity and distribution of apoE immunoreactivity following Ad-*APOE* injection is due to adenovirus-mediated delivery of the *APOE* gene since only minimal apoE immunoreactivity localised to the injection tract was observed after vehicle injection or adenovirus-mediated delivery of the GFP gene. Cellular apoE immunoreactivity adjacent to the injection tract is likely to be a response to tissue damage caused by mechanical disruption since this was observed in vehicle and Ad-GFP treated mice.

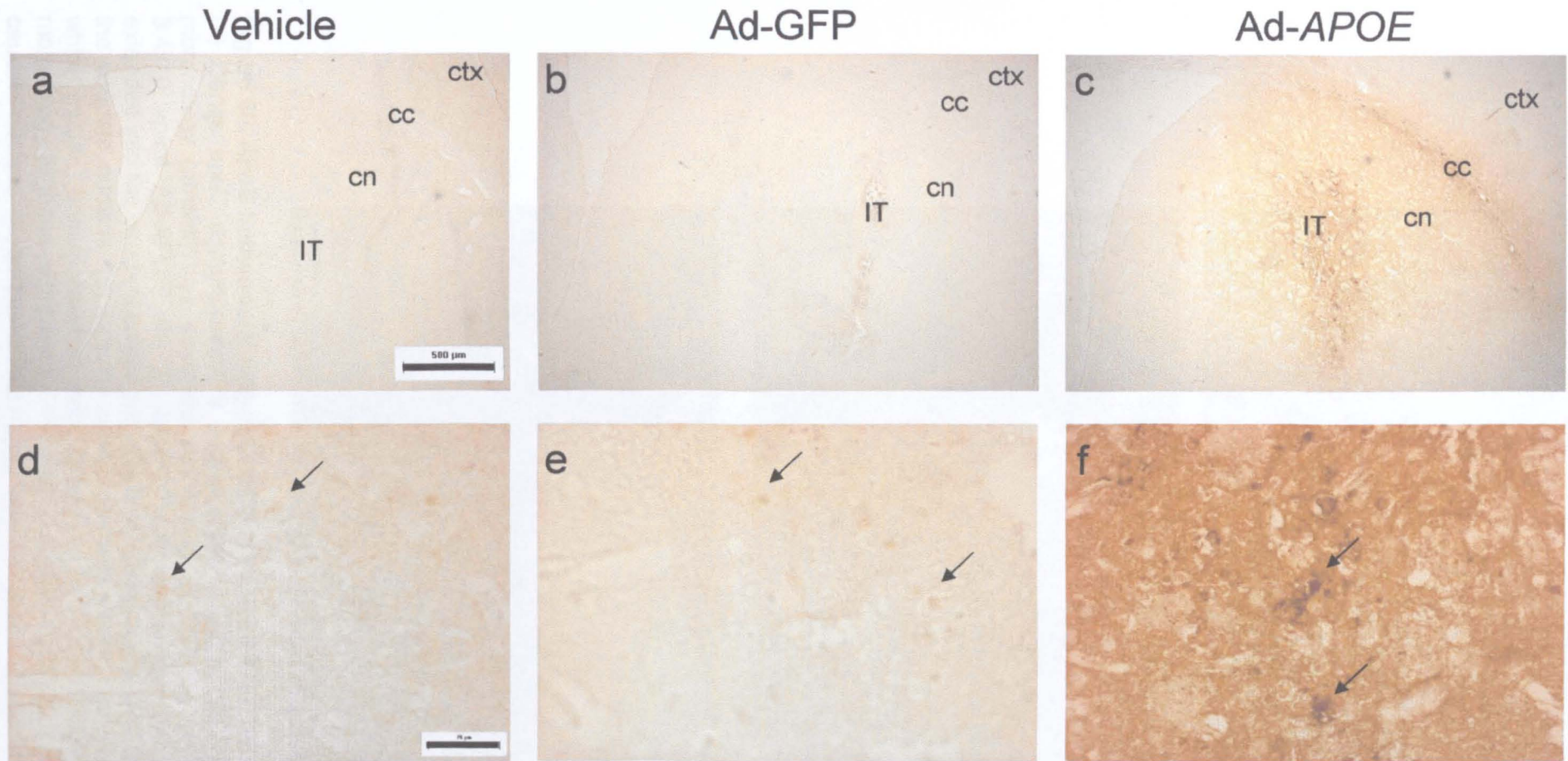


Figure 59. ApoE immunostaining after vehicle or vector administration without subsequent ischaemia

(a) Vehicle and (b) Ad-GFP injection resulted in only minimal apoE immunostaining localised to the injection tract whereas (c) Ad-APOE injection produced dense apoE immunoreactivity around the injection tract and also distant to this in the caudate nucleus, corpus callosum and deep layers of the cerebral cortex. (d,e) Faint cellular apoE immunoreactivity (arrows) was evident around the injection tract in (d) vehicle and (e) AD-GFP treated mice. In contrast, injection of (f) Ad-APOE produced intense neuropil and cellular (arrows) immunoreactivity. Photomicrographs of Ad-GFP and Ad-APOE show immunostaining after injection of highest dose (3.4×10^{11} vp/ml) of adenoviral vector. ctx, cortex; cc, corpus callosum; cn, caudate nucleus; IT, injection tract. Scale bar (a-c), $500 \mu\text{m}$; (d-f), $50 \mu\text{m}$.

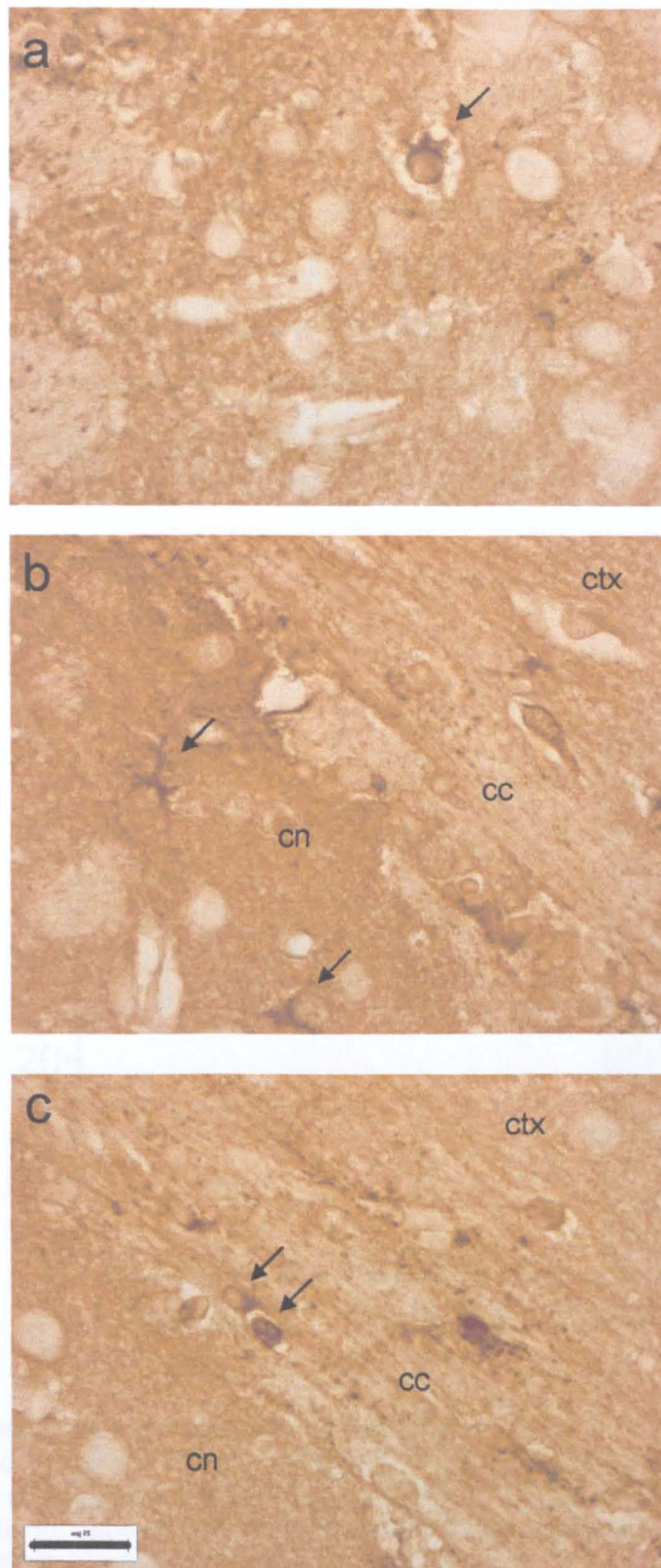


Figure 60. ApoE immunostaining after Ad-APOE injection

(a) Dense apoE immunoreactivity in the neuropil and a few cells with neuronal morphology (arrows) was observed in the caudate nucleus after administration of 3.4×10^{11} vp/ml Ad-APOE. (b) In addition, dense neuropil apoE immunoreactivity extended into the cerebral cortex and was also observed in a few glial cells (arrows) in the caudate nucleus. (c) Cellular apoE immunoreactivity was evident in subcortical white matter. Immunoreactive cells (arrows) displayed similar (oligodendrocytic) morphology to those expressing GFP after treatment with 3.4×10^{11} vp/ml Ad-GFP. cn, caudate nucleus; cc, corpus callosum; ctx, cerebral cortex. Scale bar, 25µm.

6.3.2 Effect of Ad-APOE administration on apoE levels

ApoE levels were measured 3 days after injection in mice that did not undergo focal ischaemia (Figure 61). Administration of Ad-APOE resulted in significantly higher levels of apoE compared to treatment with Ad-GFP (50.7 ± 3.0 ng apoE/mg total protein vs. 1.2 ± 0.2 ng apoE/mg total protein, $P < 0.0001$). There was no difference in the level of apoE following administration of vehicle or Ad-GFP (1.0 ± 0.4 ng apoE/mg total protein vs. 1.2 ± 0.2 ng apoE/mg total protein, $P > 0.05$).

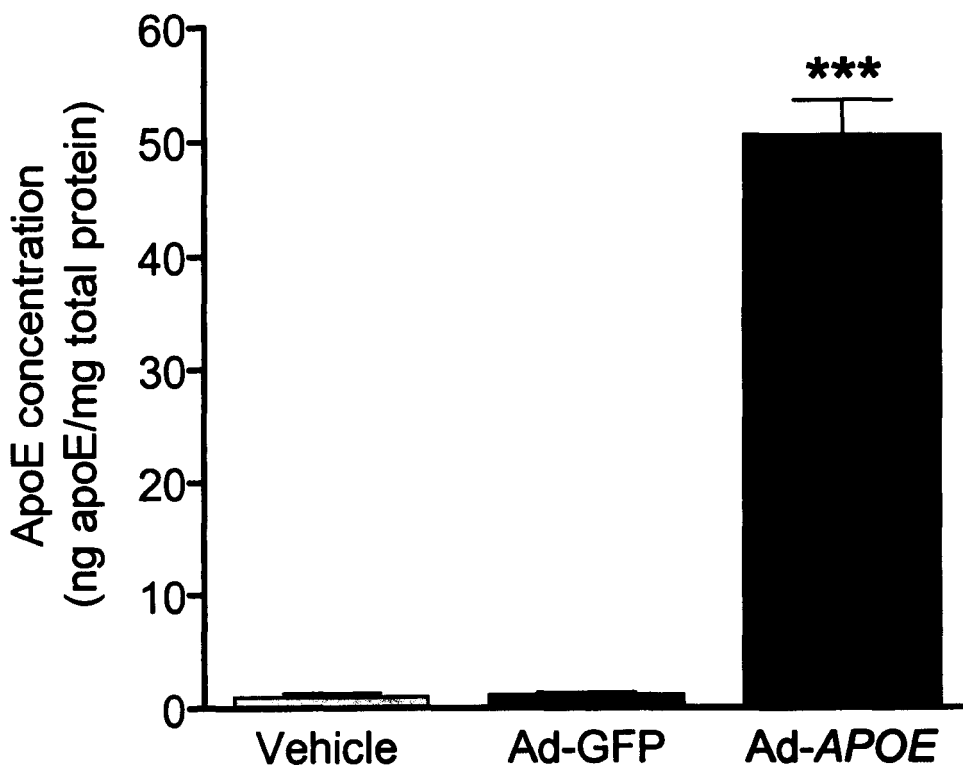


Figure 61. Quantification of apoE levels by ELISA

The level of apoE was significantly greater in Ad-APOE compared to Ad-GFP treated mice. The level of apoE was similar in vehicle and Ad-GFP treated mice. *** $P < 0.0001$ for the comparison between Ad-GFP and Ad-APOE, one-way ANOVA followed by Student's unpaired *t*-test with Bonferroni correction. $n = 4$ (each group). Data are presented as mean \pm SEM.

6.3.3 Effect of Ad-APOE administration on ischaemic damage after focal ischaemia

Administration of Ad-APOE significantly reduced the total volume of ischaemic damage in comparison to Ad-GFP treated mice ($13 \pm 3\text{mm}^3$ vs. $29 \pm 4\text{mm}^3$, $P = 0.013$) (**Figure 62**). The total volume of ischaemic damage was similar in vehicle and Ad-GFP treated mice ($27 \pm 5\text{mm}^3$ vs. $29 \pm 4\text{mm}^3$, $P > 0.05$). The volume of ischaemic damage was also similar in vehicle and Ad-GFP treated mice in the cortical ($16 \pm 4\text{mm}^3$ vs. $15 \pm 2\text{mm}^3$, $P > 0.05$) and striatal ($9 \pm 1\text{mm}^3$ vs. $10 \pm 0.5\text{mm}^3$, $P > 0.05$) components of the ischaemic injury. Administration of Ad-APOE significantly reduced the volume of ischaemic damage in comparison to Ad-GFP treated mice in both the cortex ($6 \pm 2\text{mm}^3$ vs. $15 \pm 2\text{mm}^3$, $P = 0.012$) and the striatum ($7 \pm 1\text{mm}^3$ vs. $10 \pm 1\text{mm}^3$, $P = 0.010$). In addition, there was a trend toward smaller areas of ischaemic damage at each coronal level in Ad-APOE treated mice compared to Ad-GFP treated mice. At coronal level three (injection level) the area of ischaemic damage was significantly reduced in Ad-APOE compared to Ad-GFP treated mice ($5 \pm 0.9\text{mm}^2$ vs. $9 \pm 0.5\text{mm}^2$, $P = 0.003$). There was no difference in the area of ischaemic damage between vehicle and Ad-GFP treated mice at the injection level ($P > 0.05$).

The distribution of ischaemic damage predominantly involved the striatum and cerebral cortex (**Table 11**). There was no evidence of ischaemic damage in the hemisphere contralateral to occlusion.

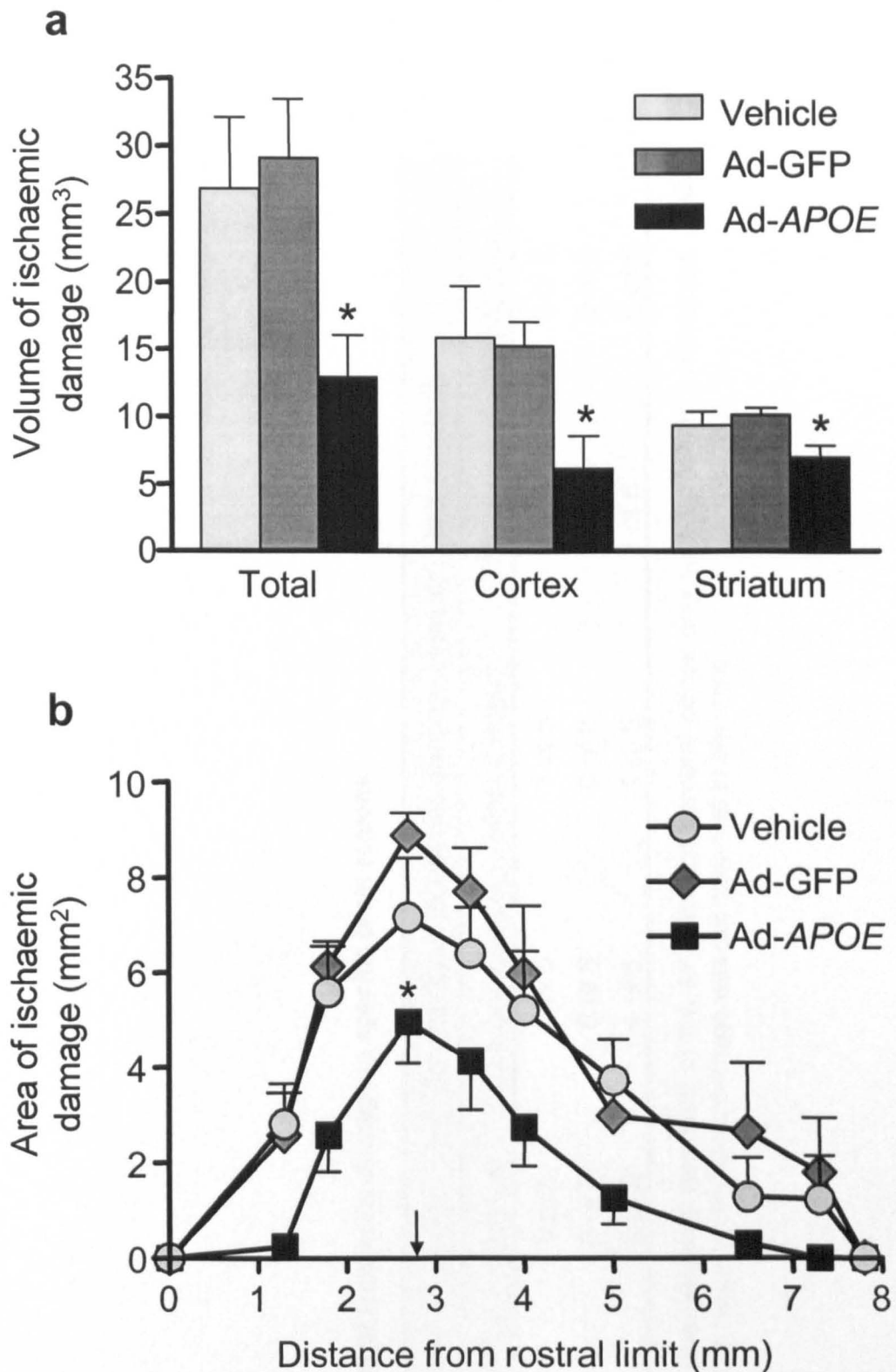


Figure 62. Measurement of ischaemic damage

(a) Administration of *Ad-APOE* significantly reduced the volume of ischaemic damage in the whole hemisphere (total), cerebral cortex and striatum in comparison to *Ad-GFP* treatment. (b) There was a trend toward reduced areas of ischaemic damage in *Ad-APOE* treated mice compared to *Ad-GFP* treated mice at each coronal level. The area of ischaemic damage was significantly reduced at the level of injection in *Ad-APOE* compared to *Ad-GFP* treated mice. * $P < 0.05$ for the comparison between *Ad-GFP* and *Ad-APOE*, one-way ANOVA followed by Student's unpaired *t*-test with Bonferroni correction. Arrow denotes injection level. $n = 5$ (vehicle); $n = 6$ (*Ad-GFP*); $n = 6$ (*Ad-APOE*). Data are presented as mean \pm SEM.

Table 11. Frequency of ischaemic damage in specific brain regions

Treatment	Frequency of ischaemic damage in specific brain regions				
	Striatum	Cerebral cortex	Hippocampus	Thalamus	Hypothalamus
Vehicle	5 of 5	5 of 5	1 of 5	1 of 5	0 of 5
Ad-GFP	6 of 6	6 of 6	0 of 6	1 of 6	0 of 6
Ad-APOE	6 of 6	4 of 6	1 of 6	1 of 6	0 of 6

Ischaemic damage was generally observed in the striatum and cerebral cortex only with infrequent involvement of the hippocampus and thalamus. Hypothalamic damage was not observed in any mice.

6.3.4 Effect of Ad-APOE administration on neurological deficit after focal ischaemia

60min focal ischaemia provoked obvious neurological deficits in all mice except one treated with Ad-APOE in which there was no observable deficit. There was a trend toward a lower neurological deficit score in Ad-APOE treated mice, although this did not reach statistical significance ($P > 0.05$) (Figure 63). There was no association between neurological deficit and the volume of ischaemic damage ($P > 0.05$).

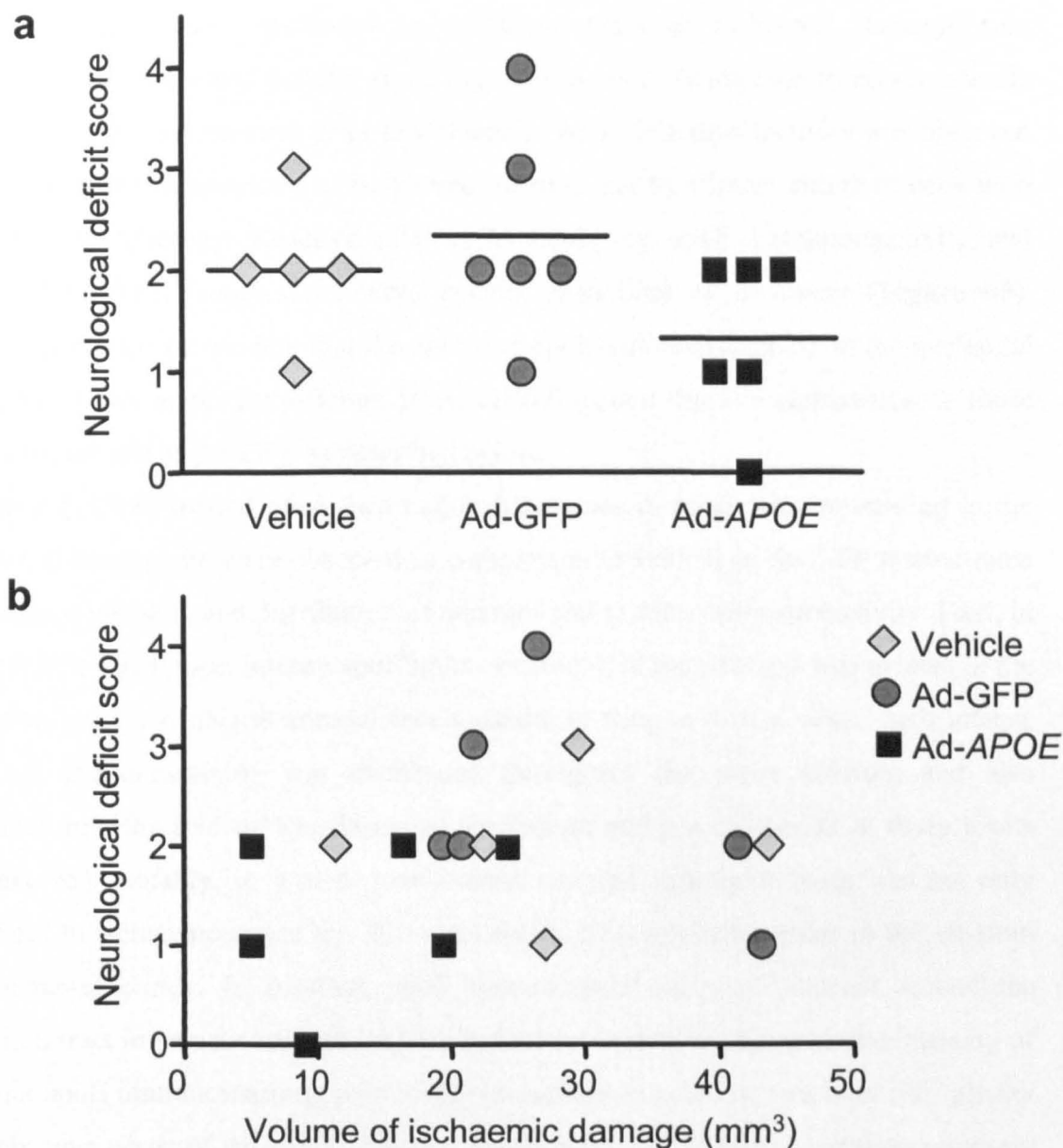


Figure 63. Neurological deficit after focal ischaemia

(a) There was a trend toward a lower neurological deficit score in mice receiving intrastriatal injection of Ad-APOE, however this was not statistically significant ($P > 0.05$, one-way ANOVA). Bars show mean. (b) There was no correlation between neurological deficit and the volume of ischaemic damage ($P > 0.05$, Spearman Rank correlation co-efficient).

6.3.5 Effect of Ad-APOE administration on apoE immunostaining after focal ischaemia

In all mice, in the hemisphere contralateral to injection and occlusion, there was minimal evidence of cellular apoE immunoreactivity regardless of vehicle, Ad-GFP or Ad-APOE treatment (**Figure 64**). ApoE immunoreactivity was present in a few cells with astrocytic morphology and was absent in neurons. Faint apoE immunostaining of the neuropil was observed in the majority of the contralateral hemisphere, including the striatum and cerebral cortex.

In the hemisphere ipsilateral to occlusion, areas of ischaemic damage were associated with increased cellular apoE immunoreactivity (compared to non-ischaemic areas) regardless of treatment prior to ischaemia. ApoE immunoreactivity was observed in cells with the morphology of ischaemic neurons and to a lesser extent in cells with astrocytic morphology. Reactive glial cells displaying apoE immunoreactivity and localised to the injection tract were evident regardless of treatment (**Figure 65**). However, it was also evident that the nature of apoE immunoreactivity in the ipsilateral hemisphere was markedly different in Ad-APOE treated mice in comparison to those receiving vehicle or Ad-GFP as described below.

In Ad-APOE treated mice, two major differences in apoE immunostaining in the ipsilateral hemisphere were observed in comparison to vehicle or Ad-GFP treated mice – increased intensity and distribution of neuropil and cellular immunoreactivity. First, in Ad-APOE treated mice, intense apoE immunostaining of the neuropil was evident at the injection level and also at coronal levels caudal to this. In 4 of 6 mice, such intense neuropil immunostaining was distributed throughout the entire striatum and also extended into the mid to deep layers of the frontal and parietal cortex at these levels (**Figure 65**). Notably, in 3 of 6 mice intense neuropil immunostaining was not only localised to ischaemic tissue but also extended to non-ischaemic tissue in the striatum and cerebral cortex. In contrast, apoE immunoreactivity was localised around the injection tract in vehicle and Ad-GFP treated mice (**Figure 65**). Second, the intensity of cellular apoE immunostaining, particularly in ischaemic neurons, was markedly greater in ischaemic tissue of Ad-APOE treated mice (**Figure 65**). Ischaemic neurons intensely immunoreactive for apoE were observed throughout the rostro-caudal extent of the striatum, including the coronal levels displaying intense neuropil immunoreactivity. Unlike vehicle and Ad-GFP treated mice, in which apoE immunoreactive ischaemic neurons were most apparent at the ischaemic border in the striatum, Ad-APOE treated

mice displayed ischaemic neurons with similarly high apoE immunoreactivity throughout the striatum. In addition, intensely apoE-immunoreactive ischaemic neurons were also visible in the cerebral cortex of some animals, notably in areas with increased neuropil immunoreactivity (**Figure 65**).

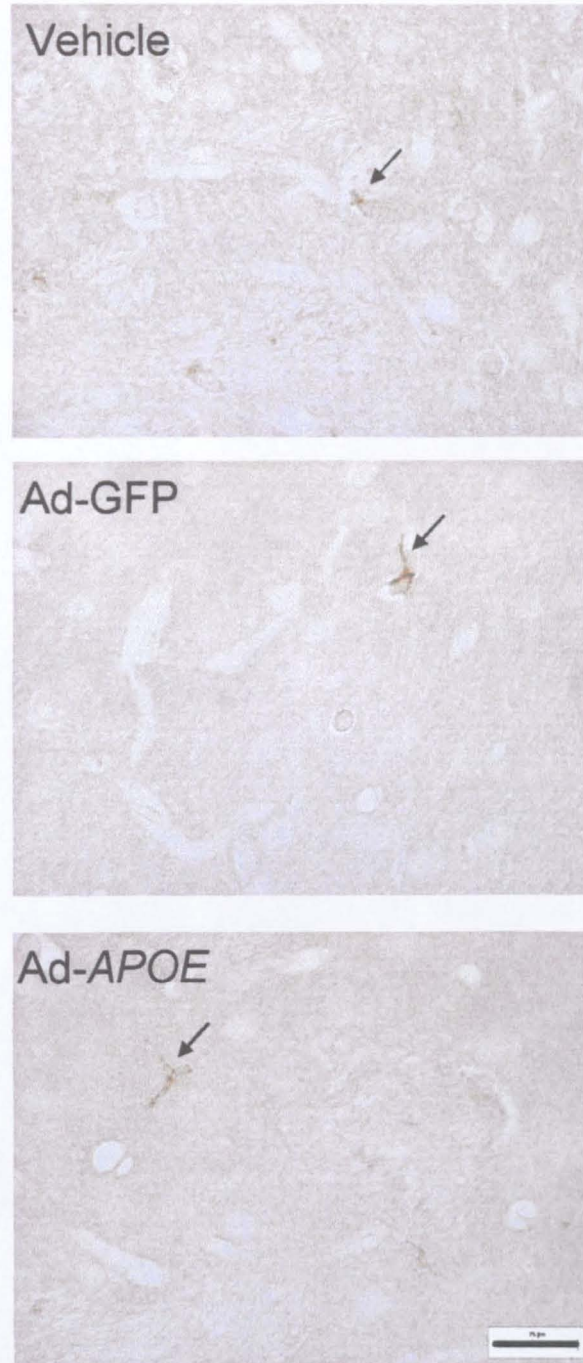


Figure 64. ApoE staining in the contralateral hemisphere after focal ischaemia
In the hemisphere contralateral to occlusion, apoE immunostaining was similar in all groups. Cellular immunostaining was confined to a few scattered apoE immunoreactive glial cells (arrows). In general, faint immunostaining of the neuropil was observed throughout the hemisphere. Photomicrographs show caudate nucleus. Scale bar, 25 μ m.

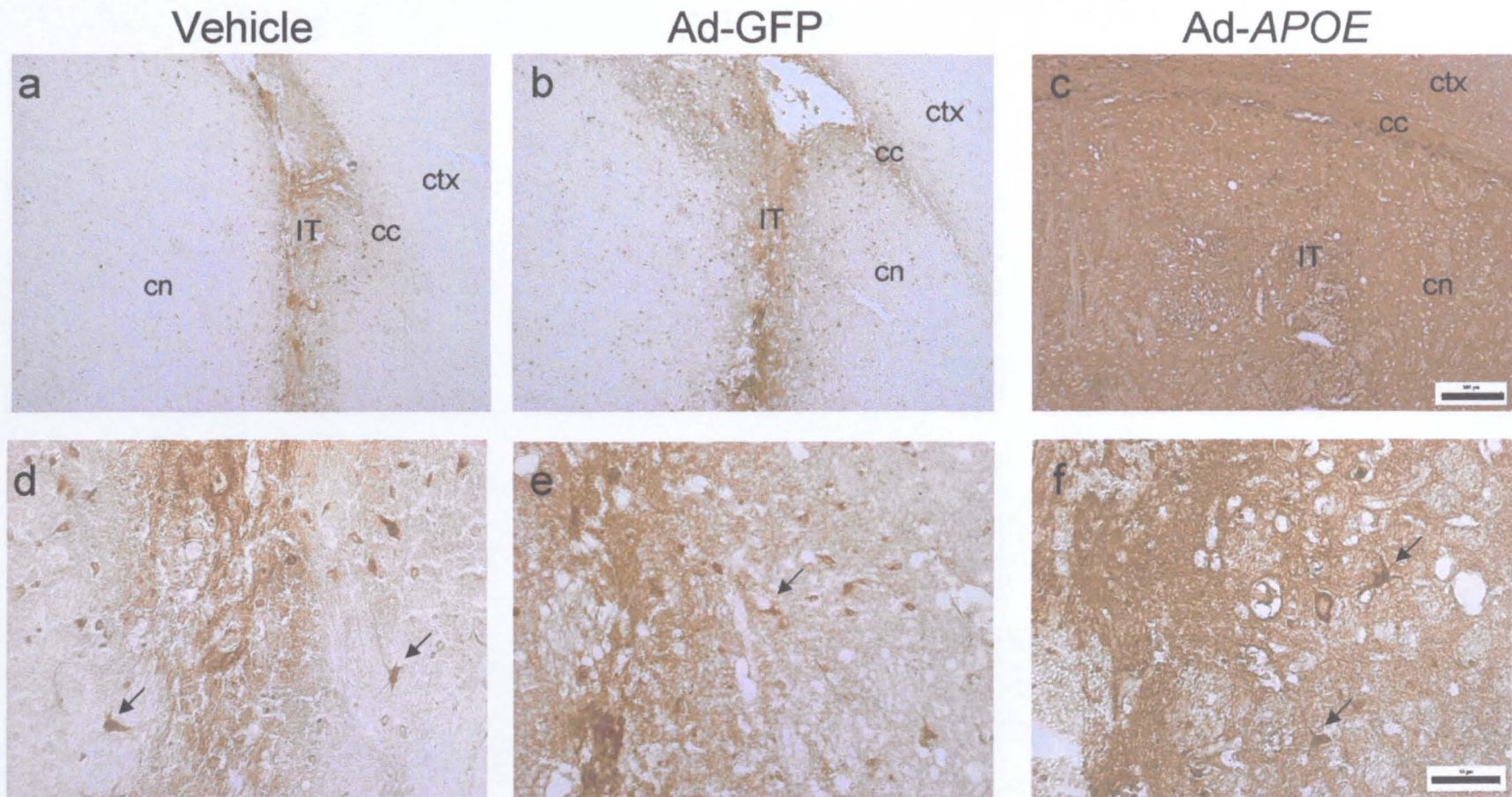


Figure 65. ApoE immunostaining in the ipsilateral hemisphere after focal ischaemia

(a,b) In vehicle and Ad-GFP treated mice, dense neuropil apoE immunoreactivity observed at low magnification was restricted to the injection tract. (c) In contrast, injection of Ad-APOE resulted in dense neuropil apoE distributed throughout the caudate nucleus and extending into the deep layers of the cerebral cortex. (d-f) In each treatment group, a small number of apoE immunoreactive cells with the morphology of reactive glial cells was observed adjacent to the injection tract (arrows). IT, injection tract; cn, caudate nucleus; cc, corpus callosum; ctx, cerebral cortex. Scale bar (a-c), 300 μ m; (d-f), 50 μ m.

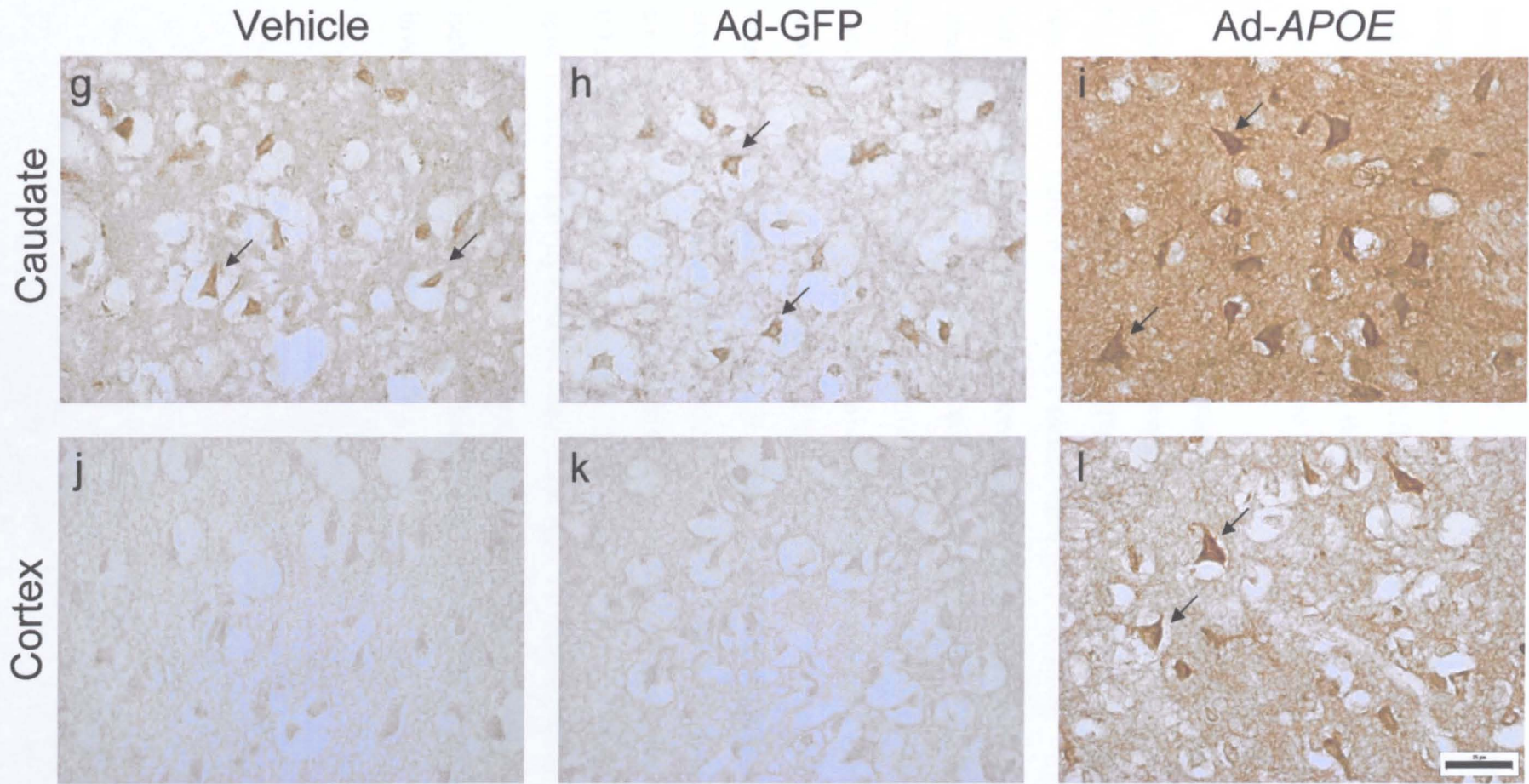


Figure 65 (cont). ApoE immunostaining in the ipsilateral hemisphere after focal ischaemia

(g-i) ApoE immunoreactivity was observed in neurons with ischaemic morphology (arrows) in the caudate nucleus of all mice. The intensity of apoE immunoreactivity was markedly greater in Ad-APOE treated mice (i). (j-k) In the cerebral cortex, minimal or no apoE immunoreactivity was observed in ischaemic neurons of vehicle and Ad-GFP treated mice (j,k), whereas intense immunoreactivity was observed in ischaemic neurons (arrows) of Ad-APOE treated mice (l) in cortical tissue also displaying dense neuropil immunoreactivity. Scale bar, 25µm.

The distribution of intense apoE immunoreactivity was assessed at low magnification (x25). Cellular apoE immunoreactivity was not readily visible at this magnification and therefore intense neuropil apoE immunoreactivity related to vehicle/vector infusion could be differentiated from the apoE response to neuronal damage and quantified accordingly. Borders between areas of intensely immunoreactive neuropil and areas of pallor were readily identifiable therefore facilitating their delineation.

Administration of Ad-*APOE* significantly increased the total volume of intense apoE immunoreactivity in comparison to Ad-GFP treated mice ($5.4 \pm 1.36\text{mm}^3$ vs. $0.6 \pm 0.13\text{mm}^3$, $P = 0.006$) (**Figure 66**). The total volume of intense apoE immunoreactivity was similar in vehicle and Ad-GFP treated mice ($0.9 \pm 0.04\text{mm}^3$ vs. $0.6 \pm 0.13\text{mm}^3$, $P > 0.05$). The volume of apoE immunoreactivity was also similar in vehicle and Ad-GFP treated mice in the cerebral cortex ($0.2 \pm 0.02\text{mm}^3$ vs. $0.1 \pm 0.06\text{mm}^3$, $P > 0.05$) and striatum ($0.7 \pm 0.02\text{mm}^3$ vs. $0.5 \pm 0.12\text{mm}^3$, $P > 0.05$). Administration of Ad-*APOE* significantly increased the volume of apoE immunoreactivity in comparison to Ad-GFP treated mice in both the cortex ($1.1 \pm 0.32\text{mm}^3$ vs. $0.1 \pm 0.06\text{mm}^3$, $P = 0.015$) and the striatum ($4.3 \pm 1.09\text{mm}^3$ vs. $0.5 \pm 0.12\text{mm}^3$, $P = 0.005$) (**Figure 66**). In addition, the area of apoE immunoreactivity was significantly larger in Ad-*APOE* treated mice compared to Ad-GFP treated mice at the level of the injection ($3.5 \pm 0.13\text{mm}^2$ vs. $0.6 \pm 0.11\text{mm}^2$, $P = 0.001$) (**Figure 66**). There was no significant difference in the area of apoE immunoreactivity between vehicle and Ad-GFP treated mice ($P > 0.05$).

In the Ad-*APOE* treated group, there was a trend toward smaller volumes of ischaemic damage in mice with larger volumes of apoE immunoreactivity (i.e. an inverse relationship) (**Appendix J**).

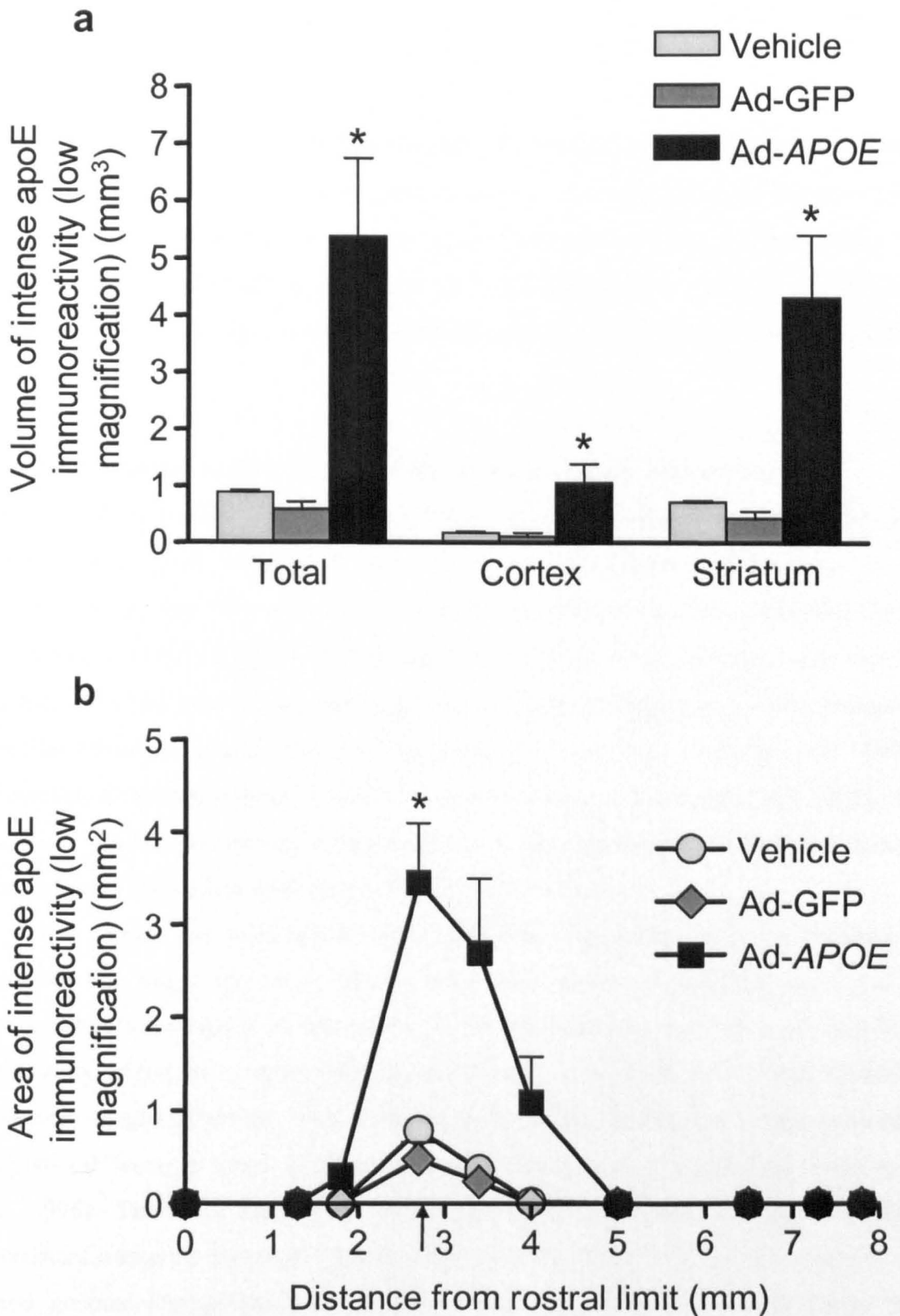


Figure 66. Volumetric measurement of apoE immunoreactivity

(a) Administration of *Ad-APOE* significantly increased the volume of intense apoE immunoreactivity (as observed at low magnification) in the whole hemisphere (total), cerebral cortex and striatum in comparison to *Ad-GFP* treatment. (b) The area of intense apoE immunoreactivity was significantly greater at level of injection in *Ad-APOE* compared to *Ad-GFP* treated mice. * $P < 0.05$ for the comparison between *Ad-GFP* and *Ad-APOE*, one-way ANOVA followed by Student's unpaired *t*-test with Bonferroni correction. Arrow denotes injection level. $n = 5$ (vehicle); $n = 6$ (*Ad-GFP*); $n = 6$ (*Ad-APOE*). Data are presented as mean \pm SEM.

6.4 Discussion

The results from the present study have demonstrated that adenovirus mediated transfer of the human *APOE* $\epsilon 3$ gene to the brain results in markedly increased levels of apoE compared to administration of control vector (Ad-GFP) or vehicle. Furthermore, the present data show that administration of Ad-*APOE* significantly reduced the volume of ischaemic damage by approximately 50% in comparison to treatment with AD-GFP or vehicle.

6.4.1 Adenoviral vector transduction and transgene expression

ApoE (and associated lipids) do not cross the blood-brain barrier and therefore modulation of apoE levels in the brain requires a direct intrathecal approach. In the present study, this was achieved by intrastriatal injection of an adenoviral vector carrying the *APOE* $\epsilon 3$ cDNA. The integrity of adenoviral vector-mediated gene transfer to the brain has been shown previously for a number of genes by demonstration of cellular transduction and transgene expression (*for review see Ooboshi et al., 2003*). However, these studies have utilised first generation adenoviral vectors (E1- and/or E3-deleted). In the present study, gene transfer to the brain was accomplished using a second generation adenoviral vector (E1, E2b, E3 deficient).

This vector has been administered previously by intramuscular or intravenous injection (to target the liver) where it has been shown to promote regression of atherosclerotic pathology in susceptible *APOE*-deficient mice (Harris *et al.*, 2002). In this study, secretion of apoE into the circulation was evident for 70 days following intravenous administration. This contrasts with another study using a first generation adenoviral vector in which apoE expression was evident for 1 month only (Kashyap *et al.*, 1995). The key feature of the second generation vector that is thought to mediate persistent transgene expression in the periphery is the deletion of the E2b region of the viral genome (Amalfitano *et al.*, 1998). Effectively, this removes the trigger that induces a cell-mediated immune response against adenovirally-transduced cells and the potentially antigenic transgene product (Amalfitano *et al.*, 1998; Hu *et al.*, 1999). Prior to the present study, however, there was no information regarding the efficacy of the current vector as a gene transfer agent to the brain. It has been indicated that weaker transgene expression may be a feature of second generation vectors (Dr Andy Baker, personal communication). Accordingly, preliminary experiments (adenoviral

application without subsequent ischaemia) were performed to assess the ability of this vector to mediate transgene expression in the brain.

The ability of the vector to successfully transduce cells in the brain and mediate transgene expression was confirmed in mice treated with an adenoviral vector containing the GFP reporter gene. At the dose of vector used in the focal ischaemia experiments, GFP expression was observed in cells distributed throughout a substantial part of the caudate nucleus and in overlying subcortical white matter. The extent of GFP expression was similar to that observed in previous studies after intrastriatal injection of similar doses of first generation adenoviral vectors (Hermann *et al.*, 2001b; Kilic *et al.*, 2002). It is also possible that additional cells were transduced but not expressing GFP at the time-point examined and therefore the number of GFP expressing cells is likely to under-represent the extent of adenoviral transduction. Cells expressing GFP displayed oligodendrocytic morphology and transduction of this cell type is supported by the observation of numerous GFP expressing cells in subcortical white matter. The present observations are in accordance with both *in vivo* and *in vitro* studies analysing the cellular specificity of adenoviral gene transfer and transgene expression driven by the CMV promoter. Such studies have shown that, although adenoviral vectors transduce both neuronal and non-neuronal cells, transduction of glial cells occurs with greater efficacy (Elshami *et al.*, 1997; Ambar *et al.*, 1999; Hermann *et al.*, 2001b; Kugler *et al.*, 2001). In addition, CMV promoter activity and transgene expression in glial cells may suppress promoter activity in neurons. Transgene expression in cultured hippocampal neurons was evident only if these cells were transduced in the absence of glia (Kugler *et al.*, 2001). In the present study, vectors were injected in the caudate nucleus (neuronal and glial populations present) therefore it is possible that transduction occurred in neurons and glia and that neuronal transgene expression was suppressed resulting in the glial-specific nature of GFP expression.

Immunohistochemical detection of apoE also provided confirmation of vector transduction and transgene expression following Ad-*APOE* administration. At the dose of vector used in the ischaemia experiments, apoE was distributed throughout a large portion of the caudate nucleus, similar to GFP expression. Interestingly, apoE immunoreactivity was predominantly observed in the neuropil. These observations suggest that secretion of apoE occurs after adenoviral transduction and transgene expression, and may result in apoE being found in non-transduced areas, such as the deep layers of the cerebral cortex. In addition, there was evidence of a few apoE

immunoreactive glial cells in the caudate nucleus and in cells of the subcortical white matter displaying similar morphology to those expressing GFP indicating that *APOE* transgene expression is also likely to be glial in origin. It seems unlikely that apoE expression was the result of a response to adenoviral transduction since only minimal apoE immunoreactivity localised to the injection tract was observed after Ad-GFP injection. In support of this, apoE ELISA showed that apoE levels were minimal after Ad-GFP injection and were markedly increased after Ad-*APOE* injection. It is also unlikely that apoE expression was a response to injection-mediated cellular injury since histological damage was minimal in all groups.

6.4.2 Adenoviral vector cytotoxicity

The lack of a significant amount of cellular damage after adenoviral vector injection (without subsequent ischaemia) suggests there were no major direct cytotoxic effects of adenoviral transduction, in particular since areas of tissue containing GFP expressing cells did not display histological damage. Direct cytotoxicity following first generation adenoviral vector transduction has been reported when doses above 10^8 particles were injected into rat brain (Gerdes *et al.*, 2000). Removal of additional viral genes in second generation vectors may attenuate this toxicity by preventing “leaky” expression of viral genes. This is supported by the finding that intracerebral injection of a gutless adenoviral vector, similar to the type used in the present study, resulted in greatly diminished toxicity (and immunogenicity) compared to a first generation vector (Zou *et al.*, 2000). In the present study, tissue and cellular injury is likely to have been the result of mechanical disruption of tissue due to needle penetration, as indicated by the presence of (minimal) damage after vehicle injection.

6.4.3 Neuroprotection by administration of Ad-*APOE*

The present data demonstrate that adenoviral vector-mediated transfer of human *APOE* $\epsilon 3$ was neuroprotective 24h after transient focal ischaemia and indicate the potential for gene transfer of *APOE* to be used as a therapeutic strategy in human stroke. The effects of administration of exogenous apoE have not previously been investigated in focal ischaemia, however the neuroprotective effects observed in the present study are consistent with those reported in a mouse model of transient global ischaemia. Human plasma-derived apoE (of mixed isoform complexed with very low density lipoprotein)

was continuously infused into a lateral ventricle prior, during and after the ischaemic insult and resulted in a reduction in the extent of ischaemic damage in selectively vulnerable regions (Horsburgh *et al.*, 2000b). In another study, neurodegeneration and cognitive impairment in *APOE*-deficient mice was attenuated by intraventricular infusion of recombinant apoE (without lipids) (Masliah *et al.*, 1997). Recombinant apoE and apoE-derived peptides have also been shown to attenuate excitotoxic damage *in vitro* (Aono *et al.*, 2002; Aono *et al.*, 2003). The present results also reinforce the greater neuroprotective effects associated with the apoE3 isoform and are consistent with the results in the previous chapter of this thesis showing that human *APOE* ϵ 3 transgenic mice display less ischaemic damage after focal ischaemia than *APOE* ϵ 4 mice.

Intrastriatal administration of Ad-*APOE* significantly reduced the volume of ischaemic damage in both the striatum and cerebral cortex and by approximately 50% in the whole hemisphere. The preliminary experiments indicated that apoE was probably secreted into the extracellular space following adenoviral transduction. Since apoE is a diffusible molecule it is possible that apoE may be able to act remote to the injection/transduction sites and in this way may facilitate attenuation of the volume of ischaemic tissue. In support of this, neuropil apoE immunoreactivity was distributed throughout a large part of the caudate nucleus and extended into the deep layers of cerebral cortex (including non-ischaemic tissue) after focal ischaemia in Ad-*APOE* treated mice. There was also a trend toward smaller amounts of ischaemic damage in Ad-*APOE* treated mice with greater distribution of apoE immunoreactivity suggesting that increased availability of apoE may promote more robust neuroprotection. However, it cannot be excluded that greater ischaemic damage reduced the pool of apoE by inhibiting transgene expression. Adenoviral transfer of genes encoding other diffusible proteins, such as GDNF and CNTF, to the brain parenchyma also resulted in reductions in infarct volume after focal ischaemia (Kitagawa *et al.*, 1999; Hermann *et al.*, 2001b). Similarly, attenuation of infarct volume after focal ischaemia was achieved by intraventricular application of adenovirus containing the interleukin-1 receptor antagonist gene, facilitating diffusion of the vector via CSF pathways and transgene expression in ependymal cells (Betz *et al.*, 1995; Yang *et al.*, 1997b; Yang *et al.*, 1999). In contrast, viral vector mediated overexpression of intraneuronal proteins that cannot diffuse through brain parenchyma (e.g. Bcl-X_L, Bcl-2, calbindin D28K) have generally

failed to attenuate infarct volume after focal ischaemia, although have protected against neuronal loss in the striatum and infarct margin (Yenari *et al.*, 2001; Kilic *et al.*, 2002; Zhao *et al.*, 2003). Thus, it appears that diffusion of the transgene product or widespread vector transduction may be necessary for global alterations in ischaemic damage.

Two principal explanations are suggested for the neuroprotective effects observed after administration of Ad-*APOE* in the present study, which may not be mutually exclusive. ELISA and immunohistochemical analysis indicated that Ad-*APOE* administration resulted in substantial elevations in the amount of apoE. It is possible that the concentration of available apoE is the key factor in determining the response to acute brain injury. In support of this, the neuroprotective effects observed in a model of global ischaemia followed intraventricular administration of human plasma-derived apoE of mixed isoform (Horsburgh *et al.*, 2000b), although it is likely that apoE was primarily of the E3 isoform since the *APOE* ϵ 3 allele occurs with greatest frequency (~78%) in humans (Davignon *et al.*, 1988). Similarly, intraventricular administration of recombinant apoE3 and apoE4 both reduced cognitive impairment and neuronal degeneration in aged *APOE*-deficient mice (Masliah *et al.*, 1997). In humans, some studies have shown lower plasma and brain levels of apoE in *APOE* ϵ 4 patients with AD (Bertrand *et al.*, 1995; Beffert *et al.*, 1999; Panza *et al.*, 2003) and it has been proposed that *APOE* ϵ 4 carriers are more susceptible to brain injury and disease as a result of reduced levels of apoE (Poirier, 1994). Alternatively, the key factor underlying neuroprotection in the present study may be apoE isoform-related since the gene encoding the “beneficial” apoE3 isoform was administered. As described previously, there is substantial *in vitro* and *in vivo* evidence for the neuroprotective and neurotrophic properties of the apoE3 isoform in the brain that appear to be independent of the level of apoE present. Notably, *APOE* ϵ 4 transgenic mice displayed a poorer outcome after global ischaemia, despite this line of mice having greater levels of apoE than *APOE* ϵ 3 mice (Horsburgh *et al.*, 2000c). In addition, using the same lines of mice for the previous study of this thesis, *APOE* ϵ 4 transgenic mice also demonstrated a poorer outcome after focal ischaemia. Other studies in human tissue have also shown higher levels of CSF-apoE in *APOE* ϵ 4 carriers (in both cognitively normal individuals and patients with AD) (Hesse *et al.*, 2000) suggesting apoE isoform- rather than apoE level-specific effects. It is also conceivable that neuroprotection was mediated by both

mechanisms described above, i.e. increasing levels of apoE by adenoviral administration of the “beneficial” apoE3 isoform. Regardless of the mechanism of neuroprotection, however, the present data indicate the clinical potential of modulating apoE3 levels in acute brain injury.

6.4.4 Inflammatory and immune responses to adenoviral vectors

The need for long-term transgene expression in acute brain injury is perhaps less critical than that required for chronic neurodegenerative conditions such as Alzheimer’s disease. Nonetheless, safe and stable prolonged expression of a therapeutic gene is likely to provide greater benefits for treatment of acute brain injury in the human CNS. For example, in the case of apoE3, which has demonstrated both neuroprotective and neurotrophic effects in experimental brain injury, long-term expression could promote both neuroprotection in the acute phase after injury and regeneration/plasticity over a longer period. Accordingly, the inflammatory and immune response (not assessed in the current study) and degree of cytotoxicity (*section 6.4.2*) provoked by adenoviral administration to the brain have important implications for gene transfer strategies in human acute brain injury. Despite the traditional belief that the brain is an immune-privileged site, there remains the capability for significant inflammatory and immune responses directed against transduced cells, the adenovirus itself and the transgene product, which can limit the duration of transgene expression (Byrnes *et al.*, 1995; Wood *et al.*, 1996). Immunity to adenoviral-mediated gene transfer is believed to comprise an early innate inflammatory and cell-mediated response against transduced cells, followed by a later humoral response (Smith *et al.*, 1997; Kajiwara *et al.*, 2000). Early infiltration of macrophages and release of the pro-inflammatory cytokines IL-1 β , IL-6 and TNF- α have been demonstrated after adenoviral vector application in the brain (Cartmell *et al.*, 1999; Zou *et al.*, 2000). In addition, T- and B-cell activation has been shown after intracerebral injection of first generation adenoviral vectors carrying the β -galactosidase reporter gene (Kajiwara *et al.*, 2000; Zou *et al.*, 2000).

Significantly, second generation vectors have been shown to elicit diminished macrophage and T-cell responses and mediate longer transgene expression (Zou, *et al.*, 2000). Furthermore, second generation vectors can sustain stable and long-term transgene expression even in the presence of an active peripheral immunisation with adenovirus that completely eliminates expression from first generation vectors within

60 days (Thomas *et al.*, 2000). Thus, reduced immunogenicity and minimal cytotoxicity offers promise of safer and more stable gene transfer with second generation adenoviral vectors.

6.4.5 Potential for adenoviral vector administration post-ischaemia

An important consideration in the present study (and previous studies) is that adenoviral application was performed prior to focal ischaemia in order that maximal transgene expression coincided with the onset of ischaemia. Such a scenario is evidently not possible clinically and so it will be necessary to establish if the neuroprotective effects of *APOE* gene transfer are also evident when vectors are administered in the post-ischaemic phase. Encouragingly, adenovirus-mediated GDNF gene transfer immediately after focal ischaemia in rats significantly reduced infarct volume, although when administration was delayed until 1h post-ischaemia the protective effects were lost, indicating a very small therapeutic time window (Zhang *et al.*, 2002).

An important issue to determine is the effect that protein synthesis inhibition, a well established feature of the ischaemic brain (Xie *et al.*, 1989; Mies, 1993; Hermann *et al.*, 2001a), has on the efficacy of gene delivery after the ischaemic insult. At present, it is unclear whether the residual protein synthesis capability would support sufficient levels of transgene expression to promote neuroprotection. It was previously shown that expression of an adenoviral vector reporter transgene (β -gal) delivered 90min after focal ischaemia was inversely related to the severity of cerebral hypoperfusion with a CBF threshold for transgene expression estimated at 40% of the resting value (Ooboshi *et al.*, 2001). Other studies have shown that expression of the β -gal reporter gene is possible, although to a lesser extent than in uninjured brain, when vectors are administered after ischaemic or traumatic insults (Abe *et al.*, 1997b; Abe *et al.*, 1997c; Kochanek *et al.*, 2001a; Zou *et al.*, 2002). It is pertinent to note that neurons contribute most strongly to the total protein synthesis rate of brain tissue and are most susceptible to protein synthesis inhibition after cerebral ischaemia (Thilmann *et al.*, 1986; Widmann *et al.*, 1992; Mies, 1993). Thus, it is possible that adenoviral transduction/transgene expression predominantly in glial cells, as observed in this study, may promote more efficient transgene expression since glial protein synthesis after ischaemia is likely to be less severely inhibited than that in neurons. In the present study, the abundant apoE immunoreactivity observed in Ad-*APOE* treated mice after focal ischaemia suggests

preservation of transgene expression and protein synthesis to a certain degree, at least in glial cells, although the extent to which apoE immunoreactivity represents apoE synthesised prior to the ischaemic insult is unknown.

An additional consideration if vectors are to be administered after the ischaemic insult is the effect of the inflammatory and immune responses induced by the ischaemic insult itself. Increased production of pro-inflammatory cytokines (e.g. IL-1 β , TNF- α) occurs rapidly after cerebral ischaemia and is associated with macrophage infiltration and microglial activation (Feuerstein *et al.*, 1998; Stoll *et al.*, 1998; del Zoppo *et al.*, 2000; Boutin *et al.*, 2001). In view of the role of the inflammatory response in limiting the duration of adenoviral vector transgene expression (*section 6.4.4*), the presence of inflammatory mediators and cells in the ischaemic brain may hamper expression of transgenes introduced during or after the ischaemic insult. Furthermore, the inflammatory response to ischaemia may be compounded by additional reactions caused by vector application (Zou *et al.*, 2002). In this regard, second generation adenoviral vectors administered after TBI in the rat were shown to induce a less pronounced immune response and a longer period of transgene expression (2 months) compared to first-generation vectors, despite the existence of an inflammatory response to TBI and a humoral immune response to the adenovirus (Zou *et al.*, 2002). Anti-inflammatory agents that dampen the inflammatory response to ischaemia may support more effective adenoviral transduction and transgene expression. Interestingly, pre-treatment with the anti-inflammatory agents cyclosporin A or flurbiprofen was shown to attenuate the inflammatory response and fever after adenoviral gene transfer (Geddes *et al.*, 1996; Cartmell *et al.*, 1999; Wilkinson and Euhus, 2001).

6.4.6 Conclusions

In summary, the present study has demonstrated that adenovirus-mediated gene transfer of *APOE* $\epsilon 3$ was neuroprotective in a model of focal cerebral ischaemia and indicates the potential of such an approach for human stroke therapy. The aims stated at the outset of the study have been achieved:

1. adenovirus-mediated gene transfer of *APOE* $\epsilon 3$ substantially increased the levels of apoE in the brain
2. adenovirus-mediated gene transfer of *APOE* $\epsilon 3$ significantly reduced ischaemic brain damage after transient focal ischaemia in mice

Chapter 7

General discussion

7. Human stroke therapy and the therapeutic potential of apoE

Currently, there is no effective treatment for stroke (and other forms of acute brain injury) in widespread use. The only approved method for treatment of acute stroke is thrombolysis, and then only in patients who satisfy stringent criteria for treatment. For the vast majority of stroke patients such intervention is unavailable and, furthermore, in the majority of patients who do meet the criteria, thrombolytic treatment is ineffective (Report of the Stroke Progress Review Group, 2002). In addition, several neuroprotective agents that have proved efficacious in animal models have failed to produce similar results in clinical trials (Green, 2002). The need for novel approaches to the development of stroke treatment is therefore apparent. One reason that has been proposed for the failure to translate pre-clinical promise into clinical success is that most strategies have targeted individual mechanisms that lead to damage (Green, 2000; Leker and Shohami, 2002). For example, blocking excitotoxic-mediated necrotic cell death may only serve to divert cells along an apoptotic pathway (Choi, 1996; Lee *et al.*, 1999). Two strategies for overcoming this problem have been suggested. The first is the use of combination drug therapy with each agent active against a different individual mechanism. In support of this, a number of studies have shown synergistic neuroprotective effects when drug combinations have been used in *in vitro* and *in vivo* models of ischaemia (Schulz *et al.*, 1998; Arias *et al.*, 1999; Schabitz *et al.*, 1999; Chen *et al.*, 2002; Zausinger *et al.*, 2003a; Zausinger *et al.*, 2003b; Culmsee *et al.*, 2004). The second strategy would be to use a single agent active against multiple mechanisms of damage. In this regard, apoE may be a candidate molecule since there is evidence that apoE, in particular the E3 isoform, can counteract the damaging effects of several pathophysiological mechanisms implicated in cerebral ischaemia, including excitotoxicity, oxidative stress, inflammation and apoptosis (*section 1.5*). In support of this, results from this thesis and previous studies suggest that restoring and/or increasing apoE levels can promote neuroprotection in the ischaemic brain.

Increasing apoE levels in the brain would therefore appear to be a tempting strategy to pursue. Several approaches could be used to augment endogenous apoE levels: (1) direct intrathecal administration of apoE in lipid-conjugated form (Horsburgh *et al.*, 2000b) or via viral vector (*chapter 6*); (2) intrathecal or systemic administration of apoE mimetic peptides (that could cross the blood-brain barrier) (Aono *et al.*, 2003); (3) administration of agents that can increase apoE expression levels. A key consideration

of any approach, however, would be the potential systemic side effects of increasing apoE levels given the fundamental role of apoE in lipid and cholesterol homeostasis in the periphery. In this regard, restricting increased apoE expression to the brain would be an important advantage. Since there is no clear evidence that apoE crosses the blood-brain barrier, direct intrathecal administration/viral vector-mediated delivery of apoE could achieve brain-specific increases in apoE. However, even with these approaches, blood-brain barrier disruption in the injured brain could result in leakage of apoE into the systemic circulation. Systemic administration of apoE mimetic peptides (containing the receptor binding region) could traverse the blood-brain barrier, although it is highly likely this approach would have systemic actions.

Another key issue relates to *APOE* polymorphism. Although the precise mechanism(s) responsible for *APOE* genotype-dependent responses to brain injury are not fully understood, there is evidence that differences may be due to beneficial properties of the apoE3 (and apoE2) isoform (that are absent in the apoE4 isoform) but also to direct toxic properties of apoE4 (*section 1.5.4*). These divergent effects of apoE isoforms could preclude development of a single drug that would benefit patients of all *APOE* genotypes. For example, a drug that indiscriminately enhances apoE expression in the brain may be beneficial in *APOE* ϵ 3 (and ϵ 2) carriers (promotes beneficial apoE3/E2 effects) but have mixed effects in *APOE* ϵ 4 carriers (compensates for effects due to apoE4 deficiency but also promotes toxic apoE4 effects). Significantly, in the periphery, increasing apoE levels could have contrasting implications to those in the brain. *APOE* ϵ 4 carriers (who have a lower plasma apoE concentration) may benefit from increased apoE reducing plasma cholesterol and risk of atherosclerosis whereas in *APOE* ϵ 2 carriers (who have a higher apoE concentration) there would be a greater risk of hyperlipoproteinaemia (Mahley and Rall, 2000). Again, this highlights the advantages of restricting the effects of an apoE-based therapeutic approach to the brain.

In view of the above pharmacogenomic issues, specifically enhancing apoE3 effects could be advantageous. This approach was employed in this thesis by indirectly increasing brain apoE3 levels via viral vector administration and resulted in a 50% reduction in ischaemic damage after focal ischaemia. Alternatively, promoting apoE3-specific effects could be achieved by administration of the apoE3 isoform (in protein/mimetic form) alone. It would be interesting to investigate the effects of administration/viral vector mediated expression of apoE3 on the response to cerebral

ischaemia in *APOE* ϵ 4 transgenic mice. Another strategy for specifically promoting the effects of apoE3 over apoE4 is based on the structural differences of these isoforms that are believed to underlie their different biochemical properties (Dong and Weisgraber, 1996; Raffai *et al.*, 2001). Small molecule compounds (e.g. GIND-25, GIND-105) have been discovered that can disrupt apoE4 domain interactions and convert the conformation of apoE4 to apoE3. Significantly, such domain alterations in apoE4 can induce apoE4 to acquire biochemical features akin to those of apoE3 *in vitro* (Xu *et al.*, 2004).

A third consideration with an apoE-based therapeutic approach would be the duration of apoE expression that could be achieved. The ability to mediate prolonged apoE expression after acute brain injury, while less important than in neurodegenerative disease, could provide more long-term benefits than a transient period of expression (although there may also be limitations to high-level long-term apoE expression, *see below*). For example, apoE (particularly apoE3) has been shown to have both neuroprotective and neurotrophic properties, which could promote neuroplasticity and long-term functional recovery. In this regard, a viral vector-mediated *APOE* gene transfer approach, as used in this thesis, would be most suitable. In the uninjured brain, there is evidence that adenoviral-mediated transgene expression can persist for months after administration, even with a subsequent immune challenge against the virus (Thomas *et al.*, 2000). It is unclear as yet if this could be achieved when the vector is administered after an ischaemic insult, although continued improvements in vector design are likely to further reduce the induction of inflammatory and immune responses that can restrict transgene expression.

Conversely, it should be considered that uncontrolled long-term overexpression of apoE could also have deleterious effects in the brain via its putative interactions with A β . It has been proposed that apoE can promote the conversion of diffuse, non-fibrillar A β deposits to the fibrillar form found in neuritic plaques (*for review, see Bales et al., 2002*). Mice that overexpress mutant APP and are *APOE* deficient display substantially less neuritic plaques than mutant APP mice expressing wild-type apoE despite similar brain A β levels, indicating that apoE expression facilitates A β fibrillogenesis and amyloid plaque formation (Bales *et al.*, 1997; Bales *et al.*, 1999; Holtzman *et al.*, 1999; Holtzman *et al.*, 2000a; Holtzman *et al.*, 2000b). This is particularly relevant in stroke therapy since most strokes occur at an advanced age when A β deposition is more

prevalent. Thus, a system to permit regulated apoE expression would have major benefits.

Several systems with the potential to regulate viral vector-mediated transgene expression are being explored and are based on the idea that transgene expression can be regulated by an inducible, co-expressed transcription factor. Induction should be reversible and should not activate other genes. The most widely explored regulation system is based on bacterial tetracycline resistance regulation (Tet system). The bacterial protein, TetR binds to its target DNA, the *tet* operator (*tetO*) only in the absence of tetracycline. Bujard and colleagues (Gossen and Bujard, 1992) engineered TetR and attached it to a eukaryotic transcription activator (tTA). In the presence of tetracycline (or a derivative) tTA cannot bind *tetO* and expression of the transgene, which is downstream of *tetO* is prevented. Conversely, in the absence of tetracycline, transgene expression can be activated. Significantly, the level of transgene expression can also be regulated with this system by modulating the dose of tetracycline administered. Studies have shown that adenoviral vector-mediated temporally controlled transgene expression in the brain can be achieved by incorporation of the Tet system (Harding *et al.*, 1997; Harding *et al.*, 1998; Ralph *et al.*, 2000; Smith-Arica *et al.*, 2000; Block *et al.*, 2003). Furthermore, cell-specific inducible transgene expression has been achieved by expressing Tet elements under the control of the NSE and GFAP promoters (Ralph *et al.*, 2000; Smith-Arica *et al.*, 2000).

Thus, it would seem that, in future, using such systems to temporally, spatially and quantitatively regulate viral vector-mediated apoE overexpression would offer the greatest clinical potential for an apoE-based therapeutic approach in human stroke.

Appendices

Appendix A. Stock solutions

Phosphate buffer (50mM, pH7.4)

10x stock solution

- In 900ml distilled H₂O dissolve:
 - 2.57g sodium dihydrogen orthophosphate (NaH₂PO₄)
 - 11.95g disodium hydrogen orthophosphate (Na₂HPO₄)
- Add 100ml distilled H₂O and pH to 7.4
- Filter and store at 4°C
- Dilute 1:10 in distilled H₂O as required

Phosphate buffered saline (50mM, pH7.4)

10x stock solution

- In 900ml distilled H₂O dissolve:
 - 2.57g sodium dihydrogen orthophosphate (NaH₂PO₄)
 - 11.95g disodium hydrogen orthophosphate (Na₂HPO₄)
 - 86.67g sodium chloride (NaCl)
- Add 100ml distilled H₂O and pH to 7.4
- Filter and store at 4°C
- Dilute 1:10 in distilled H₂O as required

Paraformaldehyde fixative (4%, pH7.4)

- Heat 900ml phosphate buffer to 65°C
- Add 40g paraformaldehyde and maintain temperature at 65°C until completely dissolved
- Add 100ml phosphate buffer and pH to 7.4
- Filter and store at 4°C

Appendix B. Summary of mouse numbers for all experiments

Experiment	Groups	<i>n</i>	Deaths	Excluded*	<i>n</i> for analysis
Chapter 4					
Comparison of 5-0 and 6-0 filament	5-0	5	0	0	5
	6-0	5	0	0	5
Effect of occlusion duration on ischaemic damage	15min	8	0	2	6
	30min	8	1	2	5
	60min	7	2	0	5
Effect of occlusion duration on cerebral blood flow	15min	6	0	0	6
	60min	6	0	0	6
	15min (sham)	4	0	0	4
	60min (sham)	4	0	0	4
Effect of occlusion duration on blood pressure	occlusion	8	0	0	8
	sham	6	0	0	6
Examination of cerebrovascular anatomy		10	0	0	10
Chapter 5					
All experiments	<i>APOE</i> 3	17	2	8	7
	<i>APOE</i> 4	20	2	11	7
Chapter 6					
Characterisation of adenoviral transduction and transgene expression	vehicle	1	0	0	1
	Ad-GFP	3	0	0	3
	Ad- <i>APOE</i>	3	0	0	3
Effect of Ad- <i>APOE</i> administration on outcome and apoE immunostaining after focal ischaemia	vehicle				5
	Ad-GFP				6
	Ad- <i>APOE</i>				6
Effect of Ad- <i>APOE</i> administration on apoE levels	vehicle	2	0	0	2
	Ad-GFP	2	0	0	2
	Ad- <i>APOE</i>	2	0	0	2

*Reasons for excluding mice are given in individual Results chapters.

Appendix C. Control and global ischaemia cohort: clinical details

Controls

	Gender	Age	Clinical event	APOE genotype
1	F	42	mycosis fungoides	2,4
2	M	72	carcinoma of lung/stomach	3,4
3	M	55	stomach lymphoma/pulmonary embolism	3,3
4	M	43	Hodgkin's lymphoma/ventricular failure	3,3
5	F	50	carcinoma of breast	3,3
6	M	47	septicaemia	3,3
7	F	64	carcinoma of breast	3,3
8	M	71	bronchopneumonia	4,4
9	F	69	renal failure	4,4
10	M	56	electrocution	?
11	M	64	hepatic failure	3,3
12	M	63	unknown progressive debilitating disease	3,3
13	F	48	pulmonary oedema	?
14	M	74	cervical myelopathy/cardiac arrest	3,4
15	F	62	volvulus of sigmoid colon	3,3
16	M	45	myocardial infarction	3,3
17	M	57	non-Hodgkin's lymphoma	2,3
18	M	59	bronchopneumonia	3,3
19	F	70	pulmonary thrombo-embolism	3,3
20	F	44	cervical lesion/sudden death	3,3
21	M	20	drug overdose	3,4
22	M	35	bronchopneumonia	2,3
23	M	52	ischaemic heart disease	3,3
24	F	24	pulmonary oedema and congestion	3,3
25	M	82	bronchopneumonia	3,3
26	F	46	septicaemia	3,4
27	M	69	acute cardiac failure	3,3
28	M	33	Crohn's disease/GI tract adenocarcinoma	3,4
29	M	60	carcinoma of lung/pulmonary thrombo-embolism	3,3
30	F	33	sudden cardiac death	3,3
31	M	62	pulmonary congestion and oedema	3,3
32	M	33	acute tracheobronchitis	3,3
33	M	62	rhabdomyolysis-hyperkalaemic cardiac arrest	3,3
34	F	21	septicaemic shock	3,4
35	M	20	inhalation of gastric contents	?
36	F	56	systemic sclerosis/cardiac failure	3,4
37	M	38	congestive cardiac failure	2,4
38	M	18	Hodgkin's lymphoma	3,3

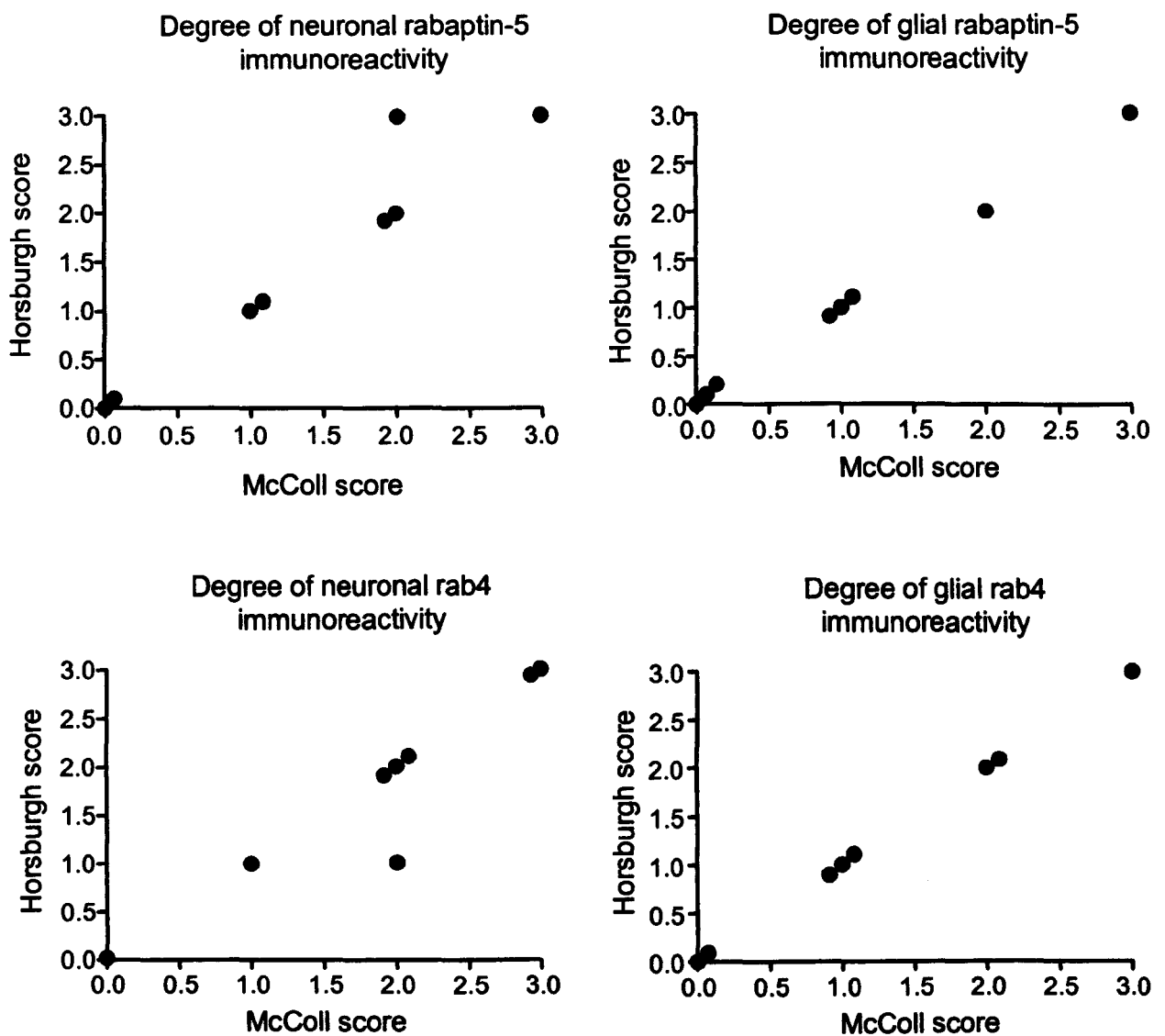
Global ischaemia

	Gender	Age	Survival	Clinical event	APOE genotype
1	F	73	3d	cardiorespiratory arrest	3,3
2	F	21	4d	cardiorespiratory arrest	3,3
3	M	30	2.5d	cardiorespiratory arrest	3,3
4	M	64	4d	arterial occlusion	3,3
5	F	48	6d	cardiorespiratory arrest	3,4
6	F	68	19d	cardiorespiratory arrest	3,3
7	M	17	3d	cardiorespiratory arrest	3,3
8	M	53	10h	cardiorespiratory arrest	3,3
9	F	50	6 weeks	cardiorespiratory arrest	3,3
10	F	50	3d	cardiorespiratory arrest	3,3
11	M	49	18h	cardiorespiratory arrest	3,4
12	M	?	3 months	cardiorespiratory arrest	3,4
13	M	73	<24h	cardiorespiratory arrest	3,3
14	M	66	1d	hypoxia-CA	3,3
15	F	62	1d	cardiorespiratory arrest	2,4
16	M	53	1d	cardiorespiratory arrest	3,4
17	M	46	10d	hypoxia	3,3
18	F	39	4d	cardiorespiratory arrest	3,3
19	M	62	9d	cardiorespiratory arrest	3,3
20	M	54	2d	cardiorespiratory arrest	3,3
21	M	25	2d	bilateral carotid artery occlusion	4,4
22	M	81	34h	cardiorespiratory arrest	3,3
23	M	68	4d	cardiorespiratory arrest	3,4
24	F	37	<1d	cardiorespiratory arrest	3,3
25	F	35	?	hypoxia	3,4
26	M	85	3h	cardiorespiratory arrest	2,3
27	M	43	3d	cardiorespiratory arrest	3,3
28	M	56	1d	cardiorespiratory arrest	2,3
29	F	38	9d	cardiorespiratory arrest	3,4
30	F	53	22d	hypoxia	3,3
31	M	23	5d	hypotension	3,3
32	M	57	10d	hypotension	3,4
33	M	43	24h	hypotension	3,3
34	M	35	36h	cardiorespiratory arrest	3,3
35	M	54	3d	hypoxia/aspiration	3,4
36	M	69	2d	cardiorespiratory arrest	3,3
37	F	62	8d	cardiorespiratory arrest	3,4
38	F	48	1d	asphyxia	3,3
39	M	47	5d	cardiorespiratory arrest	4,4
40	M	65	13d	cardiorespiratory arrest	3,3
41	F	53	36h	cardiorespiratory arrest	3,3 or 2,3
42	F	38	2d	cardiorespiratory arrest	3,4
43	F	23	11h	cardiorespiratory arrest	3,4

Appendix D. Semi-quantification of immunoreactivity in human temporal lobe: validation and reproducibility

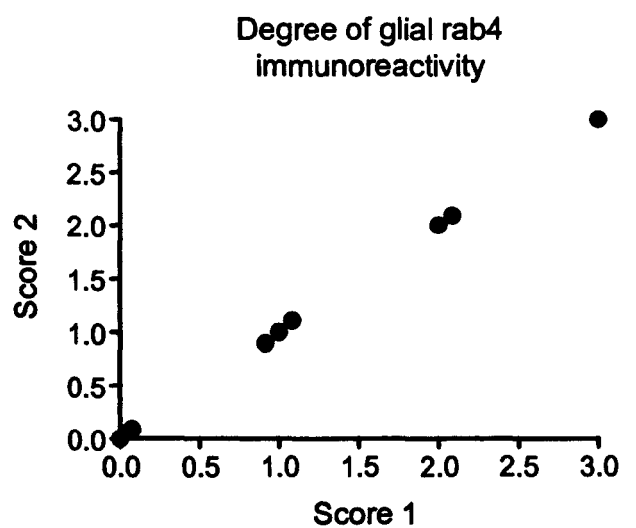
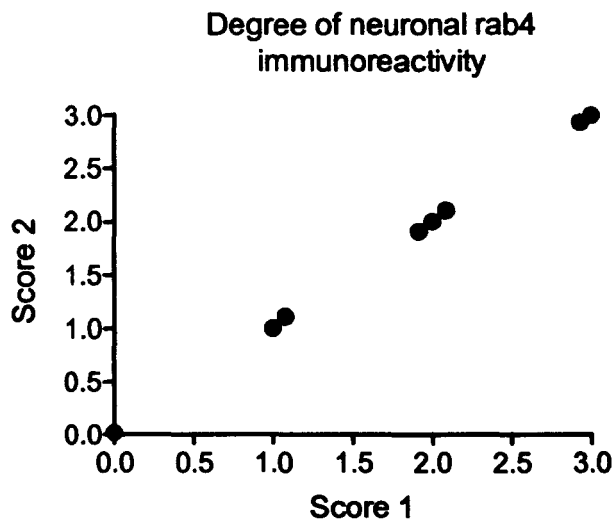
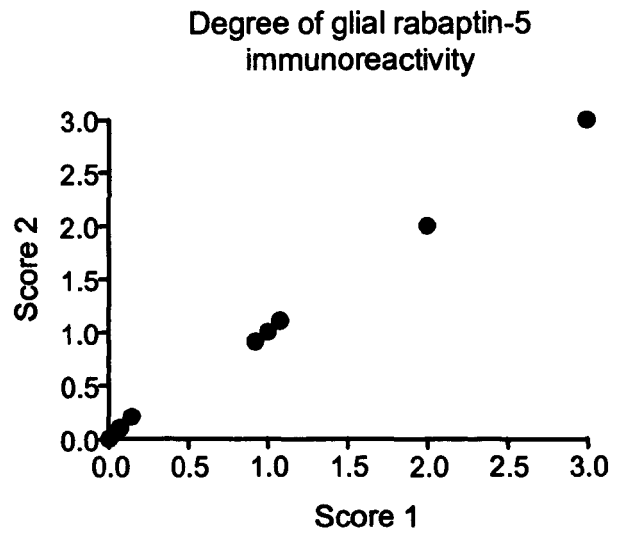
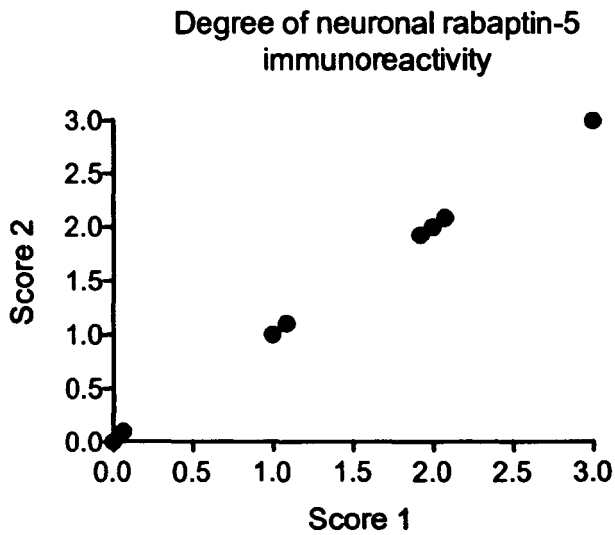
Validation

To validate my semi-quantitative analysis of immunoreactivity, my semi-quantitative scores were compared to scores assigned by Dr Karen Horsburgh who had previously used the same scoring system in this tissue. This showed that my scores were comparable to those obtained by Dr Horsburgh as shown below.



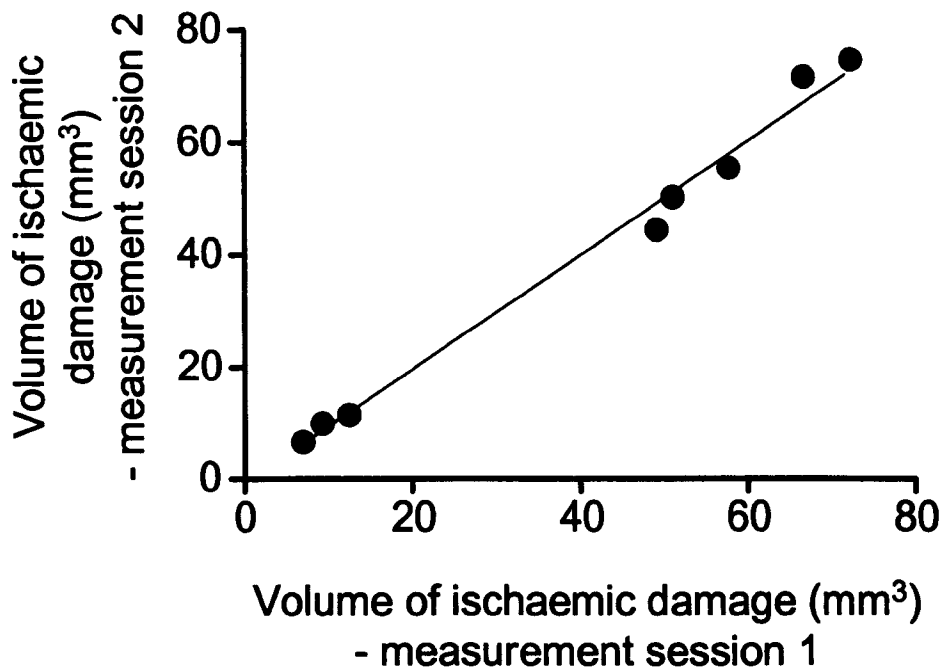
Reproducibility

To test the reproducibility of my semi-quantification, scores were compared from two separate scoring sessions. Semi-quantitative scores were comparable in both sessions indicating consistency in semi-quantification.



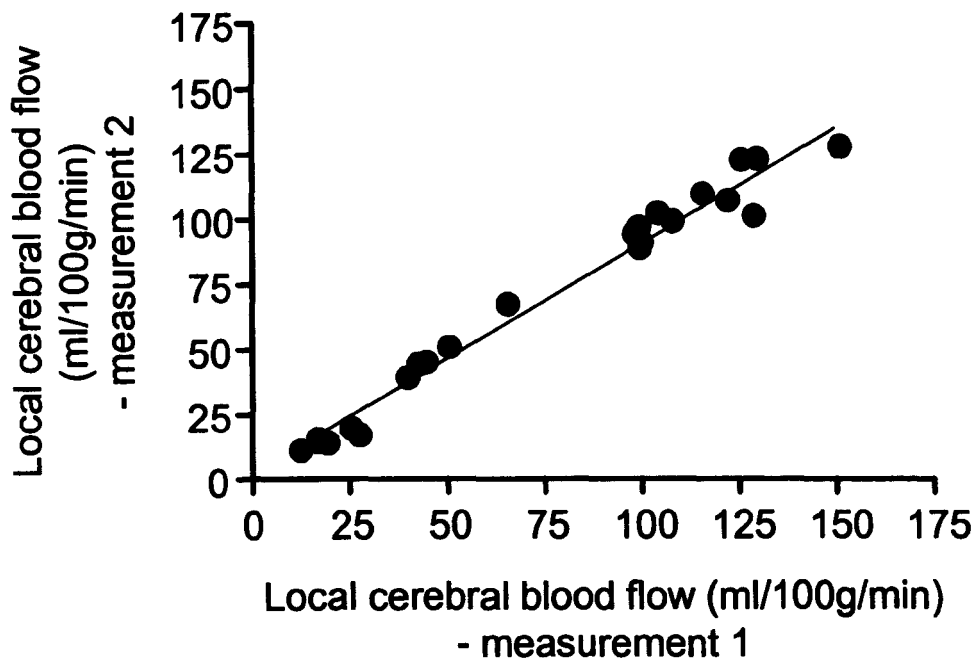
Appendix E. Volumetric measurement of ischaemic damage: reproducibility

Potential errors in quantification of ischaemic damage can arise from several sources: selection of sections at appropriate coronal levels; microscopic identification of areas of ischaemic damage; transcription to line diagrams and image analysis assessment. To test reproducibility (which incorporated all potential sources of error indicated above), the volume of ischaemic damage was measured in C57Bl/6J mice on two separate measurement sessions and compared. As shown below, reproducibility of volumetric measurement on two separate occasions was excellent ($P < 0.001$, $r^2 = 0.99$).



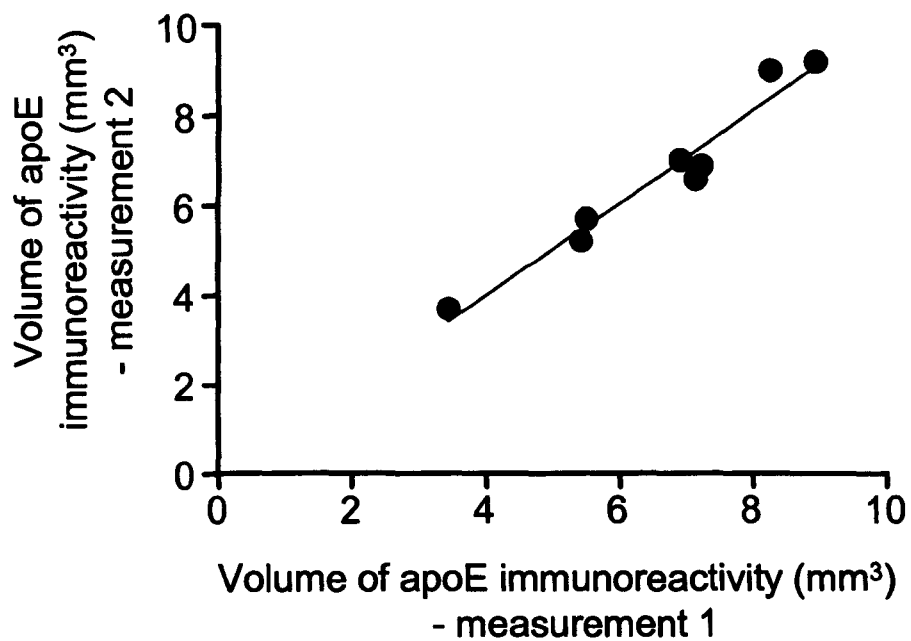
Appendix F. Measurement of local cerebral blood flow: reproducibility

Densitometric measurement is a key component in the quantification of local cerebral blood flow (LCBF) (*see section 2.11.4*). Potential errors in densitometry (e.g. calibration of image analyser, discrimination of anatomical structures) will have a major impact on the calculation of LCBF. To test reproducibility, LCBF was calculated in the 12 neuroanatomical loci ipsilateral and contralateral to occlusion using densitometric measurements of ^{14}C concentration acquired on two separate measurement sessions. As shown below, there was a high level of consistency ($P < 0.001$, $r^2 = 0.97$).



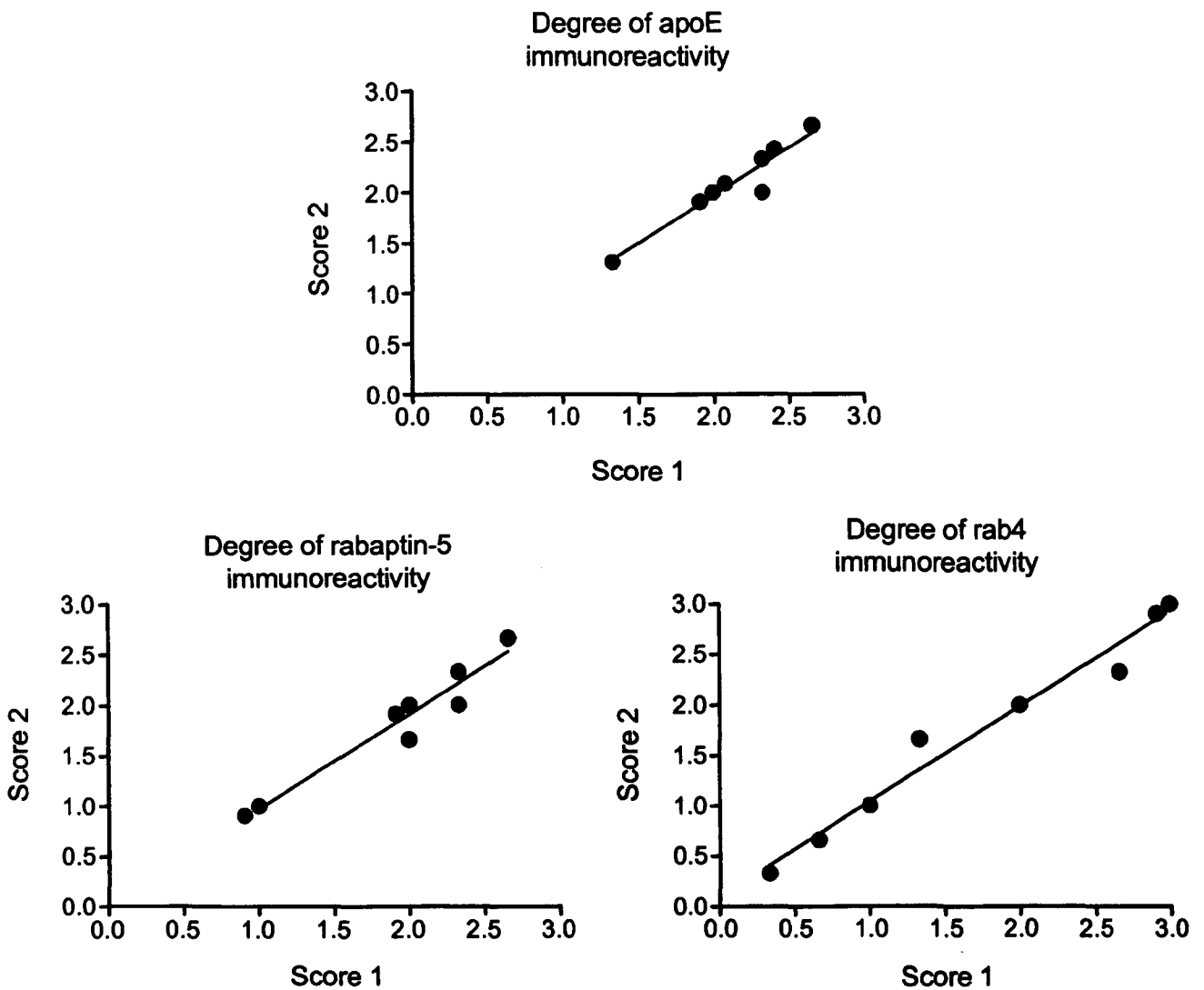
Appendix G. Volumetric measurement of apoE immunostaining in *APOE* transgenic mice: reproducibility

Similar sources of error to those encountered during volumetric measurement of ischaemic damage (*see appendix C*) can also arise during volumetric measurement of apoE immunostaining. To test reproducibility, the volume of apoE immunoreactivity was measured in *APOE* transgenic mice on two separate occasions. As shown below, there was a high level of reproducibility ($P < 0.001$, $r^2 = 0.95$; Pearson correlation)



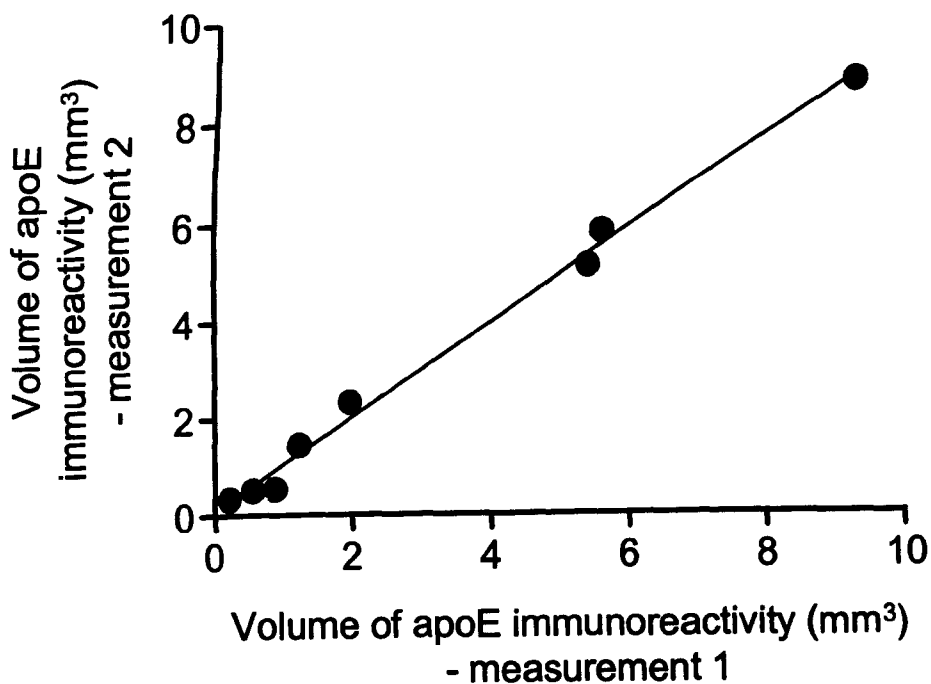
Appendix H. Semi-quantification of immunoreactivity in *APOE* transgenic mice: reproducibility

To test the reproducibility of semi-quantification of apoE, rabaptin-5 and rab4 immunoreactivity, semi-quantification was performed on two separate occasions and scores compared. As indicated below, reproducibility of semi-quantification was excellent for apoE ($P < 0.001$, $r^2 = 0.91$; Pearson correlation), rabaptin-5 ($P < 0.001$, $r^2 = 0.94$; Pearson correlation) and rab4 ($P < 0.001$, $r^2 = 0.97$; Pearson correlation).



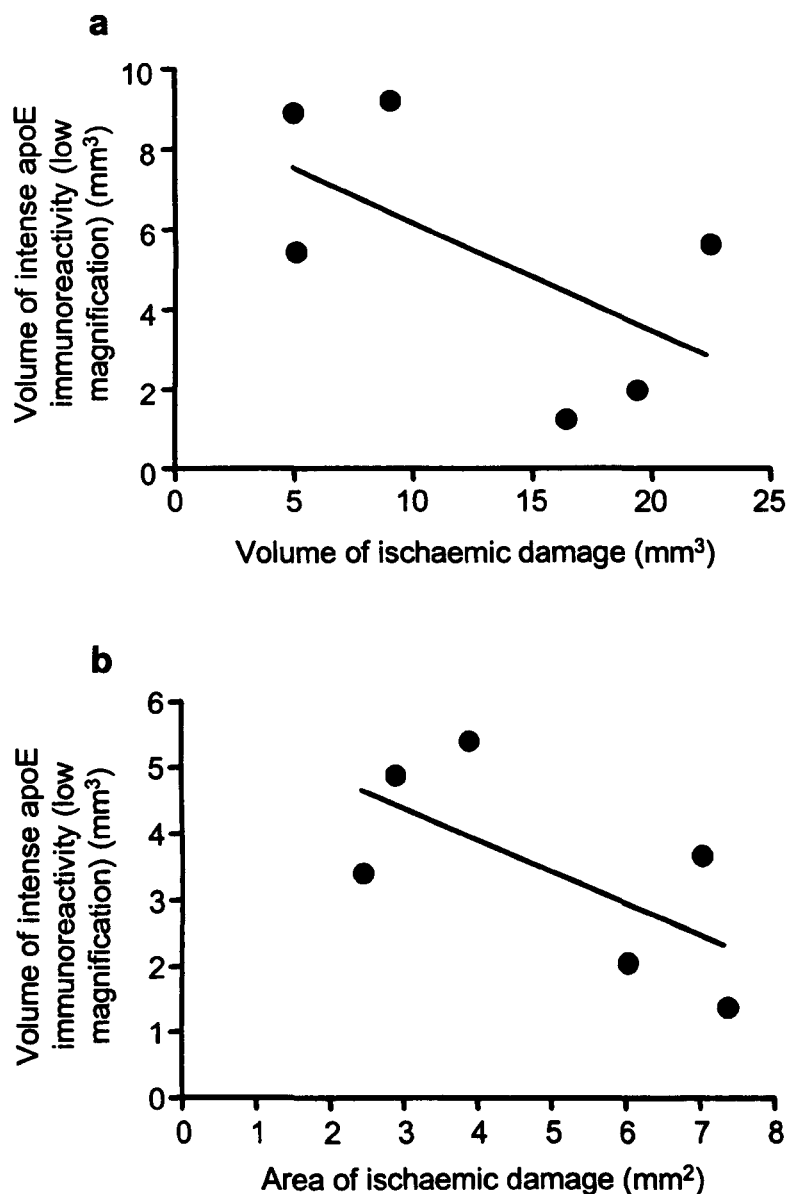
Appendix I. Volumetric measurement of apoE immunostaining after viral vector or vehicle administration: reproducibility

Reproducibility of volumetric measurement of apoE immunostaining was shown previously in *APOE* transgenic mice (see appendix D). However, in chapter 6 volumetric measurement of apoE immunostaining was performed at lower magnification (x25) (see section 6.2.4.5). To test reproducibility, the volume of apoE immunoreactivity determined at low magnification (x25) was measured on two separate occasions. There was a high level of reproducibility ($P < 0.001$, $r^2 = 0.99$; Pearson correlation).



Appendix J. Association between ischaemic damage and apoE immunoreactivity after Ad-APOE administration

Associations between (a) the volume of ischaemic damage and apoE immunoreactivity and (b) the area of ischaemic damage and apoE immunoreactivity at injection level were assessed. There was a trend toward an inverse relationship between the volume or area of ischaemic damage and apoE immunoreactivity. However, it was recognised that there were too few data points (not normally distributed) to test the statistical significance of this relationship.



References

Aarts M, Liu Y, Liu L, Besshoh S, Arundine M, Gurd JW, Wang YT, Salter MW, Tymianski M: Treatment of ischemic brain damage by perturbing NMDA receptor-PSD-95 protein interactions. **Science** 2002, **298**:846-850

Abe K: Therapeutic potential of neurotrophic factors and neural stem cells against ischemic brain injury. **J Cereb Blood Flow Metab** 2000, **20**:1393-1408

Abe K, Hayashi T, Itoyama Y: Amelioration of brain edema by topical application of glial cell line-derived neurotrophic factor in reperfused rat brain. **Neurosci Lett** 1997a, **231**:37-40

Abe K, Setoguchi Y, Hayashi T, Itoyama Y: Dissociative expression of adenoviral-mediated E. coli LacZ gene between ischemic and reperfused rat brains. **Neurosci Lett** 1997b, **226**:53-56

Abe K, Setoguchi Y, Hayashi T, Itoyama Y: In vivo adenovirus-mediated gene transfer and the expression in ischemic and reperfused rat brain. **Brain Res** 1997c, **763**:191-201

Aggerbeck LP, Wetterau JR, Weisgraber KH, Wu CS, Lindgren FT: Human apolipoprotein E3 in aqueous solution. II. Properties of the amino- and carboxyl-terminal domains. **J Biol Chem** 1988, **263**:6249-6258

Akli S, Caillaud C, Vigne E, Stratford-Perricaudet LD, Poenaru L, Perricaudet M, Kahn A, Peschanski MR: Transfer of a foreign gene into the brain using adenovirus vectors. **Nat Genet** 1993, **3**:224-228

Albanese V, Tommasino C, Spadaro A, Tomasello F: A transbasisphenoidal approach for selective occlusion of the middle cerebral artery in rats. **Experientia** 1980, **36**:302-304

Alberts MJ, Graffagnino C, McClenny C, DeLong D, Strittmatter W, Saunders AM, Roses AD: ApoE genotype and survival from intracerebral haemorrhage. **Lancet** 1995, **346**:575

Alberts MJ: Stroke genetics update. **Stroke** 2003, **34**:342-344

Ali SM, Dunn E, Oostveen JA, Hall ED, Carter DB: Induction of apolipoprotein E mRNA in the hippocampus of the gerbil after transient global ischemia. **Brain Res Mol Brain Res** 1996, **38**:37-44

Allan SM, Rothwell NJ: Inflammation in central nervous system injury. **Philos Trans R Soc Lond B Biol Sci** 2003, **358**:1669-1677

Alzheimer A: Über eine eigenartige Erkrankung der Hirnrinde (Concerning a novel disease of the cortex). **Allgemeine Zeitschrift für Psychiatrie Psychisch-Gerichtlich Medizine** 1907, **64**:146-148

Amalfitano A, Hauser MA, Hu H, Serra D, Begy CR, Chamberlain JS: Production and characterisation of improved adenovirus vectors with the E1, E2b, and E3 genes deleted. **J Virol** 1998, **72**:926-933

Ambar BB, Frei K, Malipiero U, Morelli AE, Castro MG, Lowenstein PR, Fontana A: Treatment of experimental glioma by administration of adenoviral vectors expressing Fas ligand. **Hum Gene Ther** 1999, **10**:1641-1648

Aoki K, Uchihara T, Sanjo N, Nakamura A, Ikeda K, Tsuchiya K, Wakayama Y: Increased expression of neuronal apolipoprotein E in human brain with cerebral infarction. **Stroke** 2003, **34**:875-880

Aono M, Lee Y, Grant ER, Zivin RA, Pearlstein RD, Warner DS, Bennett ER, Laskowitz DT: Apolipoprotein E protects against NMDA excitotoxicity. **Neurobiol Dis** 2002, **11**:214-220

Aono M, Bennett ER, Kim KS, Lynch JR, Myers J, Pearlstein RD, Warner DS, Laskowitz DT: Protective effect of apolipoprotein E-mimetic peptides on N-methyl-D-aspartate excitotoxicity in primary rat neuronal-glia cell cultures. **Neuroscience** 2003, **116**:437-445

Arends MJ, Morris RG, Wyllie AH: Apoptosis. The role of the endonuclease. **Am J Pathol** 1990, **136**:593-608

Arends MJ, Wyllie AH: Apoptosis: mechanisms and roles in pathology. **Int Rev Exp Pathol** 1991, **32**:223-254

Arias RL, Tasse JR, Bowlby MR: Neuroprotective interaction effects of NMDA and AMPA receptor antagonists in an in vitro model of cerebral ischemia. **Brain Res** 1999, **816**:299-308

Artiga MJ, Bullido MJ, Frank A, Sastre I, Recuero M, Garcia MA, Lendon CL, Han SW, Morris JC, Vazquez J, Goate A, Valdivieso F: Risk for Alzheimer's disease correlates with transcriptional activity of the APOE gene. **Hum Mol Genet** 1998, **7**:1887-1892

Arundine M, Tymianski M: Molecular mechanisms of calcium-dependent neurodegeneration in excitotoxicity. **Cell Calcium** 2003, **34**:325-337

Astrup J, Symon L, Branston NM, Lassen NA: Cortical evoked potential and extracellular K⁺ and H⁺ at critical levels of brain ischemia. **Stroke** 1977, **8**:51-57

Astrup J, Siesjo BK, Symon L: Thresholds in cerebral ischemia - the ischemic penumbra. **Stroke** 1981, **12**:723-725

Auer RN, Sutherland GR: Hypoxia and related conditions. **Greenfield's Neuropathology**. Edited by Graham DI, Lantos PL. London, Arnold, 2002, pp 233-280

Bacsikai BJ, Xia MQ, Strickland DK, Rebeck GW, Hyman BT: The endocytic receptor protein LRP also mediates neuronal calcium signaling via N-methyl-D-aspartate receptors. **Proc Natl Acad Sci** 2000, **97**:11551-11556

Baethmann A, Eriskat J, Stoffel M, Chapuis D, Wirth A, Plesnila N: Special aspects of severe head injury: recent developments. **Curr Opin Anaesthesiol** 1998, **11**:193-200

Bales KR, Verina T, Dodel RC, Du Y, Altstiel L, Bender M, Hyslop P, Johnstone EM, Little SP, Cummins DJ, Piccardo P, Ghetti B, Paul SM: Lack of apolipoprotein E dramatically reduces amyloid beta-peptide deposition. **Nat Genet** 1997, **17**:263-264

Bales KR, Verina T, Cummins DJ, Du Y, Dodel RC, Saura J, Fishman CE, DeLong CA, Piccardo P, Petegnief V, Ghetti B, Paul SM: Apolipoprotein E is essential for amyloid deposition in the APP(V717F) transgenic mouse model of Alzheimer's disease. **Proc Natl Acad Sci** 1999, **96**:15233-15238

Bales KR, Dodart JC, DeMattos RB, Holtzman DM, Paul SM: Apolipoprotein E, amyloid, and Alzheimer disease. **Mol Interv** 2002, **2**:363-375

Bao F, Arai H, Matsushita S, Higuchi S, Sasaki H: Expression of apolipoprotein E in normal and diverse neurodegenerative disease brain. **J Neuropathol Exp Neurol** 1996, **7**:1733-1739

Barone FC, Knudsen DJ, Nelson AH, Feuerstein GZ, Willette RN: Mouse strain differences in susceptibility to cerebral ischemia are related to cerebral vascular anatomy. **J Cereb Blood Flow Metab** 1993, **13**:683-692

Bassetti C, Bomio F, Mathis J, Hess CW: Early prognosis in coma after cardiac arrest: a prospective clinical, electrophysiological, and biochemical study of 60 patients. **J Neurol Neurosurg Psychiatry** 1996, **61**:610-615

Bederson JB, Pitts LH, Tsuji M, Nishimura MC, Davis RL, Bartkowski H: Rat middle cerebral artery occlusion: evaluation of the model and development of a neurologic examination. **Stroke** 1986, **17**:472-476

Beffert U, Danik M, Krzywkowski P, Ramassamy C, Berrada F, Poirier J: The neurobiology of apolipoproteins and their receptors in the CNS and Alzheimer's disease. **Brain Res Brain Res Rev** 1998, **27**:119-142

Beffert U, Cohn JS, Petit-Turcotte C, Tremblay M, Aumont N, Ramassamy C, Davignon J, Poirier J: Apolipoprotein E and beta-amyloid levels in the hippocampus and frontal cortex of Alzheimer's disease subjects are disease-related and apolipoprotein E genotype dependent. **Brain Res** 1999, **843**:87-94

Belayev L, Zhao W, Busto R, Ginsberg MD: Transient middle cerebral artery occlusion by intraluminal suture: I. Three-dimensional autoradiographic image-analysis of local cerebral glucose metabolism-blood flow interrelationships during ischemia and early recirculation. **J Cereb Blood Flow Metab** 1997, **17**:1266-1280

Belayev L, Busto R, Zhao W, Fernandez G, Ginsberg MD: Middle cerebral artery occlusion in the mouse by intraluminal suture coated with poly-L-lysine: neurological and histological validation. **Brain Res** 1999, **833**:181-190

Benveniste H, Drejer J, Schousboe A, Diemer NH: Elevation of the extracellular concentrations of glutamate and aspartate in rat hippocampus during transient cerebral ischemia monitored by intracerebral microdialysis. **J Neurochem** 1984, **49**:1369-1374

Berr C, Hauw JJ, Delaere P, Duyckaerts C, Amouyel P: Apolipoprotein E allele epsilon 4 is linked to increased deposition of the amyloid beta-peptide (A-beta) in cases with or without Alzheimer's disease. **Neurosci Lett** 1994, **178**:221-224

Bertrand P, Poirier J, Oda T, Finch CE, Pasinetti GM: Association of apolipoprotein E genotype with brain levels of apolipoprotein E and apolipoprotein J (clusterin) in Alzheimer disease. **Brain Res Mol Brain Res** 1995, **33**:174-178

Betz AL, Yang GY, Davidson BL: Attenuation of stroke size in rats using an adenoviral vector to induce overexpression of interleukin-1 receptor antagonist in brain. **J Cereb Blood Flow Metab** 1995, **15**:547-551

Bielenberg GW, Beck T: The effects of dizocilpine (MK-801), phencyclidine, and nimodipine on infarct size 48 h after middle cerebral artery occlusion in the rat. **Brain Res** 1991, **552**:338-342

Bielli A, Thornqvist PO, Hendrick AG, Finn R, Fitzgerald K, McCaffrey MW: The small GTPase Rab4A interacts with the central region of cytoplasmic dynein light intermediate chain-1. **Biochem Biophys Res Commun** 2001, **281**:1141-1153

Biermann V, Volpers C, Hussmann S, Stock A, Kewes H, Schiedne G, Herrmann A, Kochanek S: Targeting of high-capacity adenoviral vectors. **Hum Gene Ther** 2001, **12**:1757-1769

Block A, Puls F, Muller J, Milasinovic D, Igelmann D, Schafer P, Kupfermann N, Schmoldt A, Ameis D, Greten H: Highly suppressible expression of single-chain interleukin-12 by doxycycline following adenoviral infection with a single-vector Tet-regulatory system. **J Gene Med** 2003, **5**:190-200

Borghini I, Barja F, Pometta D, James RW: Characterization of subpopulations of lipoprotein particles isolated from human cerebrospinal fluid. **Biochim Biophys Acta** 1995, **1255**:192-200

- Boschert U, Merlo-Pich E, Higgins G, Roses AD, Catsicas S: Apolipoprotein E expression by neurons surviving excitotoxic stress. **Neurobiol Dis** 1999, **6:508-514**
- Bouma GJ, Muizelaar JP, Stringer WA, Choi SC, Fatouros P, Young HF: Ultra-early evaluation of regional cerebral blood flow in severely head-injured patients using xenon-enhanced computerized tomography. **J Neurosurg** 1992, **77:360-368**
- Boutin H, LeFeuvre RA, Horai R, Asano M, Iwakura Y, Rothwell NJ: Role of IL-1alpha and IL-1beta in ischemic brain damage. **J Neurosci** 2001, **27:5528-5534**
- Boyles JK, Pitas RE, Wilson E, Mahley RW, Taylor JM: Apolipoprotein E associated with astrocytic glia of the central nervous system and with nonmyelinating glia of the peripheral nervous system. **J Clin Invest** 1985, **76:1501-1513**
- Boyles JK, Zoellner CD, Anderson LD, Kosik LM, Pitas RE, Weisgraber KH, Hui DY, Mahley RW, Gebicke-Haerter PJ, Ignatius MJ, Shooter EM: A role for apolipoprotein E, apolipoprotein A-I, and low density lipoprotein receptors in cholesterol transport during regeneration and remyelination of the rat sciatic nerve. **J Clin Invest** 1989, **83:1015-1031**
- Branston NM, Symon L, Crockard HA, Pasztor E: Relationship between the cortical evoked potential and local cortical blood flow following acute middle cerebral artery occlusion in the baboon. **Exp Neurol** 1974, **45:195-208**
- Brecht WJ, Harris FM, Chang S, Tesseur I, Yu GQ, Xu Q, Dee Fish J, Wyss-Coray T, Buttini M, Mucke L, Mahley RW, Huang Y: Neuron-specific apolipoprotein e4 proteolysis is associated with increased tau phosphorylation in brains of transgenic mice. **J Neurosci** 2004, **24:2527-2534**
- Bressler SL, Gray MD, Sopher BL, Hu Q, Hearn MG, Pham DG, Dinulos MB, Fukuchi K, Sisodia SS, Miller MA, Distèche CM, Martin GM: cDNA cloning and chromosome mapping of the human Fe65 gene: interaction of the conserved cytoplasmic domains of the human beta-amyloid precursor protein and its homologues with the mouse Fe65 protein. **Hum Mol Genet** 1996, **5:1589-1598**
- Brinster RL, Chen HY, Trumbauer ME, Yagle MK, Palmiter RD: Factors affecting the efficiency of introducing foreign DNA into mice by microinjecting eggs. **Proc Natl Acad Sci** 1985, **82:4438-4442**
- Brown AW, Brierley JB: Anoxic-ischaemic cell change in rat brain light microscopic and fine-structural observations. **J Neurol Sci** 1972, **16:59-84**
- Brown JL, Moulton RJ, Konasiewicz SJ, Baker AJ: Cerebral oxidative metabolism and evoked potential deterioration after severe brain injury: new evidence of early posttraumatic ischemia. **Neurosurgery** 1998, **42:1057-1063**

Brown MS, Goldstein JL: A receptor-mediated pathway for cholesterol homeostasis. **Science** 1986, 232:34-47

Bu G, Maksymovitch EA, Nerbonne JM, Schwartz AL: Expression and function of the low density lipoprotein receptor-related protein (LRP) in mammalian central neurons. **J Biol Chem** 1994, 269:18521-18528

Bucci C, Parton RG, Mather IH, Stunnenberg H, Simons K, Hoflack B, Zerial M: The small GTPase rab5 functions as a regulatory factor in the early endocytic pathway. **Cell** 1992, 70:715-728

Bullido MJ, Artiga MJ, Recuero M, Sastre I, Garcia MA, Aldudo J, Lendon C, Han SW, Morris JC, Frank A, Vazquez J, Goate A, Valdivieso F: A polymorphism in the regulatory region of APOE associated with risk for Alzheimer's dementia. **Nat Genet** 1998, 18:69-71

Butcher SP, Bullock R, Graham DI, McCulloch J: Correlation between amino acid release and neuropathologic outcome in rat brain following middle cerebral artery occlusion. **Stroke** 1990, 21:1727-1733

Buttini M, Akeefe H, Lin C, Mahley RW, Pitas RE, Wyss-Coray T, Mucke L: Dominant negative effects of apolipoprotein E4 revealed in transgenic models of neurodegenerative disease. **Neuroscience** 2000, 97:207-210

Buttini M, Orth M, Bellosta S, Akeefe H, Pitas RE, Wyss-Coray T, Mucke L, Mahley RW: Expression of human apolipoprotein E3 or E4 in the brains of Apoe^{-/-} mice: isoform-specific effects on neurodegeneration. **J Neurosci** 1999, 19:4867-4880

Byrnes AP, Rusby JE, Wood MJ, Charlton HM: Adenovirus gene transfer causes inflammation in the brain. **Neuroscience** 1995, 66:1015-1024

Byrnes AP, Wood MJ, Charlton HM: Role of T cells in inflammation caused by adenovirus vectors in the brain. **Gene Ther** 1996, 3:644-651

Camarata PJ: "Brain attack": the rationale for treating stroke as a medical emergency. **Neurosurgery** 1994, 34:144-158

Carr FJ, McBride MW, Carswell HVO, Graham D, Strahorn P, Clark JS, Charchar FJ, Dominiczak AF: Genetic aspects of stroke: human and experimental studies. **J Cereb Blood Flow Metab** 2002, 22:767-773

Carroll RC, Beattie EC, von Zastrow M, Malenka RC: Role of AMPA receptor endocytosis in synaptic plasticity. **Nat Rev Neurosci** 2001, 2:315-324

Cartmell T, Southgate T, Rees GS, Castro MG, Lowenstein PR, Luheshi GN: Interleukin-1 mediates a rapid inflammatory response after injection of adenoviral vectors into the brain. **J Neurosci** 1999, 19:1517-1523

Cataldo AM, Barnett JL, Berman SA, Li J, Quarless S, Bursztajn S, Lippa C, Nixon RA: Gene expression and cellular content of cathepsin D in Alzheimer's disease brain: evidence for early up-regulation of the endosomal-lysosomal system. **Neuron** 1995, **14:671-680**

Cataldo AM, Hamilton DJ, Barnett JL, Paskevich PA, Nixon RA: Properties of the endosomal-lysosomal system in the human central nervous system: disturbances mark most neurons in populations at risk to degenerate in Alzheimer's disease. **J Neurosci** 1996, **16:186-199**

Cataldo AM, Barnett JL, Pieroni C, Nixon RA: Increased neuronal endocytosis and protease delivery to early endosomes in sporadic Alzheimer's disease: neuropathologic evidence for a mechanism of increased beta-amyloidogenesis. **J Neurosci** 1997, **17:6142-6151**

Cataldo AM, Peterhoff CM, Troncoso JC, Gomez-Isla T, Hyman BT, Nixon RA: Endocytic pathway abnormalities precede amyloid beta deposition in sporadic Alzheimer's disease and Down syndrome: differential effects of APOE genotype and presenilin mutations. **Am J Pathol** 2000, **157:277-286**

Censori B, Manara O, Agostinis C, Camerlingo M, Casto L, Galavotti B, Partziguian T, Servalli MC, Cesana B, Belloni G, Mamoli A: Dementia after first stroke. **Stroke** 1996, **27:1205-1210**

Chalmers K, Wilcock GK, Love S: APOE epsilon 4 influences the pathological phenotype of Alzheimer's disease by favouring cerebrovascular over parenchymal accumulation of A beta protein. **Neuropathol Appl Neurobiol** 2003, **29:231-238**

Chan PH: Reactive oxygen radicals in signaling and damage in the ischemic brain. **J Cereb Blood Flow Metab** 2001, **21:2-14**

Chan PH, Epstein CJ, Li Y, Huang TT, Carlson E, Kinouchi H, Yang G, Kamii H, Mikawa S, Kondo T, *et al*: Transgenic mice and knockout mutants in the study of oxidative stress in brain injury. **J Neurotrauma** 1995, **12:815-824**

Charriaut-Marlangue C, Margail I, Represa A, Popovici T, Plotkine M, Ben-Ari Y: Apoptosis and necrosis after reversible focal ischemia: an in situ DNA fragmentation analysis. **J Cereb Blood Flow Metab** 1996, **16:186-194**

Chen SD, Lee JM, Yang DI, Nassief A, Hsu CY: Combination therapy for ischemic stroke: potential of neuroprotectants plus thrombolytics. **Am J Cardiovasc Drugs** 2002, **2:303-313**

Chen WJ, Goldstein JL, Brown MS: NPXY, a sequence often found in cytoplasmic tails, is required for coated pit-mediated internalization of the low density lipoprotein receptor. **J Biol Chem** 1990, **265:3116-3123**

Chen Y, Lomnitski L, Michaelson DM, Shohami E: Motor and cognitive deficits in apolipoprotein E-deficient mice after closed head injury. **Neuroscience** 1997, **80**:1255-1262

Chiang M-F, Chang J-G, Hu C-J: Association between apolipoprotein E genotype and outcome of traumatic brain injury. **Acta Neurochir** 2003, **145**:649-654

Choi DW: Calcium-mediated neurotoxicity: relationship to specific channel types and role in ischemic damage. **Trends Neurosci** 1988, **11**:465-469

Choi DW: Ischemia-induced neuronal apoptosis. **Curr Opin Neurobiol** 1996, **6**:667-672

Clark WM, Lessov NS, Dixon MP, Eckenstein F: Monofilament intraluminal middle cerebral artery occlusion in the mouse. **Neurol Res** 1997, **19**:641-648

Connolly ES, Winfree CJ, Stern DM, Solomon RA, Pinsky DJ: Procedural and strain-related variables significantly affect outcome in a murine model of focal cerebral ischemia. **Neurosurgery** 1996, **38**:523-531

Corder EH, Saunders AM, Strittmatter WJ, Schmechel DE, Gaskell PC, Small GW, Roses AD, Haines JL, Pericak-Vance MA: Gene dose of apolipoprotein E type 4 allele and the risk of Alzheimer's disease in late onset families. **Science** 1993, **261**:921-923

Corder EH, Saunders AM, Risch NJ, Strittmatter WJ, Schmechel DE, Gaskell PC, Rimmler JB, Locke PA, Conneally PM, Schmechel KE, *et al*: Protective effect of apolipoprotein E type 2 allele for late onset Alzheimer disease. **Nat Genet** 1994, **7**:180-184

Corder EH, Saunders AM, Strittmatter WJ, Schmechel DE, Gaskell PC, Rimmler JB, Locke PA, Conneally PM, Schmechel KE, Tanzi RE, *et al*: Apolipoprotein E, survival in Alzheimer's disease patients, and the competing risks of death and Alzheimer's disease. **Neurology** 1995, **45**:1323-1328

Coria F, Rubio I, Nunez E, Sempere AP, SantaEngarcia N, Bayon C, Cuadrado N: Apolipoprotein E variants in ischemic stroke. **Stroke** 1995, **26**:2375-2376

Couderc R, Mahieux F, Bailleul S, Fenelon G, Mary R, Fermanian J: Prevalence of apolipoprotein E phenotypes in ischemic cerebrovascular disease. A case-control study. **Stroke** 1993, **24**:661-664

Crawford FC, Vanderploeg RD, Freeman MJ, Singh S, Waisman M, Michaels L, Abdullah L, Warden D, Lipsky R, Salazar A, Mullan MJ: APOE genotype influences acquisition and recall following traumatic brain injury. **Neurology** 2002, **58**:1115-1118

Crutcher KA, Clay MA, Scott SA, Tian X, Tolar M, Harmony JA: Neurite degeneration elicited by apolipoprotein E peptides. **Exp Neurol** 1994, **130**:120-126

- Culmsee C, Junker V, Kremers W, Thal S, Plesnila N, Kriegelstein J: Combination therapy in ischemic stroke: synergistic neuroprotective effects of memantine and clenbuterol. **Stroke** 2004, **35**:1197-1202
- Dampney RA, Coleman MJ, Fontes MA, Hirooka Y, Horiuchi J, Li YW, Polson JW, Potts PD, Tagawa T: Central mechanisms underlying short- and long-term regulation of the cardiovascular system. **Clin Exp Pharmacol Physiol** 2002, **29**:261-268
- Daro E, van der Sluijs P, Galli T, Mellman I: Rab4 and cellubrevin define different early endosome populations on the pathway of transferrin receptor recycling. **Proc Natl Acad Sci** 1996, **93**:9559-9564
- Davignon J, Gregg RE, Sing CF: Apolipoprotein E polymorphism and atherosclerosis. **Arteriosclerosis** 1988, **8**:1-21
- de Hoop MJ, Huber LA, Stenmark H, Williamson E, Zerial M, Parton RG, Dotti CG: The involvement of the small GTP-binding protein Rab5a in neuronal endocytosis. **Neuron** 1994, **13**:11-22
- de Knijff P, Havekes LM: Apolipoprotein E as a risk factor for coronary heart disease: a genetic and molecular biology approach. **Curr Opin Lipidol** 1996, **7**:59-63
- de la Torre JC: Alzheimer disease as a vascular disorder: nosological evidence. **Stroke** 2002, **33**:1152-1162
- de la Torre JC: Is Alzheimer's disease a neurodegenerative or a vascular disorder? Data, dogma, and dialectics. **Lancet Neurol** 2004, **3**:184-190
- DeGirolami U, Crowell RM, Marcoux FW: Selective necrosis and total necrosis in focal cerebral ischemia. Neuropathologic observations on experimental middle cerebral artery occlusion in the macaque monkey. **J Neuropathol Exp Neurol** 1984, **43**:57-71
- Dehouck B, Dehouck MP, Fruchart JC, Cecchelli R: Upregulation of the low density lipoprotein receptor at the blood-brain barrier: intercommunications between brain capillary endothelial cells and astrocytes. **J Cell Biol** 1994, **126**:465-473
- DeKroon RM, Armati PJ: The endosomal trafficking of apolipoprotein E3 and E4 in cultured human brain neurons and astrocytes. **Neurobiol Dis** 2001, **8**:78-89
- DeKroon RM, Mihovilovic M, Goodger ZV, Robinette JB, Sullivan PM, Saunders AM, Strittmatter WJ: ApoE genotype-specific inhibition of apoptosis. **J Lipid Res** 2003, **44**:1566-1573
- del Zoppo G, Ginis I, Hallenbeck JM, Iadecola C, Wang X, Feuerstein GZ: Inflammation and stroke: putative role for cytokines, adhesion molecules and iNOS in brain response to ischemia. **Brain Pathol** 2000, **10**:95-112

DeMattos RB, Thorngate FE, Williams DL: A test of the cytosolic apolipoprotein E hypothesis fails to detect the escape of apolipoprotein E from the endocytic pathway into the cytosol and shows that direct expression of apolipoprotein E in the cytosol is cytotoxic. **J Neurosci** 1999, **19**:2464-2473

Derouesne C, Cambon H, Yelink A, Dnydkaerts C, Hauw JJ: Infarcts in the middle cerebral artery territory. **Acta Neurol Scand** 1993, **87**:361-366

Diaz-Arrastia R, Gong Y, Fair S, Scott KD, Garcia MC, Carlile MC, Agostini MA, Van Ness PC: Increased risk of late posttraumatic seizures associated with inheritance of APOE epsilon4 allele. **Arch Neurol** 2003, **60**:818-822

Dickson DW, Crystal HA, Bevona C, Honer W, Vincent I, Davies P: Correlations of synaptic and pathological markers with cognition of the elderly. **Neurobiol Aging** 1995, **16**:285-304

Dienel GA, Kiessling M, Jacewicz M, Pulsinelli WA: Synthesis of heat shock proteins in rat brain cortex after transient ischemia. **J Cereb Blood Flow Metab** 1986, **6**:505-510

Dik MG, Deeg DJ, Bouter LM, Corder EH, Kok A, Jonker C: Stroke and apolipoprotein E epsilon4 are independent risk factors for cognitive decline: A population-based study. **Stroke** 2000, **31**:2431-2436

Dirnagl U, Pulsinelli W: Autoregulation of cerebral blood flow in experimental focal brain ischemia. **J Cereb Blood Flow Metab** 1990, **10**:327-336

Dirnagl U, Iadecola C, Moskowitz MA: Pathobiology of ischemic stroke: an integrated view. **Trends Neurosci** 1999, **22**:391-397

Dong LM, Weisgraber KH: Human apolipoprotein E4 domain interaction. Arginine 61 and glutamic acid 255 interact to direct the preference for very low density lipoproteins. **J Biol Chem** 1996, **271**:19053-19057

Du C, Hu R, Csernansky CA, Hsu CY, Choi DW: Very delayed infarction after mild focal cerebral ischemia: a role for apoptosis? **J Cereb Blood Flow Metab** 1996, **16**:195-201

Eichner JE, Dunn ST, Perveen G, Thompson DM, Stewart KE, Stroehla BC: Apolipoprotein E polymorphism and cardiovascular disease: a HuGE review. **Am J Epidemiol** 2002, **155**:487-495

Elshami AA, Cook JW, Amin KM, Choi H, Park JY, Coonrod L, Sun J, Molnar-Kimber K, Wilson JM, Kaiser LR, Albelda SM: The effect of promoter strength in adenoviral vectors containing herpes simplex virus thymidine kinase on cancer gene therapy in vitro and in vivo. **Cancer Gene Ther** 1997, **4**:213-221

Elshourbagy NA, Liao WS, Mahley RW, Taylor JM: Apolipoprotein E mRNA is abundant in the brain and adrenals, as well as in the liver, and is present in other peripheral tissues of rats and marmosets. **Proc Natl Acad Sci** 1985, **83:203-207**

Evans MJ: Transgenic rodents. **Animals with novel genes**. Edited by MacLean L. Cambridge, Cambridge University Press, 1994, pp 138-178

Feng Y, Press B, Wandinger-Ness A: Rab 7: an important regulator of late endocytic membrane traffic. **J Cell Biol** 1995, **131:1435-1452**

Feuerstein GZ, Wang X, Barone FC: Inflammatory gene expression in cerebral ischemia and trauma. Potential new therapeutic targets. **Ann N Y Acad Sci** 1997, **825:179-193**

Feuerstein GZ, Wang X, Barone FC: The role of cytokines in the neuropathology of stroke and neurotrauma. **Neuroimmunomodulation** 1998, **5:143-159**

Fielding CJ, Shore VG, Fielding PE: A protein cofactor of lecithin:cholesterol acyltransferase. **Biochim Biophys Res Commun** 1972, **46:1493-1498**

Fitzpatrick MO, Dewar D, Teasdale GM, Graham DI: The neuronal cytoskeleton: an insight for neurosurgeons. **Br J Neurosurg** 1996, **10:483-487**

Fleming LM, Weisgraber KH, Strittmatter WJ, Troncoso JC, Johnson GV: Differential binding of apolipoprotein E isoforms to tau and other cytoskeletal proteins. **Exp Neurol** 1996, **138:252-260**

Fleminger S, Oliver DL, Lovestone S, Rabe-Hesketh S, Giora A: Head injury as a risk factor for Alzheimer's disease: the evidence 10 years on; a partial replication. **J Neurol Neurosurg Psychiatry** 2003, **74:857-862**

Fontes MA, Tagawa T, Polson JW, Cavanagh SJ, Dampney RA: Descending pathways mediating cardiovascular response from dorsomedial hypothalamic nucleus. **Am J Physiol Heart Circ Physiol** 2001, **280:H2891-2901**

Frank A, Diez-Tejedor E, Bullido MJ, Valdivieso F, Barreiro P: APOE genotype in cerebrovascular disease and vascular dementia. **J Neurol Sci** 2002, **204:173-176**

Friedman G, Froom P, Sazbon L, Grinblatt I, Shochina M, Tsenter J, Babaey S, Yehuda B, Groswasser Z: Apolipoprotein E-epsilon4 genotype predicts a poor outcome in survivors of traumatic brain injury. **Neurology** 1999, **52:244-248**

Frikke-Schmidt R, Tybjaerg-Hansen A, Steffensen R, Jensen G, Nordestgaard BG: Apolipoprotein E genotype: epsilon3/epsilon2 women are protected while epsilon3/epsilon3 and epsilon4/epsilon4 men are susceptible to ischemic heart disease: the Copenhagen City Heart Study. **J Am Coll Cardiol** 2000, **35:1192-1199**

Frisoni GB, Bianchetti A, Govoni S, Trabucchi M, Calabresi L, Franceschini G: Association of apolipoprotein E E4 with vascular dementia. **JAMA** 1994a, **271**:1317

Frisoni GB, Calabresi L, Geroldi C, Bianchetti A, D'Acquarica AL, Govoni S, Sirtori CR, Trabucchi M, Franceschini G: Apolipoprotein E epsilon 4 allele in Alzheimer's disease and vascular dementia. **Dementia** 1994b, **5**:240-242

Fujii M, Hara H, Meng W, Vonsattel JP, Huang Z, Moskowitz MA: Strain-related differences in susceptibility to transient forebrain ischemia in SV-129 and C57black/6 mice. **Stroke** 1997, **28**:1805-1810

Fukumoto H, Ingelsson M, Garevik N, Wahlund LO, Nukina N, Yaguchi Y, Shibata M, Hyman BT, Rebeck GW, Irizarry MC: APOE epsilon 3/ epsilon 4 heterozygotes have an elevated proportion of apolipoprotein E4 in cerebrospinal fluid relative to plasma, independent of Alzheimer's disease diagnosis. **Exp Neurol** 2003, **183**:249-253

Garcia JH: A reliable method to occlude a middle cerebral artery in Wistar rats. **Stroke** 1993, **24**:1423

Gavrieli Y, Sherman Y, Ben-Sasson SA: Identification of programmed cell death in situ via specific labeling of nuclear DNA fragmentation. **J Cell Biol** 1992, **119**:493-501

Gearing M, Mirra SS, Hedreen JC, Sumi SM, Hansen LA, Heyman A: The Consortium to Establish a Registry for Alzheimer's Disease (CERAD). Part X. Neuropathology confirmation of the clinical diagnosis of Alzheimer's disease. **Neurology** 1995a, **45**:461-466

Gearing M, Schneider JA, Robbins RS, Hollister RD, Mori H, Games D, Hyman BT, Mirra SS: Regional variation in the distribution of apolipoprotein E and A beta in Alzheimer's disease. **J Neuropathol Exp Neurol** 1995b, **54**:833-841

Geddes BJ, Harding TC, Hughes DS, Byrnes AP, Lightman SL, Conde G, Uney JB: Persistent transgene expression in the hypothalamus following stereotaxic delivery of a recombinant adenovirus: suppression of the immune response with cyclosporin. **Endocrinology** 1996, **137**:5166-5169

Gerdes CA, Castro MG, Lowenstein PR: Strong promoters are the key to highly efficient, noninflammatory and noncytotoxic adenoviral-mediated transgene delivery into the brain in vivo. **Mol Ther** 2000, **2**:330-338

Gerdes LU, Gerdes C, Hansen PS, Klausen IC, Faergeman O, Dyerberg J: The apolipoprotein E polymorphism in Greenland Inuit in its global perspective. **Hum Genet** 1996, **98**:546-550

Ginsberg MD: Adventures in the pathophysiology of brain ischemia: penumbra, gene expression, neuroprotection: the 2002 Thomas Willis Lecture. **Stroke** 2003, **34**:214-223

Glockner F, Meske V, Ohm TG: Genotype-related differences of hippocampal apolipoprotein E levels only in early stages of neuropathological changes in Alzheimer's disease. **Neuroscience** 2002, **114**:1103-1114

Glover CP, Bienemann AS, Heywood DJ, Cosgrave AS, Uney JB: Adenoviral-mediated, high-level, cell-specific transgene expression: a SYN1-WPRE cassette mediates increased transgene expression with no loss of neuron specificity. **Mol Ther** 2002, **5**:509-516

Glover CP, Bienemann AS, Hopton M, Harding TC, Kew JN, Uney JB: Long-term transgene expression can be mediated in the brain by adenoviral vectors when powerful neuron-specific promoters are used. **J Gene Med** 2003, **5**:554-559

Goate A, Chartier-Harlin MC, Mullan M, Brown J, Crawford F, Fidani L, Giuffra L, Haynes A, Irving N, James L, Mant R, Newton P, Rooke K, Roques P, Talbot C, Pericak-Vance M, Roses A, Williamson R, Martin Rossor, Owen M, Hardy J: Segregation of a missense mutation in the amyloid precursor protein gene with familial Alzheimer's disease. **Nature** 1991, **349**:704-706

Golde TE, Estus S, Younkin LH, Selkoe DJ, Younkin SG: Processing of the amyloid protein precursor to potentially amyloidogenic derivatives. **Science** 1992, **255**:728-730

Gomes AR, Correia SS, Carvalho AL, Duarte CB: Regulation of AMPA receptor activity, synaptic targeting and recycling: role in synaptic plasticity. **Neurochem Res** 2003, **28**:1459-1473

Gomez-Isla T, West HL, Rebeck GW, Harr SD, Growdon JH, Locascio JJ, Perls TT, Lipsitz LA, Hyman BT: Clinical and pathological correlates of apolipoprotein E epsilon 4 in Alzheimer's disease. **Ann Neurol** 1996, **39**:62-70

Gonzalez LJ, Scheller RH: Regulation of membrane trafficking: structural insights from a Rab/effector complex. **Cell** 1999, **96**:755-758

Gordon JW, Ruddle FH: Gene transfer into mouse embryos: production of transgenic mice by pronuclear injection. **Methods Enzymol** 1983, **101**:411-433

Gordon JW, Scangos GA, Plotkin DJ, Barbosa JA, Ruddle FH: Genetic transformation of mouse embryos by microinjection of purified DNA. **Proc Natl Acad Sci** 1980, **77**:7380-7384

Gorziglia MI, Lapceovich C, Roy S, Kang Q, Kadan M, Wu V, Pechan P, Kaleko M: Generation of an adenovirus vector lacking E1, e2a, E3, and all of E4 except open reading frame 3. **J Virol** 1999, **73**:6048-6055

Gossen M, Bujard H: Tight control of gene expression in mammalian cells by tetracycline-responsive promoters. **Proc Natl Acad Sci** 1992, **89**:5547-5551

Gotthardt M, Trommsdorff M, Nevitt MF, Shelton J, Richardson JA, Stockinger W, Nimpf J, Herz J: Interactions of the low density lipoprotein receptor gene family with cytosolic adaptor and scaffold proteins suggest diverse biological functions in cellular communication and signal transduction. **J Biol Chem** 2000, **275**:25616-25624

Gournier H, Stenmark H, Rybin V, Lippe R, Zerial M: Two distinct effectors of the small GTPase Rab5 cooperate in endocytic membrane fusion. **EMBO J** 1998, **17**:1930-1940

Graham DI, Adams JH, Doyle D: Ischaemic brain damage in fatal non-missile head injuries. **J Neurol Sci** 1978, **39**:213-234

Graham DI, Ford I, Adams JH, Doyle D, Teasdale GM, Lawrence AE, McLellan DR: Ischaemic brain damage is still common in fatal non-missile head injury. **J Neurol Neurosurg Psychiatry** 1989, **52**:346-350

Graham DI, Gennarelli TA, McIntosh TK: Trauma. **Greenfield's Neuropathology**. Edited by Graham DI, Lantos PL. London, Arnold, 2002, pp 823-898

Green AR: Why do neuroprotective drugs that are so promising in animals fail in the clinic? An industry perspective. **Clin Exp Pharmacol Physiol** 2002, **29**:2030-1034

Greenamyre JT, Olson JM, Penney JBJ, Young AB: Autoradiographic characterization of N-methyl-D-aspartate-, quisqualate- and kainate-sensitive glutamate binding sites. **J Pharmacol Exp Ther** 1985, **233**:254-263

Greenberg SM, Rebeck GW, Vonsattel JP, Gomez-Isla T, Hyman BT: Apolipoprotein E epsilon 4 and cerebral hemorrhage associated with amyloid angiopathy. **Ann Neurol** 1995, **38**:254-259

Greenberg SM, Briggs ME, Hyman BT, Kokoris GJ, Takis C, Kanter DS, Kase CS, Pessin MS: Apolipoprotein E epsilon 4 is associated with the presence and earlier onset of hemorrhage in cerebral amyloid angiopathy. **Stroke** 1996, **27**:1333-1337

Greenberg SM, Vonsattel JP, Segal AZ, Chiu RI, Clatworthy AE, Liao A, Hyman BT, Rebeck GW: Association of apolipoprotein E epsilon2 and vasculopathy in cerebral amyloid angiopathy. **Neurology** 1998, **50**:961-965

Guo Z, Cupples LA, Kurz A, Auerbach SH, Volicer L, Chui H, Green RC, Sadovnick AD, Duara R, DeCarli C, Johnson K, Go RC, Growdon JH, Haines JL, Kukull WA, Farrer LA: Head injury and the risk of AD in the MIRAGE study. **Neurology** 2000, **54**:1316-1323

Guyton JR, Miller SE, Martin ME, Khan WA, Roses AD, Strittmatter WJ: Novel large apolipoprotein E-containing lipoproteins of density 1.006-1.060 g/ml in human cerebrospinal fluid. **J Neurochem** 1998, **70**:1235-1240

Haasdijk ED, Vlug A, Mulder MT, Jaarsma D: Increased apolipoprotein E expression correlates with the onset of neuronal degeneration in the spinal cord of G93A-SOD1 mice. **Neurosci Lett** 2002, **335:29-33**

Haass C, Koo EH, Mellon A, Hung AY, Selkoe DJ: Targeting of cell-surface beta-amyloid precursor protein to lysosomes: alternative processing into amyloid-bearing fragments. **Nature** 1992, **357:500-503**

Hakim AM, Evans AC, Berger L, Kuwabara H, Worsley K, Marchai G, Biel C, Pokrupa R, Diksie M, Meyer E: The effect of nimodipine on the evolution of human cerebral infarction studied by PET. **J Cereb Blood Flow Metab** 1989, **9:523-534**

Hakim AM, Hogan MJ, Carpenter S: Time course of cerebral blood flow and histological outcome after focal cerebral ischemia in rats. **Stroke** 1992, **23:1138-1144**

Hall ED, Oostveen JA, Dunn E, Carter DB: Increased amyloid protein precursor and apolipoprotein E immunoreactivity in the selectively vulnerable hippocampus following transient forebrain ischemia in gerbils. **Exp Neurol** 1995, **135:17-27**

Hamanaka H, Katoh-Fukui Y, Suzuki K, Kobayashi M, Suzuki R, Motegi Y, Nakahara Y, Takeshita A, Kawai M, Ishiguro K, Yokoyama M, Fujita SC: Altered cholesterol metabolism in human apolipoprotein E4 knock-in mice. **Hum Mol Genet** 2000, **9:353-361**

Han SH, Einstein G, Weisgraber KH, Strittmatter WJ, Saunders AM, Pericak-Vance M, Roses AD, Schmechel DE: Apolipoprotein E is localized to the cytoplasm of human cortical neurons: a light and electron microscopic study. **J Neuropathol Exp Neurol** 1994a, **53:535-544**

Han SH, Hulette C, Saunders AM, Einstein G, Pericak-Vance M, Strittmatter WJ, Roses AD, Schmechel DE: Apolipoprotein E is present in hippocampal neurons without neurofibrillary tangles in Alzheimer's disease and in age-matched controls. **Exp Neurol** 1994b, **128:13-26**

Hanlon CS, Rubinsztein DC: Arginine residues at codons 112 and 158 in the apolipoprotein E gene correspond to the ancestral state in humans. **Atherosclerosis** 1995, **112:85-90**

Hara H, Friedlander RM, Gagliardini V, Ayata C, Fink K, Huang Z, Shimizu-Sasamata M, Yuan J, Moskowitz MA: Inhibition of interleukin 1beta converting enzyme family proteases reduces ischemic and excitotoxic neuronal damage. **Proc Natl Acad Sci** 1997, **94:2007-2012**

Harding TC, Geddes BJ, Noel JD, Murphy D, Uney JB: Tetracycline-regulated transgene expression in hippocampal neurones following transfection with adenoviral vectors. **J Neurochem** 1997, **69:2620-2623**

Harding TC, Geddes BJ, Murphy D, Knight D, Uney JB: Switching transgene expression in the brain using an adenoviral tetracycline-regulatable system. **Nat Biotechnol** 1998, 16:553-555

Harris JD, Graham IR, Schepelmann S, Stannard AK, Roberts ML, Hodges BL, Hill VJ, Amalfitano A, Hassall DG, Owen JS, Dickson G: Acute regression of advanced and retardation of early aortic atheroma in immunocompetent apolipoprotein-E (apoE) deficient mice by administration of a second generation [E1(-), E3(-), polymerase(-)] adenovirus vector expressing human apoE. **Hum Mol Gen** 2002, 11:43-58

Hata R, Mies G, Wiessner C, Fritze K, Hesselbarth D, Brinker G, Hossmann K-A: A reproducible model of middle cerebral artery occlusion in mice: hemodynamic, biochemical, and magnetic resonance imaging. **J Cereb Blood Flow Metab** 1998, 18:367-375

Hayashi T, Abe K, Itoyama Y: Reduction of ischemic damage by application of vascular endothelial growth factor in rat brain after transient ischemia. **J Cereb Blood Flow Metab** 1998, 18:887-895

Heeren J, Grewal T, Jackle S, Beisiegel U: Recycling of apolipoprotein E and lipoprotein lipase through endosomal compartments in vivo. **J Biol Chem** 2001, 276:42333-42338

Heiss WD: Flow thresholds of functional and morphological damage of brain tissue. **Stroke** 1983, 14:329-331

Heiss WD, Hayakawa T, Waltz AG: Cortical neuronal function during ischemia. Effects of occlusion of one middle cerebral artery on single-unit activity in cats. **Arch Neurol** 1976, 33:813-820

Heiss WD, Kracht LW, Thiel A, Grond M, Pawlik G: Penumbra probability thresholds of cortical flumazenil binding and blood flow predicting tissue outcome in patients with cerebral ischaemia. **Brain** 2001, 124:20-29

Hendriks L, van Duijn CM, Cras P, Cruts M, Van Hul W, van Harskamp F, Warren A, McInnis MG, Antonarakis SE, Martin JJ, al. e: Presenile dementia and cerebral haemorrhage linked to a mutation at codon 692 of the beta-amyloid precursor protein gene. **Nat Genet** 1992, 1:218-221

Henon H, Pasquier F, Durieu I, Godefroy O, Lucas C, Lebert F, Leys D: Preexisting dementia in stroke patients. Baseline frequency, associated factors, and outcome. **Stroke** 1997, 28:2429-2436

Hermann DM, Kilic E, Hata R, Hossmann KA, Mies G: Relationship between metabolic dysfunctions, gene responses and delayed cell death after mild focal cerebral ischemia in mice. **Neuroscience** 2001a, 404:947-955

Hermann DM, Kilic E, Kugler S, Isenmann S, Bahr M: Adenovirus-mediated GDNF and CNTF pretreatment protects against striatal injury following transient middle cerebral artery occlusion in mice. **Neurobiol Dis** 2001b, 8:655-666

Herz J: Lipoprotein receptors: beacons to neurons? **Trends Neurosci** 2001a, 24:193-195

Herz J: The LDL receptor gene family: (un)expected signal transducers in the brain. **Neuron** 2001b, 29:571-581

Herz J, Beffert U: Apolipoprotein E receptors: linking brain development and Alzheimer's disease. **Nat Rev Neurosci** 2000, 1:51-58

Herz J, Bock HH: Lipoprotein receptors in the nervous system. **Annu Rev Biochem** 2002, 71:405-434

Herz J, Strickland DK: LRP: a multifunctional scavenger and signaling receptor. **J Clin Invest** 2001, 108:779-784

Herz J, Hamann U, Rogne S, Myklebost O, Gausepohl H, Stanley KK: Surface location and high affinity for calcium of a 500-kd liver membrane protein closely related to the LDL-receptor suggest a physiological role as lipoprotein receptor. **EMBO J** 1988, 7:4119-4127

Herz J, Clouthier DE, Hammer RE: LDL receptor-related protein internalizes and degrades uPA-PAI-1 complexes and is essential for embryo implantation. **Cell** 1992, 71:411-421

Hesse C, Larsson H, Fredman P, Minthon L, Andreasen N, Davidsson P, Blennow K: Measurement of apolipoprotein E (apoE) in cerebrospinal fluid. **Neurochem Res** 2000, 25:511-517

Hiesberger T, Trommsdorff M, Howell BW, Goffinet A, Mumby MC, Cooper JA, Herz J: Direct binding of Reelin to VLDL receptor and ApoE receptor 2 induces tyrosine phosphorylation of disabled-1 and modulates tau phosphorylation. **Neuron** 1999, 24:481-489

Hixson JE: Apolipoprotein E polymorphisms affect atherosclerosis in young males. Pathobiological Determinants of Atherosclerosis in Youth (PDAY) Research Group. **Arterioscler Thromb** 1991, 11:1237-1234

Hof PR, Young WG, Bloom FE, Belichenko PV, Celio MR: **Comparative Cytoarchitectonic Atlas of the C57BL/6 and 129/Sv Mouse Brains**. Amsterdam, Elsevier Science B.V., 2000

Holtzman DM, Bales KR, Wu S, Bhat P, Parsadanian M, Fagan AM, Chang LK, Sun Y, Paul SM: Expression of human apolipoprotein E reduces amyloid-beta deposition in a mouse model of Alzheimer's disease. **J Clin Invest** 1999, **103**:R15-R21

Holtzman DM, Bales KR, Tenkova T, Fagan AM, Parsadanian M, Sartorius LJ, Mackey B, Olney J, McKeel D, Wozniak D, Paul SM: Apolipoprotein E isoform-dependent amyloid deposition and neuritic degeneration in a mouse model of Alzheimer's disease. **Proc Natl Acad Sci** 2000a, **97**:2892-2897

Holtzman DM, Fagan AM, Mackey B, Tenkova T, Sartorius L, Paul SM, Bales K, Ashe KH, Irizarry MC, Hyman BT: Apolipoprotein E facilitates neuritic and cerebrovascular plaque formation in an Alzheimer's disease model. **Ann Neurol** 2000b, **47**:739-747

Horie Y, Fazio S, Westerlund JR, Weisgraber KH, Rall SC: The functional characteristics of a human apolipoprotein E variant (cysteine at residue 142) may explain its association with dominant expression of type III hyperlipoproteinemia. **J Biol Chem** 1992, **267**:1962-1968

Horn M, Schlote W: Delayed neuronal death and delayed neuronal recovery in the human brain following global ischemia. **Acta Neuropathol (Berl)** 1992, **85**:79-87

Horsburgh K, Nicoll JA: Selective alterations in the cellular distribution of apolipoprotein E immunoreactivity following transient cerebral ischaemia in the rat. **Neuropathol Appl Neurobiol** 1996, **22**:342-349

Horsburgh K, Fitzpatrick M, Nilsen M, Nicoll JA: Marked alterations in the cellular localisation and levels of apolipoprotein E following acute subdural haematoma in rat. **Brain Res** 1997, **763**:103-110

Horsburgh K, Graham DI, Stewart J, Nicoll JA: Influence of apolipoprotein E genotype on neuronal damage and apoE immunoreactivity in human hippocampus following global ischemia. **J Neuropathol Exp Neurol** 1999a, **58**:227-234

Horsburgh K, Kelly S, McCulloch J, Higgins GA, Roses AD, Nicoll JA: Increased neuronal damage in apolipoprotein E-deficient mice following global ischaemia. **Neuroreport** 1999b, **10**:837-841

Horsburgh K, McCarron MO, White F, Nicoll JA: The role of apolipoprotein E in Alzheimer's disease, acute brain injury and cerebrovascular disease: evidence of common mechanisms and utility of animal models. **Neurobiol Aging** 2000a, **21**:245-255

Horsburgh K, McCulloch J, Nilsen M, McCracken E, Large C, Roses AD, Nicoll JA: Intraventricular infusion of apolipoprotein E ameliorates acute neuronal damage after global cerebral ischemia in mice. **J Cereb Blood Flow Metab** 2000b, **20**:458-462

Horsburgh K, McCulloch J, Nilsen M, Roses AD, Nicoll JA: Increased neuronal damage and apoE immunoreactivity in human apolipoprotein E, E4 isoform-specific, transgenic mice after global cerebral ischaemia. **Eur J Neurosci** 2000c, 12:4309-4317

Houlden H, Crook R, Backhovens H, Prihar G, Baker M, Hutton M, Rossor M, Martin JJ, Van Broeckhoven C, Hardy J: ApoE genotype is a risk factor in nonpresenilin early-onset Alzheimer's disease families. **Am J Med Genet** 1998, 81:117-121

Howell BW, Hawkes R, Soriano P, Cooper JA: Neuronal position in the developing brain is regulated by mouse disabled-1. **Nature** 1997, 389:733-737

Hsu SM, Raine L, Fanger H: The use of antiavidin antibody and avidin-biotin-peroxidase complex in immunoperoxidase technics. **Am J Clin Pathol** 1981, 75:816-821

Hu H, Serra D, Amalfitano A: Persistence of an [E1-, polymerase-] adenovirus vector despite transduction of a neoantigen into immune-competent mice. **Hum Gene Ther** 1999, 10:355-364

Huang DY, Goedert M, Jakes R, Weisgraber KH, Garner CC, Saunders AM, Pericak-Vance MA, Schmechel DE, Roses AD, Strittmatter WJ: Isoform-specific interactions of apolipoprotein E with the microtubule-associated protein MAP2c: implications for Alzheimer's disease. **Neurosci Lett** 1994a, 182:55-58

Huang J, Kim LJ, Poisik A, Pinsky DJ, Connolly ES: Does poly-L-lysine coating of the middle cerebral artery occlusion suture improve infarct consistency in a murine model? **J Stroke Cerebrovasc Disorders** 1998, 7:296-30

Huang Y, von Eckardstein A, Wu S, Maeda N, Assmann G: A plasma lipoprotein containing only apolipoprotein E and with gamma mobility on electrophoresis releases cholesterol from cells. **Proc Natl Acad Sci** 1994b, 91:1834-1838

Huang Y, Liu XQ, Wyss-Coray T, Brecht WJ, Sanan DA, Mahley RW: Apolipoprotein E fragments present in Alzheimer's disease brains induce neurofibrillary tangle-like intracellular inclusions in neurons. **Proc Natl Acad Sci** 2001, 98:8838-8843

Ignatius MJ, Gebicke-Harter PJ, Skene JH, Schilling JW, Weisgraber KH, Mahley RW, Shooter EM: Expression of apolipoprotein E during nerve degeneration and regeneration. **Proc Natl Acad Sci** 1986, 83:1125-1129

Ignatius MJ, Gebicke-Harter PJ, Pitas RE, Shooter EM: Apolipoprotein E in nerve injury and repair. **Prog Brain Res** 1987a, 71:177-184

Ignatius MJ, Shooter EM, Pitas RE, Mahley RW: Lipoprotein uptake by neuronal growth cones in vitro. **Science** 1987b, 236:959-962

Ishibashi S, Brown MS, Goldstein JL, Gerard RD, Hammer RE, Herz J: Hypercholesterolemia in low density lipoprotein receptor knockout mice and its reversal by adenovirus-mediated gene delivery. **J Clin Invest** 1993, **92**:883-893

Isoe K, Urakami K, Sato K, Takahashi K: Apolipoprotein E in patients with dementia of the Alzheimer type and vascular dementia. **Acta Neurol Scand** 1996, **93**:133-137

Ito U, Spatz M, Walker JTJ, Klatzo I: Experimental cerebral ischemia in mongolian gerbils. I. Light microscopic observations. **Acta Neuropathol (Berl)** 1975, **32**:209-223

Jay TM, Lucignani G, Crane AM, Jehle J, Sokoloff L: Measurement of local cerebral blood flow with [14C]iodoantipyrine in the mouse. **J Cereb Blood Flow Metab** 1988, **8**:121-129

Jellinger KA, Paulus W, Wrocklage C, Litvan I: Effects of closed traumatic brain injury and genetic factors on the development of Alzheimer's disease. **Eur J Neurol** 2001, **8**:707-710

Jennett B, Teasdale G, Braakman R, Minderhoud J, Heiden J, Kurze T: Prognosis of patients with severe head injury. **Neurosurgery** 1979, **4**:283-289

Ji ZS, Miranda RD, Newhouse YM, Weisgraber KH, Huang Y, Mahley RW: Apolipoprotein E4 potentiates amyloid beta peptide-induced lysosomal leakage and apoptosis in neuronal cells. **J Biol Chem** 2002, **277**:21821-21828

Johnson EM, Deckwerth TL: Molecular mechanisms of developmental neuronal death. **Annu Rev Neurosci** 1996, **16**:31-46

Jones TH, Morawetz RB, Crowell RM, Marcoux FW, Fitzgibbon SJ, de Girolami U, Ojemann RG: Thresholds of focal cerebral ischemia in awake minkeys. **J Neurosurg** 1981, **54**:773-782

Jordan BD, Relkin NR, Ravdin LD, Jacobs AR, Bennett A, Gandy S: Apolipoprotein E epsilon4 associated with chronic traumatic brain injury in boxing. **JAMA** 1997, **278**:136-140

Jordan CA, Watkins BA, Kufta C, Dubois-Dalcq M: Infection of brain microglial cells by human immunodeficiency virus type 1 is CD4 dependent. **J Virol** 1991, **65**:736-742

Jung-Testas I, Weintraub H, Dupuis D, Eychenne B, Baulieu EE, Robel P: Low density lipoprotein-receptors in primary cultures of rat glial cells. **J Steroid Biochem Mol Biol** 1992, **42**:597-605

Kajiwara K, Byrnes AP, Charlton HM, Wood MJ, Wood KJ: Immune responses to adenoviral vectors during gene transfer in the brain. **Hum Gene Ther** 1997, **8**:253-265

- Kajiwara K, Byrnes AP, Ohmoto Y, Charlton HM, Wood MJ, Wood KJ: Humoral immune responses to adenovirus vectors in the brain. **J Neuroimmunol** 2000, **103**:8-15
- Kalaria RN: The role of cerebral ischemia in Alzheimer's disease. **Neurobiol Aging** 2000, **21**:321-330
- Kalaria RN: Small vessel disease and Alzheimer's dementia: pathological considerations. **Cerebrovasc Dis** 2002, **13 Suppl 2**:48-52
- Kalimo H, Kaste M, Haltia M: Vascular diseases. **Greenfield's Neuropathology**. Edited by Graham DI, Lantos PL. London, Arnold, 2002, pp 281-355
- Kalmijn S, Feskens EJ, Launer LJ, Kromhout D: Cerebrovascular disease, the apolipoprotein e4 allele, and cognitive decline in a community-based study of elderly men. **Stroke** 1996, **27**:2230-2235
- Kamada H, Sato K, Zhang WR, Omori N, Nagano I, Shoji M, Abe K: Spatiotemporal changes of apolipoprotein E immunoreactivity and apolipoprotein E mRNA expression after transient middle cerebral artery occlusion in rat brain. **J Neurosci Res** 2003, **73**:545-556
- Kanemitsu H, Nakagomi T, Tamura A, Tsuchiya T, Kono G, Sano K: Differences in the extent of primary ischemic damage between middle cerebral artery coagulation and intraluminal occlusion models. **J Cereb Blood Flow Metab** 2002, **22**:1196-1204
- Kaplan B, Brint S, Tanabe J, Jacewicz M, Wang X-J, Pulsinelli W: Temporal thresholds for neocortical infarction in rats subjected to reversible focal cerebral ischemia. **Stroke** 1991, **22**:1032-1039
- Karathanasis SK, Yunis I, Zannis VI: Structure, evolution, and tissue-specific synthesis of human apolipoprotein AIV. **Biochemistry** 1986, **25**:3962-3970
- Karvonen J, Kauma H, Kervinen K, Ukkola O, Rantala M, Paivansalo M, Savolainen MJ, Kesaniemi YA: Apolipoprotein E polymorphism affects carotid artery atherosclerosis in smoking hypertensive men. **J Hypertens** 2002, **20**:2371-2378
- Kashyap VS, Santamarina-Fojo S, Brown DR, Parrott CL, Applebaum-Bowden D, Meyn S, Talley G, Paigen B, Maeda N, Brewer HB: Apolipoprotein E deficiency in mice: gene replacement and prevention of atherosclerosis using adenovirus vectors. **J Clin Invest** 1995, **96**:1612-1630
- Kaufmann AM, Firlik AD, Fukui MB, Wechsler LR, Jungries CA, Yonas H: Ischemic core and penumbra in human stroke. **Stroke** 1999, **30**:93-99
- Kawagoe J, Abe K, Sato S, Nagano I, Nakamura S, Kogure K: Distributions of heat shock protein-70 mRNAs and heat shock cognate protein-70 mRNAs after transient global ischemia in gerbil brain. **J Cereb Blood Flow Metab** 1992, **12**:794-801

- Kay MA, Glorioso JC, Naldini L: Viral vectors for gene therapy: the art of turning infectious agents into vehicles of therapeutics. **Nat Med** 2001, 7:33-40
- Kelly DF, Martin NA, Kordestani R, Counelis G, Hovda DA, Bergsneider M, McBride DQ, Shalmon E, Herman D, Becker DP: Cerebral blood flow as a predictor of outcome following traumatic brain injury. **J Neurosurg** 1997, 86:633-641
- Kelly S, Bieneman A, Horsburgh K, Hughes D, Sofroniew MV, McCulloch J, Uney JB: Targeting expression of hsp70i to discrete neuronal populations using the Lmo-1 promoter: assessment of the neuroprotective effects of hsp70i in vivo and in vitro. **J Cereb Blood Flow Metab** 2001a, 21:971-982
- Kelly S, McCulloch J, Horsburgh K: Minimal ischaemic neuronal damage and HSP70 expression in MF1 strain mice following bilateral common carotid artery occlusion. **Brain Res** 2001b, 914:185-195
- Kennedy PG: Potential use of herpes simplex virus (HSV) vectors for gene therapy of neurological disorders. **Brain** 1997, 120:1245-1259
- Kerr JF, Wyllie AH, Currie AR: Apoptosis: a basic biological phenomenon with wide-ranging implications in tissue kinetics. **Br J Cancer** 1972, 26:239-257
- Kida E, Pluta R, Lossinsky AS, Golabek AA, Choi-Miura NH, Wisniewski HM, Mossakowski MJ: Complete cerebral ischemia with short-term survival in rat induced by cardiac arrest. II. Extracellular and intracellular accumulation of apolipoproteins E and J in the brain. **Brain Res** 1995, 674:341-346
- Kilic E, Hermann DM, Kugler S, Kilic U, Holzmuller H, Schmeer C, Bahr M: Adenovirus-mediated Bcl-X expression using a neuron-specific synapsin-1 promoter protects against disseminated neuronal injury and brain infarction following focal cerebral ischaemia in mice. **Neurobiol Dis** 2002, 11:275-284
- Kim DH, Iijima H, Goto K, Sakai J, Ishii H, Kim HJ, Suzuki H, Kondo H, Saeki S, Yamamoto T: Human apolipoprotein E receptor 2. A novel lipoprotein receptor of the low density lipoprotein receptor family predominantly expressed in brain. **J Biol Chem** 1996, 271:8373-8380
- Kim JS, Han SR, Chung SW, Kim BS, Lee KS, Kim YI, Yang DW, Kim KS, Kim JW: The apolipoprotein E epsilon4 haplotype is an important predictor for recurrence in ischemic cerebrovascular disease. **J Neurol Sci** 2003, 206:31-37
- Kinoshita A, Whelan CM, Smith CJ, Mikhailenko I, Rebeck GW, Strickland DK, Hyman BT: Demonstration by fluorescence resonance energy transfer of two sites of interaction between the low-density lipoprotein receptor-related protein and the amyloid precursor protein: role of the intracellular adapter protein Fe65. **J Neurosci** 2001, 21:8354-8361

Kinouchi H, Epstein CJ, Mizui T, Carlson E, Chen SF, Chan PH: Attenuation of focal cerebral ischemic injury in transgenic mice overexpressing CuZn superoxide dismutase. **Proc Natl Acad Sci** 1991, **88**:11158-11162

Kinouchi H, Sharp FR, Koistinaho J, Hicks K, Kamii H, Chan PH: Induction of heat shock hsp70 mRNA and HSP70 kDa protein in neurons in the 'penumbra' following focal cerebral ischemia in the rat. **Brain Res** 1993, **619**:334-338

Kirino T: Delayed neuronal death in the gerbil hippocampus following ischemia. **Brain Res** 1982, **239**:57-69

Kirino T, Sano K: Selective vulnerability in the gerbil hippocampus following transient ischemia. **Acta Neuropathol (Berl)** 1984, **62**:201-208

Kirino T, Tamura A, Sano K: Delayed neuronal death in the rat hippocampus following transient forebrain ischemia. **Acta Neuropathol (Berl)** 1984, **64**:139-147

Kitagawa H, Hayashi T, Mitsumoto Y, Koga N, Itoyama Y, Abe K: Reduction of ischemic brain injury by topical application of glial cell line-derived neurotrophic factor after permanent middle cerebral artery occlusion in rats. **Stroke** 1998a, **29**:1417-1422

Kitagawa H, Sasaki C, Sakai K, Mori A, Mitsumoto Y, Mori T, Fukuchi Y, Setoguchi Y, Abe K: Adenovirus-mediated gene transfer of glial cell line-derived neurotrophic factor prevents ischemic brain injury after transient middle cerebral artery occlusion in rats. **J Cereb Blood Flow Metab** 1999, **19**:1336-1344

Kitagawa K, Matsumoto M, Tsujimoto Y, Ohtsuki T, Kuwabara K, Matsushita K, Yang G, Tanabe H, Martinou J-C, Hori M, Yanagihara T: Amelioration of hippocampal neuronal damage after global ischemia by neuronal overexpression of BCL-2 in transgenic mice. **Stroke** 1998b, **29**:2616-2621

Kitagawa K, Matsumoto M, Yang G, Mabuchi T, Yagita Y, Hori M, Yanagihara T: Cerebral ischemia after bilateral carotid artery occlusion and intraluminal suture occlusion in mice: evaluation of the patency of the posterior communicating artery. **J Cereb Blood Flow Metab** 1998c, **18**:570-579

Kitagawa K, Matsumoto M, Hori M, Yanagihara T: Neuroprotective effect of apolipoprotein E against ischemia. **Ann N Y Acad Sci** 2002a, **977**:468-475

Kitagawa K, Matsumoto M, Kuwabara K, Takasawa K, Tanaka S, Sasaki T, Matsushita K, Ohtsuki T, Yanagihara T, Hori M: Protective effect of apolipoprotein E against ischemic neuronal injury is mediated through antioxidant action. **J Neurosci Res** 2002b, **68**:226-232

Knouff C, Hinsdale ME, Mezdour H, Altenburg MK, Watanabe M, Quarfordt SH, Sullivan PM, Maeda N: Apo E structure determines VLDL clearance and atherosclerosis risk in mice. **J Clin Invest** 1999, **103**:1579-1586

Koch S, Donarski N, Goetze K, Kreckel M, Stuerenburg HJ, Buhmann C, Beisiegel U: Characterization of four lipoprotein classes in human cerebrospinal fluid. **J Lipid Res** 2001, **42**:1143-1151

Kochanek PM, Janesko KL, Jenkins LW, Yan HQ, Kibbe MR, Robichaud P, Wooditch AC, Clark RS, Dixon CE, Marion DW, Billiar TR: Adenovirus-mediated transfer and expression of beta-gal in injured hippocampus after traumatic brain injury in mice. **J Neurotrauma** 2001a, **18**:73-82

Kochanek S, Schiedner G, Volpers C: High-capacity 'gutless' adenoviral vectors. **Curr Opin Mol Ther** 2001b, **3**:454-463

Koizumi J, Yoshida Y, Nakazawa T, Ooneda G: Experimental studies of ischemic brain edema: 1. A new experimental model of cerebral embolism in which recirculation can be introduced in the ischemic area. **Jpn J Stroke** 1986, **8**:1-8

Kokmen E, Whisnant JP, O'Fallon WM, Chu CP, Beard CM: Dementia after ischemic stroke: a population-based study in Rochester, Minnesota (1960-1984). **Neurology** 1996, **46**:154-159

Kokubo Y, Chowdhury AH, Date C, Yokoyama T, Sobue H, Tanaka H: Age-dependent association of apolipoprotein E genotypes with stroke subtypes in a Japanese rural population. **Stroke** 2000, **31**:2279

Koo CH, Squazzo SL: Evidence that production and release of amyloid beta-protein involves the endocytic pathway. **J Biol Chem** 1994, **269**:17386-17389

Koo EH, Squazzo SL, Selkoe DJ, Koo CH: Trafficking of cell-surface amyloid beta-protein precursor. I. Secretion, endocytosis and recycling as detected by labeled monoclonal antibody. **J Cell Sci** 1996, **109**:911-998

Kraszpulski M, Soininen H, Helisalmi S, Alafuzoff I: The load and distribution of beta-amyloid in brain tissue of patients with Alzheimer's disease. **Acta Neurol Scand** 2001, **103**:88-92

Krieger M, Herz J: Structures and functions of multiligand lipoprotein receptors: macrophage scavenger receptors and LDL receptor-related protein (LRP). **Annu Rev Biochem** 1994, **63**:601-637

Kristensen T, Moestrup SK, Gliemann J, Bendtsen L, Sand O, Sottrup-Jensen L: Evidence that the newly cloned low-density-lipoprotein receptor related protein (LRP) is the alpha 2-macroglobulin receptor. **FEBS Lett** 1990, **276**:151-155

Kristian T, Siesjo BK: Calcium in ischemic cell death. **Stroke** 1998, **29**:705-718

Kuge Y, Minematsu K, Yamaguchi T, Miyake Y: Nylon monofilament for intraluminal middle cerebral artery occlusion in rats. **Stroke** 1995, **26**:1655-1657

Kugler S, Meyn L, Holzmüller H, Gerhardt E, Isenmann S, Schulz JB, Bahr M: Neuron-specific expression of therapeutic proteins: evaluation of different cellular promoters in recombinant adenoviral vectors. **Mol Cell Neurosci** 2001, **17:78-96**

Kugler S, Kilic E, Bahr M: Human synapsin 1 gene promoter confers highly neuron-specific long-term transgene expression from an adenoviral vector in the adult rat brain depending on the transduced area. **Gene Ther** 2003, **10:337-347**

Kutner KC, Erlanger DM, Tsai J, Jordan B, Relkin NR: Lower cognitive performance of older football players possessing apolipoprotein E epsilon4. **Neurosurgery** 2000, **47:651-657**

LaDu MJ, Gilligan SM, Lukens JR, Cabana VG, Reardon CA, Van Eldik LJ, Holtzman DM: Nascent astrocyte particles differ from lipoproteins in CSF. **J Neurochem** 1998, **70:2070-2081**

Laing RJ, Jakubowski J, Laing RW: Middle cerebral artery occlusion without craniectomy in rats. Which method works best? **Stroke** 1993, **24:294-297**

Lambert JC, Berr C, Pasquier F, Delacourte A, Frigard B, Cotel D, Perez-Tur J, Mouroux V, Mohr M, Cecyrc D, Galasko D, Lendon C, Poirier J, Hardy J, Mann D, Amouyel P, Chartier-Harlin MC: Pronounced impact of Th1/E47cs mutation compared with -491 AT mutation on neural APOE gene expression and risk of developing Alzheimer's disease. **Hum Mol Genet** 1998, **7:1511-1516**

Lambert JC, Araria-Goumide L, Myllykangas L, Ellis C, Wang JC, Bullido MJ, Harris JM, Artiga MJ, Hernandez D, Kwon JM, Frigard B, Petersen RC, Cumming AM, Pasquier F, Sastre I, Tienari PJ, Frank A, Sulkava R, Morris JC, St Clair D, Mann DM, Wavrant-DeVrieze F, Ezquerra-Trabalon M, Amouyel P, Hardy J, Haltia M, Valdivieso F, Goate AM, Perez-Tur J, Lendon CL, Chartier-Harlin MC: Contribution of APOE promoter polymorphisms to Alzheimer's disease risk. **Neurology** 2002, **59:59-66**

Larson IA, Ordovas JM, DeLuca C, Barnard JR, Feussner G, Schaefer EJ: Association of apolipoprotein (Apo)E genotype with plasma apo E levels. **Atherosclerosis** 2000, **148:327-335**

Laskowitz DT, Sheng H, Bart RD, Joyner KA, Roses AD, Warner DS: Apolipoprotein E-deficient mice have increased susceptibility to focal cerebral ischemia. **J Cereb Blood Flow Metab** 1997, **17:753-759**

Laskowitz DT, Horsburgh K, Roses AD: Apolipoprotein E and the CNS response to injury. **J Cereb Blood Flow Metab** 1998, **18:465-471**

Lauderback CM, Kanski J, Hackett JM, Maeda N, Kindy MS, Butterfield DA: Apolipoprotein E modulates Alzheimer's Aβ(1-42)-induced oxidative damage to synaptosomes in an allele-specific manner. **Brain Res** 2002, **924:90-97**

Laws SM, Hone E, Taddei K, Harper C, Dean B, McClean C, Masters C, Lautenschlager N, Gandy SE, Martins RN: Variation at the APOE -491 promoter locus is associated with altered brain levels of apolipoprotein E. **Mol Psychiatry** 2002, **7:886-890**

Laws SM, Hone E, Gandy S, Martins RN: Expanding the association between the APOE gene and the risk of Alzheimer's disease: possible roles for APOE promoter polymorphisms and alterations in APOE transcription. **J Neurochem** 2003, **84:1215-1236**

Lee JM, Zipfel GJ, Choi DW: The changing landscape of ischaemic brain injury mechanisms. **Nature** 1999, **399:A7-14**

Lee SH, Kim M, Yoon BW, Kim YJ, Ma SJ, Roh JK, Lee JS, Seo JS: Targeted hsp70.1 disruption increases infarction volume after focal cerebral ischemia in mice. **Stroke** 2001, **32:2905-2912**

Lefranc D, Vermersch P, Dallongeville J, Daems-Monpeurt C, Petit H, Delacourte A: Relevance of the quantification of apolipoprotein E in the cerebrospinal fluid in Alzheimer's disease. **Neurosci Lett** 1996, **212:91-94**

Leker RR, Shohami E: Cerebral ischemia and trauma - different etiologies yet similar mechanisms: neuroprotective opportunities. **Brain Res Brain Res Rev** 2002, **39:55-73**

Lemere CA, Blusztajn JK, Yamaguchi H, Wisniewski T, Saido TC, Selkoe DJ: Sequence of deposition of heterogeneous amyloid beta-peptides and APO E in Down syndrome: implications for initial events in amyloid plaque formation. **Neurobiol Dis** 1996, **3:16-32**

Lendon CL, Martinez A, Behrens IM, Kosik KS, Madrigal L, Norton J, Neuman R, Myers A, Busfield F, Wragg M, Arcos M, Arango Viana JC, Ossa J, Ruiz A, Goate AM, Lopera F: E280A PS-1 mutation causes Alzheimer's disease but age of onset is not modified by ApoE alleles. **Hum Mutat** 1997, **10:186-195**

Leung CH, Poon WS, Yu LM, Wong GK, Ng HK: Apolipoprotein e genotype and outcome in aneurysmal subarachnoid hemorrhage. **Stroke** 2002, **33:548-552**

Levy E, Carman MD, Fernandez-Madrid IJ, Power MD, Lieberburg I, van Duinen SG, Bots GT, Luyendijk W, Frangione B: Mutation of the Alzheimer's disease amyloid gene in hereditary cerebral hemorrhage, Dutch type. **Science** 1990, **248:1124-1126**

Levy-Lahad E, Wasco W, P P, Romano DM, Oshima J, Pettingell WH, Yu CE, Jondro PD, Schmidt SD, Wang Kea: Candidate gene for the chromosome 1 familial Alzheimer's disease locus. **Science** 1995, **269:917-918**

Lewen A, Matz P, Chan PH: Free radical pathways in CNS injury. **J Neurotrauma** 2000, **17:871-89**

- Li WH, Tanimura M, Luo CC, Datta S, Chan L: The apolipoprotein multigene family: biosynthesis, structure, structure-function relationships, and evolution. **J Lipid Res** 1988, 29:245-271.
- Li Y, Chopp M, Zhang ZG, Zhang RL, Garcia JH: Neuronal survival is associated with 72-kDa heat shock protein expression after transient middle cerebral artery occlusion in the rat. **J Neurol Sci** 1993, 120:187-194
- Li Y, Chopp M, Jiang N, Yao F, Zaloga C: Temporal profile of in situ DNA fragmentation after transient middle cerebral artery occlusion in the rat. **J Cereb Blood Flow Metab** 1995a, 15:389-397
- Li Y, Chopp M, Jiang N, Zhang ZG, Zaloga C: Induction of DNA fragmentation after 10 to 120 minutes of focal cerebral ischemia in rats. **Stroke** 1995b, 26:1252-1257
- Lieberman JN, Stewart WF, Wesnes K, Troncoso J: Apolipoprotein E epsilon 4 and short-term recovery from predominantly mild brain injury. **Neurology** 2002, 58:1038-1044
- Lichtman SW, Seliger G, Tycko B, Marder K: Apolipoprotein E and functional recovery from brain injury following postacute rehabilitation. **Neurology** 2000, 55:1539-1539
- Linnik MD, Miller JA, Sprinkle-Cavallo J, Mason PJ, Thompson FY, Montgomery LR, Schroeder KK: Apoptotic DNA fragmentation in the rat cerebral cortex induced by permanent middle cerebral artery occlusion. **Brain Res Mol Brain Res** 1995, 36:116-124
- Linton MF, Gish R, Hubl ST, Butler E, Esquivel C, Bry WI, Boyles JK, Wardell MR, Young SG: Phenotypes of apolipoprotein B and apolipoprotein E after liver transplantation. **J Clin Invest** 1991, 88:270-281
- Lipton P: Ischemic cell death in brain neurons. **Physiol Rev** 1999, 79:1431-1568
- Liszczak TM, Hedley-Whyte ET, Adams JF, Han DH, Kolluri VS, Vacanti FX, Heros RC, Zervas NT: Limitations of tetrazolium salts in delineating infarcted brain. **Acta Neuropathol (Berl)** 1984, 65:150-157
- Liu Y, Kato H, Nakata N, Kogure K: Temporal profile of heat shock protein 70 synthesis in ischemic tolerance induced by preconditioning ischemia in rat hippocampus. **Neuroscience** 1993, 56:921-927
- Liu Y, Laakso MP, Karonen JO, Vanninen RL, Nuutinen J, Soimakallio S, Aronen HJ: Apolipoprotein E polymorphism and acute ischemic stroke: a diffusion- and perfusion-weighted magnetic resonance imaging study. **J Cereb Blood Flow Metab** 2002, 22:1336-1342

Ljungberg MC, Asuni A, Pearce J, Dayanandan R, Marz W, Hoffmann MM, Bertrand P, Siest G, Rupniak HT, Anderton BH, Huettinger M, Lovestone S: Apolipoprotein E (apoE) uptake and distribution in mammalian cell lines is dependent upon source of apoE and can be monitored in living cells. **Neurosci Lett** 2003, **341**:69-73

Lo EH, Dalkara T, Moskowitz MA: Mechanisms, challenges and opportunities in stroke. **Nat Rev Neurosci** 2003, **4**:399-415

Loddick SA, Rothwell NJ: Neuroprotective effects of human recombinant interleukin-1 receptor antagonist in focal cerebral ischaemia in the rat. **J Cereb Blood Flow Metab** 1996, **16**:932-940

Longa EZ, Weinstein PR, Carlson S, Cummins R: Reversible middle cerebral artery occlusion without craniectomy in rats. **Stroke** 1989, **20**:84-91

Longstreth WT, Schellenberg GD, Fahrenbruch CE, Cobb LA, Copass MK, Siscovick DS: Apolipoprotein E genotypes and outcome from out of hospital cardiac arrest. **J Neurol Neurosurg Psychiatry** 2003, **74**:1441-1443

Lorent K, Overbergh L, Moechars D, De Strooper B, Van Leuven F, Van den Berghe H: Expression in mouse embryos and in adult mouse brain of three members of the amyloid precursor protein family, of the alpha-2-macroglobulin receptor/low density lipoprotein receptor-related protein and of its ligands apolipoprotein E, lipoprotein lipase, alpha-2-macroglobulin and the 40,000 molecular weight receptor-associated protein. **Neuroscience** 1995, **65**:1009-1025

Lund-Katz S, Wehrli S, Zaiou M, Newhouse Y, Weisgraber KH, Phillips MC: Effects of polymorphism on the microenvironment of the LDL receptor-binding region of human apoE. **J Lipid Res** 2001, **42**:894-901

Luthra K, Prasad K, Kumar P, Dwivedi M, Pandey RM, Das N: Apolipoprotein E gene polymorphism in cerebrovascular disease: a case-control study. **Clin Genet** 2002, **62**:39-44

Lynch JR, Tang W, Wang H, Vitek MP, Bennett ER, Sullivan PM, Warner DS, Laskowitz DT: APOE genotype and an ApoE-mimetic peptide modify the systemic and central nervous system inflammatory response. **J Biol Chem** 2003, **278**:48529-48533

MacLeod MJ, De Lange RP, Breen G, Meiklejohn D, Lemmon H, Clair DS: Lack of association between apolipoprotein E genotype and ischaemic stroke in a Scottish population. **Eur J Clin Invest** 2001, **31**:570-576

Macrae IM: New models of focal cerebral ischaemia. **Br J Clin Pharmacol** 1992, **34**:302-308

Maeda K, Mies G, Olah L, Hossmann K-A: Quantitative measurement of local cerebral blood flow in the anesthetized mouse using intraperitoneal [¹⁴C]iodoantipyrine injection and final arterial heart blood sampling. **J Cereb Blood Flow Metab** 2000, 20:10-14

Mahley RW: Apolipoprotein E: cholesterol transport protein with expanding role in cell biology. **Science** 1988, 240:622-630

Mahley RW, Innerarity TL: Lipoprotein receptors and cholesterol homeostasis. **Biochim Biophys Acta** 1983, 737:197-222

Mahley RW, Rall SC: Apolipoprotein E: far more than a lipid transport protein. **Annu Rev Genomics Hum Genet** 2000, 1:507-537

Majid A, He YY, Gidday JM, Kaplan SS, Gonzales ER, Park TS, Fenstermacher JD, Wei L, Choi DW, Hsu CY: Differences in vulnerability to permanent focal cerebral ischemia among 3 common mouse strains. **Stroke** 2001, 31:2707-2714

Malenka RC: Synaptic plasticity and AMPA receptor trafficking. **Ann N Y Acad Sci** 2003, 1003:1-11

Malinow R, Malenka RC: AMPA receptor trafficking and synaptic plasticity. **Annu Rev Neurosci** 2002, 25:103-126

Mao Y, Yang GY, Zhou LF, Stern JD, Betz AL: Focal cerebral ischemia in the mouse: description of a model and effects of permanent and temporary occlusion. **Brain Res Mol Brain Res** 1999, 63:366-370

Margaglione M, Seripa D, Gravina C, Grandone E, Vecchione G, Cappucci G, Merla G, Papa S, Postiglione A, Di Minno G, Fazio VM: Prevalence of apolipoprotein E alleles in healthy subjects and survivors of ischemic stroke: an Italian Case-Control Study. **Stroke** 1998, 29:399-403

Marion DW, Darby J, Yonas H: Acute regional cerebral blood flow changes caused by severe head injuries. **J Neurosurg** 1991, 74:407-414

Marques MA, Tolar M, Harmony JA, Crutcher KA: A thrombin cleavage fragment of apolipoprotein E exhibits isoform-specific neurotoxicity. **Neuroreport** 1996, 7:2529-2532

Marques MA, Tolar M, Crutcher KA: Apolipoprotein E exhibits isoform-specific neurotoxicity. **Alzheimer's Res** 1997, 3:1-6

Martin LJ, Al-Abdulla NA, Brambrink AM, Kirsch JR, Sieber FE, Portera-Cailliau C: Neurodegeneration in excitotoxicity, global cerebral ischemia, and target deprivation: A perspective on the contributions of apoptosis and necrosis. **Brain Res Bull** 1998, 46:281-309

Martinou JC, Dubois-Dauphin M, Staple JK, Rodriguez I, Frankowski H, Missotten M, Albertini P, Talabot D, Catsicas S, Pietra C: Overexpression of BCL-2 in transgenic mice protects neurons from naturally occurring cell death and experimental ischemia. **Neuron** 1994, 13:1017-1030

Marz W, Scharnagl H, Kirca M, Bohl J, Gross W, Ohm TG: Apolipoprotein E polymorphism is associated with both senile plaque load and Alzheimer-type neurofibrillary tangle formation. **Ann N Y Acad Sci** 1996, 777:276-280

Masliah E, Mallory M, Alford M, Veinbergs I, Roses AD: Apolipoprotein E; role in maintaining the integrity of the aging nervous system. **Apolipoprotein E and Alzheimer's disease**. Edited by Roses AD, Weisgraber KH, Christen Y. Berlin, Springer Verlag, 1996, pp 59-73

Masliah E, Samuel W, Veinbergs I, Mallory M, Mante M, T S: Neurodegeneration and cognitive impairment in apoE-deficient mice is ameliorated by infusion of recombinant apoE. **Brain Res** 1997, 751:307-314

Massaro AR, Sacco RL, Mohr JP, Foulkes MA, Tatemichi TK, Price TR, Hier DB, Wolf PA: Clinical discriminators of lobar and deep hemorrhage: the Stroke Data Bank. **Neurology** 1991, 41:1881-1885

Matsuo Y, Onodera H, Shiga Y, Shozuhara H, Ninomiya M, Kihara T, Tamatani T, Miyasaka M, Kogure K: Role of cell adhesion molecules in brain injury after transient middle cerebral artery occlusion in the rat. **Brain Res** 1994, 656:344-352

Mayeux R, Ottman R, Tang MX, Noboa-Bauza L, Marder K, Gurland B, Stern Y: Genetic susceptibility and head injury as risk factors for Alzheimer's disease among community-dwelling elderly persons and their first-degree relatives. **Ann Neurol** 1993, 33:494-501

Mayeux R, Ottman R, Maestre G, Ngai C, Tang MX, Ginsberg H, Chun M, Tycko B, Shelanski M: Synergistic effects of traumatic head injury and apolipoprotein-epsilon 4 in patients with Alzheimer's disease. **Neurology** 1995, 45:555-557

McAuley MA: Rodent models of focal ischemia. **Cerebrovas Brain Metab Rev** 1995, 7:153-180

McCaffrey MW, Bielli A, Cantalupo G, Mora S, Roberti V, Santillo M, Drummond F, Bucci C: Rab4 affects both recycling and degradative endosomal trafficking. **FEBS Lett** 2001, 495:21-30

McCarron MO, Muir KW, Weir CJ, Dyker AG, Bone I, Nicoll JA, Lees KR: The apolipoprotein E epsilon4 allele and outcome in cerebrovascular disease. **Stroke** 1998, 29:1882-1887

- McCarron MO, DeLong D, Alberts MJ: APOE genotype as a risk factor for ischemic cerebrovascular disease: a meta-analysis. **Neurology** 1999, **53**:1308-1311
- McCarron MO, Muir KW, Nicoll JA, Stewart J, Currie Y, Brown K, Bone I: Prospective study of apolipoprotein E genotype and functional outcome following ischemic stroke. **Arch Neurol** 2000, **57**:1480-1484
- McCarron MO, Weir CJ, Muir KW, Hoffmann KL, Graffagnino C, Nicoll JA, Lees KR, Alberts MJ: Effect of apolipoprotein E genotype on in-hospital mortality following intracerebral haemorrhage. **Acta Neurol Scand** 2003, **107**:106-109
- McCracken E, Graham DI, Nilsen M, Stewart J, Nicoll JAR, Horsburgh K: 4-hydroxynonenal immunoreactivity is increased in human hippocampus after global ischemia. **Brain Pathol** 2001, **11**:414-421
- McCulloch J: Excitatory amino acid antagonists and their potential for the treatment of ischaemic brain damage in man. **Br J Clin Pharmacol** 1992, **34**:106-114
- McLauchlan H, Newell J, Morrice N, Osborne A, West M, Smythe E: A novel role for Rab5-GDI in ligand sequestration into clathrin-coated pits. **Curr Biol** 1998, **8**:34-45
- Memezawa H, Minamisawa H, Smith M-L, Siesjo BK: Ischemic penumbra in a model of reversible middle cerebral artery occlusion in the rat. **Exp Brain Res** 1992, **89**:67-78
- Meresse S, Delbart C, Fruchart JC, Cecchelli R: Low-density lipoprotein receptor on endothelium of brain capillaries. **J Neurochem** 1989, **53**:340-345
- Metzger RE, LaDu MJ, Pan JB, Getz GS, Frail DE, Falduto MT: Neurons of the human frontal cortex display apolipoprotein E immunoreactivity: implications for Alzheimer's disease. **J Neuropathol Exp Neurol** 1996, **55**:372-380
- Mies G: Inhibition of protein synthesis during repetitive cortical spreading depression. **J Neurochem** 1993, **60**:360-363
- Mirra SS, Hyman BT: Ageing and dementia. **Greenfield's Neuropathology**. Edited by Graham DI, Lantos PL. London, Arnold, 2002, pp 195-271
- Miyata M, Smith JD: Apolipoprotein E allele-specific antioxidant activity and effects on cytotoxicity by oxidative insults and beta-amyloid peptides. **Nat Genet** 1996, **14**:55-61
- Monaghan DT, Cotman CW: Distribution of N-methyl-D-aspartate-sensitive L-[3H]glutamate-binding sites in rat brain. **J Neurosci** 1985, **5**:2909-2919
- Monaghan DT, Bridges RJ, Cotman CW: The excitatory amino acid receptors: their classes, pharmacology, and distinct properties in the function of the central nervous system. **Annu Rev Pharmacol Toxicol** 1989, **29**:365-402

Montine KS, Olson SJ, Amarnath V, Whetsell WOJ, Graham DG, Montine TJ: Immunohistochemical detection of 4-hydroxy-2-nonenal adducts in Alzheimer's disease is associated with inheritance of APOE4. **Am J Pathol** 1997, **150**:437-443

Morawetz RB, Crowell RH, DeGirolami U, Marcoux FW, Jones TH, Halsey JH: Regional cerebral blood flow thresholds during cerebral ischemia. **Fed Proc** 1979, **38**:2493-2494

Mori T, Kobayashi M, Town T, Fujita SC, Asano T: Increased vulnerability to focal ischemic brain injury in human apolipoprotein E4 knock-in mice. **J Neuropathol Exp Neurol** 2003, **62**:280-291

Morral N, Parks RJ, Zhou H, Langston C, Schiedner G, Quinones J, Graham FL, Kochanek S, Beaudet AL: High doses of a helper-dependent adenoviral vector yield supraphysiological levels of alpha1-antitrypsin with negligible toxicity. **Hum Gene Ther** 1998, **9**:2709-2716

Morris JC, Storandt M, McKeel DWJ, Rubin EH, Price JL, Grant EA, Berg L: Cerebral amyloid deposition and diffuse plaques in "normal" aging: Evidence for presymptomatic and very mild Alzheimer's disease. **Neurology** 1996, **46**:707-719

Morris PG, Wilson JT, Dunn LT, Nicoll JA: Apolipoprotein E polymorphism and neuropsychological outcome following subarachnoid haemorrhage. **Acta Neurol Scand** 2004, **109**:205-209

Morsy MA, Gu M, Motzel S, Zhao J, Lin J, Su Q, Allen H, Franlin L, Parks RJ, Graham FL, Kochanek S, Bett AJ, Caskey CT: An adenoviral vector deleted for all viral coding sequences results in enhanced safety and extended expression of a leptin transgene. **Proc Natl Acad Sci** 1998, **95**:7866-7871

Mortimer JA, French LR, Hutton JT, Schuman LM: Head injury as a risk factor for Alzheimer's disease. **Neurology** 1985, **35**:264-267

Mortimer JA, van Duijn CM, Chandra V, Fratiglioni L, Graves AB, Heyman A, Jorm AF, Kokmen E, Kondo K, Rocca WA, *et al.*: Head trauma as a risk factor for Alzheimer's disease: a collaborative re-analysis of case-control studies. EURODEM Risk Factors Research Group. **Int J Epidemiol** 1991, **20 Suppl 2**:S28-35

Mouw G, Zechel JL, Zhou Y, Lust WD, Selman WR, Ratcheson RA: Caspase-9 inhibition after focal cerebral ischemia improves outcome following reversible focal ischemia. **Metab Brain Dis** 2002, **17**:143-151

Mukherjee S, Ghosh RN, Maxfield FR: Endocytosis. **Physiol Rev** 1997, **77**:759-803

Mullan M, Crawford F, Axelman K, Houlden H, Lilius L, Winblad B, Lannfelt L: A pathogenic mutation for probable Alzheimer's disease in the APP gene at the N-terminus of beta-amyloid. **Nat Genet** 1992, **1**:345-347

Muller HW, Gebicke-Harter PJ, Hangen DH, Shooter EM: A specific 37,000-dalton protein that accumulates in regenerating but not in nonregenerating mammalian nerves. **Science** 1985, **228**:499-501

Muller HW, Ignatius MJ, Hangen DH, Shooter EM: Expression of specific sheath cell proteins during peripheral nerve growth and regeneration in mammals. **J Cell Biol** 1986, **102**:393-402

Murrell J, Farlow M, Ghetti B, Benson MD: A mutation in the amyloid precursor protein associated with hereditary Alzheimer's disease. **Science** 1991, **254**:97-99

Nacmias B, Latorraca S, Piersanti P, Forleo P, Piacentini S, Bracco L, Amaducci L, Sorbi S: ApoE genotype and familial Alzheimer's disease: a possible influence on age of onset in APP717 Val-->Ile mutated families. **Neurosci Lett** 1995, **183**:1-3

Nagasawa H, Kogure K: Correlation between cerebral blood flow and histologic changes in a new rat model of middle cerebral artery occlusion. **Stroke** 1989, **20**:1037-1043

Nathan BP, Bellosta S, Sanan DA, Weisgraber KH, Mahley RW, Pitas RE: Differential effects of apolipoproteins E3 and E4 on neuronal growth in vitro. **Science** 1994, **264**:850-852

Nathan BP, Jiang Y, Wong GK, Shen F, Brewer GJ, Struble RG: Apolipoprotein E4 inhibits, and apolipoprotein E3 promotes neurite outgrowth in cultured adult mouse cortical neurons through the low-density lipoprotein receptor-related protein. **Brain Res** 2002, **928**:96-105

Navarro V, Millecamps S, Geoffroy MC, Robert JJ, Valin A, Mallet J, Gal La Salle GL: Efficient gene transfer and long-term expression in neurons using a recombinant adenovirus with a neuron-specific promoter. **Gene Ther** 1999, **6**:1884-1892

Nedergaard M: Transient focal ischemia in hyperglycemic rats is associated with increased cerebral infarction. **Brain Res** 1987, **408**:79-85

Nedergaard M: Mechanisms of brain damage in focal cerebral ischemia. **Acta Neurol Scand** 1988, **77**:81-101

Nicoll JA, Burnett C, Love S, Graham DI, Ironside JW, Vinters HV: High frequency of apolipoprotein E epsilon 2 in patients with cerebral hemorrhage due to cerebral amyloid angiopathy. **Ann Neurol** 1996, **39**:682-683

Nicoll JA, Burnett C, Love S, Graham DI, Dewar D, Ironside JW, Stewart J, Vinters HV: High frequency of apolipoprotein E epsilon 2 allele in hemorrhage due to cerebral amyloid angiopathy. **Ann Neurol** 1997, **41**:716-721

Nishino K, Nowak TS: Time course and cellular distribution of hsp27 and hsp72 stress protein expression in a quantitative gerbil model of ischemic injury and tolerance: thresholds for hsp72 induction and hilar lesioning in the context of ischemic preconditioning. **J Cereb Blood Flow Metab** 2004, **24**:167-178

Nishio M, Kohmura E, Yuguchi T, Nakajima Y, Fujinaka T, Akiyama C, Iwata A, Yoshimine T: Neuronal apolipoprotein E is not synthesized in neuron after focal ischemia in rat brain. **Neurol Res** 2003, **25**:390-394

Niskakangas T, Ohman J, Niemela M, Ilveskoski E, Kunnas TA, Karhunen PJ: Association of apolipoprotein E polymorphism with outcome after aneurysmal subarachnoid hemorrhage: a preliminary study. **Stroke** 2001, **32**:1181-1184

Nitatori T, Sato N, Waguri S, Karasawa Y, Araki H, Shibana K, Kominami E, Uchiyama Y: Delayed neuronal death in the CA1 pyramidal cell layer of the gerbil hippocampus following transient ischemia is apoptosis. **J Neurosci** 1995, **15**:1001-1011

Nixon RA, Cataldo AM: The endosomal-lysosomal system of neurons: new roles. **Trends Neurosci** 1995, **18**:489-496

Noshita N, Sugawara T, Hayashi T, Lewen A, Omar G, Chan PH: Copper/zinc superoxide dismutase attenuates neuronal cell death by preventing extracellular signal-regulated kinase activation after transient focal cerebral ischemia in mice. **J Neurosci** 2002, **22**:7923-7930

Nowak TS: Synthesis of a stress protein following transient ischemia in the gerbil. **J Neurochem** 1985, **45**:1635-1641

Nowak TS: Localization of 70 kDa stress protein mRNA induction in gerbil brain after ischemia. **J Cereb Blood Flow Metab** 1991, **11**:432-439

Nykjaer A, Willnow TE: The low-density lipoprotein receptor gene family: a cellular Swiss army knife? **Trends Cell Biol** 2002, **12**:273-280

Olichney JM, Hansen LA, Galasko D, Saitoh T, Hofstetter CR, Katzman R, Thal LJ: The apolipoprotein E epsilon 4 allele is associated with increased neuritic plaques and cerebral amyloid angiopathy in Alzheimer's disease and Lewy body variant. **Neurology** 1996, **47**:190-196

Olney JW: Neurotoxicity of excitatory amino acids. **Kainic acid as a tool in neurobiology**. Edited by McGeer EG, Olney JW, McGeer PL. New York, Raven, 1978, pp 37-70

O'Meara ES, Kukull WA, Sheppard L, Bowen JD, McCormick WC, Teri L, Pfanschmidt M, Thompson JD, Schellenberg GD, Larson EB: Head injury and risk of Alzheimer's disease by apolipoprotein E genotype. **Am J Epidemiol** 1997, **146**:373-384

O'Neal WK, Zhou H, Morral N, Aguilar-Cordova E, Pestaner J, Langston C, Mull B, Wang Y, Beaudet AL, Lee B: Toxicological comparison of E2a-deleted and first-generation adenoviral vectors expressing alpha1-antitrypsin after systemic delivery. **Hum Gene Ther** 1998, **9**:1587-1598

Ooboshi H, Ibayashi S, Takada J, Yao H, Kitazono T, Fujishima M: Adenovirus-mediated gene transfer to ischemic brain: ischemic flow threshold for transgene expression. **Stroke** 2001, **32**:1043-1047

Ooboshi H, Ibayashi S, Takeda J, Kumai Y, Iida M: Brain ischemia as a potential target of gene therapy. **Exp Gerontol** 2003, **38**:183-187

Orrenius S: Apoptosis: molecular mechanisms and implications for human disease. **J Intern Med** 1995, **237**:529-536

Osborne KA, Shigeno T, Balarsky AM, Ford I, McCulloch J, Teasdale GM, Graham DI: Quantitative assessment of early brain damage in a rat model of focal cerebral ischaemia. **J Neurol Neurosurg Psychiatry** 1987, **50**:402-410

Panza F, Solfrizzi V, Colacicco AM, Basile AM, D'Introno A, Capurso C, Sabba M, Capurso S, Capurso A: Apolipoprotein E (APOE) polymorphism influences serum APOE levels in Alzheimer's disease patients and centenarians. **Neuroreport** 2003, **14**:605-608

Park CK, Mendelow AD, Graham DI, McCulloch J, Teasdale GM: Correlation of triphenyltetrazolium chloride perfusion staining with conventional neurohistology in the detection of early brain ischaemia. **Neuropathol Appl Neurobiol** 1988a, **14**:289-298

Park CK, Nehls DG, Graham DI, Teasdale GM, McCulloch J: Focal cerebral ischaemia in the cat: treatment with the glutamate antagonist MK-801 after induction of ischaemia. **J Cereb Blood Flow Metab** 1988b, **8**:757-762

Park CK, Nehls DG, Graham DI, Teasdale GM, McCulloch J: The glutamate antagonist MK-801 reduces focal ischemic brain damage in the rat. **Ann Neurol** 1988c, **24**:543-551

Pastor P, Roe CM, Villegas A, Bedoya G, Chakraverty S, Garcia G, Tirado V, Norton J, Rios S, Martinez M, Kosik KS, Lopera F, Goate AM: Apolipoprotein Epsilon4 modifies Alzheimer's disease onset in an E280A PS1 kindred. **Ann Neurol** 2003, **54**:163-169

Paulson OB, Strandgaard S, Edvinsson L: Cerebral autoregulation. **Cerebrovasc Brain Metab Rev** 1990, **2**:161-192

Pedersen WA, Chan SL, Mattson MP: A mechanism for the neuroprotective effect of apolipoprotein E: isoform-specific modification by the lipid peroxidation product 4-hydroxynonenal. **J Neurochem** 2000, **74**:1426-1433

Pedro-Botet J, Senti M, Nogues X, Rubies-Prat J, Roquer J, D'Olhaberriague L, Olive J: Lipoprotein and apolipoprotein profile in men with ischemic stroke. Role of lipoprotein(a), triglyceride-rich lipoproteins, and apolipoprotein E polymorphism. **Stroke** 1992, **23**:1556-1562

Peng DQ, Zhao SP, Wang JL: Lipoprotein (a) and apolipoprotein E epsilon 4 as independent risk factors for ischemic stroke. **Cardiovasc Risk** 1999, **6**:1-6

Pericak-Vance MA, Bebout JL, Gaskell PC, Yamaoka LH, Hung WY, Alberts MJ, Walker AP, Bartlett RJ, Haynes CA, Welsh KA, *et al*: Linkage studies in familial Alzheimer disease: evidence for chromosome 19 linkage. **Am J Hum Genet** 1991, **48**:1034-1050

Petito CK, Pulsinelli WA: Delayed neuronal recovery and neuronal death in rat hippocampus following severe cerebral ischemia: possible relationship to abnormalities in neuronal processes. **J Cereb Blood Flow Metab** 1984, **4**:194-205

Petito CK, Feldmann E, Pulsinelli WA, Plum F: Delayed hippocampal damage in humans following cardiorespiratory arrest. **Neurology** 1987, **37**:1281-1286

Piedrahita JA, Zhang SH, Hageman JR, Oliver PM, Maeda N: Generation of mice carrying a mutant apolipoprotein E gene inactivated by gene targeting in embryonic stem cells. **Proc Natl Acad Sci** 1992, **89**:4471-4475

Pietrzik CU, Busse T, Merriam DE, Weggen S, Koo EH: The cytoplasmic domain of the LDL receptor-related protein regulates multiple steps in APP processing. **EMBO J** 2002, **21**:5691-5700

Pirttila T, Soininen H, Heinonen O, Lehtimaki T, Bogdanovic N, Paljarvi L, Kosunen O, Winblad B, Riekkinen PS, Wisniewski HM, Mehta PD: Apolipoprotein E (apoE) levels in brains from Alzheimer disease patients and controls. **Brain Res** 1996, **722**:71-77

Pitas RE, Boyles JK, Lee SH, Foss D, Mahley RW: Astrocytes synthesize apolipoprotein E and metabolize apolipoprotein E-containing lipoproteins. **Biochim Biophys Acta** 1987a, **917**:148-161

Pitas RE, Boyles JK, Lee SH, Hui D, Weisgraber KH: Lipoproteins and their receptors in the central nervous system. Characterization of the lipoproteins in cerebrospinal fluid and identification of apolipoprotein B,E(LDL) receptors in the brain. **J Biol Chem** 1987b, **262**:14352-14360

Plassman BL, Havlik RJ, Steffens DC, Helms MJ, Newman TN, Drosdick D, Phillips C, Gau BA, Welsh-Bohmer KA, Burke JR, Guralnik JM, Breitner JC: Documented head injury in early adulthood and risk of Alzheimer's disease and other dementias. **Neurology** 2000, **55**:1158-1166

- Poirier J: Apolipoprotein E in animal models of CNS injury and in Alzheimer's disease. **Trends Neurosci** 1994, **17**:525-530
- Poirier J: Apolipoprotein E and Alzheimer's disease. A role in amyloid catabolism. **Ann N Y Acad Sci** 2000, **924**:81-90
- Poirier J, Baccichet A, Dea D, Gauthier S: Cholesterol synthesis and lipoprotein reuptake during synaptic remodelling in hippocampus in adult rats. **Neuroscience** 1993a, **55**:81-90
- Poirier J, Davignon J, Bouthillier D, Kogan S, Bertrand P, Gauthier S: Apolipoprotein E polymorphism and Alzheimer's disease. **Lancet** 1993b, **342**:697-699
- Politis MJ, Pellegrino RG, Oaklander AL, Ritchie JM: Reactive glial protein synthesis and early disappearance of saxitoxin binding in degenerating rat optic nerve. **Brain Res** 1983, **273**:392-395
- Polvikoski T, Sulkava R, Haltia M, Kainulainen K, Vuorio A, Verkkoniemi A, Niinisto L, Halonen P, Kontula K: Apolipoprotein E, dementia, and cortical deposition of beta-amyloid protein. **N Engl J Med** 1995, **333**:1242-1247
- Premkumar DR, Cohen DL, Hedera P, Friedland RP, Kalaria RN: Apolipoprotein E-epsilon4 alleles in cerebral amyloid angiopathy and cerebrovascular pathology associated with Alzheimer's disease. **Am J Pathol** 1996, **148**:2083-2095
- Pulsinelli WA, Brierley JB, Plum F: Temporal profile of neuronal damage in a model of transient forebrain ischemia. **Ann Neurol** 1982, **11**:491-498
- Qiu Z, Strickland DK, Hyman BT, Rebeck GW: alpha 2-Macroglobulin exposure reduces calcium responses to N-methyl-D-aspartate via low density lipoprotein receptor-related protein in cultured hippocampal neurons. **J Biol Chem** 2002, **277**:14458-14466
- Qiu Z, Crutcher KA, Hyman BT, Rebeck GW: ApoE isoforms affect neuronal N-methyl-D-aspartate calcium responses and toxicity via receptor-mediated processes. **Neuroscience** 2003, **122**:291-303
- Raffai RL, Dong LM, Farese RV, Weisgraber KH: Introduction of human apolipoprotein E4 "domain interaction" into mouse apolipoprotein E. **Proc Natl Acad Sci** 2001, **98**:11587-11591
- Rajdev S, Hara K, Kokubo Y, Mestrlil R, Dillmann W, Weinstein PR, Sharp FR: Mice overexpressing rat heat shock protein 70 are protected against cerebral infarction. **Ann Neurol** 2000, **47**:782-791

Ralph GS, Bienemann A, Harding TC, Hopton M, Henley J, Uney JB: Targeting of tetracycline-regulatable transgene expression specifically to neuronal and glial cell populations using adenoviral vectors. **Neuroreport** 2000, **11**:2051-2055

Ramassamy C, Averill D, Beffert U, Theroux L, Lussier-Cacan S, Cohn JS, Christen Y, Schoofs A, Davignon J, Poirier J: Oxidative insults are associated with apolipoprotein E genotype in Alzheimer's disease brain. **Neurobiol Dis** 2000, **7**:23-37

Ramassamy C, Krzywkowski P, Averill D, Lussier-Cacan S, Theroux L, Christen Y, Davignon J, Poirier J: Impact of apoE deficiency on oxidative insults and antioxidant levels in the brain. **Brain Res Mol Brain Res** 2001, **86**:76-83

Rebeck GW, Reiter JS, Strickland DK, Hyman BT: Apolipoprotein E in sporadic Alzheimer's disease: allelic variation and receptor interactions. **Neuron** 1993, **11**:575-580

Refolo LM, Sambamurti K, Efthimiopoulos S, Pappolla MA, Robakis NK: Evidence that secretase cleavage of cell surface Alzheimer amyloid precursor occurs after normal endocytic internalization. **J Neurosci Res** 1995, **40**:694-706

Reivich M, Jehle J, Sokoloff L, Kety SS: Measurement of regional cerebral blood flow with antipyrine-14C in awake cats. **J Appl Physiol** 1969, **27**:296-300

Rempel-Clower NL, Zola SM, Squire LR, Amaral DG: Three cases of enduring memory impairment after bilateral damage limited to the hippocampal formation. **J Neurosci** 1996, **16**:5233-5255

Rensen PC, Jong MC, van Vark LC, van der Boom H, Hendriks WL, van Berkel TJ, Biessen EA, Havekes LM: Apolipoprotein E is resistant to intracellular degradation in vitro and in vivo. Evidence for retroendocytosis. **J Biol Chem** 2000, **275**:8564-8571

Report of the Stroke Progress Review Group (National Institute of Neurological Disorders and Stroke, Maryland). 2002, pp 1-116

Reventos J, Gordon JW: Introduction of genes into the mouse germ line. **Acta Paediatr Scand Suppl** 1990, **366**:45-56

Ringelstein EB, Biniek R, Weiller C, Ammeling B, Nolte PN, Thron A: Type and extent of hemispheric brain infarctions and clinical outcome in early and delayed middle cerebral artery recanalization. **Neurology** 1992, **42**:289-298

Robbins PD, Tahara H, Ghivizzani SC: Viral vectors for gene therapy. **Trends Biotechnol** 1998, **16**:35-40

Robertson CS, Contant CF, Gokaslan ZL, Narayan RK, Grossman RG: Cerebral blood flow, arteriovenous oxygen difference, and outcome in head injured patients. **J Neurol Neurosurg Psychiatry** 1992, **55**:594-603

Robinson RG, Shoemaker WJ, Schlumpf M, Valk T, Bloom FE: Effect of experimental cerebral infarction in rat brain on catecholamines and behaviour. **Nature** 1975, 255:332-334

Rodman JS, Seidman L, Farquhar MG: The membrane composition of coated pits, microvilli, endosomes, and lysosomes is distinctive in the rat kidney proximal tubule cell. **J Cell Biol** 1986, 102:77-87

Rogaev EI, Sherrington R, Rogaeva EA, Levesque G, Ikeda M, Liang Y, Chi H, Lin C, Holman K, Tsuda Tea: Familial Alzheimer's disease in kindreds with missense mutations in a gene on chromosome 1 related to the Alzheimer's disease type 3 gene. **Nature** 1995, 376:775-778

Roheim PS, Carey M, Forte T, Vega GL: Apolipoproteins in human cerebrospinal fluid. **Proc Natl Acad Sci** 1979, 76:4646-4649

Roine RO, Kajaste S, Kaste M: The only population-based prospective study on the frequency and severity of various neuropsychological deficits after out-of-hospital cardiac arrest. **JAMA** 1993, 269:237-242

Roses AD: Apolipoprotein E alleles as risk factors in Alzheimer's disease. **Annu Rev Med** 1996, 47:387-400

Roses AD, Einstein G, Gilbert J, Goedert M, Han SH, Huang D, Hulette C, Masliah E, Pericak-Vance MA, Saunders AM, Schmechel DE, Strittmatter WJ, Weisgraber KH, Xi PT: Morphological, biochemical, and genetic support for an apolipoprotein E effect on microtubular metabolism. **Ann N Y Acad Sci** 1996, 777:146-157

Rothwell NJ, Hopkins SJ: Cytokines and the nervous system II: Actions and mechanisms of action. **Trends Neurosci** 1995, 18:130-136

Sabo T, Lomnitski L, Nyska A, Beni S, Maronpot RR, Shohami E, Roses AD, Michaelson DM: Susceptibility of transgenic mice expressing human apolipoprotein E to closed head injury: the allele E3 is neuroprotective whereas E4 increases fatalities. **Neuroscience** 2000, 101:879-884

Sacco RL: Classification of stroke. **Clinical atlas of cerebrovascular disorders**. Edited by Fisher M. London, Wolfe, 1994, pp 2.2-2.25

Sahuquillo J, Poca MA, Garnacho A, Robles A, Coello F, Godet C, Triginer C, Rubio E: Early ischaemia after severe head injury. Preliminary results in patients with diffuse brain injuries. **Acta Neurochir (Wien)** 1993, 122:204-214

Saito A, Hayashi T, Okuno S, Ferrand-Drake M, Chan PH: Overexpression of copper/zinc superoxide dismutase in transgenic mice protects against neuronal cell death after transient focal ischemia by blocking activation of the Bad cell death signaling pathway. **J Neurosci** 2003, 23:1710-1718

- Sakurada O, Kennedy C, Jehle J, Brown JD, Carbin GL, Sokoloff L: Measurement of local cerebral blood flow with iodo [14C] antipyrine. **Am J Physiol** 1978, **234:H59-66**
- Sattler R, Xiong Z, Lu WY, Hafner M, MacDonald JF, Tymianski M: Specific coupling of NMDA receptor activation to nitric oxide neurotoxicity by PSD-95 protein. **Science** 1999, **284:1845-1848**
- Saunders AM, Strittmatter WJ, Schmechel D, George-Hyslop PH, Pericak-Vance MA, Joo SH, Rosi BL, Gusella JF, Crapper-MacLachlan DR, Alberts MJ: Association of apolipoprotein E allele epsilon 4 with late-onset familial and sporadic Alzheimer's disease. **Neurology** 1993, **43:1467-1472**
- Scarmeas N, Habeck CG, Stern Y, Anderson KE: APOE genotype and cerebral blood flow in healthy young individuals. **JAMA** 2003, **290:1581-1582**
- Schabitz WR, Li F, Irie K, Sandage BW, Locke KW, Fisher M: Synergistic effects of a combination of low-dose basic fibroblast growth factor and citicoline after temporary experimental focal ischemia. **Stroke** 1999, **30:427-431**
- Schiefermeier M, Kollegger H, Madl C, Schwarz C, Holzer M, Kofler J, Sterz F: Apolipoprotein E polymorphism: survival and neurological outcome after cardiopulmonary resuscitation. **Stroke** 2000, **31:2068-2073**
- Schiele F, De Bacquer D, Vincent-Viry M, Beisiegel U, Ehnholm C, Evans A, Kafatos A, Martins MC, Sans S, Sass C, Visvikis S, De Backer G, Siest G: Apolipoprotein E serum concentration and polymorphism in six European countries: the ApoEurope Project. **Atherosclerosis** 2000, **152:475-788**
- Schmechel DE, Saunders AM, Strittmatter WJ, Crain BJ, Hulette CM, Joo SH, Pericak-Vance MA, Goldgaber D, Roses AD: Increased amyloid beta-peptide deposition in cerebral cortex as a consequence of apolipoprotein E genotype in late-onset Alzheimer disease. **Proc Natl Acad Sci** 1993, **90:9649-9653**
- Schmid-Elsaesser R, Zausinger S, Hungerhuber E, Baethmann A, Reulen HJ: A critical reevaluation of the intraluminal thread model of focal cerebral ischemia: evidence of inadvertent premature reperfusion and subarachnoid hemorrhage in rats by laser-Doppler flowmetry. **Stroke** 1998, **29:2162-2170**
- Schneider JA, Wilson RS, Bienias JL, Evans DA, Bennett DA: Cerebral infarctions and the likelihood of dementia from Alzheimer disease pathology. **Neurology** 2004, **62:1148-1155**
- Schroder ML, Muizelaar JP, Bullock MR, Salvant JB, Povlishock JT: Focal ischemia due to traumatic contusions documented by stable xenon-CT and ultrastructural studies. **J Neurosurg** 1995, **82:966-971**

Schroder ML, Muizelaar JP, Kuta AJ, Choi SC: Thresholds for cerebral ischemia after severe head injury: relationship with late CT findings and outcome. **J Neurotrauma** 1996, 13:17-23

Schulz JB, Weller M, Matthews RT, Heneka MT, Groscurth P, Martinou JC, Lommatzsch J, von Coelln R, Wullner U, Loschmann PA, Beal MF, Dichgans J, Klockgether T: Extended therapeutic window for caspase inhibition and synergy with MK-801 in the treatment of cerebral histotoxic hypoxia. **Cell Death Differ** 1998, 5:847-857

Scremin OU: Cerebral Vascular System. **The Rat Nervous System**. Edited by Paxinos G. London, Academic Press, 1995, pp 3-35

Seitz A, Kragol M, Aglow E, Showe L, Heber-Katz E: Apolipoprotein E expression after spinal cord injury in the mouse. **J Neurosci Res** 2003, 71:417-426

Selkoe DJ: The molecular pathology of Alzheimer's disease. **Neuron** 1991, 6:487-498

Selkoe DJ, Schenk D: Alzheimer's disease: molecular understanding predicts amyloid-based therapeutics. **Annu Rev Pharmacol Toxicol** 2003, 43:545-584

Shea TB, Rogers E, Ashline D, Ortiz D, Sheu MS: Apolipoprotein E deficiency promotes increased oxidative stress and compensatory increases in antioxidants in brain tissue. **Free Radic Biol Med** 2002, 33:1115-1120

Sheng H, Laskowitz DT, Bennett E, Schmechel DE, Bart RD, Saunders AM, Pearlstein RD, Roses AD, Warner DS: Apolipoprotein E isoform-specific differences in outcome from focal ischemia in transgenic mice. **J Cereb Blood Flow Metab** 1998, 18:361-366

Sheng H, Laskowitz DT, Mackensen GB, Kudo M, Pearlstein RD, Warner DS: Apolipoprotein E deficiency worsens outcome from global cerebral ischemia in the mouse. **Stroke** 1999, 30:1118-1124

Sherrington R, Rogaev EI, Liang Y, Rogaeva EA, Levesque G, Ikeda M, Chi H, Lin C, Li G, Holman K, Tsuda T, Mar L, Foncin J-F, Bruni AC, Montesi MP, Sorbi S, Rainero I, Pinessi L, Nee L, Chumakov I, Pollen D, Brookes A, Sanseau P, Polinsky RJ, Wasco W, Da Silva HAR, Haines JL, Pericak-Vance MA, Tanzi RE, Roses AD, Fraser PE, Rommens JM, St George-Hyslop PH: Cloning of a gene bearing missense mutations in early-onset familial Alzheimer's disease. **Nature** 1995, 375:734-735

Shi N, Pardridge WM: Noninvasive gene targeting to the brain. **Proc Natl Acad Sci** 2000, 97:7567-7572

Shore VG, Shore B: Heterogeneity of human plasma very low density lipoproteins. Separation of species differing in protein components. **Biochemistry** 1973, 12:502-507

Simon RP, Swan JH, Griffiths T, Meldrum BS: Blockade of N-methyl-D-aspartate receptors may protect against ischemic damage in the brain. **Science** 1984, **226:850-852**

Skene JH, Shooter EM: Denervated sheath cells secrete a new protein after nerve injury. **Proc Natl Acad Sci** 1983, **80:4169-4173**

Simon RP, Cho H, Gwinn R, Lowenstein DH: The temporal profile of 72-kDa heat-shock protein expression following global ischemia. **J Neurosci** 1991, **11:881-889**

Skoog I, Hesse C, Aevansson O, Landahl S, Wahlstrom J, Fredman P, Blennow K: A population study of apoE genotype at the age of 85: relation to dementia, cerebrovascular disease, and mortality. **J Neurol Neurosurg Psychiatry** 1998, **64:37-43**

Skulachev VP: Cytochrome c in the apoptotic and antioxidant cascades. **FEBS Lett** 1998, **423:275-280**

Slooter AJ, de Knijff P, Hofman A, Cruts M, Breteler MM, Van Broeckhoven C, Havekes LM, van Duijn CM: Serum apolipoprotein E level is not increased in Alzheimer's disease: the Rotterdam study. **Neurosci Lett** 1998, **248:21-24**

Small GW, Mazziotta JC, Collins MT, Baxter LR, Phelps ME, Mandelkern MA, Kaplan A, La Rue A, Adamson CF, Chang L, *et al*: Apolipoprotein E type 4 allele and cerebral glucose metabolism in relatives at risk for familial Alzheimer disease. **JAMA** 1995, **273:942-947**

Smith JG, Raper SE, Wheeldon EB, Hackney D, Judy K, Wilson JM, Eck SL: Intracranial administration of adenovirus expressing HSV-TK in combination with ganciclovir produces a dose-dependent, self-limiting inflammatory response. **Hum Gene Ther** 1997, **8:943-954**

Smith ML, Auer RN, Siesjo BK: The density and distribution of ischemic brain injury in the rat following 2 - 10 min of forebrain ischemia. **Acta Neuropathol (Berl)** 1984, **64:319-332**

Smith PK, Krohn RI, Hermanson GT, Mallia AK, Gartner FH, Provenzano MD, Fujimoto EK, Goeke NM, Olson BJ, Klenk DC: Measurement of protein using bicinchoninic acid. **Anal Biochem** 1985, **150:76-85**

Smith-Arica JR, Morelli AE, Larregina AT, Smith J, Lowenstein PR, Castro MG: Cell-type-specific and regulatable transgenesis in the adult brain: adenovirus-encoded combined transcriptional targeting and inducible transgene expression. **Mol Ther** 2000, **2:579-587**

Snider BJ, Gottron FJ, Choi DW: Apoptosis and necrosis in cerebrovascular disease. **Ann N Y Acad Sci** 1999, **893:243-253**

Snipes GJ, McGuire CB, Norden JJ, Freeman JA: Nerve injury stimulates the secretion of apolipoprotein E by nonneuronal cells. **Proc Natl Acad Sci** 1986, **83**:1130-1134

Snowdon DA, Greiner LH, Mortimer JA, Riley KP, Greiner PA, Markesbery WR: Brain infarction and the clinical expression of Alzheimer disease. The Nun Study. **JAMA** 1997, **277**:813-817

Souza DR, Campos BF, Arruda EF, Yamamoto LJ, Trindade DM, Tognola WA: Influence of the polymorphism of apolipoprotein E in cerebral vascular disease. **Arq Neuropsiquiatr** 2003, **61**:7-13

St George-Hyslop P, McLachlan DC, Tsuda T, Rogaev E, Karlinsky H, Lippa CF, Pollen D, Tuda T: Alzheimer's disease and possible gene interaction. **Science** 1994, **263**:904

Stengard JH, Pekkanen J, Sulkava R, Ehnholm C, Erkinjuntti T, Nissinen A: Apolipoprotein E polymorphism, Alzheimer's disease and vascular dementia among elderly Finnish men. **Acta Neurol Scand** 1995, **92**:297-298

Stenmark H, Olkkonen VM: The Rab GTPase family. **Genome Biol** 2001, **2**:1-7

Stenmark H, Vitale G, Ullrich O, Zerial M: Rabaptin-5 is a direct effector of the small GTPase Rab5 in endocytic membrane fusion. **Cell** 1995, **83**:423-432

Stockinger W, Hengstschlager-Ottnad E, Novak S, Matus A, Huttinger M, Bauer J, Lassmann H, Schneider WJ, Nimpf J: The low density lipoprotein receptor gene family. Differential expression of two alpha2-macroglobulin receptors in the brain. **J Biol Chem** 1998, **273**:32213-32221

Stockinger W, Brandes C, Fasching D, M H, Gotthardt M, Herz J, Schneider WJ, Nimpf J: The reelin receptor ApoER2 recruits JNK-interacting proteins-1 and -2. **J Biol Chem** 2000, **275**:25625-25632

Stoll G, Jander S, Schroeter M: Inflammation and glial responses in ischemic brain lesions. **Prog Neurobiol** 1998, **56**:149-171

Strickland DK, Ashcom JD, Williams S, Burgess WH, Migliorini M, Argraves WS: Sequence identity between the alpha 2-macroglobulin receptor and low density lipoprotein receptor-related protein suggests that this molecule is a multifunctional receptor. **J Biol Chem** 1990, **265**:17401-17404

Strittmatter WJ, Bova Hill C: Molecular biology of apolipoprotein E. **Curr Opin Lipidol** 2002, **13**:119-123

Strittmatter WJ, Saunders AM, Schmechel D, Pericak-Vance M, Enghild J, Salvesen GS, Roses AD: Apolipoprotein E: high-avidity binding to beta-amyloid and increased frequency of type 4 allele in late-onset familial Alzheimer disease. **Proc Natl Acad Sci** 1993, **90**:1977-1981

Strittmatter WJ, Saunders AM, Goedert M, Weisgraber KH, Dong LM, Jakes R, Huang DY, Pericak-Vance M, Schmechel D, Roses AD: Isoform-specific interactions of apolipoprotein E with microtubule-associated protein tau: implications for Alzheimer disease. **Proc Natl Acad Sci** 1994a, **91**:11183-11186

Strittmatter WJ, Weisgraber KH, Goedert M, Saunders AM, Huang D, Corder EH, Dong LM, Jakes R, Alberts MJ, Gilbert JR, *et al*: Hypothesis: microtubule instability and paired helical filament formation in the Alzheimer disease brain are related to apolipoprotein E genotype. **Exp Neurol** 1994b, **125**:163-171

Sudlow CL, Warlow CP: Comparable studies of the incidence of stroke and its pathological types: results from an international collaboration. International Stroke Incidence Collaboration. **Stroke** 1997, **28**:491-499

Sugawara T, Noshita N, Lewen A, Gasche Y, Ferrand-Drake M, Fujimura M, Morita-Fujimura Y, Chan PH: Overexpression of copper/zinc superoxide dismutase in transgenic mice protects vulnerable neurons against ischemic damage by blocking the mitochondrial pathway of caspase activation. **J Neurosci** 2002, **22**:209-217

Sullivan PM, Mezdour H, Aratani Y, Knouff C, Najib J, Reddick RL, Quarfordt SH, Maeda N: Targeted replacement of the mouse apolipoprotein E gene with the common human APOE3 allele enhances diet-induced hypercholesterolemia and atherosclerosis. **J Biol Chem** 1997, **272**:17972-17980

Sullivan PM, Mezdour H, Quarfordt SH, Maeda N: Type III hyperlipoproteinemia and spontaneous atherosclerosis in mice resulting from gene replacement of mouse Apoe with human Apoe*2. **J Clin Invest** 1998, **102**:130-135

Sun Y, Wu S, Bu G, Onifade MK, Patel SN, LaDu MJ, Fagan AM, Holtzman DM: Glial fibrillary acidic protein-apolipoprotein E (apoE) transgenic mice: astrocyte-specific expression and differing biological effects of astrocyte-secreted apoE3 and apoE4 lipoproteins. **J Neurosci** 1998, **18**:7261-3272

Takagi N, Logan R, Teves L, Wallace MC, Gurd JW: Altered interaction between PSD-95 and the NMDA receptor following transient global ischemia. **J Neurochem** 2000, **74**:169-178

Takano K, Tatlisumak T, Bergmann AG, Gibson III DG, Fisher M: Reproducibility and reliability of middle cerebral artery occlusion using a silicone-coated suture (Koizumi) in rats. **J Neurol Sci** 1997, **153**:8-11

Talman WT: Cardiovascular regulation and lesions of the central nervous system. **Ann Neurol** 1985, 18:1-13

Tamaoka A, Miyatake F, Matsuno S, Ishii K, Nagase S, Sahara N, Ono S, Mori H, Wakabayashi K, Tsuji S, Takahashi H, Shoji S: Apolipoprotein E allele-dependent antioxidant activity in brains with Alzheimer's disease. **Neurology** 2000, 54:2319-2321

Tamura A, Asano T, Sano K: Correlation between rCBF and histological changes following temporary middle cerebral artery occlusion. **Stroke** 1980, 11:287-293

Tamura A, Graham DI, McCulloch J, Teasdale GM: Focal cerebral ischaemia in the rat: 1. Description of technique and early neuropathological consequences following middle cerebral artery occlusion. **J Cereb Blood Flow Metab** 1981, 1:53-60

Tang J, Zhao J, Zhao Y, Wang S, Chen B, Zeng W: Apolipoprotein E epsilon4 and the risk of unfavorable outcome after aneurysmal subarachnoid hemorrhage. **Surg Neurol** 2003, 60:391-396

Tatemichi TK, Desmond DW, Mayeux R, Paik M, Stern Y, Sano M, Remien RH, Williams JB, Mohr JP, Hauser WA, *et al*: Dementia after stroke: baseline frequency, risks, and clinical features in a hospitalized cohort. **Neurology** 1992, 42:1185-1193

Tatemichi TK, Paik M, Bagiella E, Desmond DW, Stern Y, Sano M, Hauser WA, Mayeux R: Risk of dementia after stroke in a hospitalized cohort: results of a longitudinal study. **Neurology** 1994, 44:1885-1891

Teasdale GM, Nicoll JA, Murray G, Fiddes M: Association of apolipoprotein E polymorphism with outcome after head injury. **Lancet** 1997, 350:1069-1071

Terent A, Marke LA, Asplund K, Norrving B, Jonsson E, O WP: Costs of stroke in Sweden. A national perspective. **Stroke** 1994, 25:2363-2369

Tesseur I, Van Dorpe J, Spittaels K, Van den Haute C, Moechars D, Van Leuven F: Expression of human apolipoprotein E4 in neurons causes hyperphosphorylation of protein tau in the brains of transgenic mice. **Am J Pathol** 2000, 156:951-964

Thaker U, McDonagh AM, Iwatsubo T, Lendon CL, Pickering-Brown SM, Mann DM: Tau load is associated with apolipoprotein E genotype and the amount of amyloid beta protein, Abeta40, in sporadic and familial Alzheimer's disease. **Neuropathol Appl Neurobiol** 2003, 29:35-44

Thilmann R, Xie Y, Kleihues P, Kiessling M: Persistent inhibition of protein synthesis precedes neuronal death in postischemic gerbil hippocampus. **Acta Neuropathol (Berl)** 1986, 71:88-93

Thomas CE, Schiedner G, Kochanek S, Castro MG, Lowenstein PR: Peripheral infection with adenovirus causes unexpected long-term brain inflammation in animals injected intracranially with first-generation, but not with high-capacity, adenovirus vectors: toward realistic long-term neurological gene therapy for chronic diseases. **Proc Natl Acad Sci** 2000, **97**:7482-7487

Thomas CE, Schiedner G, Kochanek S, Castro MG, Lowenstein PR: Preexisting antiadenoviral immunity is not a barrier to efficient and stable transduction of the brain, mediated by novel high-capacity adenovirus vectors. **Hum Gene Ther** 2001, **12**:839-846

Tolar M, Keller JN, Chan S, Mattson MP, Marques MA, Crutcher KA: Truncated apolipoprotein E (ApoE) causes increased intracellular calcium and may mediate ApoE neurotoxicity. **J Neurosci** 1999, **19**:7100-7110

Traykov L, Rigaud AS, Baudic S, Smagghe A, Boller F, Forette F: Apolipoprotein E epsilon 4 allele frequency in demented and cognitively impaired patients with and without cerebrovascular disease. **J Neurol Sci** 2002, **204**:177-181

Treger I, Fromm P, Ring H, Friedman G: Association between apolipoprotein E4 and rehabilitation outcome in hospitalized ischemic stroke patients. **Arch Phys Med Rehabil** 2003, **84**:973-976

Tripathy SK, Black HB, Goldwasser E, Leiden JM: Immune responses to transgene-encoded proteins limit the stability of gene expression after injection of replication-defective adenovirus vectors. **Nat Med** 1996, **2**:545-550

Trommsdorff M, Borg JP, Margolis B, Herz J: Interaction of cytosolic adaptor proteins with neuronal apolipoprotein E receptors and the amyloid precursor protein. **J Biol Chem** 1998, **273**:33556-33560

Trommsdorff M, Gotthardt M, Hiesberger T, Shelton J, Stockinger W, Nimpf J, Hammer RE, Richardson JA, Herz J: Reeler/Disabled-like disruption of neuronal migration in knockout mice lacking the VLDL receptor and ApoE receptor 2. **Cell** 1999, **97**:689-701

Tsai TH, Chen SL, Xiao X, Chiang YH, Lin SZ, Kuo SW, Liu DW, Tsao YP: Gene treatment of cerebral stroke by rAAV vector delivering IL-1ra in a rat model. **Neuroreport** 2003, **14**:803-807

Tsuchiya D, Hong S, Kayama T, Panter SS, Weinstein PR: Effect of suture size and carotid clip application upon blood flow and infarct volume after permanent and temporary middle cerebral artery occlusion in mice. **Brain Res** 2003a, **970**:131-139

Tsuchiya D, Hong S, Matsumori Y, Kayama T, Swanson RA, Dillman WH, Liu J, Panter SS, Weinstein PR: Overexpression of rat heat shock protein 70 reduces neuronal injury after transient focal ischemia, transient global ischemia, or kainic acid-induced seizures. **Neurosurgery** 2003b, **53**:1179-1187

Tyson GW, Teasdale GM, Graham DI, McCulloch J: Focal cerebral ischemia in the rat: topography of hemodynamic and histopathological changes. **Ann Neurol** 1984, **15**:559-567

Tyurin VA, Tyurina YY, Borisenko GG, Sokolova TV, Ritov VB, Quinn PJ, Rose M, Kochanek P, Graham SH, Kagan VE: Oxidative stress following traumatic brain injury in rats: quantitation of biomarkers and detection of free radical intermediates. **J Neurochem** 2000, **75**:2178-2189

Ulery PG, Beers J, Mikhailenko I, Tanzi RE, Rebeck GW, Hyman BT, Strickland DK: Modulation of beta-amyloid precursor protein processing by the low density lipoprotein receptor-related protein (LRP). Evidence that LRP contributes to the pathogenesis of Alzheimer's disease. **J Biol Chem** 2000, **275**:7410-7415

Utermann G, Hees M, Steinmetz A: Polymorphism of apolipoprotein E and occurrence of dysbetalipoproteinaemia in man. **Nature** 1977, **269**:604-607

Van Broeckhoven C: Presenilins and Alzheimer disease. **Nat Genet** 1995, **11**:230-232

van der Sluijs P, Hull M, Webster P, Male P, Goud B, Mellman I: The small GTP-binding protein rab4 controls an early sorting event on the endocytic pathway. **Cell** 1992, **70**:729-740

Vance JE, Campenot RB, Vance DE: The synthesis and transport of lipids for axonal growth and nerve regeneration. **Biochim Biophys Acta** 2000, **1486**:84-96

Vass K, Welch WJ, Nowak TS: Localization of 70-kDa stress protein induction in gerbil brain after ischemia. **Acta Neuropathol (Berl)** 1988, **77**:128-135

Veinbergs I, Everson A, Sagara Y, Masliah E: Neurotoxic effects of apolipoprotein E4 are mediated via dysregulation of calcium homeostasis. **J Neurosci Res** 2002, **67**:379-387

Wahl F, Obrenovitch TP, Hardy AM, Plotkine M, Boulu R, Symon L: Extracellular glutamate during focal cerebral ischaemia in rats: time course and calcium dependency. **J Neurochem** 1994, **63**:1003-1011

Wang JM, Hayashi T, Zhang WR, Sakai K, Shiro Y, Abe K: Reduction of ischemic brain injury by topical application of insulin-like growth factor-I after transient middle cerebral artery occlusion in rats. **Brain Res** 2000, **859**:381-385

Warlow C, Dennis MS, van Gijn J: What caused this transient or persisting ischaemic event? **Stroke: a practical guide to management. Oxford, Blackwell Science, 2001, pp 223-300**

Warlow C, Sudlow C, Dennis M, Wardlaw J, Sandercock P: Stroke. **Lancet 2003, 362:1211-1224**

Weisgraber KH: Apolipoprotein E: structure-function relationships. **Adv Protein Chem 1994, 45:249-302**

Wenham PR, Price WH, Blandell G: Apolipoprotein E genotyping by one-stage PCR. **Lancet 1991, 337:1158-1159**

Wetterau JR, Aggerbeck LP, Rall SC, Weisgraber KH: Human apolipoprotein E3 in aqueous solution. I. Evidence for two structural domains. **J Biol Chem 1988, 263:6240-6248**

Widmann R, Weber C, Bonnekoh P, Schlenker M, Hossmann KA: Neuronal damage after repeated 5 minutes of ischemia in the gerbil is preceded by prolonged impairment of protein metabolism. **J Cereb Blood Flow Metab 1992, 12:425-433**

Wilkinson NW, Euhus DM: Cyclosporin A does not affect adenoviral-mediated transgene expression of interleukin-2. **Int J Surg Investig 2001, 2:491-498**

Williams KR, Saunders AM, Roses AD, Armati PJ: Uptake and internalization of exogenous apolipoprotein E3 by cultured human central nervous system neurons. **Neurobiol Dis 1998, 5:271-279**

Willnow TE, Nykjaer A, Herz J: Lipoprotein receptors: new roles for ancient proteins. **Nat Cell Biol 1999, 1:E157-162**

Wilson PW, Schaefer EJ, Larson MG, Ordovas JM: Apolipoprotein E alleles and risk of coronary disease. A meta-analysis. **Arterioscler Thromb Vasc Biol 1996, 16:1250-1255**

Wolf BB, Lopes MB, VandenBerg SR, Gonias SL: Characterization and immunohistochemical localization of alpha 2-macroglobulin receptor (low-density lipoprotein receptor-related protein) in human brain. **Am J Pathol 1992, 141:37-42**

Wolfe CD: The impact of stroke. **Br Med Bull 2000, 56:275-286**

Wood MJ, Charlton HM, Wood KJ, Kajiwara K, Byrnes AP: Immune responses to adenovirus vectors in the nervous system. **Trends Neurosci 1996, 19:497-501**

Xie Y, Mies G, Hossmann KA: Ischemic threshold of brain protein synthesis after unilateral carotid artery occlusion in gerbils. **Stroke 1989, 20:620-626**

Xu PT, Schmechel D, Rothrock-Christian T, Burkhart DS, Qiu HL, Popko B, Sullivan P, Maeda N, Saunders AM, Roses AD, Gilbert JR: Human apolipoprotein E2, E3, and E4 isoform-specific transgenic mice: human-like pattern of glial and neuronal immunoreactivity in central nervous system not observed in wild-type mice. **Neurobiol Dis** 1996, **3**:229-245

Xu PT, Gilbert JR, Qiu HL, Ervin J, Rothrock-Christian TR, Hulette C, Schmechel DE: Specific regional transcription of apolipoprotein E in human brain neurons. **Am J Pathol** 1999, **154**:601-611

Xu Q, Brecht WJ, Weisgraber KH, Mahley RW, Huang Y: Apolipoprotein E4 domain interaction occurs in living neuronal cells as determined by fluorescence resonance energy transfer. **J Biol Chem** 2004, **Epub ahead of print**

Yagi T, Jikihara J, Fukumura M, Watabe K, Ohashi T, Eto Y, Hara M, Maeda M: Rescue of ischemic brain injury by adenoviral gene transfer of glial cell line-derived neurotrophic factor after transient global ischemia in gerbils. **Brain Res** 2000, **885**:273-282

Yamada M: Risk factors for cerebral amyloid angiopathy in the elderly. **Ann N Y Acad Sci** 2002, **977**:37-44

Yamauchi K, Tozuka M, Hidaka H, Hidaka E, Kondo Y, Katsuyama T: Characterization of apolipoprotein E-containing lipoproteins in cerebrospinal fluid: effect of phenotype on the distribution of apolipoprotein E. **Clin Chem** 1999a, **45**:1431-1438

Yamauchi K, Tozuka M, Nakabayashi T, Sugano M, Hidaka H, Kondo Y, Katsuyama T: Apolipoprotein E in cerebrospinal fluid: relation to phenotype and plasma apolipoprotein E concentrations. **Clin Chem** 1999b, **45**:497-504

Yamazaki T, Koo EH, Selkoe DJ: Trafficking of cell-surface amyloid beta-protein precursor. II. Endocytosis, recycling and lysosomal targeting detected by immunolocalization. **J Cell Sci** 1996, **109**:999-1008

Yanaka K, Camarata PJ, Spellman SR, McCarthy JB, Furcht LT, Low W: Antagonism of leukocyte adherence by synthetic fibronectin peptide V in a rat model of transient focal cerebral ischemia. **Neurosurgery** 1997, **40**:557-563

Yang G, Kitagawa K, Matsushita K, Mabuchi T, Yagita Y, Yanagihara T, Matsumoto M: C57BL/6 strain is most susceptible to cerebral ischemia following bilateral common carotid occlusion among seven mouse strains: selective neuronal death in the murine transient forebrain ischemia. **Brain Res** 1997a, **752**:209-218

Yang G-Y, Zhao Y-J, Davidson BL, Betz AL: Overexpression of interleukin-1 receptor antagonist in the mouse brain reduces ischemic brain injury. **Brain Res** 1997b, **751**:181-188

Yang G-Y, Mao Y, Zhon L-F, Ye W, Liu X-H, Gong C, Betz AL: Attenuation of temporary focal cerebral ischemic injury in the mouse following transfection with interleukin-1 receptor antagonist. **Brain Res Mol Brain Res** 1999, **72**:129-137

Yang J, Feng G, Zhang J, Hui Z, Breen G, St Clair D, He L: Is ApoE gene a risk factor for vascular dementia in Han Chinese? **Int J Mol Med** 2002, **7**:217-219

Yenari MA, Minami M, Sun GH, Meier TJ, Kunis DM, McLaughlin JR, Ho DY, Sapolsky RM, Steinberg GK: Calbindin D28K overexpression protects striatal neurons from transient focal cerebral ischemia. **Stroke** 2001, **32**:1028-1035

Zaiou M, Arnold KS, Newhouse YM, Innerarity TL, Weisgraber KH, Segall ML, Phillips MC, Lund-Katz S: Apolipoprotein E;-low density lipoprotein receptor interaction. Influences of basic residue and amphipathic alpha-helix organization in the ligand. **J Lipid Res** 2000, **41**:1087-1095

Zambrano N, Buxbaum JD, Minopoli G, Fiore F, De Candia P, De Renzis S, Faraonio R, Sabo S, Cheetham J, Sudol M, Russo T: Interaction of the phosphotyrosine interaction/phosphotyrosine binding-related domains of Fe65 with wild-type and mutant Alzheimer's beta-amyloid precursor proteins. **J Biol Chem** 1997, **272**:6399-6405

Zannis VI, Breslow JL, Utermann G, Mahley RW, Weisgraber KH, Havel RJ, Goldstein JL, Brown MS, Schonfeld G, Hazzard WR, Blum C: Proposed nomenclature of apoE isoproteins, apoE genotypes, and phenotypes. **J Lipid Res** 1982, **23**:911-914

Zausinger S, Scholler K, Plesnila N, Schmid-Elsaesser R: Combination drug therapy and mild hypothermia after transient focal cerebral ischemia in rats. **Stroke** 2003a, **34**:2246-2251

Zausinger S, Westermaier T, Plesnila N, Steiger HJ, Schmid-Elsaesser R: Neuroprotection in transient focal cerebral ischemia by combination drug therapy and mild hypothermia: comparison with customary therapeutic regimen. **Stroke** 2003b, **34**:1526-1532

Zhang W, Stanimirovic D: Current and future therapeutic strategies to target inflammation in stroke. **Curr Drug Targets Inflamm Allergy** 2002, **1**:151-166

Zhang WR, Kitagawa H, Hayashi T, Sasaki C, Sakai K, Warita H, Shiro Y, Suenaga H, Ohmae H, Tsuji S, Itoh T, Nishimura O, Nagasaki H, Abe K: Topical application of neurotrophin-3 attenuates ischemic brain injury after transient middle cerebral artery occlusion in rats. **Brain Res** 1999, **842**:211-214

Zhang WR, Hayashi T, Iwai M, Nagano I, Sato K, Manabe Y, Abe K: Time dependent amelioration against ischemic brain damage by glial cell line-derived neurotrophic factor after transient middle cerebral artery occlusion in rat. **Brain Res** 2001, **903**:253-256

Zhang WR, Sato K, Iwai M, Nagano I, Manabe Y, Abe K: Therapeutic time window of adenovirus-mediated GDNF gene transfer after transient middle cerebral artery occlusion in rat. **Brain Res** 2002, **947:140-145**

Zhang Y, Sclachetzki F, Pardridge WM: Global non-viral gene transfer to the primate brain following intravenous administration. **Mol Ther** 2003, **7:11-18**

Zhao H, Yenari MA, Cheng D, Sapolsky RM, Steinberg GK: Bcl-2 overexpression protects against neuron loss within the ischemic margin following experimental stroke and inhibits cytochrome c translocation and caspase-3 activity. **J Neurochem** 2003, **85:1026-1036**

Zhao W, Belayev L, Ginsberg MD: Transient middle cerebral artery occlusion by intraluminal suture: II. Neurological deficits, and pixel-based correlation of histopathology with local blood flow and glucose utilization. **J Cereb Blood Flow Metab** 1997, **17:1281-1290**

Zhu L, Fratiglioni L, Guo Z, Basun H, Corder EH, Winblad B, Viitanen M: Incidence of dementia in relation to stroke and the apolipoprotein E epsilon4 allele in the very old. Findings from a population-based longitudinal study. **Stroke** 2000, **31:53-60**

Zipfel GJ, Babcock DJ, Lee JM, Choi DW: Neuronal apoptosis after CNS injury: the roles of glutamate and calcium. **J Neurotrauma** 2000, **17:857-869**

Zou L, Zhou H, Pastore L, Yang K: Prolonged transgene expression mediated by a helper-dependent adenoviral vector (hdAd) in the central nervous system. **Mol Ther** 2000, **2:105-113**

Zou L, Yotnda P, Zhao T, Yuan X, Long Y, Zhou H, Yang K: Reduced inflammatory reactions to the inoculation of helper-dependent adenoviral vectors in traumatically injured rat brain. **J Cereb Blood Flow Metab** 2002, **22:959-970**

